

WORKING GUIDE TO RESERVOIR ROCK PROPERTIES AND FLUID FLOW

TAREK AHMED



AMSTERDAM • BOSTON • HEIDELBERG • LONDON NEW YORK • OXFORD • PARIS • SAN DIEGO SAN FRANCISCO • SINGAPORE • SYDNEY • TOKYO Guif Professional Publishing is an imprint of Elsevier



Gulf Professional Publishing is an imprint of Elsevier 30 Corporate Drive, Suite 400, Burlington, MA 01803, USA Linacre House, Jordan Hill, Oxford OX2 8DP, UK

Copyright © 2006, 2010, Elsevier Inc. All rights reserved.

Material in the work originally appeared in *Reservoir Engineering Handbook, Third Edition* by Tarek Ahmed (Elsevier Inc. 2006).

No part of this publication may be reproduced, stored in a retrieval system, or transmitted in any form or by any means, electronic, mechanical, photocopying, recording, or otherwise, without the prior written permission of the publisher.

Permissions may be sought directly from Elsevier's Science & Technology Rights Department in Oxford, UK: phone: (+44) 1865 843830, fax: (+44) 1865 853333, E-mail: permissions@elsevier.com. You may also complete your request online via the Elsevier homepage (http://www.elsevier.com), by selecting "Support & Contact" then "Copyright and Permission" and then "Obtaining Permissions."

Library of Congress Cataloging-in-Publication Data

A catalog record for this book is available from the Library of Congress.

British Library Cataloguing-in-Publication Data

A catalogue record for this book is available from the British Library.

ISBN: 978-1-85617-825-9

For information on all Gulf Professional Publishing publications visit our Web site at www.elsevierdirect.com

09 10 11 12 13 10 9 8 7 6 5 4 3 2 1

Printed in the United States of America

Working together to grow libraries in developing countries

www.elsevier.com | www.bookaid.org | www.sabre.org

ELSEVIER

BOOK AID International

Sabre Foundation

Contents

1

FUNDAMENTALS OF RESERVOIR FLUID BEHAVIOR

Section 1.1 Classification of Reservoirs and Reservoir Fluids	1
Pressure-Temperature Diagram 2	
Oil Reservoirs 3	
Gas Reservoirs 9	
Undefined Petroleum Fractions 25	

Section 1.2 Problems 29

Section 1.3 References 30

2

FUNDAMENTALS OF ROCK PROPERTIES

Section 2.1 Porosity	32
Absolute Porosity 32	
Effective Porosity 33	

Section 2.2 Saturation 36
Average Saturation 38

Section 2.3 Wettability 40

Section 2.4 Surface and Interfacial Tension 40

Section 2.5 Capillary Pressure 43
Capillary Pressure of Reservoir Rocks 46
Capillary Hysteresis 49
Initial Saturation Distribution in a Reservoir 51
Leverett J-Function 61
Converting Laboratory Capillary Pressure Data 64

Section 2.6 Permeability 65
The Klinkenberg Effect 71
Averaging Absolute Permeabilities 76
Absolute Penneability Correlations 84

vi CONTENTS

Section 2.7 Rock Compressibility 87
Section 2.8 Net Pay Thickness 92
Section 2.9 Reservoir Heterogeneity 93 Vertical Heterogeneity 94
Section 2.10 Areal Heterogeneity 104
Section 2.11 Problems 110
Section 2.12 References 115
3
FUNDAMENTALS OF RESERVOIR FLUID FLOW
Section 3.1 Types of Fluids 117 Incompressible Fluids 118 Slightly Compressible Fluids 118 Compressible Fluids 119
Section 3.2 Flow Regimes 120 Steady-State Flow 121 Unsteady-State Flow 121 Pseudosteady-State Flow 121
Section 3.3 Reservoir Geometry 122 Radial Flow 122 Linear Flow 123 Spherical and Hemispherical Flow 123
Section 3.4 Number of Flowing Fluids in the Reservoir 125
Section 3.5 Fluid Flow Equations 125 Darcy's Law 125
Section 3.6 Steady-State Flow 127 Linear Flow of Incompressible Fluids 128 Linear Flow of Slightly Compressible Fluids 132 Linear Flow of Compressible Fluids (Gases) 133 Radial Flow of Incompressible Fluids 138 Radial Flow of Slightly Compressible Fluids 143 Radial Flow of Compressible Gases 144 Horizontal Multiple-Phase Flow 151 Section 3.7 Unsteady-State Flow 153 Basic Transient Flow Equation 155 Radial Flow of Slightly Compressible Fluids 159

CONTENTS vii

Section 3.8 Constant-Terminal-Pressure Solution	162
Section 3.9 Constant-Terminal-Rate Solution The E _I -Function Solution 163	163
The Dimensionless Pressure Drop (pp) Solution 170	
Radial Flow of Compressible Fluids 179	
The m(p)-Solution Method (Exact Solution) 181	
The Pressure-Squared Approximation Method (p ² -Method)	183
The Pressure-Approximation Method 185	
Section 3.10 Pseudosteady-State Flow 188	
Radial Flow of Slightly Compressible Fluids 193	
Radial Flow of Compressible Fluids (Gases) 201	
Pressure-Squared Approximation Method 201	

Radial Flow of Slightly Compressible Fluids 193
Radial Flow of Compressible Fluids (Gases) 201
Pressure-Squared Approximation Method 201
Pressure-Approximation Method 202
Skin Factor 202
Turbulent Flow Factor 208

Section 3.11 Principle of Superposition 211 Effects

Effects of Variable Flow Rates 215
Effects of the Reservoir Boundary 218
Accounting for Pressure-Change Effects 221

Section 3.12 Transient Well Testing 221
Drawdown Test 222
Pressure Buildup Test 233

Section 3.13 Problems 241

Section 3.14 References 245

INDEX 247

1

Fundamentals of Reservoir Fluid Behavior

Naturally occurring hydrocarbon systems found in petroleum reservoirs are mixtures of organic compounds that exhibit multiphase behavior over wide ranges of pressures and temperatures. These hydrocarbon accumulations may occur in the gaseous state, the liquid state, the solid state, or in various combinations of gas, liquid, and solid.

These differences in phase behavior, coupled with the physical properties of reservoir rock, which determine the relative ease with which gas and liquid are transmitted or retained, result in many diverse types of hydrocarbon reservoirs with complex behaviors. Frequently, petroleum engineers have the task to study the behavior and characteristics of a petroleum reservoir and to determine the course of future development and production that would maximize the profit.

The objective of this chapter is to review the basic principles of reservoir fluid phase behavior and illustrate the use of phase diagrams in classifying types of reservoirs and the native hydrocarbon systems.

SECTION 1.1 CLASSIFICATION OF RESERVOIRS AND RESERVOIR FLUIDS

Petroleum reservoirs are broadly classified as oil or gas reservoirs. These broad classifications are further subdivided depending on

- The composition of the reservoir hydrocarbon mixture.
- Initial reservoir pressure and temperature.
- Pressure and temperature of the surface production.

The conditions under which these phases exist are a matter of considerable practical importance. The experimental or the mathematical

determinations of these conditions are conveniently expressed in different types of diagrams, commonly called *phase diagrams*. One such diagram is called the *pressure-temperature diagram*.

Pressure-Temperature Diagram

Figure 1-1 shows a typical pressure-temperature diagram of a multicomponent system with a specific overall composition. Although a different hydrocarbon system would have a different phase diagram, the general configuration is similar.

These multicomponent pressure-temperature diagrams are essentially used to

- Classify reservoirs.
- Classify the naturally occurring hydrocarbon systems.
- Describe the phase behavior of the reservoir fluid.

To fully understand the significance of the pressure-temperature diagrams, it is necessary to identify and define the following key points on these diagrams:

Cricondentherm (T_{ct}). The cricondentherm is defined as the
maximum temperature above which liquid cannot be formed
regardless of pressure (point E). The corresponding pressure is
termed the *cricondentherm pressure* p_{ct}.

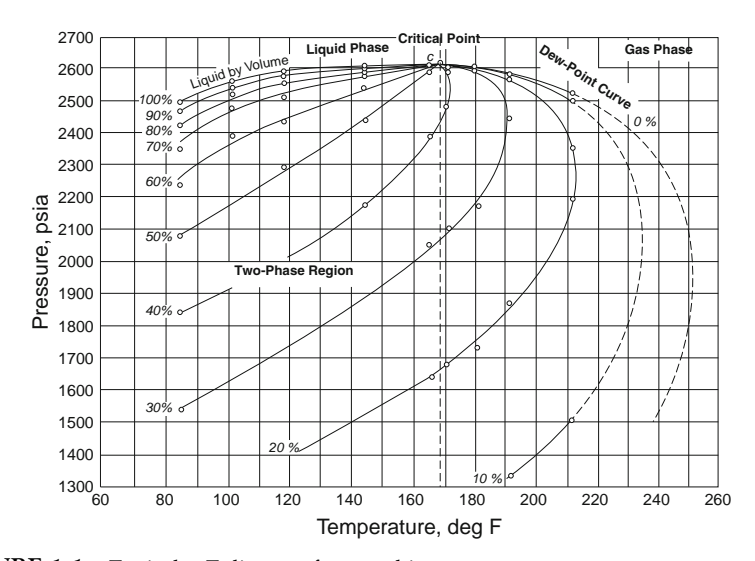


FIGURE 1-1 Typical p-T diagram for a multicomponent system.

- Cricondenbar (P_{cb}). The cricondenbar is the maximum pressure above which no gas can be formed regardless of temperature (point D). The corresponding temperature is called the *cricondenbar* temperature T_{cb}.
- **Critical Point.** The critical point for a multicomponent mixture refers to the state of pressure and temperature at which all intensive properties of the gas and liquid phases are equal (point C). At the critical point, the corresponding pressure and temperature are called the *critical pressure* p_c and *critical temperature* T_c of the mixture.
- **Phase Envelope (Two-Phase Region).** The region enclosed by the bubble-point curve and the dew-point curve (line BCA), wherein gas and liquid coexist in equilibrium, is identified as the phase envelope of the hydrocarbon system.
- **Quality Lines.** The dashed lines within the phase diagram are called *quality lines*. They describe the pressure and temperature conditions for equal volumes of liquids. Note that the quality lines converge at the critical point (point C).
- **Bubble-Point Curve.** The bubble-point curve (line BC) is defined as the line separating the liquid-phase region from the two-phase region.
- **Dew-Point Curve.** The dew-point curve (line AC) is defined as the line separating the vapor-phase region from the two-phase region.

In general, reservoirs are conveniently classified on the basis of the location of the point representing the initial reservoir pressure p_i and temperature T with respect to the pressure-temperature diagram of the reservoir fluid. Accordingly, reservoirs can be classified into basically two types. These are

- Oil Reservoirs. If the reservoir temperature T is less than the critical temperature T_c of the reservoir fluid, the reservoir is classified as an oil reservoir.
- **Gas Reservoirs.** If the reservoir temperature is greater than the critical temperature of the hydrocarbon fluid, the reservoir is considered a gas reservoir.

Oil Reservoirs

Depending upon initial reservoir pressure p_i, oil reservoirs can be subclassified into the following categories:

1. **Undersaturated Oil Reservoir.** If the initial reservoir pressure p_i (as represented by point 1 in Figure 1-1) is greater than the bubble-point pressure p_b of the reservoir fluid, the reservoir is labeled an *undersaturated oil reservoir*.

- 2. **Saturated Oil Reservoir.** When the initial reservoir pressure is equal to the bubble-point pressure of the reservoir fluid, as shown in Figure 1-1 by point 2, the reservoir is called a *saturated oil reservoir*.
- 3. **Gas-Cap Reservoir.** If the initial reservoir pressure is below the bubble-point pressure of the reservoir fluid, as indicated by point 3 in Figure 1-1, the reservoir is termed a *gas-cap* or *two-phase reservoir*, in which the gas or vapor phase is underlain by an oil phase. The appropriate quality line gives the ratio of the gas-cap volume to reservoir oil volume.

Crude oils cover a wide range in physical properties and chemical compositions, and it is often important to be able to group them into broad categories of related oils. In general, crude oils are commonly classified into the following types:

- Ordinary black oil.
- Low-shrinkage crude oil.
- High-shrinkage (volatile) crude oil.
- Near-critical crude oil.

These classifications are essentially based upon the properties exhibited by the crude oil, including physical properties, composition, gas-oil ratio, appearance, and pressure-temperature phase diagrams:

1. **Ordinary Black Oil.** A typical pressure-temperature phase diagram for ordinary black oil is shown in Figure 1-2. It should be noted that quality lines, which are approximately equally spaced, characterize

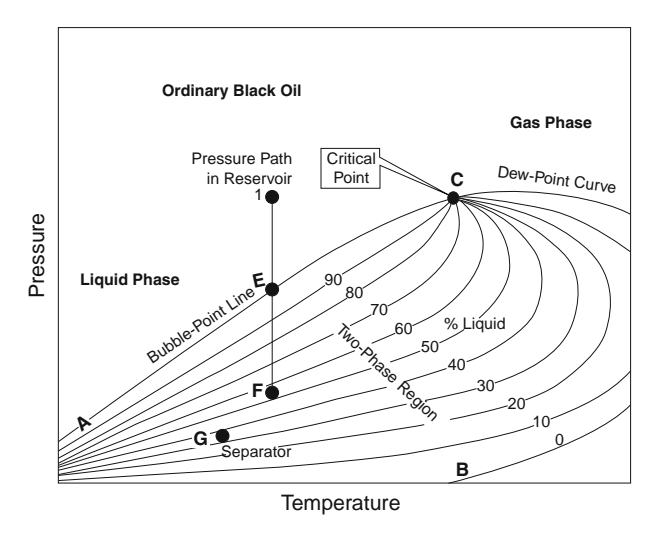


FIGURE 1-2 A typical p-T diagram for an ordinary black oil.

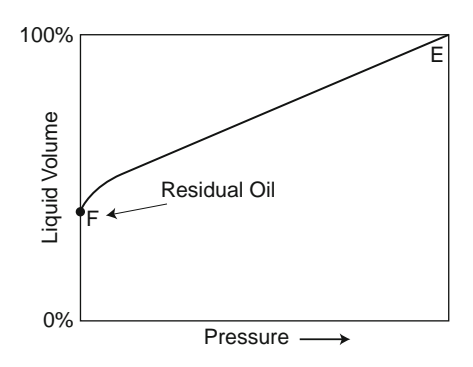


FIGURE 1-3 Liquid-shrinkage curve for black oil.

this black oil phase diagram. Following the pressure reduction path as indicated by the vertical line EF in Figure 1-2, the liquid-shrinkage curve, as shown in Figure 1-3, is prepared by plotting the liquid volume percent as a function of pressure. The liquid-shrinkage curve approximates a straight line except at very low pressures. When produced, ordinary black oils usually yield gas-oil ratios between 200–700 scf/STB and oil gravities of 15 to 40 API. The stock-tank oil is usually brown to dark green in color.

2. **Low-Shrinkage Oil.** A typical pressure-temperature phase diagram for low-shrinkage oil is shown in Figure 1-4. The diagram is characterized by quality lines that are closely spaced near the dew-point curve. The liquid-shrinkage curve, as given in Figure 1-5,

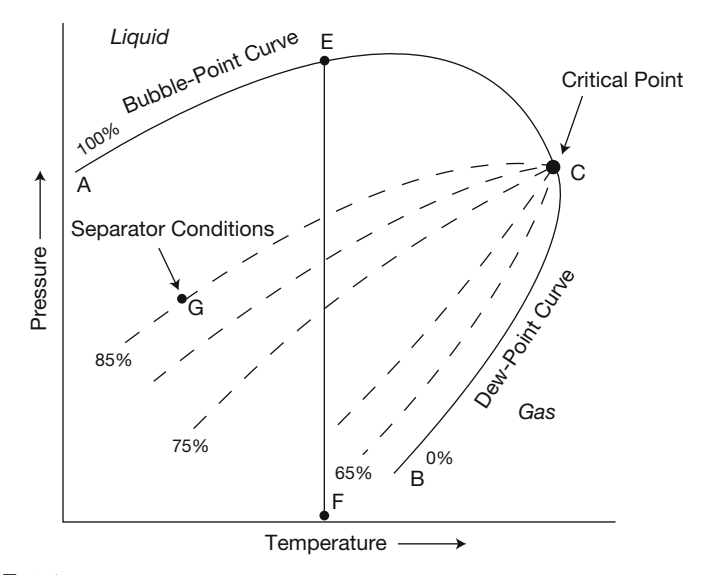
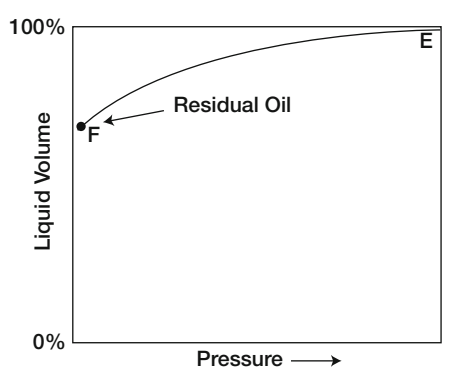


FIGURE 1-4 A typical phase diagram for a low-shrinkage oil.

FIGURE 1-5 Oil-shrinkage curve for low-shrinkage oil.



shows the shrinkage characteristics of this category of crude oils. The other associated properties of this type of crude oil are

- Oil formation volume factor less than 1.2 bbl/STB.
- Gas-oil ratio less than 200 scf/STB.
- Oil gravity less than 35° API.
- Black or deeply colored.
- Substantial liquid recovery at separator conditions as indicated by point G on the 85% quality line of Figure 1-4.
- 3. **Volatile Crude Oil.** The phase diagram for a volatile (high-shrinkage) crude oil is given in Figure 1-6. Note that the quality lines are close

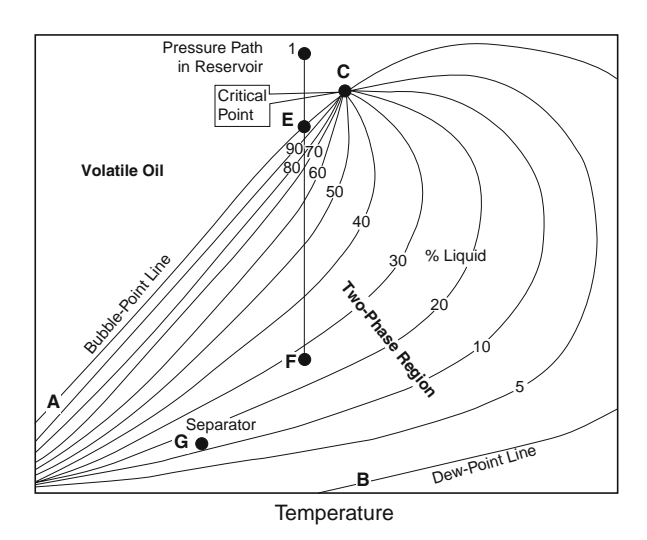


FIGURE 1-6 A typical p-T diagram for a volatile crude oil.

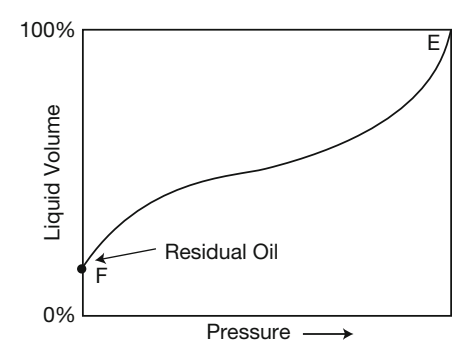


FIGURE 1-7 A typical liquid-shrinkage curve for a volatile crude oil.

together near the bubble point and are more widely spaced at lower pressures. This type of crude oil is commonly characterized by a high liquid shrinkage immediately below the bubble point as shown in Figure 1-7. The other characteristic properties of this oil include

- Oil formation volume factor less than 2 bbl/STB.
- Gas-oil ratios between 2,000 and 3,200 scf/STB.
- Oil gravities between 45° and 55° API.
- Lower liquid recovery of separator conditions as indicated by point G in Figure 1-6.
- Greenish to orange in color.

Another characteristic of volatile oil reservoirs is that the API gravity of the stock-tank liquid will increase in the later life of the reservoirs.

4. Near-Critical Crude Oil. If the reservoir temperature T is near the critical temperature T_c of the hydrocarbon system, as shown in Figure 1-8, the hydrocarbon mixture is identified as a near-critical crude oil. Because all the quality lines converge at the critical point, an isothermal pressure drop (as shown by the vertical line EF in Figure 1-8) may shrink the crude oil from 100% of the hydrocarbon pore volume at the bubble point to 55% or less at a pressure 10 to 50 psi below the bubble point. The shrinkage characteristic behavior of the near-critical crude oil is shown in Figure 1-9. The near-critical crude oil is characterized by a high GOR in excess of 3,000 scf/STB with an oil formation volume factor of 2.0 bbl/STB or higher. The compositions of near-critical oils are usually characterized by 12.5 to 20 mol% heptanes-plus, 35% or more of ethane through hexanes, and the remainder methane.

Figure 1-10 compares the characteristic shape of the liquid-shrinkage curve for each crude oil type.

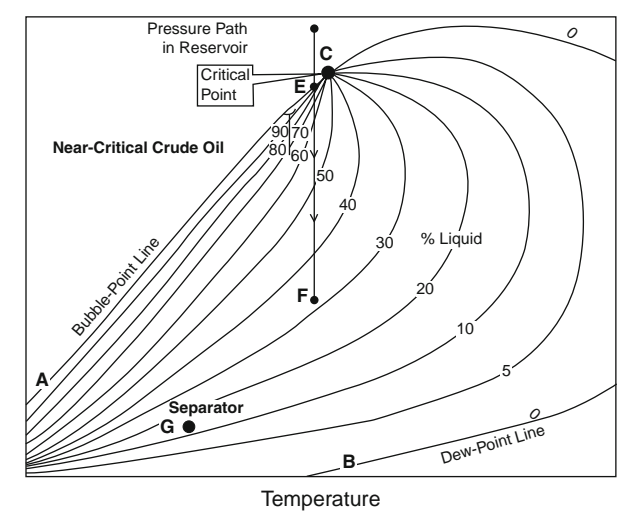
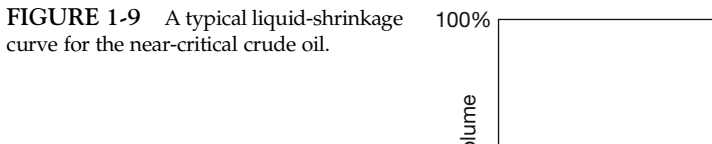
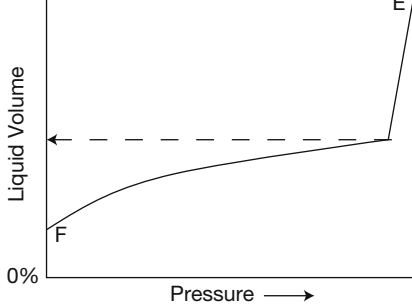


FIGURE 1-8 A schematic phase diagram for the near-critical crude oil.





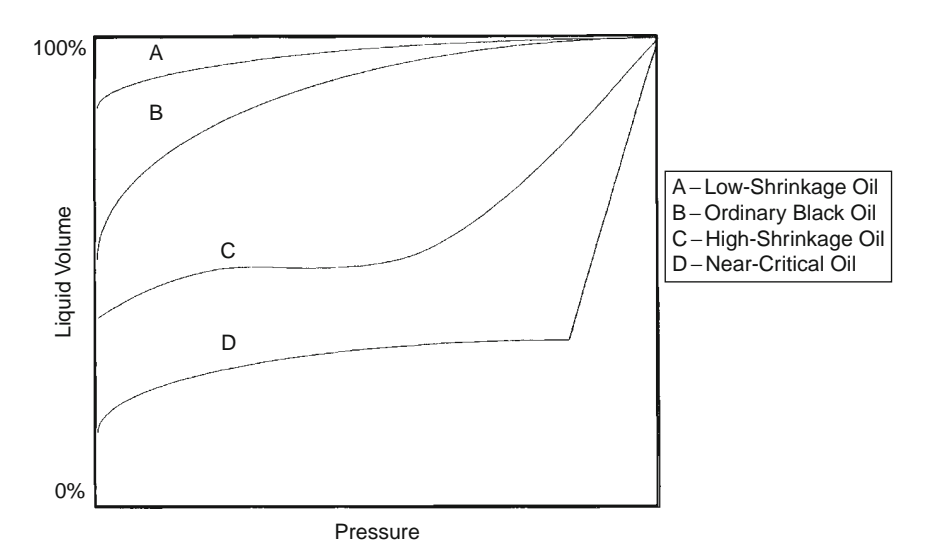


FIGURE 1-10 Liquid shrinkage for crude oil systems.

Gas Reservoirs

In general, if the reservoir temperature is above the critical temperature of the hydrocarbon system, the reservoir is classified as a natural gas reservoir. On the basis of their phase diagrams and the prevailing reservoir conditions, natural gases can be classified into four categories:

- Retrograde gas-condensate
- Near-critical gas-condensate
- Wet gas
- Dry gas

Retrograde Gas-Condensate Reservoir. If the reservoir temperature T lies between the critical temperature T_c and cricondentherm T_{ct} of the reservoir fluid, the reservoir is classified as a retrograde gas-condensate reservoir. This category of gas reservoir is a unique type of hydrocarbon accumulation in that the special thermodynamic behavior of the reservoir fluid is the controlling factor in the development and the depletion process of the reservoir. When the pressure is decreased on these mixtures, instead of expanding (if a gas) or vaporizing (if a liquid) as might be expected, they vaporize instead of condensing.

Consider that the initial condition of a retrograde gas reservoir is represented by point 1 on the pressure-temperature phase diagram of Figure 1-11. Because the reservoir pressure is above the upper dewpoint pressure, the hydrocarbon system exists as a single phase (i.e., vapor phase) in the reservoir. As the reservoir pressure declines isothermally during production from the initial pressure (point 1) to the

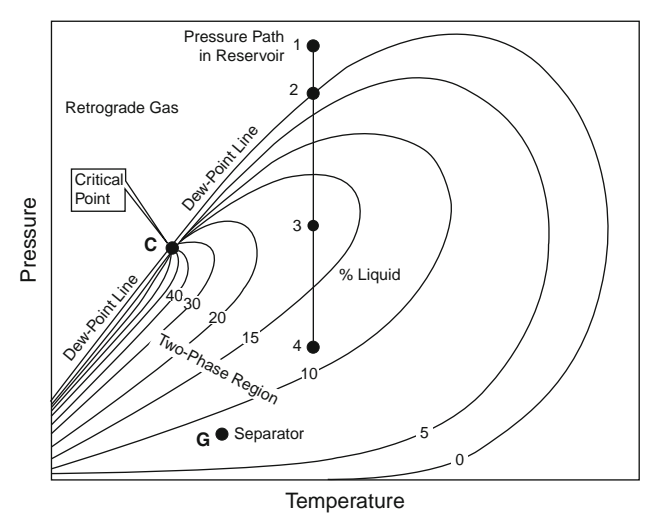


FIGURE 1-11 A typical phase diagram of a retrograde system.

upper dew-point pressure (point 2), the attraction between the molecules of the light and heavy components causes them to move further apart. As this occurs, attraction between the heavy component molecules becomes more effective; thus, liquid begins to condense.

This retrograde condensation process continues with decreasing pressure until the liquid dropout reaches its maximum at point 3. Further reduction in pressure permits the heavy molecules to commence the normal vaporization process. This is the process whereby fewer gas molecules strike the liquid surface and cause more molecules to leave than enter the liquid phase. The vaporization process continues until the reservoir pressure reaches the lower dew-point pressure. This means that all the liquid that formed must vaporize because the system is essentially all vapors at the lower dew point.

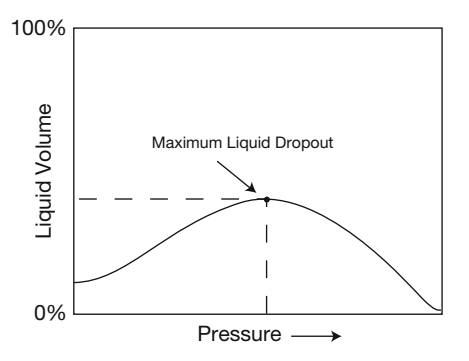
Figure 1-12 shows a typical liquid shrinkage volume curve for a condensate system. The curve is commonly called the *liquid dropout curve*. In most gas-condensate reservoirs, the condensed liquid volume seldom exceeds more than 15–19% of the pore volume. This liquid saturation is not large enough to allow any liquid flow. It should be recognized, however, that around the wellbore, where the pressure drop is high, enough liquid dropout might accumulate to give two-phase flow of gas and retrograde liquid.

The associated physical characteristics of this category are

- Gas-oil ratios between 8,000 and 70,000 scf/STB. Generally, the gas-oil ratio for a condensate system increases with time due to the liquid dropout and the loss of heavy components in the liquid.
- Condensate gravity above 50° APL.
- Stock-tank liquid is usually water-white or slightly colored.

There is a fairly sharp dividing line between oils and condensates from a compositional standpoint. Reservoir fluids that contain heptanes and are heavier in concentrations of more than 12.5 mol% are almost always in the liquid phase in the reservoir. Oils have been observed with

FIGURE 1-12 A typical liquid dropout curve.



heptanes and heavier concentrations as low as 10% and condensates as high as 15.5%. These cases are rare, however, and usually have very high tank liquid gravities.

Near-Critical Gas-Condensate Reservoir. If the reservoir temperature is near the critical temperature, as shown in Figure 1-13, the hydrocarbon mixture is classified as a near-critical gas condensate. The volumetric behavior of this category of natural gas is described through the isothermal pressure declines as shown by the vertical line 1–3 in Figure 1-13 and also by the corresponding liquid dropout curve of Figure 1-14. Because all the quality lines converge at the critical point, a rapid liquid buildup will immediately occur below the dew point (Figure 1-14) as the pressure is reduced to point 2.

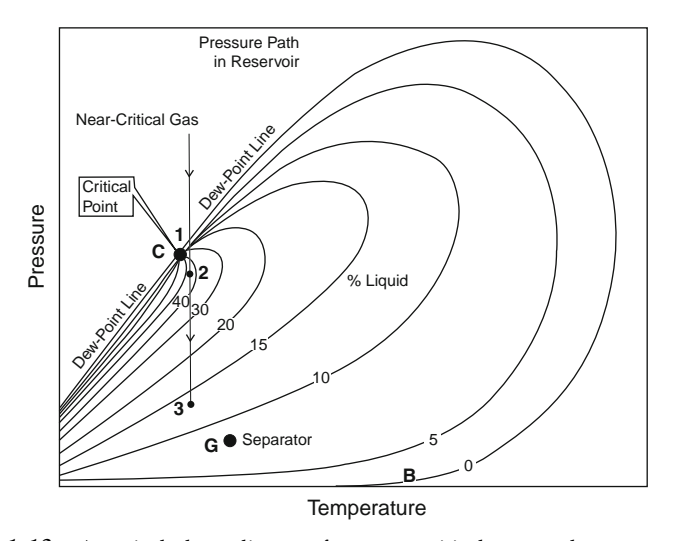


FIGURE 1-13 A typical phase diagram for a near-critical gas-condensate reservoir.

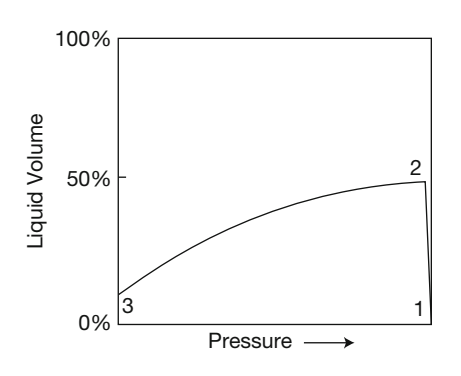


FIGURE 1-14 Liquid-shrinkage curve for a near-critical gas-condensate system.

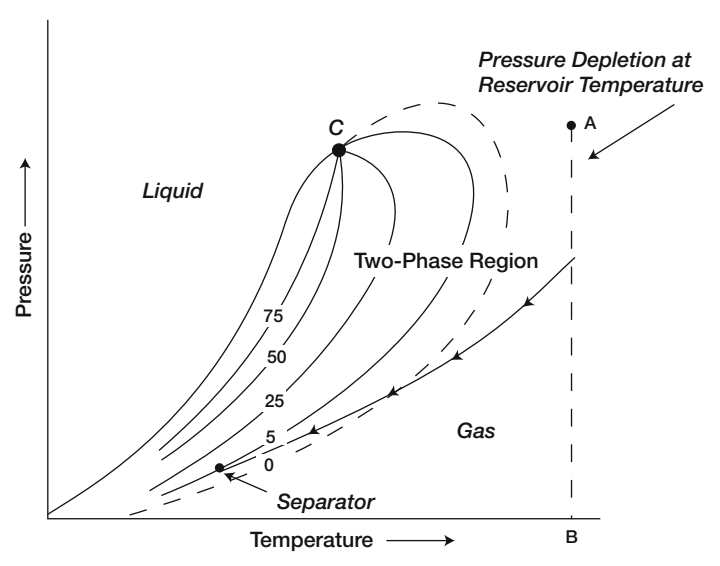


FIGURE 1-15 Phase diagram for a wet gas. (After Clark, N.J., Elements of Petroleum Reservoirs, SPE, 1969.)

This behavior can be justified by the fact that several quality lines are crossed very rapidly by the isothermal reduction in pressure. At the point where the liquid ceases to build up and begins to shrink again, the reservoir goes from the retrograde region to a normal vaporization region.

Wet-Gas Reservoir. A typical phase diagram of a wet gas is shown in Figure 1-15, where reservoir temperature is above the cricondentherm of the hydrocarbon mixture. Because the reservoir temperature exceeds the cricondentherm of the hydrocarbon system, the reservoir fluid will always remain in the vapor-phase region as the reservoir is depleted isothermally, along the vertical line A–B.

As the produced gas flows to the surface, however, the pressure and temperature of the gas will decline. If the gas enters the two-phase region, a liquid phase will condense out of the gas and be produced from the surface separators. This is caused by a sufficient decrease in the kinetic energy of heavy molecules with temperature drop and their subsequent change to liquid through the attractive forces between molecules.

Wet-gas reservoirs are characterized by the following properties:

- Gas-oil ratios between 60,000 and 100,000 scf/STB.
- Stock-tank oil gravity above 60° API.
- Liquid is water-white in color.
- Separator conditions, i.e., separator pressure and temperature, lie within the two-phase region.

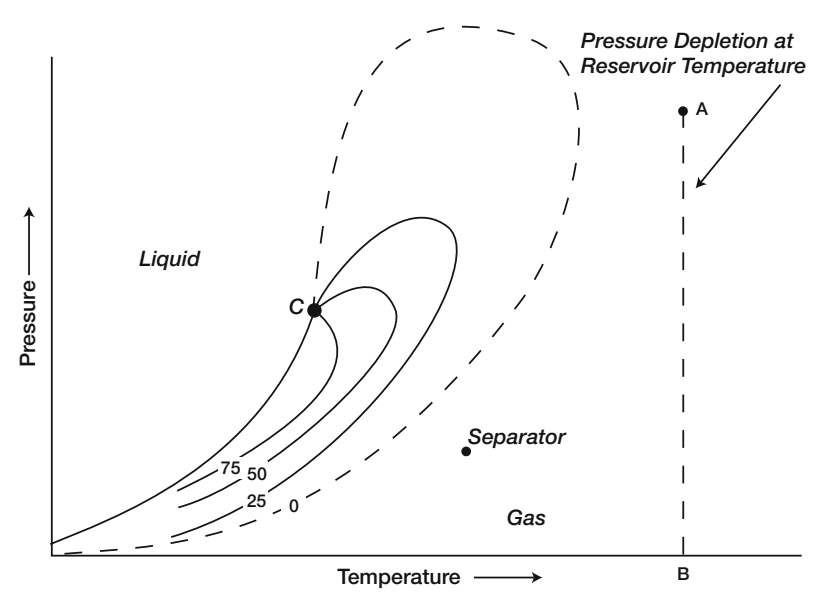


FIGURE 1-16 Phase diagram for a dry gas. (After Clark, N.J., Elements of Petroleum Reservoirs, SPE, 1969.)

Dry-Gas Reservoir. The hydrocarbon mixture exists as a gas both in the reservoir and in the surface facilities. The only liquid associated with the gas from a dry-gas reservoir is water. A phase diagram of a dry-gas reservoir is given in Figure 1-16. Usually a system having a gas-oil ratio greater than 100,000 scf/STB is considered to be a dry gas.

Kinetic energy of the mixture is so high and attraction between molecules so small that none of them coalesce to a liquid at stock-tank conditions of temperature and pressure.

It should be pointed out that the classification of hydrocarbon fluids might also be characterized by the initial composition of the system. McCain (1994) suggested that the heavy components in the hydrocarbon mixtures have the strongest effect on fluid characteristics. The ternary diagram, as shown in Figure 1-17, with equilateral triangles can be conveniently used to roughly define the compositional boundaries that separate different types of hydrocarbon systems.

From the foregoing discussion, it can be observed that hydrocarbon mixtures may exist in either the gaseous or liquid state, depending on the reservoir and operating conditions to which they are subjected. The qualitative concepts presented may be of aid in developing quantitative analyses. Empirical equations of state are commonly used as a quantitative tool in describing and classifying the hydrocarbon system. These equations of state require

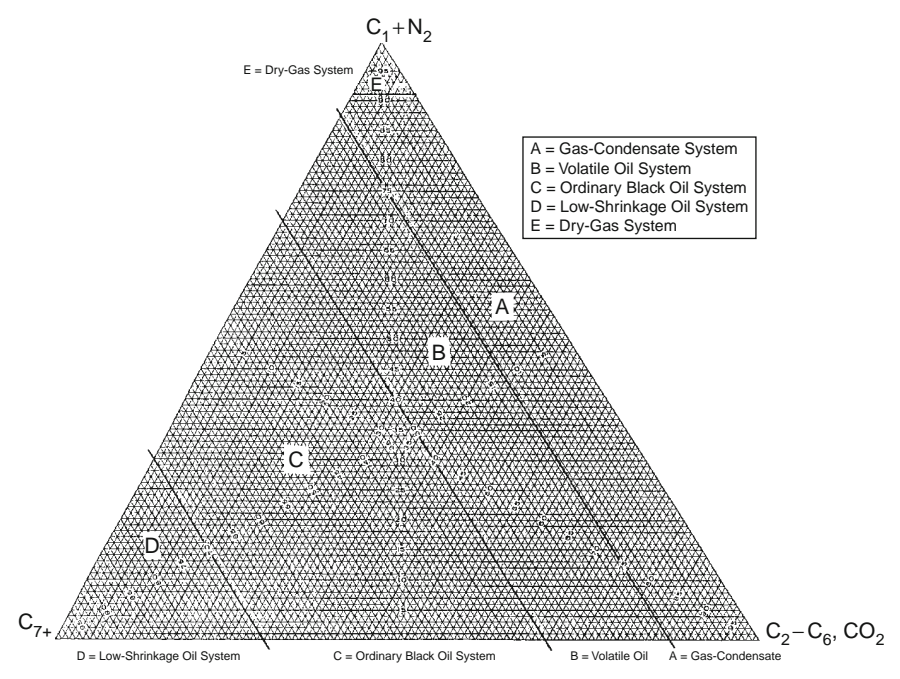


FIGURE 1-17 Compositions of various reservoir fluid types.

- Detailed compositional analyses of the hydrocarbon system.
- Complete descriptions of the physical and critical properties of the mixture's individual components.

Many characteristic properties of these individual components (in other words, pure substances) have been measured and compiled over the years. These properties provide vital information for calculating the thermodynamic properties of pure components, as well as their mixtures. The most important of these properties are

- Critical pressure, p_c.
- Critical temperature, T_c.
- Critical volume, V_c.
- Critical compressibility factor, z_c.
- Acentric factor, T.
- Molecular weight, M.

Table 1-1 documents these properties for a number of hydrocarbon and nonhydrocarbon components.

Katz and Firoozabadi (1978) presented a generalized set of physical properties for the petroleum fractions C_6 through C_{45} . The tabulated properties include the average boiling point, specific gravity, and

 TABLE 1-1
 Physical Properties for Pure Components

				Phy	sical Constar	nts					
	See Note No.→		Α.	В.		C.	D.				
								Critical constants			
Number	Compound	Formula	Molar mass (molecular weight)	Boiling point, °F 14.696 psia	Vapor pressure, psia 100°F	Freezing point, °F 14.696 psia	Refractive index, $\eta_D~60^{\circ}F$	Pressure, psia	Temperature, °F	Volume, ft ³ /1 bm	Number
1	Methane	CH_4	16.043	-258.73	(5000)	-296.44	1.00042	666.4	-116.67	0.0988	1
2	Ethane	C_2H_6	30.070	-127.49	(800)	-297.04	1.20971	706.5	89.92	0.0783	2
3	Propane	C_3H_8	44.097	-43.75	188.64	-305.73	1.29480	616.0	206.06	0.0727	3
4	Isobutane	C_4H_{10}	58.123	10.78	72.581	-255.28	1.3245*	527.9	274.46	0.0714	4
5	n-Butane	C_4H_{10}	58.123	31.08	51.706	-217.05	1.33588*	550.6	305.62	0.0703	5
6	Isopentane	C_5H_{12}	72.150	82.12	20.445	-255.82	1.35631	490.4	369.10	0.0679	6
7	n-Pentane	C_5H_{12}	72.150	96.92	15.574	-201.51	1.35992	488.6	385.8	0.0675	7
8	Neopentane	C_5H_{12}	72.150	49.10	36.69	2.17	1.342	464.0	321.13	0.0673	8
9	n-Hexane	C_6H_{14}	86.177	155.72	4.9597	-139.58	1.37708	436.9	453.6	0.0688	9

 TABLE 1-1
 Physical Properties for Pure Components—Cont'd

-				Phy	sical Consta	nts					
	See Note No.→		Α.	В.		C.	D.				
								Critical constants			
Number	Compound	Formula	Molar mass (molecular weight)	Boiling point, °F 14.696 psia	Vapor pressure, psia 100°F	Freezing point, °F 14.696 psia	Refractive index, $\eta_D~60^{\circ}F$	Pressure, psia	${\sf Temperature,}^{\circ}{\sf F}$	Volume, ft ³ /1 bm	Number
10	2-Methylpentane	C ₆ H ₁₄	86.177	140.47	6.769	-244.62	1.37387	436.6	435.83	0.0682	10
11	3-Methylpentane	C_6H_{14}	86.177	145.89	6.103		1.37888	453.1	448.4	0.0682	11
12	Neohexane	C_6H_{14}	86.177	121.52	9.859	-147.72	1.37126	446.8	420.13	0.0667	12
13	2,3-Dimethylbutane	C_6H_{14}	86.177	136.36	7.406	-199.38	1.37730	453.5	440.29	0.0665	13
14	n-Heptane	C_7H_{16}	100.204	209.16	1.620	-131.05	1.38989	396.8	512.7	0.0691	14
15	2-Methylhexane	C_7H_{16}	100.204	194.09	2.272	-180.89	1.38714	396.5	495.00	0.0673	15
16	3-Methylhexane	C_7H_{16}	100.204	197.33	2.131		1.39091	408.1	503.80	0.0646	16
17	3-Ethylpentane	C_7H_{16}	100.204	200.25	2.013	-181.48	1.39566	419.3	513.39	0.0665	17
18	2,2-Dimethylpentane	C_7H_{16}	100.204	174.54	3.494	-190.86	1.38446	402.2	477.23	0.0665	18
19	2, 4-Dimethylpentane	C_7H_{16}	100.204	176.89	3.293	-182.63	1.38379	396.9	475.95	0.0668	19

20	3, 3-Dimethylpentane	C_7H_{16}	100.204	186.91	2.774	-210.01	1.38564	427.2	505.87	0.0662	20
21	Triptane	C_7H_{16}	100.204	177.58	3.375	-12.81	1.39168	428.4	496.44	0.0636	21
22	n-Octane	C_8H_{18}	114.231	258.21	0.53694	-70.18	1.39956	360.7	564.22	0.0690	22
23	Dilsobutyl	C_8H_{18}	114.231	228.39	1.102	-132.11	1.39461	360.6	530.44	0.0676	23
24	Isooctane	C_8H_{18}	114.231	210.63	1.709	-161.27	1.38624	372.4	519.46	0.0656	24
25	n-Nonane	C_9H_{20}	128.258	303.47	0.17953	-64.28	1.40746	331.8	610.68	0.0684	25
26	n-Decane	$C_{10}H_{22}$	142.285	345.48	0.06088	-21.36	1.41385	305.2	652.0	0.0679	26
27	Cyclopentane	C_5H_{10}	70.134	120.65	9.915	-136.91	1.40896	653.8	461.2	0.0594	27
28	Methylcyclopentane	C_6H_{12}	84.161	161.25	4.503	-224.40	1.41210	548.9	499.35	0.0607	28
29	Cyclohexane	C_6H_{12}	84.161	177.29	3.266	43.77	1.42862	590.8	536.6	0.0586	29
30	Methylcyclohexane	C_7H_{14}	98.188	213.68	1.609	-195.87	1.42538	503.5	570.27	0.0600	30
31	Ethene (Ethylene)	C_2H_4	28.054	-154.73	(1400)	-272.47	(1.228)	731.0	48.54	0.0746	31
32	Propene (Propylene)	C_3H_6	42.081	-53.84	227.7	-301.45	1.3130	668.6	197.17	0.0689	32
33	1-Butene (Butylene)	C_4H_8	56.108	20.79	62.10	-301.63	1.3494	583.5	295.48	0.0685	33
34	cis-2-Butene	C_4H_8	56.108	38.69	45.95	-218.06	1.3665	612.1	324.37	0.0668	34
35	trans-2-Butene	C_4H_8	56.108	33.58	49.87	-157.96	1.3563	587.4	311.86	0.0679	35
36	Isobutene	C_4H_8	56.108	19.59	63.02	-220.65	1.3512	580.2	292.55	0.0682	36
37	1-Pentene	C_5H_{10}	70.134	85.93	19.12	-265.39	1.37426	511.8	376.93	0.0676	37
38	1,2-Butadiene	C_4H_6	54.092	51.53	36.53	-213.16		(653.)	(340.)	(0.065)	38

Continued

 TABLE 1-1
 Physical Properties for Pure Components—Cont'd

				Phy	sical Constar	nts					
	See Note No.→		Α.	В.		C.	D.				
								Critical constants			
Number	Compound	Formula	Molar mass (molecular weight)	Boiling point, °F 14.696 psia	Vapor pressure, psia 100°F	Freezing point, °F 14.696 psia	Refractive index, $\eta_D~60^\circ F$	Pressure, psia	Temperature, °F	Volume, ft ³ /1 bm	Number
39	1,3-Butadiene	C_4H_6	54.092	24.06	59.46	-164.02	1.3975	627.5	305.	0.0654	39
40	Isoprene	C_5H_8	68.119	93.31	16.68	-230.73	1.42498	(558.)	(412.)	(0.065)	40
41	Acetylene	C_2H_2	26.038	-120.49		-114.5		890.4	95.34	0.0695	41
42	Benzene	C_6H_6	78.114	176.18	3.225	41.95	1.50396	710.4	552.22	0.0531	42
43	Toluene	C_7H_8	92.141	231.13	1.033	-139.00	1.49942	595.5	605.57	0.0550	43
44	Ethylbenzene	C_8H_{10}	106.167	277.16	0.3716	-138.966	1.49826	523.0	651.29	0.0565	44
45	o-Xylene	C_8H_{10}	106.167	291.97	0.2643	-13.59	1.50767	541.6	674.92	0.0557	45
46	m-Xylene	C_8H_{10}	106.167	282.41	0.3265	-54.18	1.49951	512.9	651.02	0.0567	46
47	p-Xylene	C_8H_{10}	106.167	281.07	0.3424	55.83	1.49810	509.2	649.54	0.0570	47

48	Styrene	C_8H_8	104.152	293.25	0.2582	-23.10	1.54937	587.8	(703.)	0.0534	48
49	Isopropylbenzene	C_9H_{12}	120.194	306.34	0.1884	-140.814	1.49372	465.4	676.3	0.0572	49
50	Methyl alcohol	CH ₄ O	32.042	148.44	4.629	-143.79	1.33034	1174.	463.08	0.0590	50
51	Ethyl alcohol	C_2H_6O	46.069	172.90	2.312	-173.4	1.36346	890.1	465.39	0.0581	51
52	Carbon monoxide	CO	28.010	-312.68		-337.00	1.00036	507.5	-220.43	0.0532	52
53	Carbon dioxide	CO_2	44.010	-109.257		-69.83	1.00048	1071.	87.91	0.0344	53
54	Hydrogen sulfide	H_2S	34.08	-76.497	394.59	-121.88	1.00060	1300.	212.45	0.0461	54
55	Sulfur dioxide	SO_2	64.06	14.11	85.46	-103.86	1.00062	1143.	315.8	0.0305	55
56	Ammonia	NH_3	17.0305	-27.99	211.9	-107.88	1.00036	1646.	270.2	0.0681	56
57	Air	$N_2 + O_2$	28.9625	-317.8			1.00028	546.9	-221.31	0.0517	57
58	Hydrogen	H_2	2.0159	-422.955		-435.26	1.00013	188.1	-399.9	0.5165	58
59	Oxygen	O_2	31.9988	-297.332		-361.820	1.00027	731.4	-181.43	0.0367	59
60	Nitrogen	N_2	28.0134	-320.451		-346.00	1.00028	493.1	-232.51	0.0510	60
61	Chlorine	Cl_2	70.906	-29.13	157.3	-149.73	1.3878	1157.	290.75	0.0280	61
62	Water	H_2O	18.0153	212.000	0.9501	32.00	1.33335	3198.8	705.16	0.0497s	62
63	Helium	Не	4.0026	-452.09			1.00003	32.99	-450.31	0.2300	63
64	Hydrogen chloride	HCl	36.461	-121.27	906.71	-173.52	1.00042	1205.	124.77	0.0356	64

Continued

 TABLE 1-1
 Physical Properties for Pure Components—Cont'd

					Phy	ysical Consta	nts					
	E. Density of liquid 14.696 psia, 60°F		F.	F. G. H.			I.	į	J.			
			coefficient of		tor of sia,	14.	Ideal gas 14.696 psia, 60°F			ic Heat .696 psia bm.°F)		
Number	Relative density (specific gravity) 60°F/60°F	l bm/gal.	gal./Ib mole	Temperature coeffi density, $1/^{\circ} \mathrm{F}$	Acentric factor, ®	Compressibility factor of real gas, Z 14.696 psia, 60°F	Relative density (specific gravity) Air = 1	ft³ gas/1 bm	ft ³ gas/gal. liquid	Cp, Ideal gas	Cp, Liquid	Number
1	(0.3)	(2.5)	(6.4172)		0.0104	0.9980	0.5539	23.654	(59.135)	0.52669		1
2	0.35619	2.9696	10.126		0.0979	0.9919	1.0382	12.620	37.476	0.40782	0.97225	2
3	0.50699	4.2268	10.433	-0.00162	0.1522	0.9825	1.5226	8.6059	36.375	0.38852	0.61996	3
4	0.56287	4.6927	12.386	-0.00119	0.1852	0.9711	2.0068	6.5291	30.639	0.38669	0.57066	4
5	0.58401	4.8690	11.937	-0.00106	0.1995	0.9667	2.0068	6.5291	31.790	0.39499	0.57272	5
6	0.62470	5.2082	13.853	-0.00090	0.2280		2.4912	5.2596	27.393	0.38440	0.53331	6
7	0.63112	5.2617	13.712	-0.00086	0.2514		2.4912	5.2596	27.674	0.38825	0.54363	7
8	0.59666	4.9744	14.504	-0.00106	0.1963	0.9582	2.4912	5.2596	26.163	0.39038	0.55021	8
9	0.66383	5.5344	15.571	-0.00075	0.2994		2.9755	4.4035	24.371	0.38628	0.53327	9
10	0.65785	5.4846	15.713	-0.00076	0.2780		2.9755	4.4035	24.152	0.38526	0.52732	10
11	0.66901	5.5776	15.451	-0.00076	0.2732		2.9755	4.4035	24.561	0.37902	0.51876	11

21

12	0.65385	5.4512	15.809	-0.00076	0.2326		2.9755	4.4035	24.005	0.38231	0.51367	12
13	0.66631	5.5551	15.513	-0.00076	0.2469		2.9755	4.4035	24.462	0.37762	0.51308	13
14	0.68820	5.7376	17.464	-0.00068	0.3494		3.4598	3.7872	21.729	0.38447	0.52802	14
15	0.68310	5.6951	17.595	-0.00070	0.3298		3.4598	3.7872	21.568	0.38041	0.52199	15
16	0.69165	5.7664	17.377	-0.00070	0.3232		3.4598	3.7872	21.838	0.37882	0.51019	16
17	0.70276	5.8590	17.103	-0.00069	0.3105		3.4598	3.7872	22.189	0.38646	0.51410	17
18	0.67829	5.6550	17.720	-0.00070	0.2871		3.4598	3.7872	21.416	0.38594	0.51678	18
19	0.67733	5.6470	17.745	-0.00073	0.3026		3.4598	3.7872	21.386	0.39414	0.52440	19
20	0.69772	5.8170	17.226	-0.00067	0.2674		3.4598	3.7872	22.030	0.38306	0.50138	20
21	0.69457	5.7907	17.304	-0.00068	0.2503		3.4598	3.7872	21.930	0.37724	0.49920	21
22	0.70696	5.8940	19.381	-0.00064	0.3977		3.9441	3.3220	19.580	0.38331	0.52406	22
23	0.69793	5.8187	19.632	-0.00067	0.3564		3.9441	3.3220	19.330	0.37571	0.51130	23
24	0.69624	5.8046	19.679	-0.00065	0.3035		3.9441	3.3220	19.283	0.38222	0.48951	24
25	0.72187	6.0183	21.311	-0.00061	0.4445		4.4284	2.9588	17.807	0.38246	0.52244	25
26	0.73421	6.1212	23.245	-0.00057	0.4898		4.9127	2.6671	16.326	0.38179	0.52103	26
27	0.75050	6.2570	11.209	-0.00073	0.1950		2.4215	5.4110	33.856	0.27199	0.42182	27
28	0.75349	6.2819	13.397	-0.00069	0.2302		2.9059	4.5090	28.325	0.30100	0.44126	28
29	0.78347	6.5319	12.885	-0.00065	0.2096		2.9059	4.5090	29.452	0.28817	0.43584	29
30	0.77400	6.4529	15.216	-0.00062	0.2358		3.3902	3.8649	24.940	0.31700	0.44012	30
31					0.0865	0.9936	0.9686	13.527		0.35697		31
32	0.52095	4.3432	9.6889	-0.00173	0.1356	0.9844	1.4529	9.0179	39.167	0.35714	0.57116	32

Continued

 TABLE 1-1
 Physical Properties for Pure Components—Cont'd

					Phy	sical Consta	nts					
	E. Density of liquid 14.696 psia, 60°F		F.	G.	H.	I.			J.			
			ient of		tor of sia,	Ideal gas 14.696 psia, 60°F			Specific Heat 60°F, 14.696 psia Btu/(1 bm.°F)			
Number	Relative density (specific gravity) 60°F/60°F	l bm/gal.	gal./lb mole	Temperature coefficient of density, $1/^{\circ}F$	Acentric factor, @	Compressibility factor of real gas, Z 14.696 psia, 60°F	Relative density (specific gravity) Air = 1	ft³ gas/1 bm	ft ³ gas/gal. liquid	Cp, Ideal gas	Cp, Liquid	Number
33	0.60107	5.0112	11.197	-0.00112	0.1941	0.9699	1.9373	6.7636	33.894	0.35446	0.54533	33
34	0.62717	5.2288	10.731	-0.00105	0.2029	0.9665	1.9373	6.7636	35.366	0.33754	0.52980	34
35	0.60996	5.0853	11.033	-0.00106	0.2128	0.9667	1.9373	6.7636	34.395	0.35574	0.54215	35
36	0.60040	5.0056	11.209	-0.00117	0.1999	0.9700	1.9373	6.7636	33.856	0.37690	0.54839	36
37	0.64571	5.3834	13.028	-0.00089	0.2333		2.4215	5.4110	29.129	0.36351	0.51782	37
38	0.65799	5.4857	9.8605	-0.00101	0.2540	(0.969)	1.8677	7.0156	38.485	0.34347	0.54029	38
39	0.62723	5.2293	10.344	-0.00110	0.2007	(0.965)	1.8677	7.0156	36.687	0.34120	0.53447	39
40	0.68615	5.7205	11.908	-0.00082	0.1568		2.3520	5.5710	31.869	0.35072	0.51933	40
41	(0.41796)	(3.4842)	(7.473)		0.1949	0.9930	0.8990	14.574		0.39754		41
42	0.88448	7.3740	10.593	-0.00067	0.2093		2.6971	4.8581	35.824	0.24296	0.40989	42
43	0.87190	7.2691	12.676	-0.00059	0.2633		3.1814	4.1184	29.937	0.26370	0.40095	43

44	0.87168	7.2673	14.609	-0.00056	0.3027		3.6657	3.5744	25.976	0.27792	0.41139	44
45	0.88467	7.3756	14.394	-0.00052	0.3942		3.6657	3.5744	26.363	0.28964	0.41620	45
46	0.86875	7.2429	14.658	-0.00053	0.3257		3.6657	3.5744	25.889	0.27427	0.40545	46
47	0.86578	7.2181	14.708	-0.00056	0.3216		3.6657	3.5744	25.800	0.27471	0.40255	47
48	0.91108	7.5958	13.712	-0.00053	(0.2412)		3.5961	3.6435	27.675	0.27110	0.41220	48
49	0.86634	7.2228	16.641	-0.00055	0.3260		4.1500	3.1573	22.804	0.29170	0.42053	49
50	0.79626	6.6385	4.8267	-0.00066	0.5649		1.1063	11.843	78.622	0.32316	0.59187	50
51	0.79399	6.6196	6.9595	-0.00058	0.6438		1.5906	8.2372	54.527	0.33222	0.56610	51
52	0.78939	6.5812	4.2561		0.0484	0.9959	0.9671	13.548	89.163	0.24847		52
53	0.81802	6.8199	6.4532	-0.00583	0.2667	0.9943	1.5196	8.6229	58.807	0.19911		53
54	0.80144	6.6817	5.1005	-0.00157	0.0948	0.9846	1.1767	11.135	74.401	0.23827	0.50418	54
55	1.3974	11.650	5.4987		0.2548	0.9802	2.2118	5.9238	69.012	0.14804	0.32460	55
56	0.61832	5.1550	3.3037		0.2557	0.9877	0.5880	22.283	114.87	0.49677	1.1209	56
57	0.87476	7.2930	3.9713			1.0000	1.0000	13.103	95.557	0.23988		57
58	0.071070	0.59252	3.4022		-0.2202	1.0006	0.06960	188.25	111.54	3.4038		58
59	1.1421	9.5221	3.3605		0.0216	0.9992	1.1048	11.859	112.93	0.21892		59
60	0.80940	6.7481	4.1513		0.0372	0.9997	0.9672	13.546	91.413	0.24828		60
61	1.4244	11.875	5.9710		0.0878	(0.9875)	2.4482	5.3519	63.554	0.11377		61
62	1.00000	8.33712	2.1609	-0.00009	0.3443		0.62202	21.065	175.62	0.44457	0.99974	62
63	0.12510	1.0430	3.8376		0.	1.0006	0.1382	94.814	98.891	1.2404		63
64	0.85129	7.0973	5.1373	-0.00300	0.1259	0.9923	1.2589	10.408	73.869	0.19086		64

molecular weight. The authors proposed a set of tabulated properties that were generated by analyzing the physical properties of 26 condensates and crude oil systems. These generalized properties are given in Table 1-2.

TABLE 1-2 Generalized Physical Properties

Group	T _b (°R)	γ	K	M	$T_c(^{\circ}R)$	P _c (psia)	ω	V _c (ft ³ /lb)	Group
C ₆	607	0.690	12.27	84	923	483	0.250	0.06395	C ₆
C_7	658	0.727	11.96	96	985	453	0.280	0.06289	C_7
C_8	702	0.749	11.87	107	1,036	419	0.312	0.06264	C_8
C_9	748	0.768	11.82	121	1,085	383	0.348	0.06258	C_9
C_{10}	791	0.782	11.83	134	1,128	351	0.385	0.06273	C_{10}
C_{11}	829	0.793	11.85	147	1,166	325	0.419	0.06291	C_{11}
C_{12}	867	0.804	11.86	161	1,203	302	0.454	0.06306	C_{12}
C_{13}	901	0.815	11.85	175	1,236	286	0.484	0.06311	C_{13}
C_{14}	936	0.826	11.84	190	1,270	270	0.516	0.06316	C_{14}
C_{15}	971	0.836	11.84	206	1,304	255	0.550	0.06325	C_{15}
C_{16}	1,002	0.843	11.87	222	1,332	241	0.582	0.06342	C_{16}
C_{17}	1,032	0.851	11.87	237	1,360	230	0.613	0.06350	C_{17}
C_{18}	1,055	0.856	11.89	251	1,380	222	0.638	0.06362	C_{18}
C_{19}	1,077	0.861	11.91	263	1,400	214	0.662	0.06372	C_{19}
C_{20}	1,101	0.866	11.92	275	1,421	207	0.690	0.06384	C_{20}
C_{21}	1,124	0.871	11.94	291	1,442	200	0.717	0.06394	C_{21}
C_{22}	1,146	0.876	11.95	300	1,461	193	0.743	0.06402	C_{22}
C_{23}	1,167	0.881	11.95	312	1,480	188	0.768	0.06408	C_{23}
C_{24}	1,187	0.885	11.96	324	1,497	182	0.793	0.06417	C_{24}
C_{25}	1,207	0.888	11.99	337	1,515	177	0.819	0.06431	C_{25}
C_{26}	1,226	0.892	12.00	349	1,531	173	0.844	0.06438	C_{26}
C_{27}	1,244	0.896	12.00	360	1,547	169	0.868	0.06443	C_{27}
C_{28}	1,262	0.899	12.02	372	1,562	165	0.894	0.06454	C_{28}
C_{29}	1,277	0.902	12.03	382	1,574	161	0.915	0.06459	C_{29}
C_{30}	1,294	0.905	12.04	394	1,589	158	0.941	0.06468	C_{30}
C_{31}	1,310	0.909	12.04	404	1,603	143	0.897	0.06469	C_{31}
C ₃₂	1,326	0.912	12.05	415	1,616	138	0.909	0.06475	C_{32}

Group	T _b (°R)	γ	K	M	T _c (°R)	P _c (psia)	ω	V _c (ft ³ /lb)	Group
C ₃₃	1,341	0.915	12.05	426	1,629	134	0.921	0.06480	C ₃₃
C_{34}	1,355	0.917	12.07	437	1,640	130	0.932	0.06489	C_{34}
C ₃₅	1,368	0.920	12.07	445	1,651	127	0.942	0.06490	C_{35}
C ₃₆	1,382	0.922	12.08	456	1,662	124	0.954	0.06499	C_{36}
C ₃₇	1,394	0.925	12.08	464	1,673	121	0.964	0.06499	C_{37}
C ₃₈	1,407	0.927	12.09	475	1,683	118	0.975	0.06506	C_{38}
C_{39}	1,419	0.929	12.10	484	1,693	115	0.985	0.06511	C_{39}
C_{40}	1,432	0.931	12.11	495	1,703	112	0.997	0.06517	C_{40}
C_{41}	1,442	0.933	12.11	502	1,712	110	1.006	0.06520	C_{41}
C_{42}	1,453	0.934	12.13	512	1,720	108	1.016	0.06529	C_{42}
C_{43}	1,464	0.936	12.13	521	1,729	105	1.026	0.06532	C_{43}
C_{44}	1,477	0.938	12.14	531	1,739	103	1.038	0.06538	C_{44}
C_{45}	1,487	0.940	12.14	539	1,747	101	1.048	0.06540	C_{45}

TABLE 1-2 Generalized Physical Properties—Cont'd

Permission to publish by the Society of Petroleum Engineers of AIME. Copyright SPE-AIME.

Ahmed (1985) correlated Katz-Firoozabadi–tabulated physical properties with the number of carbon atoms of the fraction by using a regression model. The generalized equation has the following form:

$$\theta = a_1 + a_2 n + a_3 n^2 + a_4 n^3 + (a_5/n) \tag{1-1}$$

where

 θ = any physical property

n = number of carbon atoms, that is, 6, 7, ..., 45

 $a_1-a_5 = \text{coefficients of the equation and are given in Table 1-3}$

Undefined Petroleum Fractions

Nearly all naturally occurring hydrocarbon systems contain a quantity of heavy fractions that are not well defined and are not mixtures of discretely identified components. These heavy fractions are often lumped together and identified as the plus fraction, e.g., C_{7+} fraction.

A proper description of the physical properties of the plus fractions and other undefined petroleum fractions in hydrocarbon mixtures

TABLE 1-3 Coefficients of Equation 1-1

θ	a_1	a_2	a ₃	a_4	a_5
M	-131.11375	24.96156	-0.34079022	2.4941184×10^{-3}	468.32575
T _c , °R	915.53747	41.421337	-0.7586859	5.8675351×10^{-3}	-1.3028779×10^3
P _c , psia	275.56275	-12.522269	0.29926384	$-2.8452129 \times 10^{-3}$	1.7117226×10^{-3}
T _b , °R	434.38878	50.125279	-0.9097293	7.0280657×10^{-3}	-601.85651
T	-0.50862704	8.700211×10^{-2}	$-1.8484814 \times 10^{-3}$	1.4663890×10^{-5}	1.8518106
γ	0.86714949	3.4143408×10^{-3}	-2.839627×10^{-5}	2.4943308×10^{-8}	-1.1627984
V _c , ft ³ /lb	5.223458×10^{-2}	$7.87091369 \times 10^{-4}$	$-1.9324432 \times 10^{-5}$	1.7547264×10^{-7}	4.4017952×10^{-2}

is essential in performing reliable phase behavior calculations and compositional modeling studies. Frequently, a distillation analysis or a chromatographic analysis is available for this undefined fraction. Other physical properties, such as molecular weight and specific gravity, may also be measured for the entire fraction or for various cuts of it.

To use any of the thermodynamic property-prediction models, e.g., equations, of state, to predict the phase and volumetric behavior of complex hydrocarbon mixtures, one must be able to provide the acentric factor, along with the critical temperature and critical pressure, for both the defined and undefined (heavy) fractions in the mixture. The problem of how to adequately characterize these undefined plus fractions in terms of their critical properties and acentric factors has been long recognized in the petroleum industry.

Riazi and Daubert (1987) developed a simple two-parameter equation for predicting the physical properties of pure compounds and undefined hydrocarbon mixtures. The proposed generalized empirical equation is based on the use of the molecular weight M and specific gravity γ of the undefined petroleum fraction as the correlating parameters. Their mathematical expression has the following form:

$$\theta = a(M)^b \gamma^c EXP[d(M) + e\gamma + f(M)\gamma]$$
 (1-2)

where θ = any physical property

a-f = constants for each property as given in Table 1-4

 γ = specific gravity of the fraction

M = molecular weight

 T_c = critical temperature, ${}^{\circ}R$

 P_c = critical pressure, psia (Table 1-4)

 $T_b = boiling point temperature, °R$

 $V_c = critical volume, ft^3/lb$

TABLE 1-4 Correlation Constants for Equation 1-2

θ	a	b	c	d	e	f
$T_{c\prime}$ $^{\circ}R$	544.4	0.2998	1.0555	-1.3478×10^{-4}	-0.61641	0.0
P _c , psia	4.5203×10^4	-0.8063	1.6015	-1.8078×10^{-3}	-0.3084	0.0
$V_{\rm c} \ {\rm ft}^3/{\rm lb}$	1.206×10^{-2}	0.20378	-1.3036	-2.657×10^{-3}	0.5287	2.6012×10^{-3}
$T_{b\prime}\ ^{\circ}R$	6.77857	0.401673	-1.58262	3.77409×10^{-3}	2.984036	-4.25288×10^{-3}

Edmister (1958) proposed a correlation for estimating the acentric factor T of pure fluids and petroleum fractions. The equation, widely used in the petroleum industry, requires boiling point, critical temperature, and critical pressure. The proposed expression is given by the following relationship:

$$\omega = \frac{3[\log(p_c/14.70)]}{7[(T_c/T_b - 1)]} - 1 \tag{1-3}$$

where T = acentric factor

 p_c = critical pressure, psia T_c = critical temperature, ${}^{\circ}R$ T_b = normal boiling point, ${}^{\circ}R$

If the acentric factor is available from another correlation, the Edmister equation can be rearranged to solve for any of the three other properties (providing the other two are known).

The critical compressibility factor is another property that is often used in thermodynamic-property prediction models. It is defined as the component compressibility factor calculated at its critical point. This property can be conveniently computed by the real gas equation of state at the critical point, or

$$z_{c} = \frac{p_{c}V_{c}M}{RT_{c}} \tag{1-4}$$

where R = universal gas constant, 10.73 psia-ft³/lb-mol. °R

 $V_c = critical volume, ft^3/lb$

M = molecular weight

The accuracy of Equation 1-4 depends on the accuracy of the values of $p_{c\prime}$, $T_{c\prime}$ and V_c used in evaluating the critical compressibility factor. Table 1-5 presents a summary of the critical compressibility estimation methods.

TABLE 1-5	Critical	Compressibility	Estimation	Methods
-----------	----------	-----------------	------------	---------

Method	Year	\mathbf{z}_{c}	Equation No.
Haugen, Watson, and Ragatz	1959	$z_c = 1/(1.28 \omega + 3.41)$	1-5
Reid, Prausnitz, and Sherwood	1977	$z_c = 0.291 - 0.080 \omega$	1-6
Salerno et al.	1985	$z_c = 0.291 - 0.080 \ \omega - 0.016 \ \omega^2$	1-7
Nath	1985	$z_c = 0.2918 - 0.0928$	1-8

Example 1-1

Estimate the critical properties and the acentric factor of the heptanesplus fraction, i.e., C_{7+} , with a measured molecular weight of 150 and specific gravity of 0.78.

Solution

Step 1. Use Equation 1-2 to estimate T_c , p_c , V_c , and T_b :

- $T_c = 544.2 (150)^{0.2998} (0.78)^{1.0555} exp[-1.3478 \times 10^{-4} (150) 0.61641 (0.78) + 0] = 1139.4 \, {}^{\circ}R$
- $p_c = 4.5203 \times 10^4 (150)^{-0.8063} (0.78)^{1.6015} exp[-1.8078 \times 10^{-3} (150) 0.3084 (0.78) + 0] = 320.3 psia$
- $V_c = 1.206 \times 10^{-2} (150)^{0.20378} (0.78)^{-1.3036} exp[-2.657 \times 10^{-3} (150) + 0.5287 (0.78) = 2.6012 \times 10^{-3} (150) (0.78)] = 0.06035 ft^3/lb$
- $T_b = 6.77857 (150)^{0.401673} (0.78)^{-1.58262} exp[3.77409 \times 10^{-3} (150) + 2.984036 (0.78) 4.25288 \times 10^{-3} (150) (0.78)] = 825.26 \, {}^{\circ}R$

Step 2. Use Edmister's Equation (Equation 1-3) to estimate the acentric factor:

$$\omega = \frac{3[\log(320.3/14.7)]}{7[1139.4/825.26 - 1]} - 1 = 0.5067$$

SECTION 1.2 PROBLEMS

 The following is a list of the compositional analyses of different hydrocarbon systems. The compositions are expressed in terms of mol%.

Component	System #1	System #2	System #3	System #4
C_1	68.00	25.07	60.00	12.15
C_2	9.68	11.67	8.15	3.10
C_3	5.34	9.36	4.85	2.51
C_4	3.48	6.00	3.12	2.61
C_5	1.78	3.98	1.41	2.78
C_6	1.73	3.26	2.47	4.85
C ₇₊	9.99	40.66	20.00	72.00

Classify these hydrocarbon systems.

2. If a petroleum fraction has a measured molecular weight of 190 and a specific gravity of 0.8762, characterize this fraction by calculating the boiling point, critical temperature, critical pressure, and critical volume of the fraction. Use the Riazi and Daubert correlation.

3. Calculate the acentric factor and critical compressibility factor of the component in the above problem.

SECTION 1.3 REFERENCES

- T. Ahmed, Composition Modeling of Tyler and Mission Canyon Formation Oils with CO2 and Lean Gases, final report submitted to the Montana's on a New Track for Science (MONTS) program (Montana National Science Foundation Grant Program), 1985
- [2] W.C. Edmister, Applied Hydrocarbon Thermodynamic, Part 4: Compressibility Factors and Equations of State, Petroleum Refiner. 37 (1958) 173–179.
- [3] O.A. Haugen, K.M. Watson, R.A. Ragatz, Chemical Process Principles, 2nd ed., Wiley, New York, 1959.
- [4] D.L. Katz, A. Firoozabadi, Predicting Phase Behavior of Condensate/Crude-Oil Systems Using Methane Interaction Coefficients, JPT (1978) 1649–1655.
- [5] W.D. McCain, Heavy Components Control Reservoir Fluid Behavior, JPT (1994) 746–750.
- [6] J. Nath, Acentric Factor and Critical Volumes for Normal Fluids, Ind. Eng. Chem. Fundam. 21(3) (1985) 325–326.
- [7] R. Reid, J.M. Prausnitz, T. Sherwood, The Properties of Gases and Liquids, 3rd ed., McGraw-Hill, 1977.
- [8] M.R. Riazi, T.E. Daubert, Characterization Parameters for Petroleum Fractions, Ind. Eng. Chem. Res. 26(24) (1987) 755–759.
- [9] S. Salerno, et al., Prediction of Vapor Pressures and Saturated Volume, Fluid Phase Equilibria 27 (1985) 15–34.

Fundamentals of Rock Properties

The material of which a petroleum reservoir rock may be composed can range from very loose and unconsolidated sand to a very hard and dense sandstone, limestone, or dolomite. The grains may be bonded together with a number of materials, the most common of which are silica, calcite, and clay. Knowledge of the physical properties of the rock and the existing interaction between the hydrocarbon system and the formation is essential in understanding and evaluating the performance of a given reservoir.

Rock properties are determined by performing laboratory analyses on cores from the reservoir to be evaluated. The cores are removed from the reservoir environment, with subsequent changes in the core bulk volume, pore volume, reservoir fluid saturations, and, sometimes, formation wettability. The effect of these changes on rock properties may range from negligible to substantial, depending on characteristics of the formation and property of interest, and should be evaluated in the testing program.

Basically two main categories of core analysis tests are performed on core samples regarding physical properties of reservoir rocks. These are

Routine Core Analysis Tests

- Porosity
- Permeability
- Saturation

Special Tests

- Overburden pressure
- Capillary pressure
- Relative permeability
- Wettability
- Surface and interfacial tension

These rock property data are essential for reservoir engineering calculations as they directly affect both the quantity and the distribution of hydrocarbons and, when combined with fluid properties, control the flow of the existing phases (i.e., gas, oil, and water) within the reservoir.

SECTION 2.1 POROSITY

The porosity of a rock is a measure of the storage capacity (pore volume) that is capable of holding fluids. Quantitatively, the porosity is the ratio of the pore volume to the total volume (bulk volume). This important rock property is determined mathematically by the following generalized relationship:

$$\phi = \frac{pore\ volume}{bulk\ volume}$$

where $\phi = porosity$

As the sediments were deposited and the rocks were being formed during past geological times, some void spaces that developed became isolated from the other void spaces by excessive cementation. Therefore, many of the void spaces are interconnected while some of the pore spaces are completely isolated. This leads to two distinct types of porosity, namely,

- Absolute porosity
- Effective porosity

Absolute Porosity

The absolute porosity is defined as the ratio of the total pore space in the rock to that of the bulk volume. A rock may have considerable absolute porosity and yet have no conductivity to fluid for lack of pore interconnection. The absolute porosity is generally expressed mathematically by the following relationships:

$$\phi_a = \frac{\text{total pore volume}}{\text{bulk volume}}$$
 (2-1)

or

$$\varphi_{a} = \frac{bulk\ volume - grain\ volume}{bulk\ volume} \tag{2-2}$$

where ϕ_a = absolute porosity

Effective Porosity

The effective porosity is the percentage of *interconnected* pore space with respect to bulk volume, or

$$\phi = \frac{\text{interconnected pore volume}}{\text{bulk volume}}$$
 (2-3)

where ϕ = effective porosity

The effective porosity is the value that is used in all reservoir engineering calculations because it represents the interconnected pore space that contains the recoverable hydrocarbon fluids.

Porosity may be classified according to the mode of origin as original or induced.

The *original* porosity is that developed in the deposition of the material, while *induced* porosity is that developed by some geologic process subsequent to deposition of the rock. The intergranular porosity of sandstones and the intercrystalline and oolitic porosity of some limestones typify original porosity. Induced porosity is typified by fracture development as found in shales and limestones and by the slugs or solution cavities commonly found in limestones. Rocks having original porosity are more uniform in their characteristics than those in which a large part of the porosity is included. For direct quantitative measurement of porosity, reliance must be placed on formation samples obtained by coring.

Since effective porosity is the porosity value of interest to the petroleum engineer, particular attention should be paid to the methods used to determine porosity. For example, if the porosity of a rock sample was determined by saturating the rock sample 100% with a fluid of known density and then determining, by weighing, the increased weight due to the saturating fluid, this would yield an effective porosity measurement because the saturating fluid could enter only the interconnected pore spaces. On the other hand, if the rock sample was crushed with a mortar and pestle to determine the actual volume of the solids in the core sample, then an absolute porosity measurement would result because the identity of any isolated pores would be lost in the crushing process.

One important application of the effective porosity is its use in determining the original hydrocarbon volume in place. Consider a reservoir with an areal extent of A acres and an average thickness of h feet. The total bulk volume of the reservoir can be determined from the following expressions:

Bulk volume =
$$43,560 \text{ Ah}, \text{ ft}^3$$
 (2-4)

or

Bulk volume =
$$7,758$$
 Ah, bbl (2-5)

where A = areal extent, acres

h = average thickness

The reservoir pore volume PV can then be determined by combining Equations 2-4 and 2-5 with 2-3. Expressing the reservoir pore volume in cubic feet gives

$$PV = 43,560 \text{ Ah}\phi, \text{ ft}^3$$
 (2-6)

Expressing the reservoir pore volume in barrels gives

$$PV = 7,758 \text{ Ah}\phi, \text{ bbl}$$
 (2-7)

Example 2-1

An oil reservoir exists at its bubble-point pressure of 3,000 psia and temperature of 160°F. The oil has an API gravity of 42° and a gas-oil ratio of 600 scf/STB. The specific gravity of the solution gas is 0.65. The following additional data are available:

- Reservoir area = 640 acres
- Average thickness = 10 ft
- Connate water saturation = 0.25
- Effective porosity = 15%

Calculate the initial oil in place in STB.

Solution

Step 1. Determine the specific gravity of the stock-tank oil using the API gravity. The API gravity scale is related to the specific gravity (γ_0) by

$$^{\circ}$$
API = $\frac{141.5}{\gamma_0}$ - 131.5

Therefore,

$$\gamma_o = \frac{141.5}{42 + 131.5} = 0.8156$$

Step 2. Calculate the initial oil formation volume factor by applying Standing's equation:

$$B_0 = 0.9759 + 0.000120 \left[R_s \left(\frac{\gamma_g}{\gamma_o} \right)^{0.5} + 1.25 (T - 460) \right]^{1.2}$$

where B_0 = oil formation volume factor

 R_s = gas solubility

 γ_g = specific gravity of the solution gas

 γ_0 = specific gravity of the stock-tank oil

 $T = temperature, {}^{\circ}R$

This gives

$$B_0 = 0.9759 + 0.00012 \left[600 \left(\frac{0.65}{0.8156} \right)^{0.5} + 1.25(160) \right]^{1.2}$$

= 1,396 bbl/STB

Step 3. Calculate the pore volume from Equation 2-7:

Pore volume =
$$7758(640)(10)(0.15) = 7,447,680$$
 bbl

Step 4. Calculate the initial oil in place:

Initial oil in place =
$$12,412,800(1-0.25)/1.306 = 4,276,998$$
 STB

The reservoir rock may generally show large variations in porosity vertically but does not show very great variations in porosity parallel to the bedding planes. In this case, the arithmetic average porosity or the thickness-weighted average porosity is used to describe the average reservoir porosity. A change in sedimentation or depositional conditions, however, can cause the porosity in one portion of the reservoir to be greatly different from that in another area. In such cases, the areal-weighted average or the volume-weighted average porosity is used to characterize the average rock porosity. These averaging techniques are expressed mathematically in the following forms:

Arithmetic average
$$\phi = \Sigma \phi_i / n$$
 (2-8)

Thickness-weighted average
$$\phi = \Sigma \phi_i h_i / \Sigma h_i$$
 (2-9)

Areal-weighted average
$$\phi = \Sigma \phi_i A_i / \Sigma A_i$$
 (2-10)

Volumetric-weighted average
$$\phi = \Sigma \phi_i A_i h_i / \Sigma A_i h_i$$
 (2-11)

where n = total number of core samples

h_i = thickness of core sample i or reservoir area i

 ϕ_i = porosity of core sample i or reservoir area i

 A_i = reservoir area i

Example 2-2

Calculate the arithmetic average and thickness-weighted average from the following measurements:

Sample	Thickness, ft	Porosity, %
1	1.0	10
2	1.5	12
3	1.0	11
4	2.0	13
5	2.1	14
6	1.1	10

Solution

• Arithmetic average:

$$\varphi = \frac{10+12+11+13+14+10}{6} = 11.67\%$$

• Thickness-weighted average:

$$\begin{split} \varphi &= \frac{(1)(10) + (1.5)(12) + (1)(11) + (2)(13) + (2.1)(14) + (1.1)(10)}{1 + 1.5 + 1 + 2 + 2.1 + 1.1} \\ &= 12.11\% \end{split}$$

SECTION 2.2 SATURATION

Saturation is defined as that fraction, or percent, of the pore volume occupied by a particular fluid (oil, gas, or water). This property is expressed mathematically by the following relationship:

$$fluid\ saturation = \frac{total\ volume\ of\ fluid}{pore\ volume}$$

Applying this mathematical concept of saturation to each reservoir fluid gives

$$S_o = \frac{\text{volume of oil}}{\text{pore volume}}$$
 (2-12)

$$S_g = \frac{\text{volume of gas}}{\text{pore volume}}$$
 (2-13)

$$S_{w} = \frac{\text{volume of water}}{\text{pore volume}}$$
 (2-14)

where S_0 = oil saturation

 S_g = gas saturation

 $S_{\rm w}$ = water saturation

Thus, all saturation values are based on *pore volume* and not on gross reservoir volume.

The saturation of each individual phase ranges between 0 and 100%. By definition, the sum of the saturations is 100%; therefore,

$$S_g + S_o + S_w = 1.0$$
 (2-15)

The fluids in most reservoirs are believed to have reached a state of equilibrium and, therefore, will have become separated according to their density, that is, oil overlain by gas and underlain by water. In addition to the bottom (or edge) water, connate water will be distributed throughout the oil and gas zones. The water in these zones will have been reduced to some irreducible minimum. The forces retaining the water in the oil and gas zones are referred to as *capillary forces* because they are important only in pore spaces of capillary size.

Connate (interstitial) water saturation $S_{\rm wc}$ is important primarily because it reduces the amount of space available between oil and gas. It is generally not uniformly distributed throughout the reservoir but varies with permeability, lithology, and height above the free water table.

Another particular phase saturation of interest is called the *critical saturation* and it is associated with each reservoir fluid. The definition and significance of the critical saturation for each phase is described next.

Critical Oil Saturation, S_{oc}

For the oil phase to flow, the saturation of the oil must exceed a certain value, which is termed *critical oil saturation*. At this particular saturation, the oil remains in the pores and, for all practical purposes, will not flow.

Residual Oil Saturation, Sor

During the displacing process of the crude oil system from the porous media by water or gas injection (or encroachment), some remaining oil will be left that is quantitatively characterized by a saturation value that is larger than the *critical oil saturation*. This saturation value is called the *residual oil saturation*, S_{or}. The term *residual saturation* is usually associated

with the nonwetting phase when it is being displaced by a wetting phase.

Movable Oil Saturation, Som

Movable oil saturation S_{om} is another saturation of interest and is defined as the fraction of pore volume occupied by movable oil as expressed by the following equation:

$$S_{om} = 1 - S_{wc} - S_{oc}$$

where S_{wc} = connate water saturation S_{oc} = critical oil saturation

Critical Gas Saturation, S_{gc}

As the reservoir pressure declines below the bubble-point pressure, gas evolves from the oil phase and consequently the saturation of the gas increases as the reservoir pressure declines. The gas phase remains immobile until its saturation exceeds a certain saturation, called *critical gas saturation*, above which gas begins to move.

Critical Water Saturation, Swc

The critical water saturation, connate water saturation, and irreducible water saturation are extensively used interchangeably to define the maximum water saturation at which the water phase will remain immobile.

Average Saturation

Proper averaging of saturation data requires that the saturation values be weighted by both the interval *thickness* h_i and interval *porosity* ϕ . The average saturation of each reservoir fluid is calculated from the following equations:

$$S_{o} = \frac{\sum_{i=1}^{n} \phi_{i} h_{i} S_{oi}}{\sum_{i=1}^{n} \phi_{i} h_{i}}$$
(2-16)

$$S_{w} = \frac{\sum_{i=1}^{n} \phi_{i} h_{i} S_{wi}}{\sum_{i=1}^{n} \phi_{i} h_{i}}$$
(2-17)

$$S_{g} = \frac{\sum_{i=1}^{n} \varphi_{i} \ h_{i} \ S_{gi}}{\sum_{i=1}^{n} \varphi_{i} \ h_{i}}$$
(2-18)

where the subscript i refers to any individual measurement and h_i represents the depth interval to which ϕ_i , S_{oi} , S_{gi} , and S_{wi} apply.

Example 2-3Calculate average oil and connate water saturation from the following measurements:

Sample	h _i , ft	ф,%	S ₀ ,%	S _{wc} , %
1	1.0	10	75	25
2	1.5	12	77	23
3	1.0	11	79	21
4	2.0	13	74	26
5	2.1	14	78	22
6	1.1	10	75	25

Solution

Construct the following table and calculate the average saturation for the oil and water phase:

Sample	h _i , ft	ф	фh	So	S _o φh	S_{wc}	S _{wc} φh
1	1.0	0.10	0.100	0.75	0.0750	0.25	0.0250
2	1.5	0.12	0.180	0.77	0.1386	0.23	0.0414
3	1.0	0.11	0.110	0.79	0.0869	0.21	0.0231
4	2.0	0.13	0.260	0.74	0.1924	0.26	0.0676
5	2.1	0.14	0.294	0.78	0.2293	0.22	0.0647
6	1.1	0.10	0.110	0.75	0.0825	0.25	0.0275
			1.054		0.8047		0.2493

Calculate average oil saturation by applying Equation 2-16:

$$S_o = \frac{0.8047}{1.054} = 0.7635$$

Calculate average water saturation by applying Equation 2-17:

$$S_{\rm w} = \frac{0.2493}{1.054} = 0.2365$$

SECTION 2.3 WETTABILITY

Wettability is defined as the tendency of one fluid to spread on or adhere to a solid surface in the presence of other immiscible fluids. The concept of wettability is illustrated in Figure 2-1. Small *drops* of three liquids—mercury, oil, and water—are placed on a clean glass plate. The three droplets are then observed from one side as illustrated in Figure 2-1. It is noted that the mercury retains a spherical shape, the oil droplet develops an approximately hemispherical shape, but the water tends to spread over the glass surface.

The tendency of a liquid to spread over the surface of a solid is an indication of the *wetting* characteristics of the liquid for the solid. This spreading tendency can be expressed more conveniently by measuring the angle of contact at the *liquid-solid* surface. This angle, which is always measured through the liquid to the solid, is called the *contact angle* θ .

The contact angle θ has achieved significance as a measure of wettability. As shown in Figure 2-1, as the contact angle decreases, the wetting characteristics of the liquid increase. Complete wettability would be evidenced by a zero contact angle, and complete nonwetting would be evidenced by a contact angle of 180° . There have been various definitions of *intermediate* wettability but, in much of the published literature, contact angles of 60° to 90° will tend to repel the liquid.

The wettability of reservoir rocks to the fluids is important in that the distribution of the fluids in the porous media is a function of wettability. Because of the attractive forces, the wetting phase tends to occupy the smaller pores of the rock and the nonwetting phase occupies the more open channels.

SECTION 2.4 SURFACE AND INTERFACIAL TENSION

In dealing with multiphase systems, it is necessary to consider the effect of the forces at the interface when two immiscible fluids are in contact. When these two fluids are liquid and gas, the term *surface tension* is

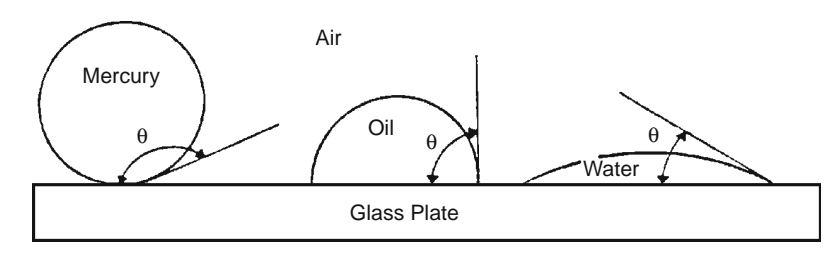


FIGURE 2-1 Illustration of wettability.

used to describe the forces acting on the interface. When the interface is between two liquids, the acting forces are called *interfacial tension*.

Surfaces of liquids are usually blanketed with what acts as a thin film. Although this apparent film possesses little strength, it nevertheless acts like a thin membrane and resists being broken. This is believed to be caused by attraction between molecules within a given system. All molecules are attracted one to the other in proportion to the product of their masses and inversely as the squares of the distance between them.

Consider the two immiscible, fluids, air (or gas) and water (or oil), as shown schematically in Figure 2-2. A liquid molecule, which is remote from the interface, is surrounded by other liquid molecules, thus having a resulting net attractive force on the molecule of zero. A molecule at the interface, however, has a force acting on it from the air (gas) molecules lying immediately above the interface and from liquid molecules lying below the interface.

Resulting forces are unbalanced and give rise to surface tension. The unbalanced attraction force between the molecules creates a membrane-like surface with a measurable tension, i.e., surface tension. As a matter of fact, if carefully placed, a needle will float on the surface of the liquid, supported by the thin membrane even though it is considerably more dense than the liquid.

The surface or interfacial tension has the units of force per unit of length, e.g., dynes/cm, and is usually denoted by the symbol σ .

If a glass capillary tube is placed in a large open vessel containing water, the combination of surface tension and wettability of tube to water will cause water to rise in the tube above the water level in the container outside the tube as shown in Figure 2-3.

The water will rise in the tube until the total force acting to pull the liquid upward is balanced by the weight of the column of liquid being

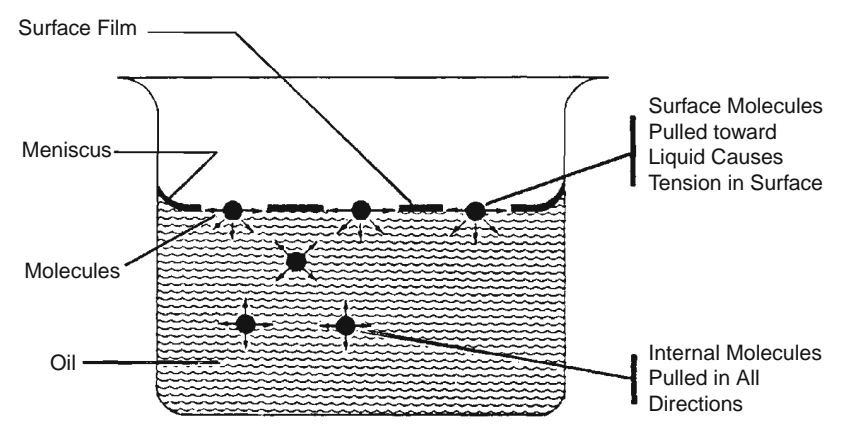
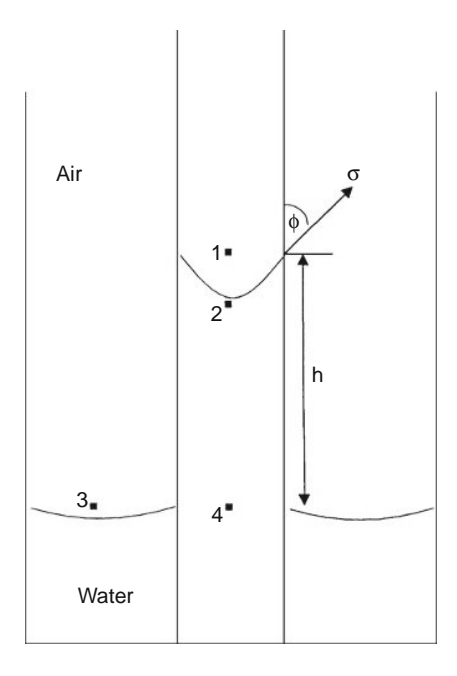


FIGURE 2-2 Illustration of surface tension. (After Clark, N.J., Elements of Petroleum Reservoirs, SPE, 1969.)

FIGURE 2-3 Pressure relations in capillary tubes.



supported in the tube. Assuming the radius of the capillary tube is r, the total upward force $F_{\rm up}$, which holds the liquid up, is equal to the force per unit length of surface times the total length of surface, or

$$F_{up} = (2\pi r)(\sigma_{gw})(\cos \theta) \tag{2-19}$$

where σ_{gw} = surface tension between air (gas) and water (oil), dynes/cm

 θ = contact angle r = radius, cm

The upward force is counteracted by the weight of the water, which is equivalent to a downward force of mass times acceleration, or

$$F_{down} = \pi r^2 h(\rho_w - \rho_{air})g \tag{2-20}$$

where h = height to which the liquid is held, cm

 $g = acceleration due to gravity, cm/sec^2$

 $\rho_{\rm w}$ = density of water, gm/cm³

 ρ_{air} = density of gas, gm/cm³

Because the density of air is negligible in comparison with the density of water, Equation 2-20 is reduced to

$$F_{down} = \pi r^2 \rho_w g \tag{2-21}$$

Equating Equation 2-19 with 2-21 and solving for the surface tension gives

$$\sigma_{gw} = \frac{rh\rho_w g}{2\cos\theta} \tag{2-22}$$

The generality of Equations 2-19 through 2-22 will not be lost by applying them to the behavior of two liquids, i.e., water and oil. Because the density of oil is not negligible, Equation 2-22 becomes

$$\sigma_{\text{ow}} = \frac{\text{rhg}(\rho_{\text{w}} - \rho_{\text{o}})}{2\cos\theta}$$
 (2-23)

where ρ_0 = density of oil, gm/cm³

 σ_{ow} = interfacial tension between the oil and the water, dynes/cm

SECTION 2.5 CAPILLARY PRESSURE

The capillary forces in a petroleum reservoir are the result of the combined effect of the surface and interfacial tensions of the rock and fluids, the pore size and geometry, and the wetting characteristics of the system. Any curved surface between two immiscible fluids has the tendency to contract into the smallest possible area per unit volume. This is true whether the fluids are oil and water, water and gas (even air), or oil and gas. When two immiscible fluids are in contact, a discontinuity in pressure exists between the two fluids, which depends upon the curvature of the interface separating the fluids. We call this pressure difference the *capillary pressure* and it is referred to by p_c.

The displacement of one fluid by another in the pores of a porous medium is either aided or opposed by the surface forces of capillary pressure. As a consequence, in order to maintain a porous medium partially saturated with nonwetting fluid and while the medium is also exposed to wetting fluid, it is necessary to maintain the pressure in the nonwetting fluid at a value greater than that in the wetting fluid.

Denoting the pressure in the wetting fluid by $p_{\rm w}$ and that in the non-wetting fluid by $p_{\rm nw}$, the capillary pressure can be expressed as

$$\label{eq:capillary pressure} \begin{split} \text{Capillary pressure} &= (\text{pressure of the nonwetting phase}) \\ &- (\text{pressure of the wetting phase}) \\ p_c &= p_{nw} - p_w \end{split} \tag{2-24}$$

That is, the pressure excess in the nonwetting fluid is the capillary pressure, and this quantity is a function of saturation. This is the defining equation for capillary pressure in a porous medium.

There are three types of capillary pressure:

- Water-oil capillary pressure (denoted P_{cwo}).
- Gas-oil capillary pressure (denoted P_{cgo}).
- Gas-water capillary pressure (denoted P_{cgw}).

Applying the mathematical definition of the capillary pressure as expressed by Equation 2-24, the three types of capillary pressure can be written as

$$\begin{aligned} p_{cwo} &= p_o - p_w \\ p_{cgo} &= p_g - p_o \\ p_{cgw} &= p_g - p_w \end{aligned}$$

where p_g , p_o , and p_w represent the pressure of gas, oil, and water, respectively.

If all the three phases are continuous, then

$$p_{cgw} = p_{cgo} + p_{cwo}$$

Referring to Figure 2-3, the pressure difference across the interface between points 1 and 2 is essentially the capillary pressure, i.e.,

$$p_{c} = p_{1} - p_{2} \tag{2-25}$$

The pressure of the water phase at point 2 is equal to the pressure at point 4 minus the head of the water, or

$$p_2 = p_4 - gh\rho_w \tag{2-26}$$

The pressure just above the interface at point 1 represents the pressure of the air and is given by

$$p_1 = p_3 - gh\rho_{air} \tag{2-27}$$

It should be noted that the pressure at point 4 within the capillary tube is the same as that at point 3 outside the tube. Subtracting Equation 2-26 from 2-27 gives

$$p_{c}=gh(\rho_{w}-\rho_{air})=gh\Delta\rho \tag{2-28}$$

where $\Delta \rho$ is the density difference between the wetting and nonwetting phase. The density of the air (gas) is negligible in comparison with the water density.

In practical units, Equation 2-28 can be expressed as

$$p_c = \left(\frac{h}{144}\right)\!\Delta\rho$$

where p_c = capillary pressure, psi

h = capillary rise, ft

 $\Delta \rho$ = density difference, lb/ft³

In the case of an oil-water system, Equation 2-28 can be written as

$$p_c = gh(\rho_w - \rho_o) = gh\Delta\rho \tag{2-29}$$

and in practical units as

$$p_c = \left(\frac{h}{144}\right)(\rho_w - \rho_o)$$

The capillary pressure equation can be expressed in terms of the surface and interfacial tension by combining Equations 2-28 and 2-29 with Equations 2-22 and 2-23 to give

• Gas-Liquid System.

$$P_{c} = \frac{2\sigma_{gw}(\cos\theta)}{r}$$
 (2-30)

and

$$h = \frac{2\sigma_{gw}(\cos\theta)}{rg(\rho_w - \rho_{gas})}$$
 (2-31)

where ρ_w = water density, gm/cm³

 σ_{gw} = gas-water surface tension, dynes/cm

r = capillary radius, cm

 θ = contact angle

h = capillary rise, cm

 $g = acceleration due to gravity, cm/sec^2$

 p_c = capillary pressure, dynes/cm²

• Oil-Water System.

$$p_{c} = \frac{2\sigma_{ow}(\cos\theta)}{r}$$
 (2-32)

and

$$h = \frac{2\sigma_{wo}(\cos\theta)}{rg(\rho_w - \rho_o)}$$
 (2-33)

where σ_{wo} is the water-oil interfacial tension.

Example 2-4

Calculate the pressure difference, i.e., capillary pressure, and capillary rise in an oil-water system from the following data:

$$\begin{array}{ll} \theta = 30^{\circ} & \rho_w = 1.0 \ gm/cm^3 & \rho_o = 0.75 \ gm/cm^3 \\ r = 10^{-4} \ cm & \sigma_{ow} = 25 \ dynes/cm \end{array}$$

Solution

Step 1. Apply Equation 2-32 to give

$$p_c = \frac{(2)(25)(\cos 30^\circ)}{0.0001} = 4.33 \times 10^5 \text{ dynes/cm}^2$$

Since 1 dyne/cm² = 1.45×10^{B5} psi,

$$p_{c} = 6.28 \text{ psi}$$

This result indicates that the oil-phase pressure is 6.28 psi higher than the water-phase pressure.

Step 2. Calculate the capillary rise by applying Equation 2-33.

$$h = \frac{(2)(25)(\cos 30^\circ)}{(0.0001)(980.7)(1.0 - 0.75)} = 1766 \text{ cm} = 75.9 \text{ ft}$$

Capillary Pressure of Reservoir Rocks

The interfacial phenomena just described for a single capillary tube also exist when bundles of interconnected capillaries of varying sizes exist in a porous medium. The capillary pressure that exists within a porous medium between two immiscible phases is a function of the interfacial tensions and the average size of the capillaries, which, in turn, control the curvature of the interface. In addition, the curvature is also a function of the saturation distribution of the fluids involved.

Laboratory experiments have been developed to simulate the displacing forces in a reservoir in order to determine the magnitude of the capillary forces in a reservoir and, thereby, determine the fluid saturation distributions and connate water saturation. One such experiment is called the *restored capillary pressure technique*, which was developed primarily to determine the magnitude of the connate water saturation. A diagrammatic sketch of this equipment is shown in Figure 2-4.

Briefly, this procedure consists of saturating a core 100% with the reservoir water and then placing the core on a porous membrane, which is saturated 100% with water and is permeable to the water only, under the pressure drops imposed during the experiment. Air is then admitted into the core chamber and the pressure is increased until a small amount of water is displaced through the porous, semipermeable membrane into the graduated cylinder. Pressure is held constant until no more water is displaced, which may require several days or even several weeks, after

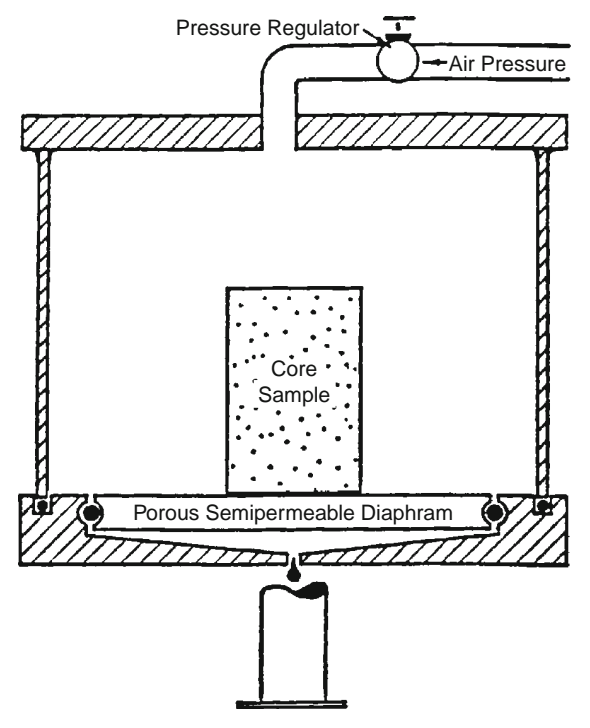


FIGURE 2-4 Capillary pressure equipment. (After Cole, F., 1969.)

which the core is removed from the apparatus and the water saturation determined by weighing. The core is then replaced in the apparatus, the pressure is increased, and the procedure is repeated until the water saturation is reduced to a minimum.

The data from such an experiment are shown in Figure 2-5. Since the pressure required to displace the wetting phase from the core is exactly equal to the capillary forces holding the remaining water within the core after equilibrium has been reached, the pressure data can be plotted as capillary pressure data. Two important phenomena can be observed in Figure 2-5. First, a finite capillary pressure at 100% water saturation is necessary to force the nonwetting phase into a capillary filled with the wetting phase. This minimum capillary pressure is known as the displacement pressure, p_d.

If the largest capillary opening is considered as circular with a radius of r, the pressure needed for forcing the nonwetting fluid out of the core is

$$P_c = \frac{2\sigma(\cos\,\theta)}{r}$$

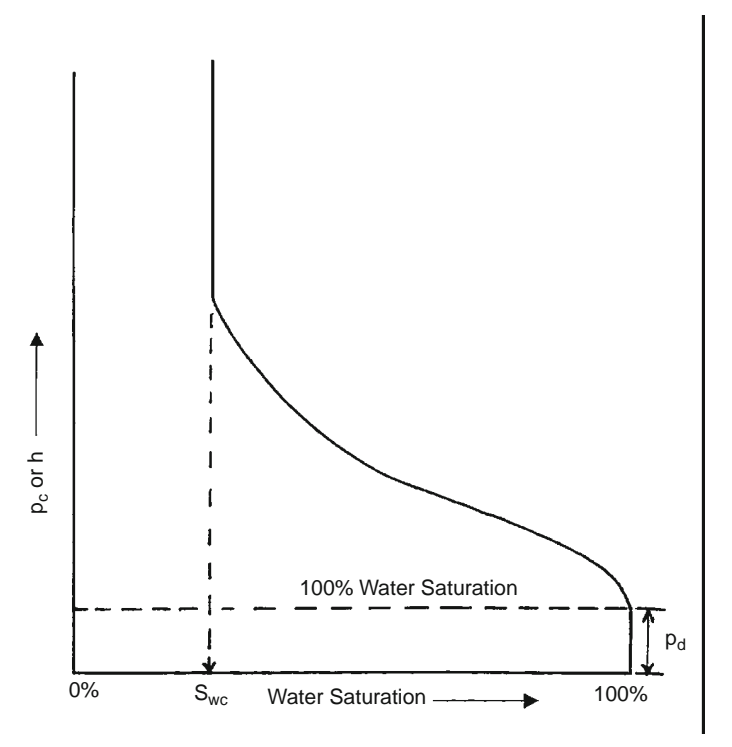


FIGURE 2-5 Capillary pressure curve.

This is the minimum pressure that is required to displace the wetting phase from the largest capillary pore because any capillary of smaller radius will require a higher pressure.

As the wetting phase is displaced, the second phenomenon of any immiscible displacement process is encountered, that is, reaching some finite minimum irreducible saturation. This irreducible water saturation is referred to as *connate water*.

It is possible from the capillary pressure curve to calculate the average size of the pores making up a stated fraction of the total pore space. Let p_c be the average capillary pressure for the 10% between saturation of 40% and 50%. The average capillary radius is obtained from

$$r = \frac{2\sigma(\cos\,\theta)}{p_c}$$

This equation may be solved for r providing that the interfacial tension σ and the angle of contact θ may be evaluated.

Figure 2-6 is an example of typical oil-water capillary pressure curves. In this case, capillary pressure is plotted versus water saturation for four

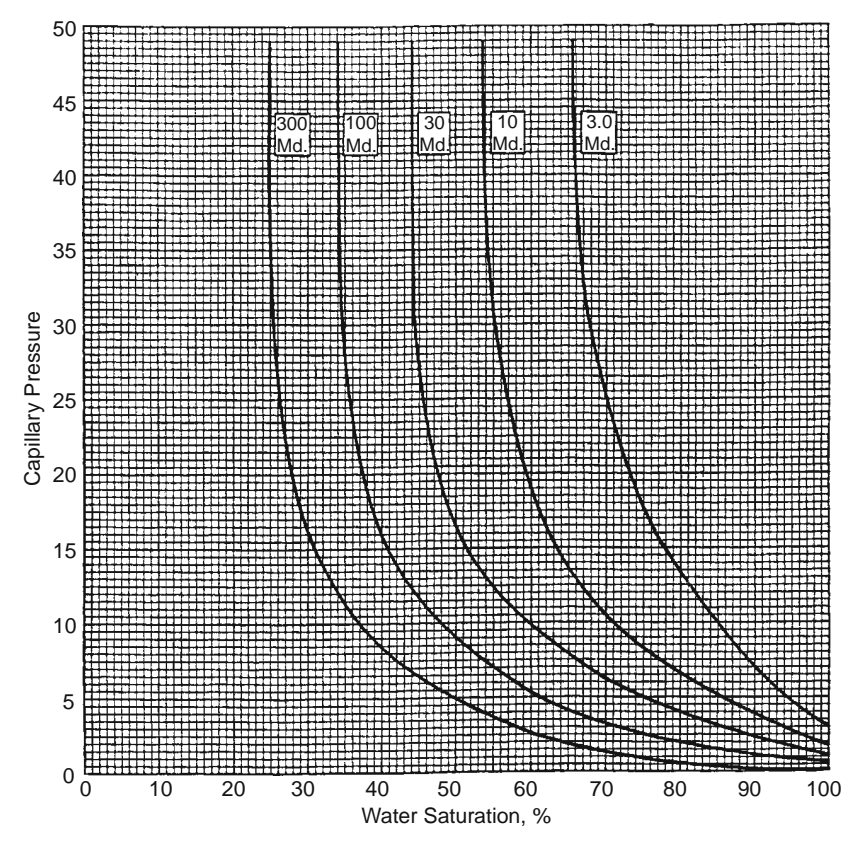


FIGURE 2-6 Variation of capillary pressure with permeability.

rock samples with permeabilities increasing from k_1 to k_4 . It can be seen that, for decreases in permeability, there are corresponding increases in capillary pressure at a constant value of water saturation. This is a reflection of the influence of pore size since the smaller-diameter pores will invariably have the lower permeabilities. Also, as would be expected, the capillary pressure for any sample increases with decreasing water saturation, another indication of the effect of the radius of curvature of the water-oil interface.

Capillary Hysteresis

It is generally agreed that the pore spaces of reservoir rocks were originally filled with water, after which oil moved into the reservoir, displacing some of the water and reducing the water to some residual saturation. When discovered, the reservoir pore spaces are filled with a connate-water saturation and an oil saturation. All laboratory

experiments are designed to duplicate the saturation history of the reservoir. The process of generating the capillary pressure curve by displacing the wetting phase, i.e., water, with the nonwetting phase (such as with gas or oil) is called the *drainage process*.

This drainage process establishes the fluid saturations found when the reservoir is discovered. The other principal flow process of interest involves reversing the drainage process by displacing the nonwetting phase (such as with oil) with the wetting phase, (e.g., water). This displacing process is termed the *imbibition process* and the resulting curve is termed the *capillary pressure imbibition curve*. The process of *saturating* and *desaturating* a core with the nonwetting phase is called *capillary hysteresis*. Figure 2-7 shows typical drainage and imbibition capillary pressure curves. The two capillary pressure-saturation curves are not the same.

This difference in the saturating and desaturating of the capillary-pressure curves is closely related to the fact that the advancing and receding contact angles of fluid interfaces on solids are different. Frequently, in natural crude oil-brine systems, the contact angle or wettability may change with time. Thus, if a rock sample that has been

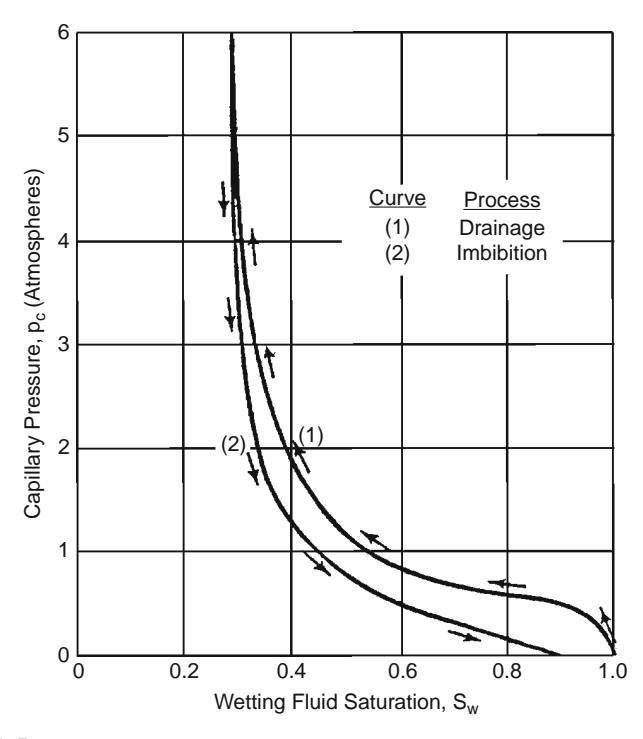


FIGURE 2-7 Capillary pressure hysteresis.

thoroughly cleaned with volatile solvents is exposed to crude oil for a period of time, it will behave as though it were oil wet. But if it is exposed to brine after cleaning, it will appear water wet. At the present time, one of the greatest unsolved problems in the petroleum industry is that of wettability of reservoir rock.

Another mechanism, which was proposed by McCardell (1955), to account for capillary hysteresis is called the *ink-bottle effect*. This phenomenon can be easily observed in a capillary tube having variations in radius along its length. Consider a capillary tube of axial symmetry having roughly sinusoidal variations in radius. When such a tube has its lower end immersed in water, the water will rise in the tube until the hydrostatic fluid head in the tube becomes equal to the capillary pressure. If the tube is then lifted to a higher level in the water, some water will drain out, establishing a new equilibrium level in the tube.

When the meniscus is advancing and it approaches a constriction, it *jumps* through the neck, whereas when receding, it halts without passing through the neck. This phenomenon explains why a given capillary pressure corresponds to a higher saturation on the drainage curve than on the imbibition curve.

Initial Saturation Distribution in a Reservoir

An important application of the concept of capillary pressures pertains to the fluid distribution in a reservoir prior to its exploitation. The capillary pressure-saturation data can be converted into height-saturation data by arranging Equation 2-29 and solving for the height h above the free-water level.

$$h = \frac{144 p_c}{\Delta \rho} \tag{2-34}$$

where p_c = capillary pressure, psia

 $\Delta \rho$ = density difference between the wetting and nonwetting phase, lb/ft³

h = height above the free-water level, ft

Figure 2-8 shows a plot of the water saturation distribution as a function of distance from the free-water level in an oil-water system.

It is essential at this point to introduce and define four important concepts:

- Transition zone.
- Water-oil contact (WOC).
- Gas-oil contact (GOC).
- Free-water level (FWL).

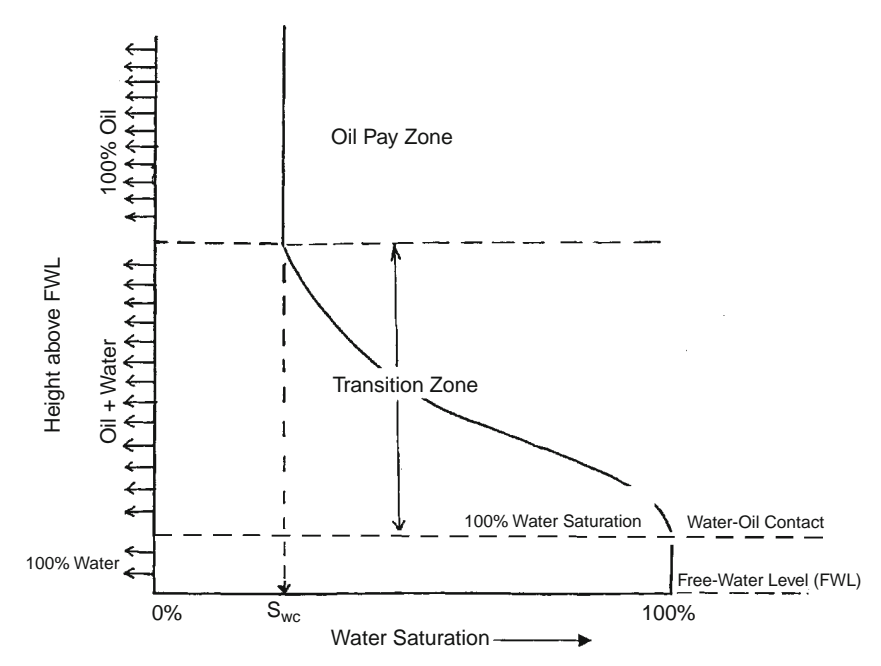


FIGURE 2-8 Water saturation profile.

Figure 2-9 illustrates an idealized gas, oil, and water distribution in a reservoir. The figure indicates that the saturations are gradually changing from 100% water in the water zone to irreducible water saturation some vertical distance above the water zone. This vertical area is referred to as the *transition zone*, which must exist in any reservoir where there is a bottom water table. The transition zone is then defined as the vertical thickness over which the water saturation ranges from 100% saturation to irreducible water saturation $S_{\rm wc}$. The important concept to be gained from Figure 2-9 is that there is no abrupt change from 100% water to maximum oil saturation. The creation of the oil-water transition zone is one of the major effects of capillary forces in a petroleum reservoir.

Similarly, the total liquid saturation (i.e., oil and water) is smoothly changing from 100% in the oil zone to the connate water saturation in the gas cap zone. A similar transition exists between the oil and gas zone. Figure 2-8 serves as a definition of what is meant by gas-oil and water-oil contacts. The WOC is defined as the "uppermost depth in the reservoir where a 100% water saturation exists." The GOC is defined as the "minimum depth at which a 100% liquid, i.e., oil + water, saturation exists in the reservoir."

Section A of Figure 2-10 shows a schematic illustration of a core that is represented by five different pore sizes and completely saturated with

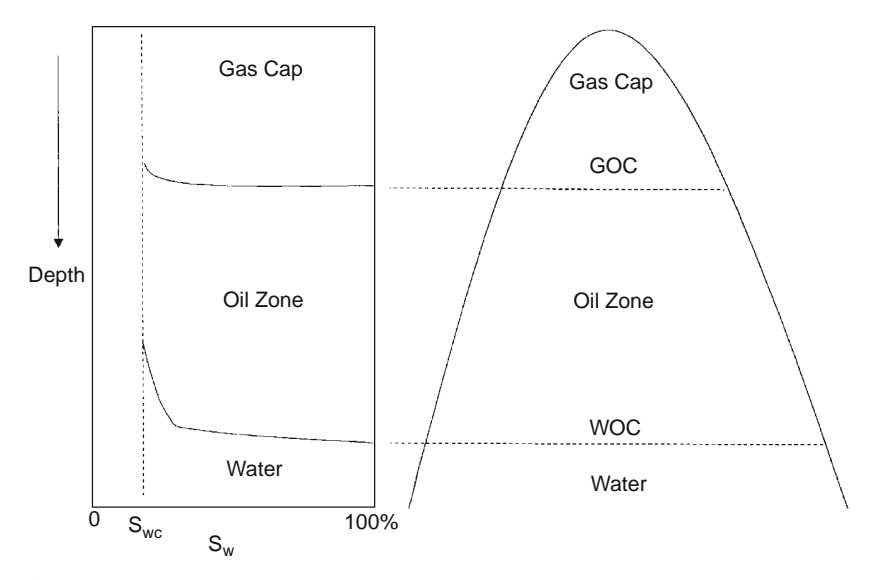


FIGURE 2-9 Initial saturation profile in a combination-drive reservoir.

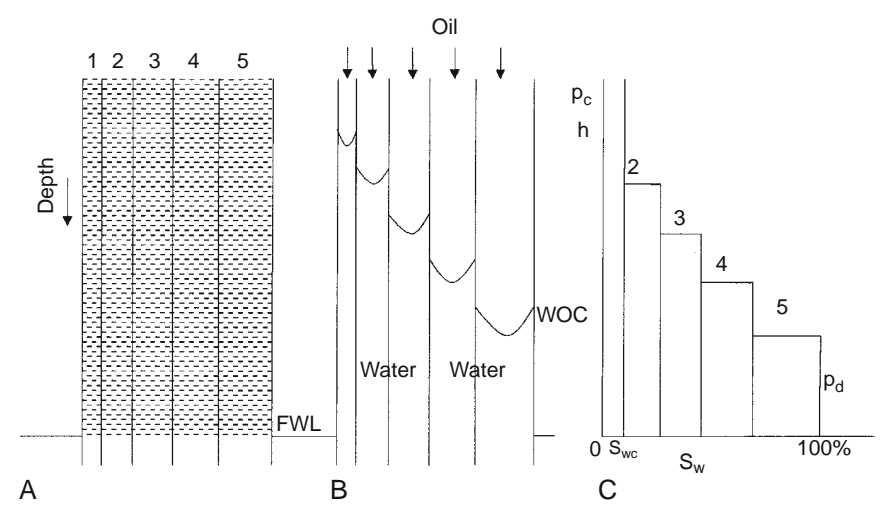


FIGURE 2-10 Relationship between saturation profile and pore-size distribution.

water, i.e., wetting phase. Assume that we subject the core to oil (the nonwetting phase) with increasing pressure until some water is displaced from the core, i.e., displacement pressure p_d . This water displacement will occur from the largest pore size. The oil pressure will have to increase to displace the water in the second largest pore. This sequential process is shown in sections B and C of Figure 2-10.

It should be noted that there is a difference between the free-water level (FWL) and the depth at which 100% water saturation exists. From a reservoir engineering standpoint, the free-water level is defined by *zero capillary pressure*. Obviously, if the largest pore is so large that there is no capillary rise in this size pore, then the free-water level and 100% water saturation level, i.e., WOC, will be the same. This concept can be expressed mathematically by the following relationship:

$$FWL = WOC + \frac{144 p_d}{\Delta \rho}$$
 (2-35)

where p_d = displacement pressure, psi

 $\Delta \rho$ = density difference, lb/ft³

FWL = free-water level, ft

WOC = water-oil contact, ft

Example 2-5

The reservoir capillary pressure-saturation data of the Big Butte Oil Reservoir is shown graphically in Figure 2-11. Geophysical log interpretations and core analysis establish the WOC at 5023 ft. The following additional data are available:

- Oil density = 43.5 lb/ft^3
- Water density = 64.1 lb/ft^3
- Interfacial tension = 50 dynes/cm

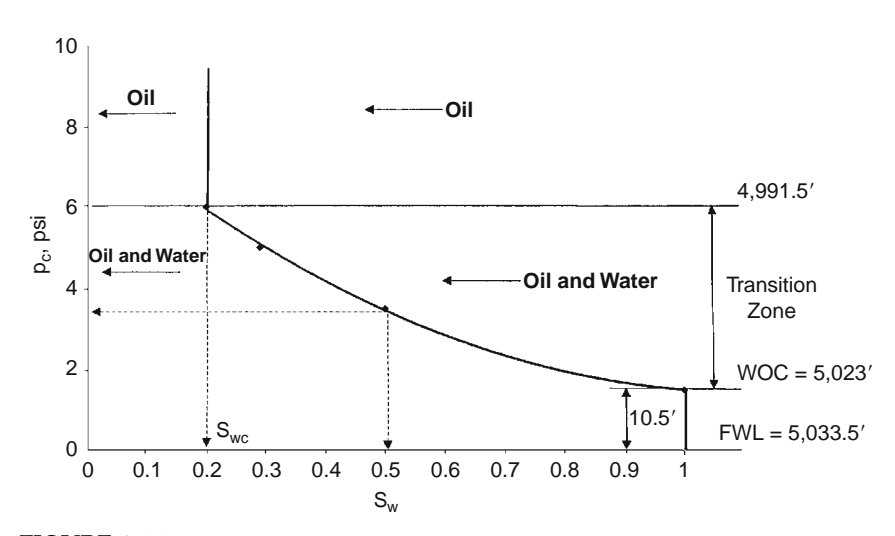


FIGURE 2-11 Capillary pressure-saturation data.

Calculate

- Connate-water saturation (S_{wc})
- Depth to FWL
- Thickness of the transition zone
- Depth to reach 50% water saturation

Solution

- a. From Figure 2-11, connate-water saturation is 20%.
- b. Applying Equation 2-35 with a displacement pressure of 1.5 psi gives

$$FWL = 5,023 + \frac{(144)(1.5)}{(64.1 - 43.5)} = 5,033.5 \text{ ft}$$

c. Thickness of transition zone =
$$\frac{144(6.0 - 1.5)}{(64.1 - 43.5)}$$
 = 31.5 ft

d. P_c at 50% water saturation = 3.5 psia Equivalent height above the FWL = (144) (3.5)/(64.1 – 432.5) = 24.5 ft Depth to 50% water saturation = 5,033.5 – 24.5 = 5,009 ft

This example indicates that only oil will flow in the interval between the top of the pay zone and depth of 4,991.5 ft. In the transition zone, i.e., the interval from 4,991.5 ft to the WOC, oil production would be accompanied by simultaneous water production.

It should be pointed out that the thickness of the transition zone may range from a few feet to several hundred feet in some reservoirs. Recalling the capillary rise equation, i.e., height above FWL,

$$h=\frac{2\sigma(\,cos\,\varphi)}{rg\Delta\rho}$$

This relationship suggests that the height above FWL increases with decreasing the density difference $\Delta \rho$.

From a practical standpoint, this means that, in a gas reservoir having a gas-water contact, the thickness of the transition zone will be a minimum since $\Delta \rho$ will be large. Also, if all other factors remain unchanged, a low API gravity oil reservoir with an oil-water contact will have a longer transition zone than a high API gravity oil reservoir. Cole (1969) illustrated this concept graphically in Figure 2-12.

The previous expression also shows that, as the radius of the pore r increases, the volume of h decreases. Therefore, a reservoir rock system with small pore sizes will have a longer transition zone than a reservoir rock system comprising large pore sizes.

The reservoir pore size can often be related approximately to permeability, and where this applies, it can be stated that high permeability

FIGURE 2-12 Variation of transition zone with fluid gravity. (After Cole, F., 1969.)

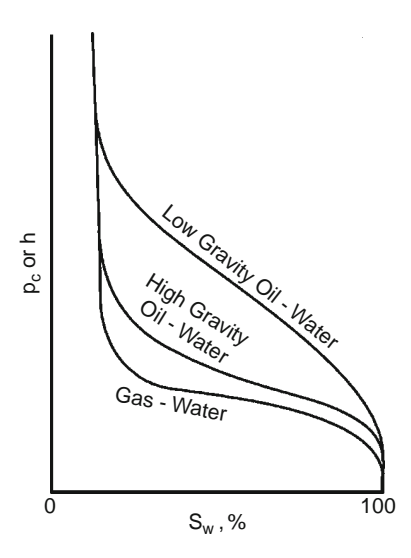
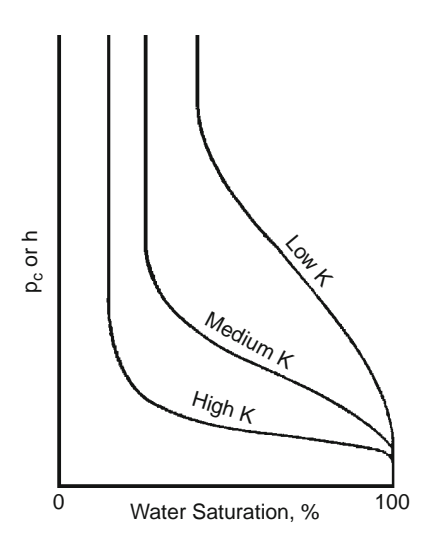


FIGURE 2-13 Variation of transition zone with permeability.



reservoirs will have shorter transition zones than low permeability reservoirs as shown graphically in Figure 2-13. As shown by Cole (Figure 2-14), a tilted water-oil contact could be caused by a change in permeability across the reservoir. It should be emphasized that the factor responsible for this change in the location of the water-oil contact is actually a change in the size of the pores in the reservoir rock system.

The previous discussion of capillary forces in reservoir rocks has assumed that the reservoir pore sizes, i.e., permeabilities, are essentially uniform. Cole (1969) discussed the effect of reservoir nonuniformity on

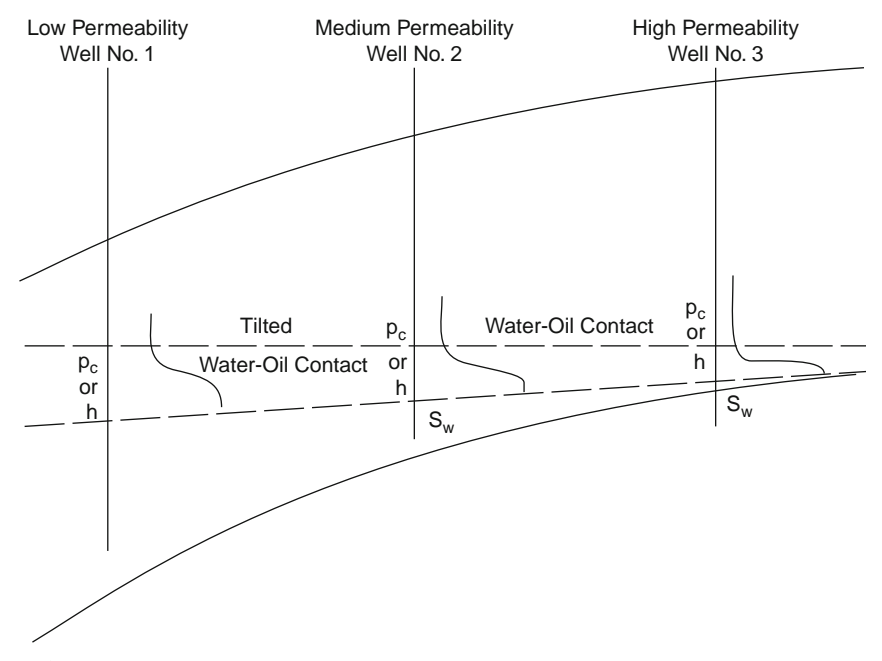


FIGURE 2-14 Tilted WOC. (After Cole, F., 1969.)

the distribution of the fluid saturation through the formation. Figure 2-15 shows a hypothetical reservoir rock system that comprises seven layers. In addition, the seven layers are characterized by only two different pore sizes, i.e., permeabilities, and corresponding capillary pressure curves as shown in section A of Figure 2-15. The resulting capillary pressure curve for the layered reservoir would resemble that shown in section B of Figure 2-15. If a well were drilled at the point shown in section B of Figure 2-15, layers 1 and 3 would not produce water, while layer 2, which is above layer 3, would produce water since it is located in the transition zone.

Example 2-6

A four-layer oil reservoir is characterized by a set of reservoir capillary pressure-saturation curves as shown in Figure 2-16. The following data are also available:

Layer	Depth, ft	Permeability, md
1	4000-4010	80
2	4010-4020	190
3	4020-4035	70
4	4035-4060	100

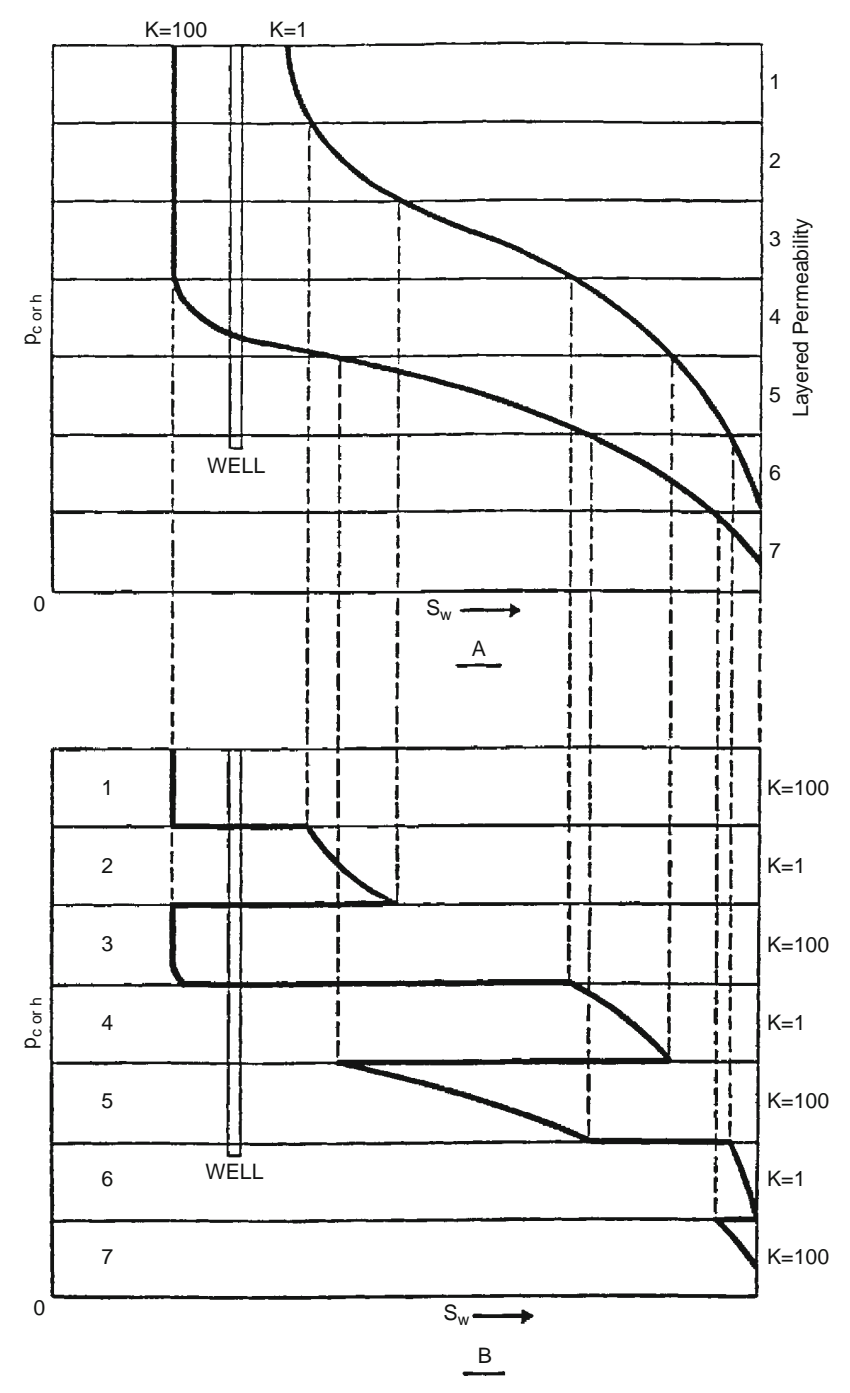


FIGURE 2-15 Effect of permeability on water saturation profile. (After Cole, F., 1969.)

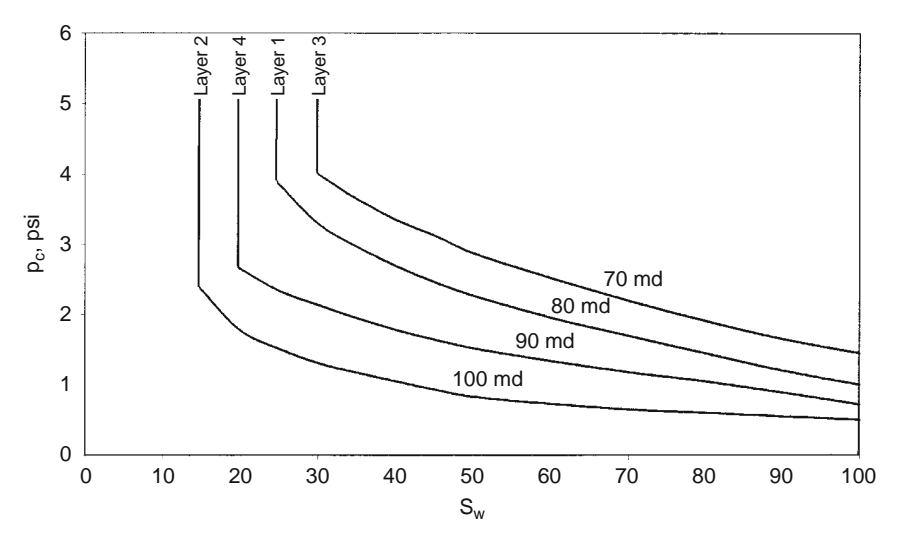


FIGURE 2-16 Variation of pc with k.

WOC =
$$4,060 \text{ ft}$$

Water density = 65.2 lb/ft^3
Oil density = 55.2 lb/ft^3

Calculate and plot water saturation versus depth for this reservoir.

Solution

Step 1. Establish the FWL by determining the displacement pressure p_d for the bottom layer, i.e., layer 4, and apply Equation 2-37:

• $p_d = 0.75 \text{ psi:}$

$$FWL = 4,060 + \frac{(144)(0.75)}{(65.2 - 55.2)} = 4,070.8 \text{ ft}$$

Step 2. The top of the bottom layer is located at a depth of 4,035 ft, which is 35.8 ft above the FWL. Using that height h of 35.8 ft, calculate the capillary pressure at the top of the bottom layer:

$$p_c = \left(\frac{h}{144}\right) \Delta \rho = \left(\frac{35.8}{144}\right) (65.2 - 55.2) = 2.486 \text{ psi}$$

• From the capillary pressure-saturation curve designated for layer 4, read the water saturation that corresponds to a p_c of 2.486 to give $S_w = 0.23$.

 Assume different values of water saturations and convert the corresponding capillary pressures into height above the FWL by applying Equation 2-34.

$$h = \frac{144 \, p_c}{\rho_w - \rho_o}$$

$S_{\mathbf{w}}$	p _c , psi	h, ft	Depth = FWL - h
0.23	2.486	35.8	4035
0.25	2.350	33.84	4037
0.30	2.150	30.96	4040
0.40	1.800	25.92	4045
0.50	1.530	22.03	4049
0.60	1.340	19.30	4052
0.70	1.200	17.28	4054
0.80	1.050	15.12	4056
0.90	0.900	12.96	4058

Step 3. The top of layer 3 is located at a distance of 50.8 ft from the FWL (i.e., h = 4,070.8 - 4,020 = 50.8 ft). Calculate the capillary pressure at the top of the third layer:

•
$$p_c = \left(\frac{50.8}{144}\right)(65.2 - 55.2) = 3.53 \text{ psi.}$$

- The corresponding water saturation as read from the curve designated for layer 3 is 0.370.
- Construct the following table for layer 3.

S _w	p _c , psi	h, ft	Depth = FWL - h
0.37	3.53	50.8	4020
0.40	3.35	48.2	4023
0.50	2.75	39.6	4031
0.60	2.50	36.0	4035

Step 4. Distance from the FWL to the top of layer 2 is

$$h = 4,070.8 - 4,010 = 60.8 \, ft$$

•
$$p_c = \left(\frac{60.8}{144}\right)(65.2 - 55.2) = 4.22 \text{ psi.}$$

• S_w at p_c of 4.22 psi is 0.15.

The distance from the FWL to the bottom of the layer is 50.8 ft, which corresponds to a p_c of 3.53 psi and an S_w of 0.15. This indicates that the second layer has a uniform water saturation of 15%.

Step 5. For layer 1, the distance from the FWL to the top of the layer is

- h = 4,070.8 4,000 = 70.8 ft.
- $p_c = \left(\frac{70.8}{144}\right)(10) = 4.92 \text{ psi.}$
- S_w at the top of layer 1 = 0.25.
- The capillary pressure at the bottom of the layer is 3.53 psi with a corresponding water saturation of 0.27.

Step 6. Figure 2-17 documents the calculated results graphically. The figure indicates that layer 2 will produce 100% oil while all remaining layers produce oil and water simultaneously.

Leverett J-Function

Capillary pressure data are obtained on small core samples that represent an extremely small part of the reservoir and, therefore, it is necessary to combine all capillary data to classify a particular reservoir. The

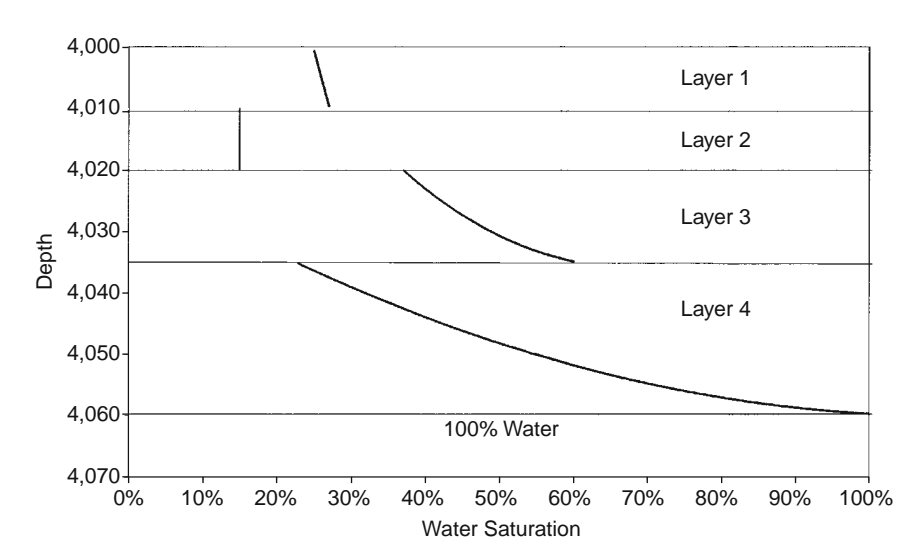


FIGURE 2-17 Water saturation profile.

fact that the capillary pressure-saturation curves of nearly all naturally porous materials have many features in common has led to attempts to devise some general equation describing all such curves. Leverett (1941) approached the problem from the standpoint of dimensional analysis.

Realizing that capillary pressure should depend on the porosity, interfacial tension, and mean pore radius, Leverett defined the dimensionless function of saturation, which he called the J-function, as

$$J(S_w) = 0.21645 \frac{p_c}{\sigma} \sqrt{\frac{k}{\varphi}}$$
 (2-36)

where $J(S_w)$ = Leverett J-function

 p_c = capillary pressure, psi

 σ = interfacial tension, dynes/cm

k = permeability, md

 ϕ = fractional porosity

In doing so, Leverett interpreted the ratio of permeability, k, to porosity, ϕ , as being proportional to the square of a mean pore radius.

The J-function was originally proposed as a means of converting all capillary-pressure data to a universal curve. There are significant differences in correlation of the J-function with water saturation from formation to formation, so that no universal curve can be obtained. For the same formation, however, this dimensionless capillary-pressure function serves quite well in many cases to remove discrepancies in the $p_{\rm c}$ versus $S_{\rm w}$ curves and reduce them to a common curve. This is shown for various unconsolidated sands in Figure 2-18.

Example 2-7

A laboratory capillary pressure test was conducted on a core sample taken from the Nameless Field. The core has a porosity and permeability of 16% and 80 md, respectively. The capillary pressure-saturation data are given as follows:

p _c , psi
0.50
0.60
0.75
1.05
1.75

The interfacial tension is measured at 50 dynes/cm. Further reservoir engineering analysis indicated that the reservoir is better described at

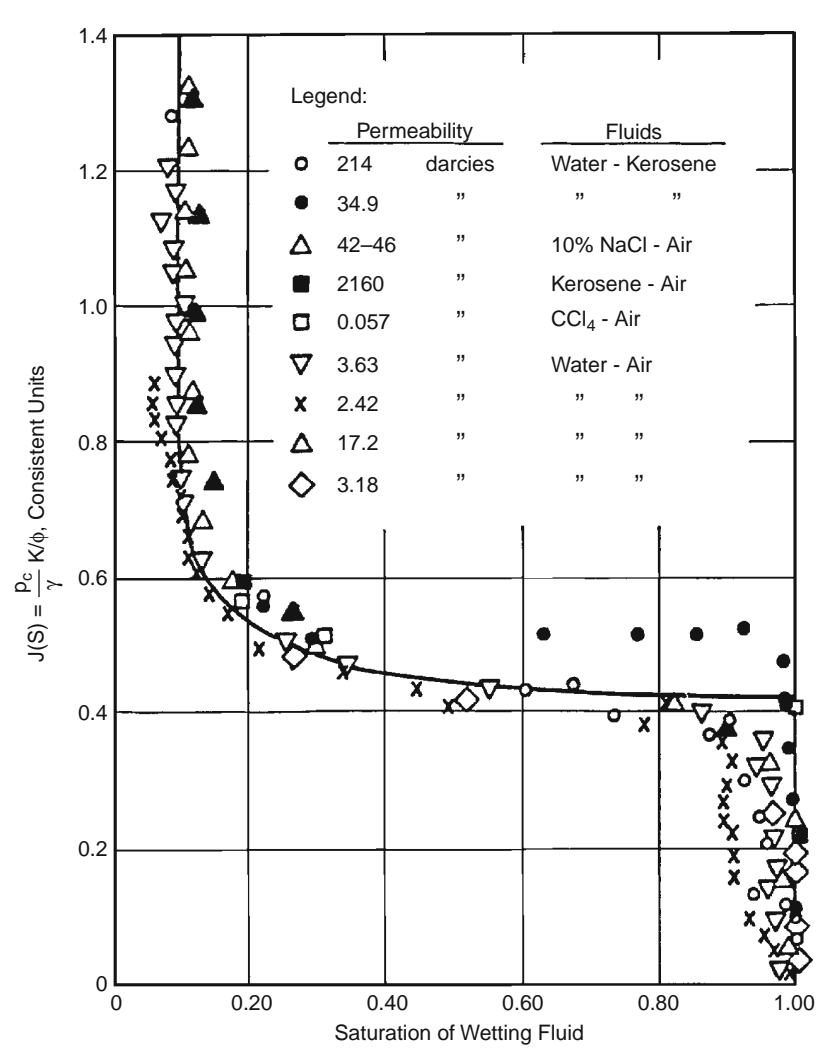


FIGURE 2-18 The Leverett J-function for unconsolidated sands. (After Leverett, 1941.)

a porosity value of 19% and an absolute permeability of 120 md. Generate the capillary pressure data for the reservoir.

Solution

Step 1. Calculate the J-function using the measured capillary pressure data:

$$J(S_w) = 0.21645 (p_c/50) \sqrt{80/0.16} = 0.096799 \ p_c$$

S _w	p _c , psi	$J(S_w) = 0.096799(p_c)$
1.0	0.50	0.048
0.8	0.60	0.058
0.6	0.75	0.073
0.4	1.05	0.102
0.2	1.75	0.169

Step 2. Using the new porosity and permeability values, solve Equation2-36 for the capillary pressure p_c:

$$\begin{split} p_c &= J(S_w)\sigma \left/ \left[0.21645\sqrt{\frac{k}{\varphi}}\right] \right. \\ p_c &= J(S_w)50 \left/ \left[0.21645\sqrt{\frac{120}{0.19}}\right] \right. \\ p_c &= 9.192\ J(S_w) \end{split}$$

Step 3. Reconstruct the capillary pressure-saturation table.

S _w	J(S _w)	$p_c = 9.192 \text{ J(S}_w)$
1.0	0.048	0.441
0.8	0.058	0.533
0.6	0.073	0.671
0.4	0.102	0.938
0.2	0.169	1.553

Converting Laboratory Capillary Pressure Data

For experimental convenience, it is common in the laboratory determination of capillary pressure to use air-mercury or air-brine systems, rather than the actual water-oil system characteristic of the reservoir. Since the laboratory fluid system does not have the same surface tension as the reservoir system, it becomes necessary to convert laboratory capillary pressure to reservoir capillary pressure. By assuming that the Leverett J-function is a property of rock and does not change from the laboratory to the reservoir, we can calculate reservoir capillary pressure as follows:

$$(p_c)_{res} = (p_c)_{lab} \frac{\sigma_{res}}{\sigma_{lab}}$$

Even after the laboratory capillary pressure has been corrected for surface tension, it may be necessary to make further corrections for permeability and porosity. The reason for this is that the core sample that was used in performing the laboratory capillary pressure test may not be representative of the average reservoir permeability and porosity. If we assume that the J-function will be invariant for a given rock type over a range of porosity and permeability values, then the reservoir capillary pressure can be expressed as

$$(p_c)_{res} = (p_c)_{lab} \frac{\sigma_{res}}{\sigma_{lab}} \sqrt{(\phi_{res} k_{core})/(\phi_{core} k_{res})}$$
(2-37)

where $(p_c)_{res}$ = reservoir capillary pressure

 σ_{res} = reservoir surface or interfacial tension

 k_{res} = reservoir permeability

 ϕ_{res} = reservoir porosity

 $(p_c)_{lab}$ = laboratory-measured capillary pressure

 ϕ_{core} = core porosity k_{core} = core permeability

SECTION 2.6 PERMEABILITY

Permeability is a property of the porous medium that measures the capacity and ability of the formation to transmit fluids. The rock permeability, k, is a very important rock property because it controls the directional movement and the flow rate of the reservoir fluids in the formation. This rock characterization was first defined mathematically by Henry Darcy in 1856. In fact, the equation that defines permeability in terms of measurable quantities is called *Darcy's Law*.

Darcy developed a fluid flow equation that has since become one of the standard mathematical tools of the petroleum engineer. If a horizontal linear flow of an incompressible fluid is established through a core sample of length L and a cross-section of area A, then the governing fluid flow equation is defined as

$$v = -\frac{k \, dp}{\mu \, dL} \tag{2-38}$$

where v = apparent fluid flowing velocity, cm/sec

k = proportionality constant, or permeability, darcys

 μ = viscosity of the flowing fluid, cp

dp/dL = pressure drop per unit length, atm/cm

The velocity, v, in Equation 2-38 is not the actual velocity of the flowing fluid but is the apparent velocity determined by dividing the flow

rate by the cross-sectional area across which fluid is flowing. Substituting the relationship, q/A, in place of ν in Equation 2-38 and solving for q results in

$$q = -\frac{kA}{\mu} \frac{dp}{dL}$$
 (2-39)

where q = flow rate through the porous medium, cm^3/sec A = cross-sectional area across which flow occurs, cm^2

With a flow rate of 1 cubic centimeter per second across a cross-sectional area of 1 square centimeter with a fluid of 1 centipoise viscosity and a pressure gradient at 1 atmosphere per centimeter of length, it is obvious that k is unity. For the units just described, k has been arbitrarily assigned a unit called *darcy* in honor of the man responsible for the development of the theory of flow through porous media. Thus, when all other parts of Equation 2-39 have values of unity, k has a value of 1 darcy.

One darcy is a relatively high permeability, as the permeabilities of most reservoir rocks are less that 1 darcy. In order to avoid the use of fractions in describing permeabilities, the term *millidarcy* is used. As the term indicates, 1 millidarcy, i.e., 1 md, is equal to one-thousandth of 1 darcy, or

$$1 \text{ darcy} = 1000 \text{ md}$$

The negative sign in Equation 2-39 is necessary, as the pressure increases in one direction while the length increases in the opposite direction.

Equation 2-39 can be integrated when the geometry of the system through which fluid flows is known. For the simple linear system shown in Figure 2-19, the integration is performed as follows:

$$q\int\limits_{0}^{L}dL=-\frac{kA}{\mu}\int\limits_{p_{1}}^{p_{2}}dp$$

Integrating the above expression yields

$$qL = -\frac{kA}{\mu}(p_2 - p_1)$$

It should be pointed out that the volumetric flow rate, q, is constant for liquids because the density does not change significantly with pressure.

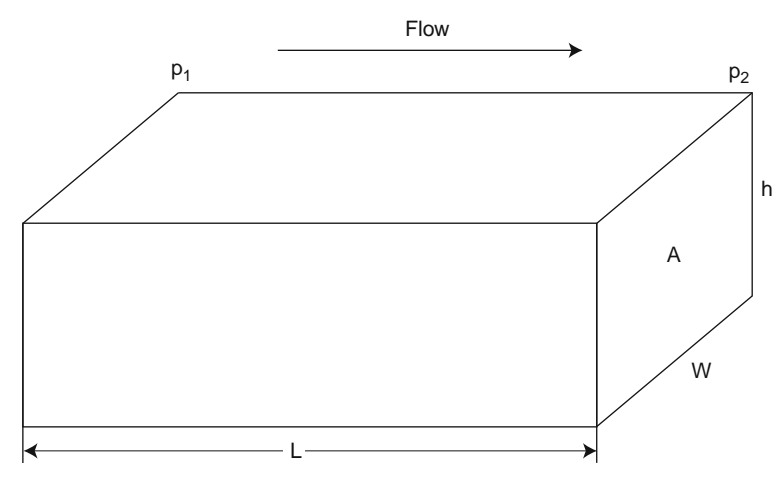


FIGURE 2-19 Linear flow model.

Since p_1 is greater than p_2 , the pressure terms can be rearranged, which will eliminate the negative term in the equation. The resulting equation is

$$q = \frac{kA(p_1 - p_2)}{\mu L}$$
 (2-40)

Equation 2-40 is the conventional linear flow equation used in fluid flow calculations.

Standard laboratory analysis procedures will generally provide reliable data on permeability of core samples. If the rock is not homogeneous, the whole core analysis technique will probably yield more accurate results than the analysis of core plugs (small pieces cut from the core). Procedures that have been used for improving the accuracy of the permeability determination include cutting the core with an oilbase mud, employing a pressure-core barrel, and conducting the permeability tests with reservoir oil.

Permeability is reduced by overburden pressure, and this factor should be considered in estimating permeability of the reservoir rock in deep wells because permeability is an isotropic property of porous rock in some defined regions of the system, that is. In other words, it is directional. Routine core analysis is generally concerned with plug samples drilled parallel to bedding planes and, hence, parallel to direction of flow in the reservoir. These yield horizontal permeabilities (k_h) .

The measured permeability on plugs that are drilled perpendicular to bedding planes is referred to as *vertical permeability* (k_v). Figure 2-20 shows a schematic illustration of the concept of the core plug and the associated permeability.

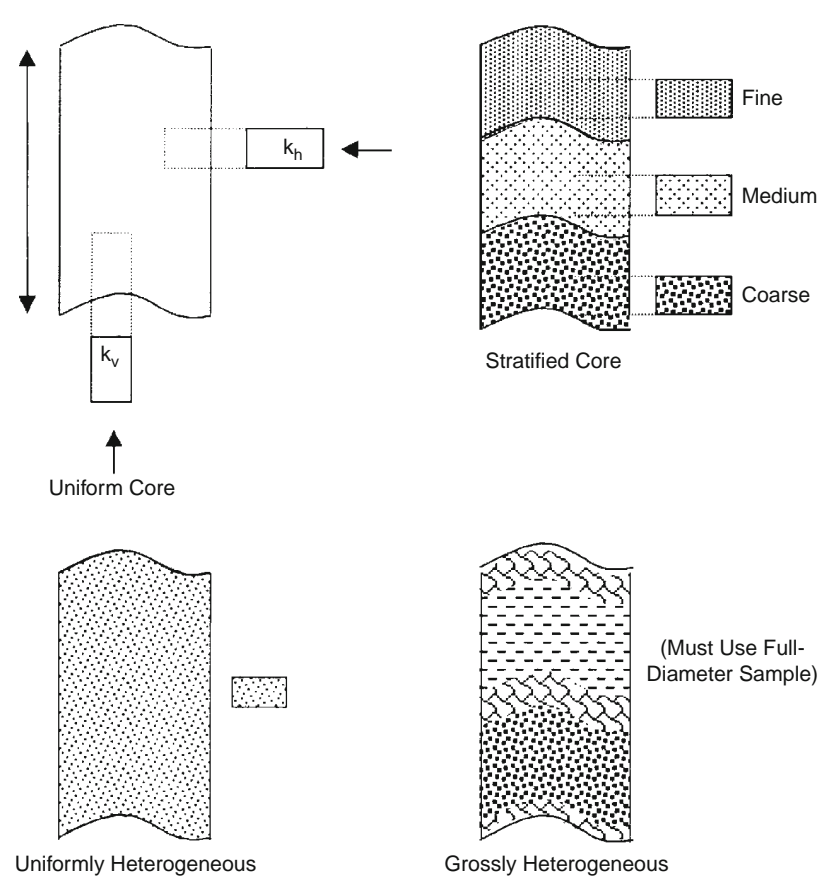


FIGURE 2-20 Representative samples of porous media.

As shown in Figure 2-20, several factors must be considered as possible sources of error in determining reservoir permeability. These factors are

- 1. Core sample may not be representative of the reservoir rock because of reservoir heterogeneity.
- 2. Core recovery may be incomplete.
- 3. Permeability of the core may be altered when it is cut or when it is cleaned and dried in preparation for analysis. This problem is likely to occur when the rock contains reactive clays.
- 4. Sampling process may be biased. There is a temptation to select the best parts of the core for analysis.

Permeability is measured by passing a fluid of known viscosity $\boldsymbol{\mu}$ through a core plug of measured dimensions (A and L) and then

measuring flow rate q and pressure drop Δp . Solving Equation 2-40 for the permeability gives

$$k = \frac{q \, \mu L}{A \, \Delta p}$$

where L = length of core, cm $A = cross-sectional area, cm^2$

The following conditions must exist during the measurement of permeability:

- Laminar (viscous) flow.
- No reaction between fluid and rock.
- Only a single phase present at 100% pore space saturation.

This measured permeability at 100% saturation of a single phase is called the *absolute permeability* of the rock.

Example 2-8

A brine is used to measure the absolute permeability of a core plug. The rock sample is 4 cm long and 3 cm² in cross section. The brine has a viscosity of 1.0 cp and is flowing at a constant rate of 0.5 cm³/sec under a 2.0 atm pressure differential. Calculate the absolute permeability.

Solution

Applying Darcy's equation, i.e., Equation 2-40, gives

$$0.5 = \frac{(k)(3)(2)}{(1)(4)}$$

$$k = 0.333 \ darcys$$

Example 2-9

Rework the preceding example assuming that an oil of 2.0 cp is used to measure the permeability. Under the same differential pressure, the flow rate is 0.25 cm³/sec.

Solution

Applying Darcy's equation yields

$$0.25 = \frac{(k)(3)(2)}{(2)(4)}$$

$$k = 0.333 \text{ darcys}$$

Dry gas is usually used (air, N₂, He) in permeability determination because of its convenience and availability, and to minimize fluid-rock reactions.

The measurement of the permeability should be restricted to the low (laminar/viscous) flow rate region, where the pressure remains proportional to the flow rate within the experimental error. For high flow rates, Darcy's equation as expressed by Equation 2-40 is inappropriate to describe the relationship of flow rate and pressure drop.

In using dry gas in measuring the permeability, the gas volumetric flow rate q varies with pressure because the gas is a highly compressible fluid. Therefore, the value of q at the average pressure in the core must be used in Equation 2-40. Assuming the used gases follow the ideal gas behavior (at low pressures), the following relationships apply:

$$p_1V_1=p_2V_2=p_mV_m$$

In terms of the flow rate q, this equation can be equivalently expressed as

$$p_1 q_1 = p_2 q_2 = p_m q_m (2-41)$$

with the mean pressure p_m expressed as

$$p_{m} = \frac{p_1 + p_2}{2}$$

where p_1 , p_2 , p_m = inlet, outlet, and mean pressures, respectively, atm V_1 , V_2 , V_m = inlet, outlet, and mean gas volume, respectively, cm³ q_1 , q_2 , q_m = inlet, outlet, and mean gas flow rate, respectively, cm³/sec

The gas flow rate is usually measured at base (atmospheric) pressure p_b , and therefore the term $Q_{\rm gsc}$ is introduced into Equation 2-41 to produce

$$Q_{gsc}p_b = q_m p_m$$

where Q_{gsc} = gas flow rate at standard conditions, cm³/sec p_b = base pressure (atmospheric pressure), atm

Substituting Darcy's Law in the previous expression gives

$$Q_{gsc}p_b = \frac{kA(p_1-p_2)}{\mu_gL} \bigg(\frac{p_1+p_2}{2}\bigg)$$

or

$$Q_{gsc} = \frac{kA(p_1^2 - p_2^2)}{2\mu_g L p_b}$$
 (2-42)

where k = absolute permeability, darcys

 μ_g = gas viscosity, cp

 p_b = base pressure, atm

 p_1 = inlet (upstream) pressure, atm

 p_2 = outlet (downstream) pressure, atm

L = length of the core, cm

A = cross-sectional area, cm²

 Q_{gsc} = gas flow rate at standard conditions, cm³/sec

The Klinkenberg Effect

Klinkenberg (1941) discovered that permeability measurements made with air as the flowing fluid showed different results from permeability measurements made with a liquid as the flowing fluid. The permeability of a core sample measured by flowing air is always greater than the permeability obtained when a liquid is the flowing fluid. Klinkenberg postulated, on the basis of his laboratory experiments, that liquids had a zero velocity at the sand grain surface, while gases exhibited some finite velocity at the sand grain surface. In other words, the gases exhibited *slippage* at the sand grain surface. This slippage resulted in a higher flow rate for the gas at a given pressure differential. Klinkenberg also found that for a given porous medium, as the mean pressure increased the calculated permeability decreased.

Mean pressure is defined as upstream flowing plus downstream flowing pressure divided by 2, $[p_m = (p_1 + p_2)/2]$. If a plot of measured permeability versus $1/p_m$ were extrapolated to the point where $1/p_m = 0$, in other words, where $p_m =$ infinity, this permeability would be approximately equal to the liquid permeability. A graph of this nature is shown in Figure 2-21. The absolute permeability is determined by extrapolation as shown in Figure 2-21.

The magnitude of the Klinkenberg effect varies with the core permeability and the type of gas used in the experiment as shown in Figures 2-22 and 2-23. The resulting straight-line relationship can be expressed as

$$k_{g} = k_{L} + c \left[\frac{1}{p_{m}} \right] \tag{2-43}$$

where k_g = measured gas permeability

 $p_m = mean pressure$

k_L = equivalent liquid permeability, i.e., absolute permeability, k

c = slope of the line

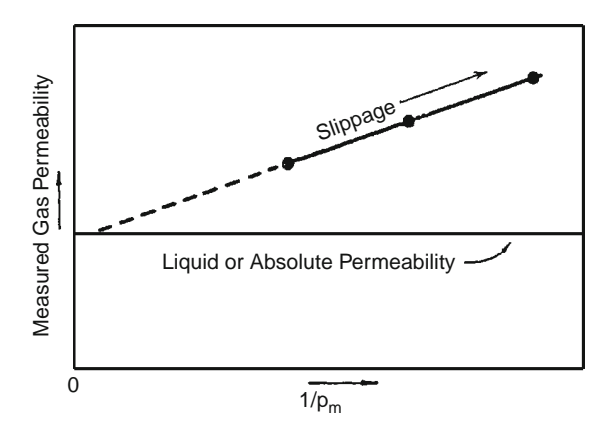


FIGURE 2-21 The Klinkenberg effect in gas permeability measurements.

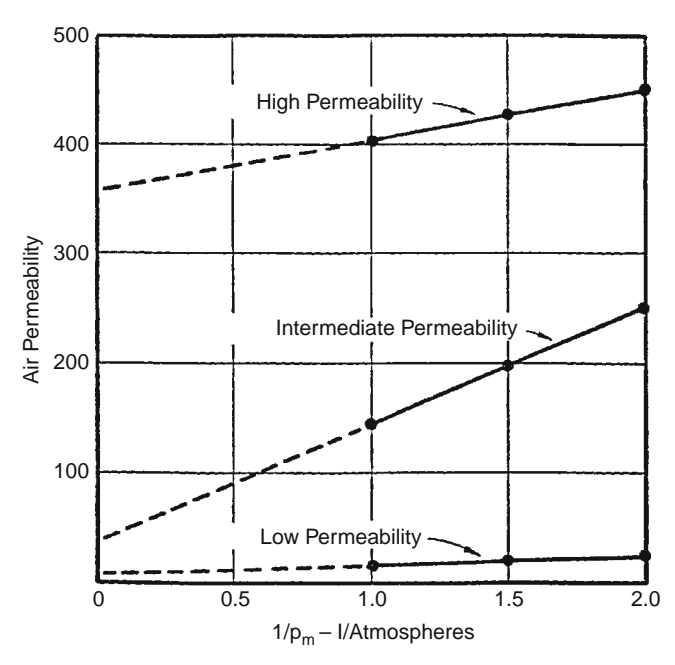


FIGURE 2-22 Effect of permeability on the magnitude of the Klinkenberg effect. (After Cole, F., 1969.)

Klinkenberg suggested that the slope c is a function of the following factors:

• Absolute permeability k, i.e., permeability of medium to a single phase completely filling the pores of the medium k_L.

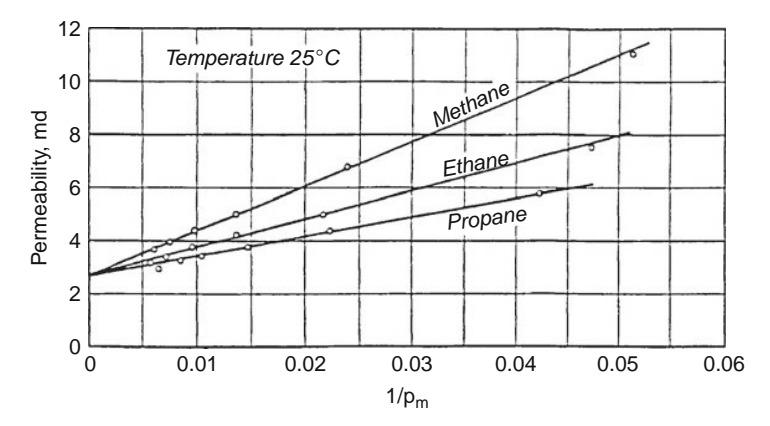


FIGURE 2-23 Effect of gas pressure on measured permeability for various gases. (After Calhoun, J., 1976.)

- Type of gas used in measuring the permeability, e.g., air.
- Average radius of the rock capillaries.

Klinkenberg expressed the slope c by the following relationship:

$$c = bk_L (2-44)$$

where k_L = equivalent liquid permeability, i.e., absolute permeability, k b = constant that depends on the size of the pore openings and is inversely proportional to the radius of capillaries

Combining Equation 2-44 with 2-43 gives

$$k_{g} = k_{L} + (bk_{L}) \left[\frac{1}{p_{m}} \right] \tag{2-45}$$

where k_g is the gas permeability as measured at the average pressure p_m . Jones (1972) studied the gas slip phenomena for a group of cores for which porosity, liquid permeability k_L (absolute permeability), and air permeability were determined. He correlated the parameter b with the liquid permeability by the following expression:

$$b = 6.9 k_{\rm I}^{-0.36} \tag{2-46}$$

The usual measurement of permeability is made with air at mean pressure just above atmospheric pressure (1 atm). To evaluate the slip phenomenon and the Klinkenberg effect, it is necessary to at least measure the gas permeability at two mean-pressure levels. In the absence of such data, Equations 2-45 and 2-46 can be combined and arranged to give

$$6.9 k_{L}^{0.64} + p_{m}k_{L} - p_{m}k_{g} = 0 (2-47)$$

where p_m = mean pressure, psi

 k_g = air permeability at p_m , psi

 k_L = absolute permeability (k), md

Equation 2-47 can be used to calculate the absolute permeability when only one gas permeability measurement (k_g) of a core sample is made at p_m . This nonlinear equation can be solved iteratively by using the Newton-Raphson iterative methods. The proposed solution method can be conveniently written as

$$k_{i+1} = k_i - \frac{f(k_i)}{f'(k_i)} \label{eq:ki}$$

where k_i = initial guess of the absolute permeability, md

 k_{i+1} = new permeability value to be used for the next iteration

i = iteration level

 $f(k_i)$ = Equation 2-47 as evaluated by using the assumed value of k_i

 $f'(k_i)$ = first-derivative of Equation 2-47 as evaluated at k_i

The first derivative of Equation 2-47 with respect to k_i is

$$f'(k_i) = 4.416 \ k_i^{-0.36} + p_m \tag{2-48}$$

The iterative procedure is repeated until convergence is achieved, when $f(k_i)$ approaches zero or when no changes in the calculated values of k_i are observed.

Example 2-10

The permeability of a core plug is measured by air. Only one measurement is made at a mean pressure of 2.152 psi. The air permeability is 46.6 md. Estimate the absolute permeability of the core sample. Compare the result with the actual absolute permeability of 23.66 md.

Solution

Step 1. Substitute the given values of p_m and k_g into Equations 2-47 and 2-48, to give

$$f(k_i) = 6.9 \; k_i^{0.64} + 2.152 \; k_i - (2.152)(46.6) \; f'(k_i) = 4.416 \; k_i^{-0.36} + 2.152$$

Step 2. Assume $k_i = 30$ and apply the Newton-Raphson method to find the required solution as follows:

i	$\mathbf{k_{i}}$	f(k _i)	$f'(k_i)$	$k_{i\ +\ 1}$
1 2	30.000 22.719	25.12 -0.466	3.45 3.29	22.719 22.861
3	22.861	0.414	3.29	22.848

After three iterations, the Newton-Raphson method converges to an absolute value for the permeability of 22.848 md.

Equation 2-39 can be expanded to describe flow in any porous medium where the geometry of the system is not too complex to integrate. For example, the flow into a wellbore is not linear but is more often radial. Figure 2-24 illustrates the type of flow that is typical of that occurring in the vicinity of a producing well. For a radial flow, Darcy's equation in a differential form can be written as

$$q = \frac{kA}{\mu} \frac{dp}{dr}$$

Integrating Darcy's equation gives

$$q \int_{r_w}^{r_e} dr = \frac{kA}{\mu} \int_{p_{wf}}^{p_e} dp$$

The term dL has been replaced by dr, as the length term has now become a radius term. The minus sign is no longer required for the radial system shown in Figure 2-24, as the radius increases in the same

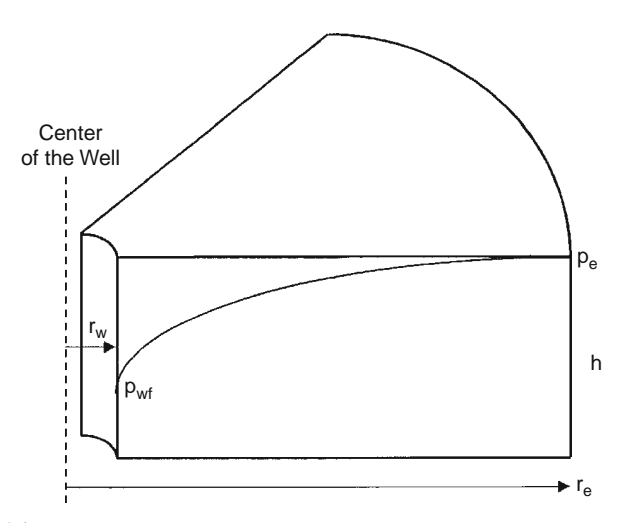


FIGURE 2-24 Radial flow model.

direction as the pressure. In other words, as the radius increases going away from the wellbore, the pressure also increases. At any point in the reservoir, the cross-sectional area across which flow occurs will be the surface area of a cylinder, which is $2\pi rh$. Since the cross-sectional area is related to r, A must be included within the integral sign as follows:

$$q \int_{r_{w}}^{r_{e}} \frac{dr}{2\pi rh} = \frac{k}{\mu} \int_{p_{wf}}^{p_{e}} dp$$

Rearranging,

and integrating,

$$\frac{q}{2\pi h}(\,ln\;r_e-\,ln\;r_w)=\frac{k}{\mu}(p_e-p_{wf})$$

Solving for the flow rate, q, results in

$$q = \frac{2\pi kh(p_e - p_{wf})}{\mu \ln(r_e/r_w)}$$
 (2-49)

This equation assumes that the reservoir is homogeneous and is completely saturated with a single liquid phase (appropriate modifications will be discussed in later sections to account for the presence of other fluids), where

q = flow rate, reservoir cm³/sec k = absolute permeability, darcy

h = thickness, cm

r_e = drainage radius, cm

 $r_{\rm w}$ = wellbore radius, cm

 p_e = pressure at drainage radius, atm

 p_{wf} = bottom-hole flowing pressure

 μ = viscosity, cp

Averaging Absolute Permeabilities

The most difficult reservoir properties to determine usually are the level and distribution of the absolute permeability throughout the reservoir. They are more variable than porosity and more difficult to measure. Yet an adequate knowledge of permeability distribution is critical to the prediction of reservoir depletion by any recovery process. It is rare to encounter a homogeneous reservoir in actual practice. In many cases,

the reservoir contains distinct layers, blocks, or concentric rings of varying permeabilities. Also, because smaller-scale heterogeneities always exist, core permeabilities must be averaged to represent the flow characteristics of the entire reservoir or individual reservoir layers (units). The proper way of averaging the permeability data depends on how permeabilities were distributed as the rock was deposited.

Three simple permeability-averaging techniques are commonly used to determine an appropriate average permeability to represent an equivalent homogeneous system:

- Weighted-average permeability.
- Harmonic-average permeability.
- Geometric-average permeability.

Weighted-Average Permeability

This averaging method is used to determine the average permeability of layered-parallel beds with different permeabilities. Consider the case where the flow system comprises three parallel layers that are separated from one another by thin impermeable barriers, i.e., no cross flow, as shown in Figure 2-25. All the layers have the same width w with a cross-sectional area of A.

The flow from each layer can be calculated by applying Darcy's equation in a linear form, as expressed by Equation 2-40, to give

Layer 1

$$q_1 = \frac{k_1 w h_1 \Delta p}{\mu L}$$

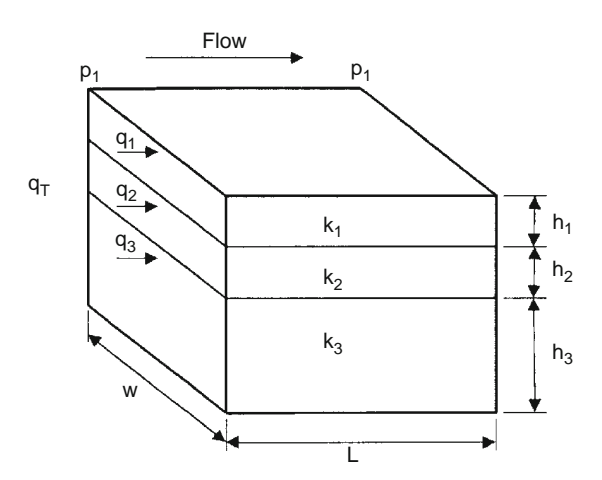


FIGURE 2-25 Linear flow through layered beds.

Layer 2

$$q_2 = \frac{k_2 w h_2 \Delta p}{\mu L}$$

Layer 3

$$q_3 = \frac{k_3 w h_3 \Delta p}{u L}$$

The total flow rate from the entire system is expressed as

$$q_t = \frac{k_{avg}wh_t\Delta p}{\mathfrak{u}L}$$

where q_t = total flow rate

 k_{avg} = average permeability for the entire model

w = width of the formation

 $\Delta p = p_1 B p_2$

 h_t = total thickness

The total flow rate q_t is equal to the sum of the flow rates through each layer, or

$$\boldsymbol{q}_t = \boldsymbol{q}_1 + \boldsymbol{q}_2 + \boldsymbol{q}_3$$

Combining the preceding expressions gives

$$\frac{k_{avg}wh_t\Delta p}{\mu L} = \frac{k_1wh_1\Delta p}{\mu L} + \frac{k_2wh_2\Delta p}{\mu L} + \frac{k_3wh_3\Delta p}{\mu L}$$

or

$$k_{avg}h_{t} = k_{1}h_{1} + k_{2}h_{2} + k_{3}h_{3}$$

$$k_{avg} = \frac{k_{1}h_{1} + k_{2}h_{2} + k_{3}h_{3}}{h_{t}}$$

The average absolute permeability for a parallel-layered system can be expressed in the following form:

$$k_{\text{avg}} = \frac{\sum_{j=1}^{n} k_j h_j}{\sum_{j=1}^{n} h_j}$$
 (2-50)

Equation 2-50 is commonly used to determine the average permeability of a reservoir from core analysis data.

Figure 2-26 shows a similar layered system with variable-width layers. Assuming no cross-flow between the layers, the average

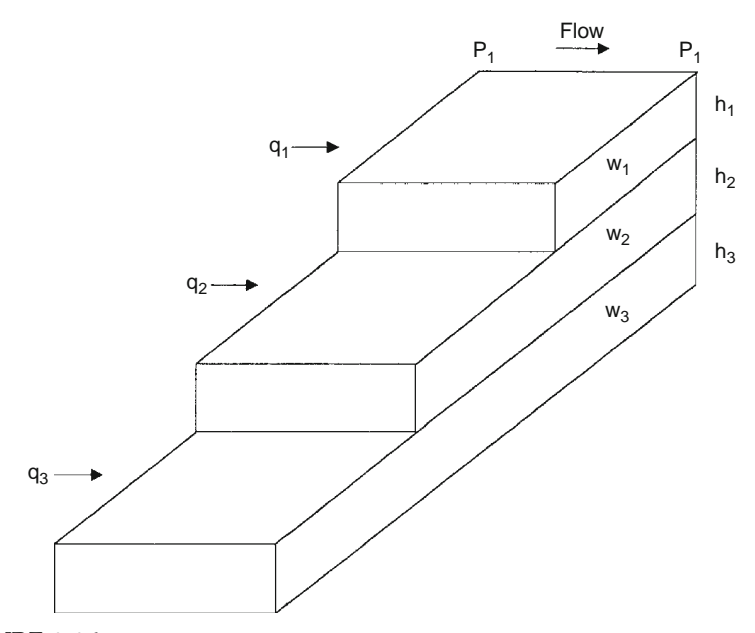


FIGURE 2-26 Linear flow through layered beds with variable area.

permeability can be approximated in a manner similar to the previous derivation to give

$$k_{\text{avg}} = \frac{\sum_{j=1}^{n} k_j A_j}{\sum_{j=1}^{n} A_j}$$
 (2-51)

with

$$A_j = h_j w_j$$

where A_j = cross-sectional area of layer j w_j = width of layer j

Example 2-11

Given the following permeability data from a core analysis report, calculate the average permeability of the reservoir.

Depth, ft	Permeability, md
3998-02	200
4002-04	130
4004-06	170
4006-08	180
4008-10	140

Solution

h _i , ft	k _i	h _i k _i
4	200	800
2	130	260
2	170	340
2	180	360
2	140	280
$h_t = 12$		$\Sigma h_i k_i = 2040$

$$k_{avg} = \frac{2,040}{12} = 170 \text{ md}$$

Harmonic-Average Permeability

Permeability variations can occur laterally in a reservoir as well as in the vicinity of a wellbore. Consider Figure 2-27, which shows fluid flow through a series combination of beds with different permeabilities.

For a steady-state flow, the flow rate is constant and the total pressure drop Δp is equal to the sum of the pressure drops across each bed, or

$$\Delta p = \Delta p_1 + \Delta p_2 + \Delta p_3$$

Substituting for the pressure drop by applying Darcy's equation, i.e., Equation 2-40, gives

$$\frac{q\mu L}{Ak_{avg}} = \frac{q\mu L_1}{Ak_1} + \frac{q\mu L_2}{Ak_2} + \frac{q\mu L_3}{Ak_3}$$

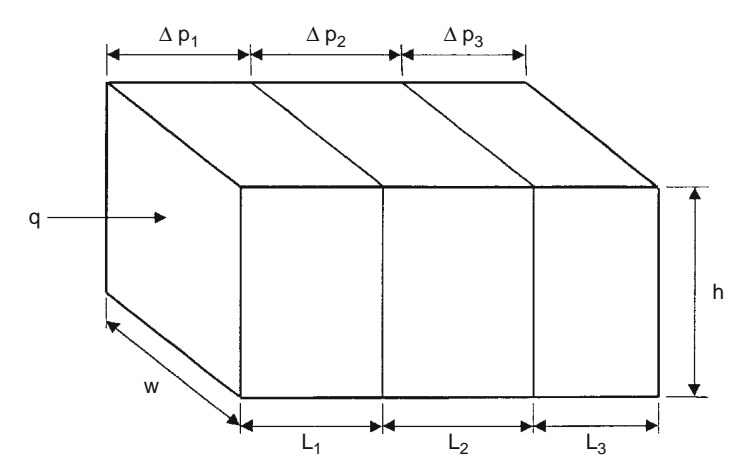


FIGURE 2-27 Linear flow through series beds.

Canceling the identical terms and simplifying gives

$$k_{avg} = \frac{L}{(L/k)_1 + (L/k)_2 + (L/k)_3}$$

This equation can be expressed in a more generalized form to give

$$k_{\text{avg}} = \frac{\sum_{i=1}^{n} L_i}{\sum_{i=1}^{n} (L/k)_i}$$
 (2-52)

where L_i = length of each bed

 k_i = absolute permeability of each bed

In the radial system shown in Figure 2-28, the preceding averaging methodology can be applied to produce the following generalized expression:

$$k_{\text{avg}} = \frac{\ln(r_{\text{e}}/r_{\text{w}})}{\sum_{j=1}^{n} \left[\frac{\ln(r_{j}/r_{j-1})}{k_{j}}\right]}$$
(2-53)

The relationship in Equation 2-53 can be used as a basis for estimating a number of useful quantities in production work. For example, the effects of mud invasion, acidizing, or well shooting can be estimated from it.

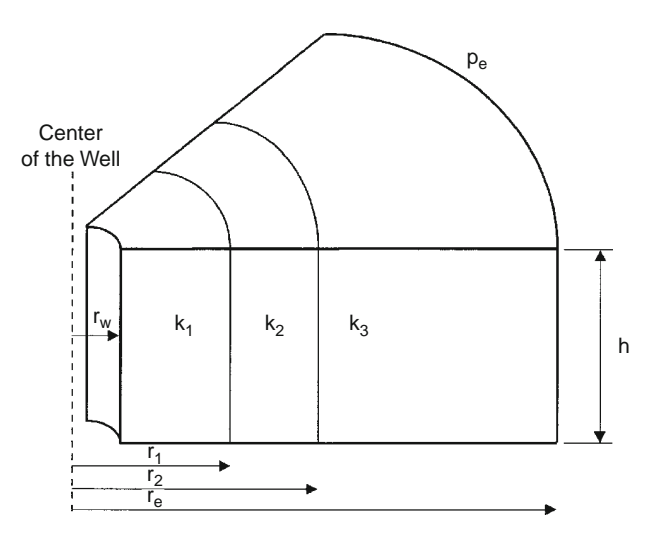


FIGURE 2-28 Flow through series beds.

Example 2-12

A hydrocarbon reservoir is characterized by five distinct formation segments that are connected in series. Each segment has the same formation thickness. The length and permeability of each section of the five-bed reservoir follow:

Length, ft	Permeability, md
150	80
200	50
300	30
500	20
200	10

Calculate the average permeability of the reservoir by assuming

- a. Linear flow system.
- b. Radial flow system.

Solution

For a linear system

L _i , ft	$\mathbf{k_{i}}$	L _i /k _i
150	80	1.8750
200	50	4.0000
300	30	10.000
500	20	25.000
200	10	20.000
1350		$\Sigma L_i/k_i = 60.875$

Using Equation 2-52 gives

$$k_{avg} = \frac{1350}{60.875} = 22.18 \,\text{md}$$

For a radial system

The solution of the radial system can be conveniently expressed in the following tabulated form. The solution is based on Equation 2-53 and assumes a wellbore radius of 0.25 ft:

Segment	r _i , ft	ln(r _i /r _{iB1})	$\mathbf{k_{i}}$	[ln(r _i /r _{iB1})]/k _i
Wellbore	0.25	_	_	_
1	150	6.397	80	0.080
2	350	0.847	50	0.017
3	650	0.619	30	10.021
4	1150	0.571	20	0.029
5	1350	0.160	10	0.016
				0.163

From Equation 2-53,

$$k_{avg} = \frac{ln(1350/0.25)}{0.163} = 52.72 \text{ md}$$

Geometric-Average Permeability

Warren and Price (1961) illustrated experimentally that the most probable behavior of a heterogeneous formation approaches that of a uniform system having a permeability that is equal to the geometric average. The geometric average is defined mathematically by the following relationship:

$$k_{avg} = exp \left[\frac{\sum_{i=1}^{n} (h_i ln(k_i))}{\sum_{i=1}^{n} h_i} \right]$$
 (2-54)

where k_i = permeability of core sample i

 h_i = thickness of core sample i

n = total number of samples

If the thicknesses (h_i) of all core samples are the same, Equation 2-57 can be simplified as follows:

$$k_{avg} = (k_1 k_2 k_3 \dots k_n)^{\frac{1}{n}}$$
 (2-55)

Example 2-13

Given the following core data, calculate the geometric average permeability:

Sample	h _i , ft	k _i , md
1	1.0	10
2	1.0	30
3	0.5	100
4	1.5	40
5	2.0	80
6	1.5	70
7	1.0	15
8	1.0	50
9	1.5	35
10	0.5	20

Solution

Sample	h _i , ft	k _i , md	h _i * Ln (k _i)
1	1.0	10	2.303
2	1.0	30	3.401
3	0.5	100	2.303
4	1.5	40	5.533
5	2.0	80	8.764
6	1.5	70	6.373
7	1.0	15	2.708
8	1.0	50	3.912
9	1.5	35	5.333
10	0.5	20	1.498
11.5			42.128

$$k_{avg} = exp\left[\frac{42.128}{11.5}\right] = 39 \text{ md}$$

Absolute Permeability Correlations

The determination of connate water by capillary-pressure measurements has allowed the evaluation of connate-water values on samples of varying permeability and within a given reservoir to a wider extent and to a greater accuracy than was possible beforehand. These measurements have accumulated to the point where it is possible to correlate connate-water content with the permeability of the sample in a given reservoir and, to a certain extent, between reservoirs.

Calhoun (1976) suggested that, in an ideal pore configuration of uniform structure, the irreducible connate water would be independent of permeability, lower permeabilities being obtained merely by a scaled reduction in particle size. In an actual porous system formed by deposition of graded particles or by some other natural means, the connate water might be expected to increase as permeability decreases. This conclusion results from the thought that lower permeabilities result from increasing nonuniformity of pore structure by a gradation of particles rather than by a scaled reduction of particles. In this sense, connatewater content is a function of permeability only insofar as permeability is dependent upon the variation of pore structure. Thus, for unconsolidated sands formed of uniform particles of one size, the connate-water content would be independent of permeability.

Calhoun (1976) pointed out that any correlation found between various reservoir properties would be anticipated to apply only within the rather narrow limits of a single reservoir or perhaps of a given formation. Beyond these bounds, a general correspondence between permeability and pore structure would not be known. It would be anticipated,

however, that, for formations of similar characteristics, a similar dependence of permeability on pore structure and, consequently, a similar correlation of connate water and permeability would be found.

It has been generally considered for many years that connate water reaches higher values in lower permeabilities. This observation amounts to nothing more than a trend. The data from capillary-pressure measurements have indicated that the relationship is semilogarithmic, although it is not yet certain from published data that this is the exact relationship. No generalizations are apparent from this amount of data, although it can now be quite generally stated that within a given reservoir the connate water (if an irreducible value) will increase proportionally to the decrease in the logarithm of the permeability. It is apparent, moreover, that one cannot state the value of connate water expected in any new formation unless one knows something of its pore makeup.

Experience indicates a general relationship between reservoir porosity (ϕ) and irreducible water saturation (S_{wc}) provided the rock type and/or the grain size does not vary over the zone of interest. This relationship is defined by the equation

$$C = (S_{wi})(\varphi)$$

where C is a constant for a particular rock type and/or grain size.

Several investigators suggest that the constant C that describes the rock type can be correlated with the absolute permeability of the rock. Two commonly used empirical methods are the Timur equation and the Morris-Biggs equation.

The Timur Equation

Timur (1968) proposed the following expression for estimating the permeability from connate-water saturation and porosity:

$$k = 8.58102 \frac{\phi^{4.4}}{S_{wc}^2} \tag{2-56}$$

The Morris-Biggs Equation

Morris and Biggs (1967) presented the following two expressions for estimating the permeability of oil and gas reservoirs.

For an oil reservoir,

$$k = 62.5 \left(\frac{\phi^3}{S_{wc}}\right)^2 \tag{2-57}$$

For a gas reservoir,

$$k = 2.5 \left(\frac{\phi^3}{S_{wc}}\right)^2 \tag{2-58}$$

where k = absolute permeability, darcy

 ϕ = porosity, fraction

 S_{wc} = connate-water saturation, fraction

Example 2-14

Estimate the absolute permeability of an oil zone with a connate-water saturation and average porosity of 25% and 19%, respectively.

Solution

Applying the Timur equation,

$$k = 8.58102 \frac{(0.19)^{4.4}}{(0.25)^2} = 0.0921 \text{ darcy}$$

From the Morris and Biggs correlation,

$$k = 62.5 \left[\frac{(0.29)^3}{0.25} \right]^2 = 0.047 \text{ darcy}$$

In the previous discussion of Darcy's Law and absolute permeability measurements, it was assumed that the entire porous medium is fully saturated with a single phase, i.e., 100% saturation. In a hydrocarbon reservoir, however, the rocks are usually saturated with two or more fluids.

Therefore, the concept of absolute permeability must be modified to describe the fluid flowing behavior when more than one fluid is present in the reservoir. If a core sample is partially saturated with a fluid (other than the test fluid) and both saturations are maintained constant throughout the flow, the measured permeability to the test fluid will be reduced below the permeability to the other fluid, which could be measured if the core were 100% saturated with the test fluid.

As the saturation of a particular phase decreases, the permeability to that phase also decreases. The measured permeability is referred to as the *effective permeability* and is a relative measure of the conductance of the porous medium for one fluid when the medium is saturated with more than one fluid. This implies that the effective permeability is an associated property with each reservoir fluid, i.e., gas, oil, or water. These effective permeabilities for the three reservoir fluids are represented by

 k_g = effective gas permeability

 k_o = effective oil permeability

 k_w = effective water permeability

One of the phenomena of multiphase effective permeabilities is that the sum of the effective permeabilities is always less than or equal to the absolute permeability, i.e.,

$$k_g + k_o + k_w \le k$$

The effective permeability is used mathematically in Darcy's Law in place of the absolute permeability. For example, the expression for flow through the linear system under a partial saturation of oil is written

$$q_o = \frac{k_o A(p_1 - p_2)}{\mu_o L}$$
 (2-59)

where $q_o = oil$ flow rate, cc/sec

 μ_{o} = oil viscosity, cm

 k_o = oil effective permeability, darcys

Effective permeabilities are normally measured directly in the laboratory on small core samples. Owing to the many possible combinations of saturation for a single medium, however, laboratory data are usually summarized and reported as relative permeability. Relative permeability is defined as the ratio of the effective permeability to a given fluid at a definite saturation to the permeability at 100% saturation. The terminology most widely used is simply $k_{\rm g}/k$, $k_{\rm o}/k$, $k_{\rm w}/k$, meaning the relative permeability to gas, oil, and water, respectively. Since k is a constant for a given porous material, the relative permeability varies with the fluid saturation in the same fashion as does the effective permeability. The relative permeability to a fluid will vary from a value of zero at some low saturation of that fluid to a value of 1.0 at 100% saturation of that fluid. Thus, the relative permeability can be expressed symbolically as

$$k_{rg} = \frac{k_g}{k}$$
$$k_{ro} = \frac{k_o}{k}$$
$$k_{rw} = \frac{k_w}{k}$$

which are relative permeabilities to gas, oil, and water, respectively.

SECTION 2.7 ROCK COMPRESSIBILITY

A reservoir thousands of feet underground is subjected to an overburden pressure caused by the weight of the overlying formations. Overburden pressures vary from area to area depending on factors such as depth, nature of the structure, consolidation of the formation, and possibly the geologic age and history of the rocks. Depth of the formation is the most important consideration, and a typical value of overburden pressure is approximately 1 psi per foot of depth.

The weight of the overburden simply applies a compressive force to the reservoir. The pressure in the rock pore spaces does not normally approach the overburden pressure. A typical pore pressure, commonly referred to as the *reservoir pressure*, is approximately 0.5 psi per foot of depth, assuming that the reservoir is sufficiently consolidated so the overburden pressure is not transmitted to the fluids in the pore spaces.

The pressure difference between overburden and internal pore pressure is referred to as the *effective overburden* pressure. During pressure depletion operations, the internal pore pressure decreases and, therefore, the effective overburden pressure increases. This increase causes the following effects:

- The bulk volume of the reservoir rock is reduced.
- Sand grains within the pore spaces expand.

These two volume changes tend to reduce the pore space and, therefore, the porosity of the rock. Often these data exhibit relationships with both porosity and the effective overburden pressure. Compressibility typically decreases with increasing porosity and effective overburden pressure.

Geertsma (1957) pointed out that three different types of compressibility must be distinguished in rocks:

 Rock-Matrix Compressibility, c_r, is defined as the fractional change in volume of the solid rock material (grains) with a unit change in pressure.
 Mathematically, the rock compressibility coefficient is given by

$$c_{r} = -\frac{1}{V_{r}} \left(\frac{\partial V_{r}}{\partial p} \right)_{T} \tag{2-60}$$

where c_r = rock-matrix compressibility, psi⁻¹

 V_r = volume of solids

The subscript T indicates that the derivative is taken at constant temperature.

• Rock-Bulk Compressibility, c_B, is defined as the fractional change in volume of the bulk volume of the rock with a unit change in pressure. The rock-bulk compressibility is defined mathematically by

$$c_{\rm B} = -\frac{1}{V_{\rm B}} \left(\frac{\partial V_{\rm B}}{\partial p} \right)_{\rm T} \tag{2-61}$$

where c_B = rock-bulk compressibility coefficient, psi⁻¹ V_B = bulk volume

Pore Compressibility, c_p, is defined as the fractional change in pore
volume of the rock with a unit change in pressure and is given by the
following relationship:

$$c_{p} = \frac{-1}{V_{p}} \left(\frac{\partial V_{p}}{\partial p} \right)_{T} \tag{2-62}$$

where p = pore pressure, psi

 c_p = pore compressibility coefficient, psi⁻¹

 V_p = pore volume

Equation 2-62 can be expressed in terms of the porosity ϕ by noting that ϕ increases with the increase in the pore pressure, or

$$c_p = \frac{1}{\varphi} \frac{\partial \varphi}{\partial p}$$

For most petroleum reservoirs, the rock and bulk compressibility are considered small in comparison with the pore compressibility c_p . The *formation compressibility* c_f is the term commonly used to describe the total compressibility of the formation and is set equal to c_p , i.e.,

$$c_{\rm f} = c_{\rm p} = \frac{1}{\phi} \frac{\partial \phi}{\partial p} \tag{2-63}$$

Typical values for the formation compressibility range from 3×10^{-6} to 25×10^{-6} psi⁻¹. Equation 2-62 can be rewritten as

$$c_f = \frac{1}{V_p} \frac{\Delta V_p}{\Delta p}$$

or

$$\Delta V_p = c_f V_p \Delta p \tag{2-64}$$

where ΔV_p and Δp are the change in the pore volume and pore pressure, respectively.

Geertsma (1957) suggested that the bulk compressibility c_B is related to the pore compressibility c_p by the following expression:

$$c_{\rm B} \cong c_{\rm p} \phi$$
 (2-65)

Geertsma has stated that in a reservoir only the vertical component of hydraulic stress is constant and that the stress components in the horizontal plane are characterized by the boundary condition that there is no bulk deformation in those directions. For those boundary conditions, he developed the following approximation for sandstones:

$$c_p(reservoir) = 1/2c_p(laboratory) \\$$

Example 2-15

Calculate the reduction in the pore volume of a reservoir due to a pressure drop of 10 psi. The reservoir original pore volume is 1 million barrels with an estimated formation compressibility of 10×10^{-6} psi⁻¹.

Solution

Applying Equation 2-64 gives

$$\Delta V_p = (10\times 10^{-6})(1\times 10^6)(10) = 100 \ bbl$$

Although this value is small, it becomes an important factor in undersaturated reservoirs when calculations are made to determine initial oil-in-place and aquifer contents.

The reduction in the pore volume due to pressure decline can also be expressed in terms of the changes in the reservoir porosity. Equation 2-63 can be rearranged, to give

$$c_f\partial p=\left(\frac{1}{\varphi}\right)\!\partial\varphi$$

Integrating the above relation gives

$$\begin{split} c_f \int\limits_{p_o}^p \partial p &= \int\limits_{\varphi_o}^\varphi \frac{\partial \varphi}{\varphi} \\ c_f(p-p_o) &= ln \left(\frac{\varphi}{\varphi_o}\right) \end{split}$$

or

$$\phi = \phi_o e^{c_f(p - p_o)} \tag{2-66}$$

where p_o = original pressure, psi

 ϕ_0 = original porosity

p = current pressure, psi

 ϕ = porosity at pressure p

Note that the e^x expansion series is expressed as

$$e^{x} = 1 + x + \frac{x^{2}}{2!} + \frac{x^{3}}{3!} + \dots$$

Using the expansion series and truncating the series after the first two terms gives

$$\phi = \phi_0 \left[1 + c_f(p - p_0) \right] \tag{2-67}$$

Example 2-16

Given the following data,

- $c_f = 10 \times 10^{-6}$.
- Original pressure = 5,000 psi.
- Original porosity = 18%.
- Current pressure = 4,500 psi.

calculate the porosity at 4,500 psi.

Solution

$$\phi = 0.18 \left[1 + (10 \times 10^{-6})(4,500 - 5,000) \right] = 0.179$$

It should be pointed out that the total reservoir compressibility c_t is extensively used in the transient flow equation and the material balance equation as defined by the following expression:

$$c_t = S_o c_o + S_w c_s + S_g c_g + c_f$$
 (2-68)

where S_o , S_w , S_g = oil, water, and gas saturation c_o = oil compressibility, psi^{-1} c_w = water compressibility, psi^{-1} c_g = gas compressibility, psi^{-1} c_t = total reservoir compressibility

For undersaturated oil reservoirs, the reservoir pressure is above the bubble-point pressure, i.e., no initial gas cap, which reduces Equation 2-68 to

$$c_t = S_o c_o + S_w c_w + c_f$$

In general, the formation compressibility c_f is the same order of magnitude as the compressibility of the oil and water and, therefore, cannot be regulated.

Several authors have attempted to correlate the pore compressibility with various parameters including the formation porosity. Hall (1953) correlated the pore compressibility with porosity as given by the following relationship:

$$c_f = (1.782/\phi^{0.438})10^{-6} \tag{2-69}$$

where c_f = formation compressibility, psi^{-1} ϕ = porosity, fraction Newman (1973) used 79 samples for consolidated sandstones and limestones to develop a correlation between the formation compressibility and porosity. The proposed generalized hyperbolic form of the equation is

$$c_f = \frac{a}{[1 + cb\phi]}$$

where

For Consolidated Sandstones

$$a = 97.32 \times 10^{-6}$$

 $b = 0.699993$
 $c = 79.8181$

For Limestones

$$\begin{aligned} a &= 0.8535 \\ b &= 1.075 \\ c &= 2.202 \times 10^6 \end{aligned}$$

Example 2-17

Estimate the compressibility coefficient of a sandstone formation that is characterized by a porosity of 0.2, using

- a. Hall's correlation.
- b. Newman's correlation.

Solution

a. Hall's correlation:

$$c_f = (1.782/0.2^{0.438})10^{-6} = 3.606 \times 10^{-6} \text{ psi}^{-1}$$

b. Newman's correlation:

$$c_f = \frac{97.32 \times 10^{-6}}{\left[1 + (0.699993)(79.8181)(0.2)\right]^{1/0.699993}} = 2.74 \times 10^{-6} \, psi^{-1}$$

SECTION 2.8 NET PAY THICKNESS

A fundamental prerequisite to reservoir performance prediction is a satisfactory knowledge of the volume of oil originally in place. The reservoir is necessarily confined to certain geologic and fluid boundaries, i.e., GOC, WOC, and GWC, so accuracy is imperative. Within the confines of such boundaries, oil is contained in what is commonly referred to as *gross pay*. *Net pay* is that part of the reservoir thickness that contributes to oil recovery and is defined by imposing the following criteria:

- Lower limit of porosity.
- Lower limit of permeability.
- Upper limit of water saturation.

All available measurements performed on reservoir samples and in wells, such as core analysis and well logs, are extensively used in evaluating the reservoir net thickness.

The choice of lower limits of porosity and permeability will depend upon such individual characteristics as

- Total reservoir volume.
- Total range of permeability values.
- Total range of porosity values.
- Distribution of the permeability and porosity values.

SECTION 2.9 RESERVOIR HETEROGENEITY

It has been proposed that most reservoirs are laid down in a body of water by a long-term process, spanning a variety of depositional environments, in both time and space. As a result of subsequent physical and chemical reorganization, such as compaction, solution, dolomitization, and cementation, the reservoir characteristics are further changed. Thus, the heterogeneity of reservoirs is, for the most part, dependent upon the depositional environments and subsequent events.

The main geologic characteristic of all the physical rock properties that have a bearing on reservoir behavior when producing oil and gas is the extreme variability in such properties within the reservoir itself, both laterally and vertically, and within short distances. It is important to recognize that there are no homogeneous reservoirs, only varying degrees of heterogeneity.

The reservoir heterogeneity is then defined as a variation in reservoir properties as a function of space. Ideally, if the reservoir is homogeneous, measuring a reservoir property at any location will allow us to fully describe the reservoir. The task of reservoir description is very simple for homogeneous reservoirs. On the other hand, if the reservoir is heterogeneous, the reservoir properties vary as a function of spatial location. These properties may include permeability, porosity, thickness, saturation, faults and fractures, rock facies, and rock characteristics. For a proper reservoir description, we need to predict the variation in these reservoir

properties as a function of spatial location. There are essentially two types of heterogeneity:

- Vertical heterogeneity.
- Areal heterogeneity.

Geostatistical methods are used extensively in the petroleum industry to quantitatively describe the two types of reservoir heterogeneity. It is obvious that the reservoir may be nonuniform in all intensive properties such as permeability, porosity, wettability, and connate-water saturation. We will discuss heterogeneity of the reservoir in terms of permeability.

Vertical Heterogeneity

One of the first problems encountered by the reservoir engineer in predicting or interpreting fluid displacement behavior during secondary recovery and enhanced oil recovery processes is that of organizing and using the large amount of data available from core analysis. Permeabilities pose particular problems in organization because they usually vary by more than an order of magnitude between different strata. The engineer must then be able to

- Describe the degree of the vertical heterogeneity in mathematical terms, and
- Describe and define the proper permeability stratification of the pay zone. This task is commonly called the *zoning* or *layering problem*.

It is appropriate to be able to describe the degree of heterogeneity within a particular system in quantitative terms. The *degree of homogeneity* of a reservoir property is a number that characterizes the departure from uniformity or constancy of that particular measured property through the thickness of the reservoir. A formation is said to have a uniformity coefficient of zero in a specified property when that property is constant throughout the formation thickness. A completely heterogeneous formation has a uniformity coefficient of unity. Between the two extremes, formations have uniformity coefficients between 0 and 1. The following are the two most widely used descriptors of the vertical heterogeneity of the formation:

- Dykstra-Parsons permeability variation V.
- Lorenz coefficient L.

The Dykstra-Parsons Permeability Variation

Dykstra and Parsons (1950) introduced the concept of the permeability variation coefficient V, which is a statistical measure of nonuniformity of a set of data. It is generally applied to the property of permeability but can

be extended to treat other rock properties. It is generally recognized that the permeability data are log-normally distributed. That is, the geologic processes that create permeability in reservoir rocks appear to leave permeabilities distributed around the geometric mean. Dykstra and Parsons recognized this feature and introduced the permeability variation that characterizes a particular distribution. The required computational steps for determining the coefficient V are summarized next:

- Step 1. Arrange the core samples in decreasing permeability sequence, i.e., descending order.
- *Step* 2. For each sample, calculate the percentage of thickness with permeability greater than this sample.
- Step 3. Using log-probability graph paper, plot permeability values on the log scale and the percent of thickness on the probability scale. This special graph paper is shown in Figure 2-29.
- Step 4. Draw the best straight line through the points.

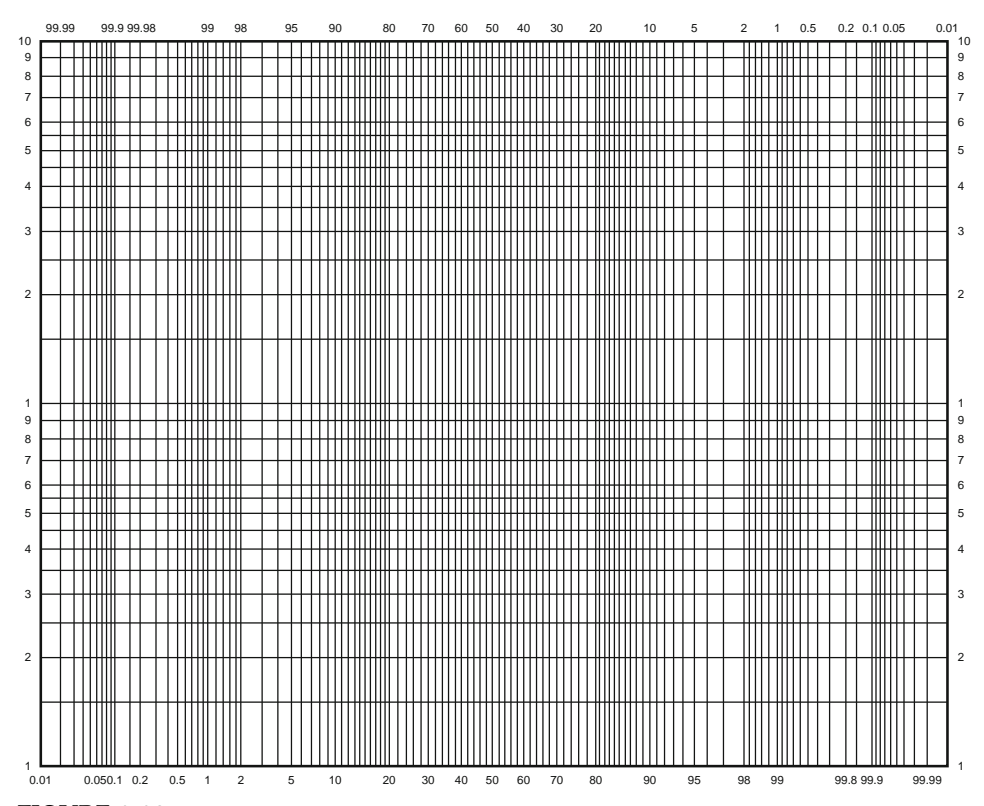


FIGURE 2-29 Probability-log scale.

Step 5. Read the corresponding permeability values at 84.1% and 50% of thickness. These two values are designated as $k_{84.1}$ and k_{50} .

Step 6. The Dykstra-Parsons permeability variation is defined by the following expression:

$$V = \frac{k_{50} - k_{84.1}}{k_{50}} \tag{2-70}$$

Example 2-18

The following conventional core analysis data are available from three wells:

Well #1			Well	#2		Well #3		
Depth ft	k md	ф %	Dept ft	k md	ф %	Dept ft	k md	ф %
5389–5391	166	17.4	5397-5398.5	72	15.7	5401-5403	28	14.0
-5393	435	18.0	-539.95	100	15.6	-5405	40	13.7
-5395	147	16.7	-5402	49	15.2	-5407	20	12.2
-5397	196	17.4	-5404.5	90	15.4	-5409	32	13.6
-5399	254	19.2	-5407	91	16.1	-5411	35	14.2
-5401	105	16.8	-5409	44	14.1	-5413	27	12.6
-5403	158	16.8	-5411	62	15.6	-5415	27	12.3
-5405	153	15.9	-5413	49	14.9	-5417	9	10.6
-5406	128	17.6	-5415	49	14.8	-5419	30	14.1
-5409	172	17.2	-5417	83	15.2			

Calculate the Dykstra-Parsons permeability variation.

Solution

Step 1. Arrange all of the permeability data in descending order and calculate percent of thickness with greater permeability as follows:

k, md	h, ft	h with greater k	% of h with greater k
435	2	0	0
254	2	2	3.6
196	2	4	7.1
172	3	6	10.7
166	2	9	16.1
158	2	11	19.6
153	2	13	23.2
147	2	15	26.8

128	1	17	30.4
105	2	18	32.1
100	1	20	35.7
91	2.5	21	37.5
90	2.5	23.5	42.0
83	2	26	46.4
72	1.5	28	50
62	2	29.5	52.7
49	6.5	31.5	56.3
44	2	38	67.9
40	2	40	71.4
35	2	42	75.0
32	2	44	78.6
30	2	46	82.1
28	2	48	85.7
27	2	50	89.3
20	2	52	92.9
9	2	54	96.4
	Total = 56'		

Step 2. Plot the permeability versus percent of thickness with greater k on a log-probability scale as shown in Figure 2-30 and read

$$k_{50} = 68 \text{ md}$$

 $k_{84.1} = 29.5$

Step 3. Calculate V by applying Equation 2-70.

$$V = \frac{68 - 29.5}{68} = 0.57$$

It should be noted that if all the permeabilities were equal, the numerator of Equation 2-70 would be 0, and the V would also be 0. This would be the case for a completely homogeneous system. The Dykstra-Parsons method is commonly referred to as a *permeability ordering technique*.

In water flooding calculations, it is frequently desired to divide the reservoir into layers that have equal thickness and different permeability. The log-probability scale can be used in this case to assign the permeability scale into equal percent increments and to read the corresponding permeability at the midpoint of each interval.

Example 2-19

Using the data given in Example 2-18, determine the average layer permeability for a 10-layered system, assuming a uniform porosity.

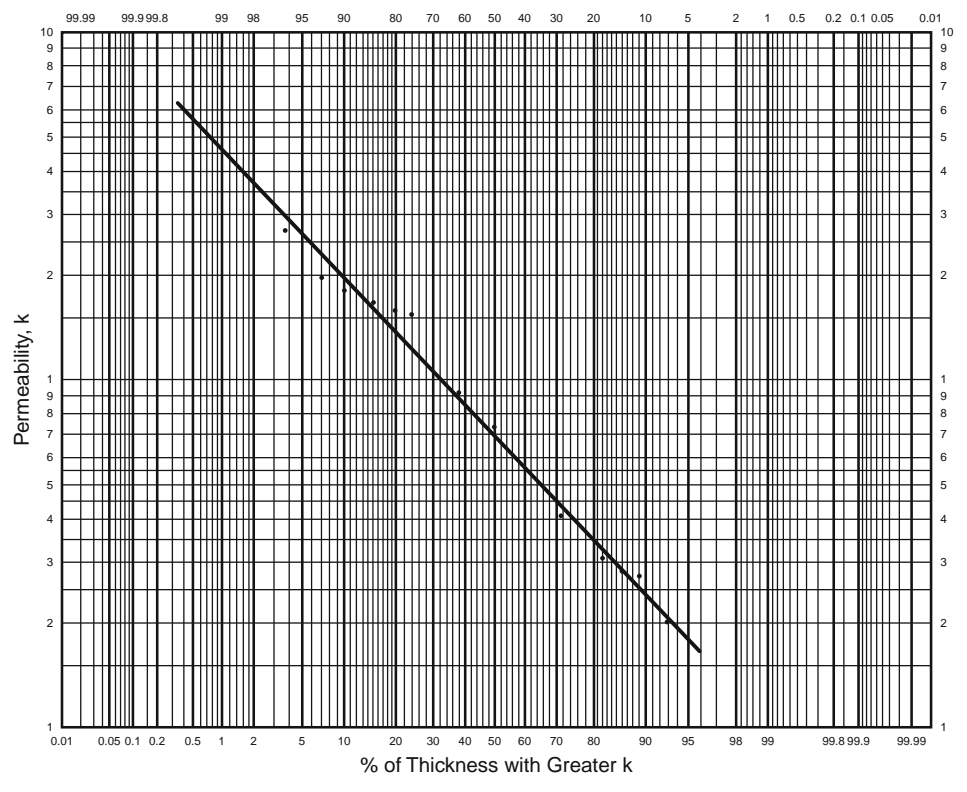


FIGURE 2-30 Percent of h versus k.

Solution

Using the Dykstra-Parsons's log-probability plot as shown in Figure 2-30, determine the permeability for the 10-layered system as follows:

Layer	% Probability	k, md
1	5	265
2	15	160
3	25	120
4	35	94
5	45	76
6	55	60
7	65	49
8	75	39
9	85	29
10	95	18

Although permeability and porosity are not related in a strict technical sense, they should correlate in rock of similar lithology and pore size distribution. In many cases, the logarithm of permeability versus porosity plots is frequently made and the best straight line is drawn through the points.

Lorenz Coefficient L

Schmalz and Rahme (1950) introduced a single parameter that describes the degree of heterogeneity within a pay zone section. The term is called the *Lorenz coefficient* and varies between 0, for a completely homogeneous system, and 1, for a completely heterogeneous system.

The following steps summarize the methodology of calculating the Lorenz coefficient:

- Step 1. Arrange all the available permeability values in descending order.
- Step 2. Calculate the cumulative permeability capacity Σ kh and cumulative volume capacity Σ ϕ h.
- *Step 3.* Normalize both cumulative capacities such that each cumulative capacity ranges from 0 to 1.
- Step 4. Plot the normalized cumulative permeability capacity versus the normalized cumulative volume capacity on a Cartesian scale.

Figure 2-31 shows an illustration of the flow capacity distribution. A completely uniform system would have all permeabilities equal,

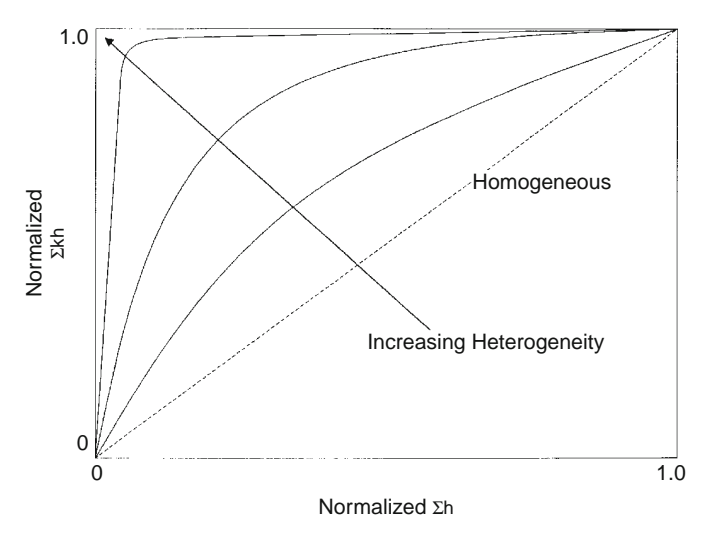


FIGURE 2-31 Normalized flow capacity.

and a plot of the normalized Σ kh versus Σ ϕ h would be a straight line. Figure 2-31 indicates that, as the degree of contrast between high and low values of permeability increases, the plot exhibits greater concavity toward the upper left corner. This would indicate more heterogeneity; i.e., the severity of deviation from a straight line is an indication of the degree of heterogeneity. The plot can be used to describe the reservoir heterogeneity quantitatively by calculating the Lorenz coefficient. The coefficient is defined by the following expression:

$$L = \frac{\text{area above the straight line}}{\text{area below the straight line}}$$
 (2-71)

where the Lorenz coefficient L can vary between 0 and 1:

0 = completely homogeneous1 = completely heterogeneous

Figure 2-32 shows the relation of the permeability variation V and Lorenz coefficient L for log-normal permeability distributions as proposed by Warren and Price (1961). This relationship can be expressed mathematically by the following two expressions.

Lorenz coefficient in terms of permeability variation:

$$L = 0.0116356 + 0.339794 V + 1.066405 V^{2} - 0.3852407 V^{3}$$
 (2-72)

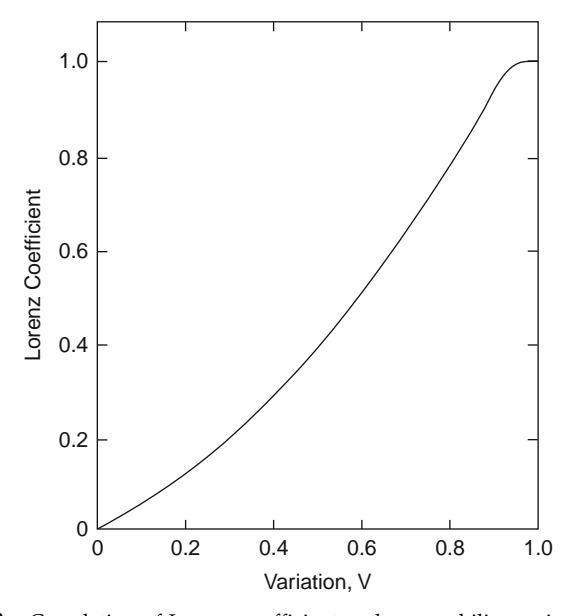


FIGURE 2-32 Correlation of Lorenz coefficient and permeability variation.

Permeability variation in terms of Lorenz coefficient:

$$V = -5.05971(10^{-4}) + 1.747525 L - 1.468855 L^2 + 0.701023 L^3$$
 (2-73)

These two expressions are applicable between 0 < L < 1 and 0 < V < 1.

Example 2-20

Using the data given in Example 2-18, calculate the Lorenz coefficient assuming a uniform porosity.

Solution

Step 1. Tabulate the permeability data in descending order and calculate the normalized Σ kh and Σ h as shown in the table:

k, md	h, ft	kh	Σ kh	Σkh/5646.5	Σh	Σh/56
435	2	870	870	0.154	2	0.036
254	2	508	1378	0.244	4	0.071
196	2	392	1770	0.313	6	0.107
172	3	516	2286	0.405	9	0.161
166	2	332	2618	0.464	11	0.196
158	2	316	2934	0.520	13	0.232
153	2	306	3240	0.574	15	0.268
147	2	294	3534	0.626	17	0.304
128	1	128	3662	0.649	18	0.321
105	2	210	3872	0.686	20	0.357
100	1	100	3972	0.703	21	0.375
91	2.5	227.5	4199.5	0.744	23.5	0.420
90	2.5	225	4424.5	0.784	26	0.464
83	2	166	4590.5	0.813	28	0.50
72	1.5	108	4698.5	0.832	29.5	0.527
62	2	124	4822.5	0.854	31.5	0.563
49	6.5	294	5116.5	0.906	38.0	0.679
44	2	88	5204.5	0.922	40.0	0.714
40	2	80	5284.5	0.936	42	0.750
35	2	70	5354.4	0.948	44	0.786
32	2	64	5418.5	0.960	46	0.821
30	2	60	5478.5	0.970	48	0.857
28	2	56	5534.5	0.980	50	0.893
27	2	54	5588.5	0.990	52	0.929
20	2	40	5628.5	0.997	54	0.964
9	2	18	5646.5	1.000	56	1.000

Step 2. Plot the normalized capacities on a Cartesian scale as shown in Figure 2-33.

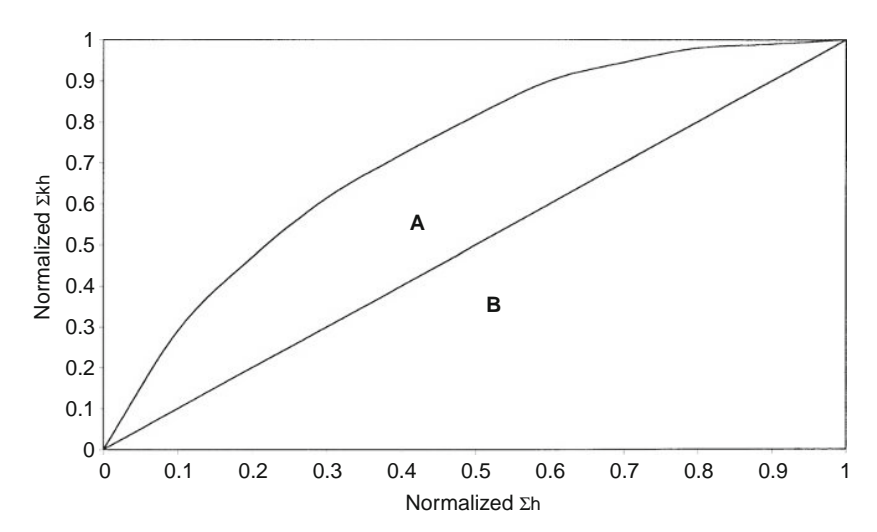


FIGURE 2-33 Normalized flow capacity for Example 2-20.

Step 3. Calculate the Lorenz coefficient by dividing the area above the straight line (area A) by the area under the straight line (area B) to give

$$L = 0.42$$

A plot of the cumulative permeability capacity Σ kh versus Σ h (without normalization) is commonly constructed as shown in Figure 2-34 and used to assign average permeability values for a selected number of reservoir layers. If the intervals of the thickness are chosen as shown in Figure 2-34, then the average values of permeability for each thickness interval (layer) can be calculated by dividing the incremental (kh) by the incremental thickness.

It should be noted that it is not necessary that equal thickness sections be chosen. They may be selected at irregular increments as desired. There are also some advantages to selecting layer properties so that each layer has the same permeability thickness product.

Example 2-21

Using the data given in Example 2-18, calculate the average permeability for a 10-layered system reservoir. Compare the results with those of the Dykstra-Parsons method.

Solution

Step 1. Using the calculated values of Σ kh and Σ h of Example 2-20, plot Σ kh versus Σ h on a Cartesian coordinate scale as shown in Figure 2-35.

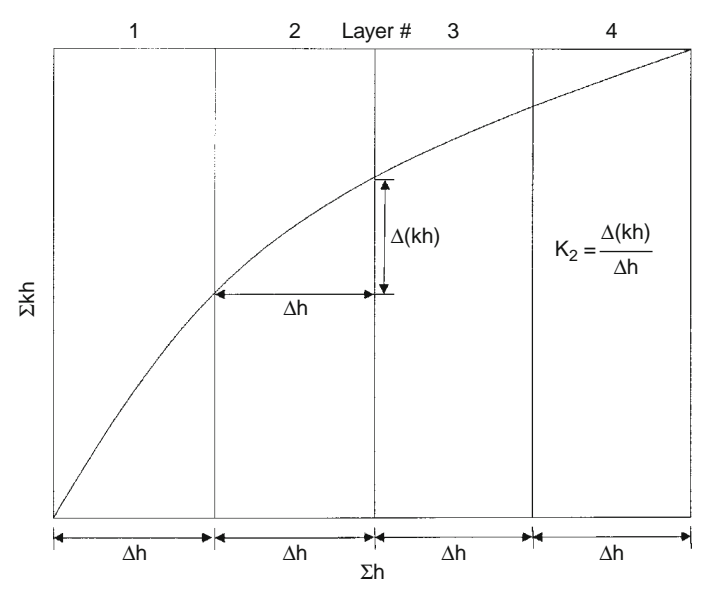


FIGURE 2-34 Cumulative permeability capacity versus cumulative thickness.

Step 2. Divide the x-axis into 10 equal segments,* each with 5.6 ft.

Step 3. Calculate the average permeability \bar{k} for each interval, to give

Layer	$\bar{\mathbf{k}}$	$ar{k}$ from Dykstra-Parsons, Example 2-19
1	289	265
2	196.4	160
3	142.9	120
4	107.1	94
5	83.9	76
6	67.9	60
7	44.6	49
8	35.7	39
9	32.1	29
10	17.2	18

The permeability sequencing (ordering) methods of zonation do not consider the physical location of the rocks within the vertical column. All the data are considered to be a statistical sampling, which will describe the statistical distribution of permeability, porosity, and

^{*}It should be noted that the 56 ft *does not* equal the reservoir net thickness. It essentially represents the cumulative thickness of the core samples.

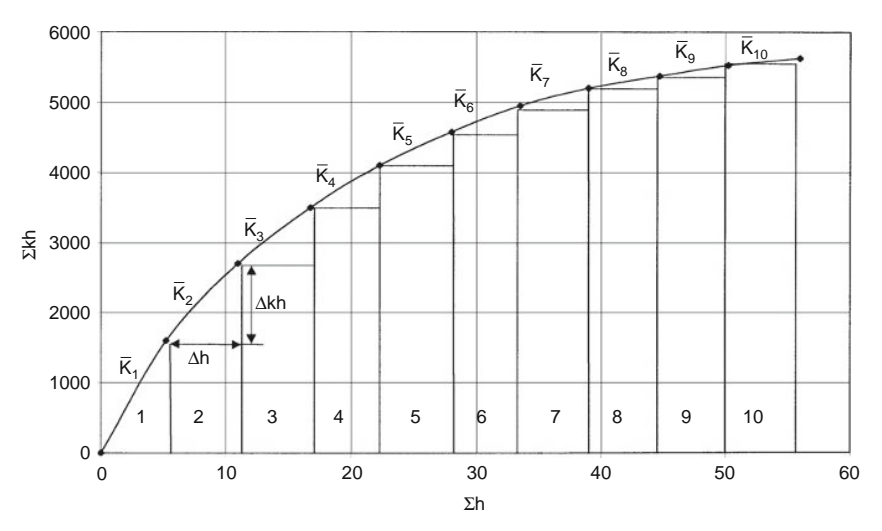


FIGURE 2-35 Cumulative kh versus cumulative h (Example 2-21).

thickness within the reservoir. All the values of equal permeability are presumed to be in communication with each other.

Miller and Lents (1947) suggested that the fluid movement in the reservoir remains in the same relative vertical position, i.e., remains in the same elevation, and that the permeability in this elevation (layer) is better described by the *geometric mean average permeability*. This method is called the *positional method*. Thus, to describe the layering system, or a reservoir using the positional approach, it is necessary to calculate the geometric mean average permeability (Equations 2-54 and 2-55) for each elevation and treat each of these as an individual layer.

SECTION 2.10 AREAL HETEROGENEITY

Since the early stages of oil production, engineers have recognized that most reservoirs vary in permeability and other rock properties in the lateral direction. To understand and predict the behavior of an underground reservoir, one must have as accurate and detailed knowledge as possible of the subsurface. Indeed, water and gas displacement is conditioned by the storage geometry (structural shape, thickness of strata) and the local values of the physical parameters (variable from one point to another) characteristic of the porous rock. Hence, prediction accuracy is closely related to the detail in which the reservoir is described.

Johnson, Careenkorn, and Woods (1966) devised a well testing procedure, called *pulse testing*, to generate rock properties data between wells. In this procedure, a series of producing rate changes or pluses is made at

one well with the response being measured at adjacent wells. The technique provides a measure of the formation flow capacity (kh) and storage capacity (ϕ h). The most difficult reservoir properties to define usually are the level and distribution of permeability. They are more variable than porosity and more difficult to measure. Yet an adequate knowledge of permeability distribution is critical to the prediction of reservoir depletion by any recovery process.

A variety of geostatistical estimation techniques has been developed in an attempt to describe accurately the spatial distribution of rock properties. The concept of spatial continuity suggests that data points close to one another are more likely to be similar than are data points farther apart from one another. One of the best geostatistical tools to represent this continuity is a visual map showing a data set value with regard to its location. Automatic or computer contouring and girding are used to prepare these maps. These methods involve interpolating between known data points, such as elevation or permeability, and extrapolating beyond these known data values. These rock properties are commonly called *regionalized variables*. These variables usually have the following contradictory characteristics:

- A random characteristic showing erratic behavior from point to point.
- A structural characteristic reflecting the connections among data points.

For example, net thickness values from a limited number of wells in a field may show randomness or erratic behavior. They also can display a connecting or smoothing behavior as more wells are drilled or spaced close together.

To study regionalized variables, a proper formulation must take this double aspect of randomness and structure into account. In geostatistics, a variogram is used to describe the randomness and spatial correlations of the regionalized variables.

Several conventional interpolation and extrapolation methods can be applied to values of a regionalized variable at different locations. Most of these methods use the following generalized expression:

$$Z^{*}(x) = \sum_{i=1}^{n} \lambda_{i} Z(x_{i})$$
 (2-74)

with

$$\sum_{i=1}^{R} \lambda_i = 1 \tag{2-75}$$

where $Z^*(x)$ = estimate of the regionalized variable at location x

 $Z(x_i)$ = measured value of the regionalized variable at position x_i

 λ_i = weight factor

n = number of nearby data points

The difference between the commonly used interpolation and extrapolation methods is in the mathematical algorithm employed to compute the weighting factors λ_i . Compared to other interpolation methods, the geostatistical originality stems from the intuition that the accuracy of the estimation at a given point (and the λ_i) depends on two factors, the first one being of a geometrical nature, the second related to the statistical spatial characteristics of the considered phenomenon.

The first factor is the geometry of the problem that is the relative positions of the measured points to the one to be estimated. When a point is well surrounded by experimental points, it can be estimated with more accuracy than one located in an isolated area. This fact is taken into account by classical interpolation methods (polynomial, multiple regression, least-squares) but these appear to be inapplicable as soon as the studied phenomenon shows irregular variations or measurement errors.

Five simple conventional interpolation and/or extrapolation methods are briefly discussed next:

- The Polygon Method. This technique is essentially based on assigning the nearest measured value of the regionalized variable to the designated location. This implies that all the weighting factors, i.e., λ_i , in Equation 2-72 are set equal to 0 except the corresponding λ_i for the nearest point, which is set equal to 1.
- The Inverse Distance Method. With *inverse distance*, data points are weighted during interpolation such that the influences of one data point relative to another decline with distance from the desired location. The inverse distance method assigns a weight factor λ_i to each measured regionalized variable by the inverse distance between the measured value and the point being estimated, or

$$\lambda_{i} = \left(\frac{1}{d_{i}}\right) / \sum_{i=1}^{n} \left(\frac{1}{d_{i}}\right) \tag{2-76}$$

where d_i = distance between the measured value and location of interest

n = number of nearby points

• The Inverse Distance Squared Method. This method assigns a weight to each measured regionalized variable by the inverse distance squared of the sample to the point being estimated, i.e.,

$$\lambda_{i} = \left(\frac{1}{d_{i}}\right)^{2} / \sum_{i=1}^{n} \left(\frac{1}{d_{i}}\right)^{2} \tag{2-77}$$

While this method accounts for all nearby wells with recorded rock properties, it gives proportionately more weight to near wells than the previous method.

Example 2-22

Figure 2-36 shows a schematic illustration of the locations of four wells and distances between the wells and point x. The average permeability in each well location follows:

Well #	Permeability, md
1	73
2	110
3	200
4	140

Estimate the permeability at location x by the polygon method and the two inverse distance methods.

Solution

The Polygon Method The well location nearest to point x is Well #1 with a distance of 170 ft. The recorded average permeability at this well is 73 md; therefore, the permeability in location x is

$$k = (1)(73) + (0)(110) + (0)(200) + (0)(140) = 73 \ md$$

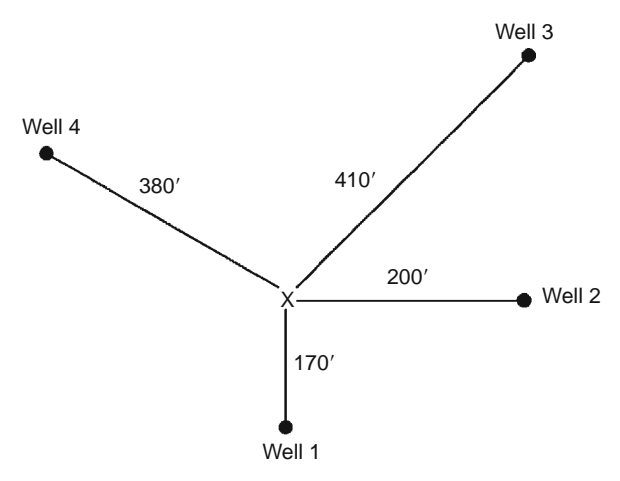


FIGURE 2-36 Well locations for Example 2-22.

The Inverse Distance Method

Step 1. Calculate the weighting factors by applying Equation 2-76:

Distance d _i ft	1/d _i	$\lambda_i = (1/d_i)/0.0159$	k, md
170	0.0059	0.3711	73
200	0.0050	0.3145	110
410	0.0024	0.1509	200
380	0.0026	0.1635	140
	Sum = 0.0159		

Step 2. Estimate the permeability at location x by applying Equation 2-74:

$$k = (0.3711)(73) + (0.3145)(110) + (0.1509)(200) + (0.1635)(140)$$
 = 114.8 md

The Inverse Distance Squared Method

Step 1. Apply Equation 2-77 to determine the weighting factors.

d _i , ft	$(1/d_i)^2$	$\lambda_i = (1/d_i)^2/0.00007$	k, md
170	0.000035	0.4795	73
200	0.000025	0.3425	110
410	0.00006	0.0822	200
380	0.000007	0.958	140
	Sum = 0.000073		

Step 2. Estimate the permeability in location x by using Equation 2-72:

$$k = (0.4795)(73) + (0.3425)(110) + (0.0822)(200) + (0.0958)(140)$$

= 102.5 md

• The Triangulation Method. The triangulation method is designed to remove possible discontinuities between adjacent points by fitting a plane through three samples that surround the point being estimated. The method is based on selecting the nearest three locations with measured data values that form a triangle, as shown in Figure 2-37.

The equation of the plane can be expressed generally as

$$Z = ax + by + c$$

where Z is a regionalized value, for example, permeability, k, at the coordinate "x and y." Given the coordinates and the regionalized

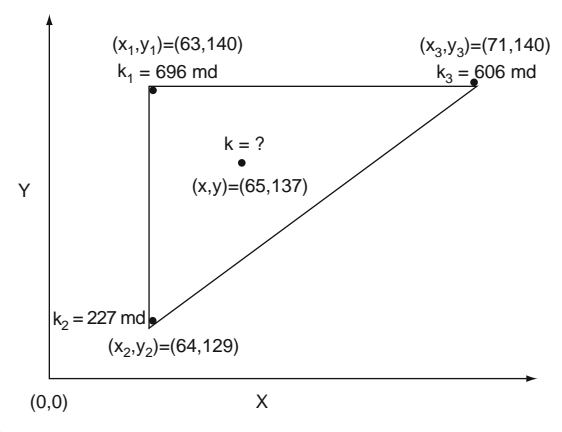


FIGURE 2-37 Triangulation method.

value of three nearby samples, as shown in Figure 2-37 for absolute permeabilities, the coefficients a, b, and c can be determined by solving the following three equations:

$$\begin{aligned} k_1 &= a\,x_1 + by_1 + c \\ k_2 &= a\,x_2 + by_2 + c \\ k_3 &= a\,_{x3} + by_3 + c \end{aligned}$$

Substituting permeability values and coordinates into this system of equations gives

$$63 a + 140 b + c = 696$$

 $64 a + 129 b + c = 227$
 $71 a + 140 b + c = 606$

Solving these three expressions yields

$$a = -11.25$$
 $b = 41.614$ $c = -4421.159$

or

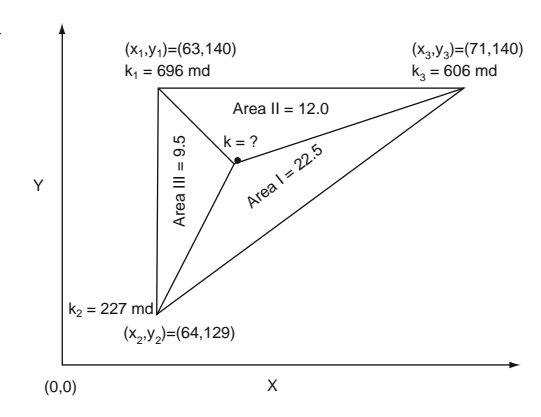
$$k = -11.25 x + 41.614 y - 4421.159$$

This relationship estimates the value of permeability at any location within that specific triangular. To estimate the permeability at the coordinates (x,y) = (65,137), then,

$$k = -11.25(65) + 41.614(137) - 4421.159 = 548.7 \,\text{md}$$

• **Delaunay Triangulation.** Figure 2-38 shows the Delaunay triangle for the same samples given in Figure 2-37 for the triangulation method. The sample permeability values at these locations are k₁, k₂, and k₃. Instead of solving the three simultaneous equations and substituting

FIGURE 2-38 Delaunay triangulation method.



the coordinates of the point of interest into the solution, the permeability value can be directly calculated from

$$k = \frac{(k_1)(\text{area I}) + (k_1)(\text{area II}) + (k_3)(\text{area III})}{(\text{area I}) + (\text{area II}) + (\text{area III})}$$

The triangulation method is essentially a weighted linear combination in which each value is weighted according to the *area of the opposite triangle*. Using the data given in Figure 2-38, the permeability value at the designated location is

$$k = \frac{(k_1)(\text{area I}) + (k_1)(\text{area II}) + (k_3)(\text{area III})}{(\text{area I}) + (\text{area II}) + (\text{area III})}$$

$$k = \frac{(696)(22.25) + (227)(12.0) + (606)(9.5)}{(22.25) + (12) + (9.5)} = 548.7 \, \text{md}$$

SECTION 2.11 PROBLEMS

1. Given

$$\begin{array}{lll} p_i = 3{,}500 & p_b = 3{,}500 & T = 160^\circ F \\ A = 1{,}000 \, acres & h = 25 \, ft & S_{wi} = 30\% \\ \varphi = 12\% & API = 45^\circ & R_{sb} = 750 \, scf/STB \\ \gamma_g = 0.7 & \end{array}$$

calculate

- a. Initial oil in place as expressed in STB.
- b. Volume of gas originally dissolved in the oil.

					•1 1 1
2. The following	measurements o	n nav	70ne	are	available.
Z. THE TOHOWING	incubal circino o	II Puy	LOTIC	uic	avanabic.

Sample	Thickness, ft	ф, %	S _{oi} , %
1	2	12	75
2	3	16	74
3	1	10	73
4	4	14	76
5	2	15	75
6	2	15	72

Calculate

- a. Average porosity.
- b. Average oil and water saturations (assuming no gas).
- 3. The capillary pressure data for a water-oil system follow:

S_{w}	P_c
0.25	35
0.30	16
0.40	8.5
0.50	5
1.0	0

The core sample used in generalizing the capillary pressure data was taken from a layer that is characterized by an absolute permeability of 300 md and a porosity of 17%. Generate the capillary pressure data for a different layer that is characterized by a porosity and permeability of 15%, 200 md, respectively. The interfacial tension is measured at 35 dynes/cm.

4. A five-layer oil reservoir is characterized by a set of capillary pressure-saturation curves as shown in Figure 2-6. The following additional data are also available:

Layer	Depth, ft	Permeability
1	6000–6016	10
2	6016-6025	300
3	6025-6040	100
4	6040-6055	30
5	6055-6070	3

- WOC = 6.070 ft
- Water density = 65 lb/ft^3
- Oil density = 32 lb/ft^3

Calculate and plot the water and oil saturation profiles for this reservoir.

5. Assuming a steady-state laminar flow, calculate the permeability from the following measurement made on a core sample by using air:

$$\begin{array}{ll} flow \ rate = 2cm^3/sec & T = 65^\circ F \\ upstream \ pressure = 2 \ atm & downstream \ pressure = 1 \ atm \\ A = 2 \ cm^2 & L = 3 \ cm & viscosity = 0.018 \ cp \end{array}$$

6. Calculate average permeability from the following core analysis data:

Depth, ft	k, md
4000–4002	50
4002-4005	20
4005-4006	70
4006-4008	100
4008-4010	85

- 7. Calculate the average permeability of a formation that consists of four beds in series, assuming
 - a. Linear system.
 - b. Radial system with $r_w = 0.3$ and $r_e = 1,450$ ft.

Bed	Length of bed linear or radial	k, md
1	400	70
2	250	400
3	300	100
4	500	60

- 8. Estimate the absolute permeability of a formation that is characterized by an average porosity and connate-water saturation of 15% and 20% md, respectively.
- 9. Given

Depth, ft	k, md
4100–4101	295
4101-4102	262
4102-4103	88
4103-4104	87
4104-4105	168
4105–4106	71
4106-4107	62
4107-4108	187

4109-4110 77 4110-4111 127 4111-4112 161 4112-4113 50 4113-4114 58 4114-4115 109 4115-4116 228 4116-4117 282 4117-4118 776 4118-4119 87 4119-4120 47 4120-4121 16 4121-4122 35 4122-4123 47 4123-4124 54 4124-4125 273 4125-4126 454 4126-4127 308 4127-4128 159	4108-4109	369
4111-4112 161 4112-4113 50 4113-4114 58 4114-4115 109 4115-4116 228 4116-4117 282 4117-4118 776 4118-4119 87 4119-4120 47 4120-4121 16 4121-4122 35 4122-4123 47 4123-4124 54 4124-4125 273 4125-4126 454 4126-4127 308 4127-4128 159	4109-4110	77
4112-4113 50 4113-4114 58 4114-4115 109 4115-4116 228 4116-4117 282 4117-4118 776 4118-4119 87 4119-4120 47 4120-4121 16 4121-4122 35 4122-4123 47 4123-4124 54 4124-4125 273 4125-4126 454 4126-4127 308 4127-4128 159	4110-4111	127
4113-4114 58 4114-4115 109 4115-4116 228 4116-4117 282 4117-4118 776 4118-4119 87 4119-4120 47 4120-4121 16 4121-4122 35 4122-4123 47 4123-4124 54 4124-4125 273 4125-4126 454 4126-4127 308 4127-4128 159	4111-4112	161
4114-4115 109 4115-4116 228 4116-4117 282 4117-4118 776 4118-4119 87 4119-4120 47 4120-4121 16 4121-4122 35 4122-4123 47 4123-4124 54 4124-4125 273 4125-4126 454 4126-4127 308 4127-4128 159	4112-4113	50
4115-4116 228 4116-4117 282 4117-4118 776 4118-4119 87 4119-4120 47 4120-4121 16 4121-4122 35 4122-4123 47 4123-4124 54 4124-4125 273 4125-4126 454 4126-4127 308 4127-4128 159	4113-4114	58
4116-4117 282 4117-4118 776 4118-4119 87 4119-4120 47 4120-4121 16 4121-4122 35 4122-4123 47 4123-4124 54 4124-4125 273 4125-4126 454 4126-4127 308 4127-4128 159	4114-4115	109
4117-4118 776 4118-4119 87 4119-4120 47 4120-4121 16 4121-4122 35 4122-4123 47 4123-4124 54 4124-4125 273 4125-4126 454 4126-4127 308 4127-4128 159	4115-4116	228
4118-4119 87 4119-4120 47 4120-4121 16 4121-4122 35 4122-4123 47 4123-4124 54 4124-4125 273 4125-4126 454 4126-4127 308 4127-4128 159	4116-4117	282
4119-4120 47 4120-4121 16 4121-4122 35 4122-4123 47 4123-4124 54 4124-4125 273 4125-4126 454 4126-4127 308 4127-4128 159	4117-4118	776
4120-4121 16 4121-4122 35 4122-4123 47 4123-4124 54 4124-4125 273 4125-4126 454 4126-4127 308 4127-4128 159	4118-4119	87
4121-4122 35 4122-4123 47 4123-4124 54 4124-4125 273 4125-4126 454 4126-4127 308 4127-4128 159	4119-4120	47
4122-4123 47 4123-4124 54 4124-4125 273 4125-4126 454 4126-4127 308 4127-4128 159	4120-4121	16
4123-4124 54 4124-4125 273 4125-4126 454 4126-4127 308 4127-4128 159	4121-4122	35
4124-4125 273 4125-4126 454 4126-4127 308 4127-4128 159	4122-4123	47
4125–4126 454 4126–4127 308 4127–4128 159	4123-4124	54
4126–4127 308 4127–4128 159	4124-4125	273
4127–4128 159	4125-4126	454
	4126-4127	308
	4127–4128	159
4128–4129 178	4128–4129	178

calculate

- a. Average permeability.
- b. Permeability variation.
- c. Lorenz coefficient.
- d. Permeability for each layer, assuming four-layer reservoir system with equal length.
- 10. Three layers 4, 6, and 10 ft thick, respectively, are conducting fluid in parallel flow. The depth to the top of the first layer is recorded as 5,012 ft. A core analysis report shows the following permeability data for each layer.

Layer #1		Layer #2		Layer #3	
Depth ft	Permeability md	Depth ft	Permeability md	Depth ft	Permeability md
5012–5013	485	5016–5017	210	5022-5023	100
5013-5014	50	5017-5018	205	5023-5024	95
5014-5015	395	5018-5019	60	5024-5025	20
5015-5016	110	5019-5020	203	5025-5026	96
		5020-5021	105	5026-5027	98
		5021-5022	195	5027-5028	30
				5028-5029	89
				5029-5030	86
				5030-5031	90
				5031-5032	10

Calculate the *average* permeability of the entire pay zone (i.e., 5,012–5,032 ft).

11. A well has a radius of 0.25 ft and a drainage radius of 660 ft. The sand that penetrates is 15 ft thick and has an absolute permeability of 50 md. The sand contains crude oil with the following PVT properties:

Pressure, psia	B _o , bbl/STB	μ ₀ , cp	
3500	1.827	1.123	
3250	1.842	1.114	
3000	1.858	1.105	
2746*	1.866	1.100	
2598	1.821	1.196	
2400	1.771	1.337	
2200	1.725	1.497	
600	1.599	2.100	

^{*}Bubble point.

The reservoir pressure (i.e., p_e) and the bubble-point pressure are 3,500 and 2,746 psia, respectively. If the bottom-hole flowing pressure is 2,500 psia, calculate the oil-flow rate.

12. Test runs on three core samples from three wells in a mythical field yielded the following three sets of values for water saturation (S_w) , porosity (ϕ) , and permeability (k). It is believed that these three properties can be used to determine the recovery fraction (RF).

Core 1	Core 2	Core 3
0.185	0.157	0.484
0.476	0.527	0.637
0.614	0.138	0.799
0.283	0.212	0.141
	0.185 0.476 0.614	0.185 0.157 0.476 0.527 0.614 0.138

The recovery factor can be expressed by the following equation:

$$RF = a_o \, \varphi + a_1 \, S_w + a_2 \, k$$

where a_0 , a_1 , and a_2 are constants.

Calculate RF if

$$S_w = 0.75, \, \varphi = 0.20, \text{and } k = 0.85$$

SECTION 2.12 REFERENCES

- J.R. Calhoun, Fundamentals of Reservoir Engineering, University of Oklahoma Press, 1976.
- [2] F. Cole, Reservoir Engineering Manual, Gulf Publishing Company, Houston, 1969.
- [3] H. Dykstra, and R.L. Parsons, In The Prediction of Oil Recovery by Water Flood, in: Secondary Recovery of Oil in the United States, second ed., API, 1950, pp. 160–174.
- [4] J. Geertsma, The Effect of Fluid Pressure Decline on Volumetric Changes of Porous Rocks, Trans. AIME (1957) 210, 331–340.
- [5] H.N. Hall, Compressibility of Reservoir Rocks, Trans. AIME (1953) 309.
- [6] O. Hustad, and H. Holt, Gravity Stable Displacement of Oil by Gas after Water Flooding, in: SPE Paper 24116, SPE/DOE Symposium on EOR, Tulsa, OK, April 22–24, 1972.
- [7] C.R. Johnson, R.A. Careenkorn, and E.G. Woods, Pulse Testing: A New Method for Describing Reservoir Flow Properties between Wells, JPT (1966) 1599–1604.
- [8] S.C. Jones, A Rapid Accurate Unsteady State Klinkenberg Parameter, SPEJ 12(5) (1972) 383–397.
- [9] L.J. Klinkenberg, The Permeability of Porous Media to Liquids and Gases, in: API Drilling and Production Practice, 1941, p. 200.
- [10] M.C. Leverett, Capillary Behavior in Porous Solids, Trans. AIME (1941).
- [11] W.M. McCardell, A Review of the Physical Basis for the Use of the J-Function, Eighth Oil Recovery Conference, Texas Petroleum Research Committee, 1955.
- [12] M.G. Miller, M.R. Lents, Performance of Bodcaw Reservoir, Cotton Valley Field Cycling Project: New Methods of Predicting Gas-Condensate Reservoir, SPEJ (1966) 239
- [13] R.L. Morris, W.P. Biggs, Using Log-Derived Values of Water Saturation and Porosity, SPWLA Paper X (1967).
- [14] G.H. Newman, Pore-Volume Compressibility, JPT (1973) 129–134.
- [15] J.P. Schmalz, H.D. Rahme, The Variation of Waterflood Performance with Variation in Permeability Profile, Prod. Monthly 15(9) (1950) 9–12.
- [16] A. Timur, An Investigation of Permeability, Porosity, and Residual Water Saturation Relationships, AIME (1968).
- [17] J.E. Warren, and H.S. Price, Flow in Heterogeneous Porous Media, SPEJ (1961) 153–169.

Fundamentals of Reservoir Fluid Flow

Flow in porous media is a very complex phenomenon and as such cannot be described as explicitly as flow through pipes or conduits. It is rather easy to measure the length and diameter of a pipe and compute its flow capacity as a function of pressure; in porous media, however, flow is different in that there are no clear-cut flow paths that lend themselves to measurement.

The analysis of fluid flow in porous media has evolved throughout the years along two fronts—the experimental and the analytical. Physicists, engineers, hydrologists, and the like, have examined experimentally the behavior of various fluids as they flow through porous media ranging from sand packs to fused Pyrex glass. On the basis of their analyses, they have attempted to formulate laws and correlations that can then be utilized to make analytical predictions for similar systems.

The main objective of this part is to present the mathematical relationships that are designed to describe the flow behavior of the reservoir fluids. The mathematical forms of these relationships will vary depending upon the characteristics of the reservoir. The primary reservoir characteristics that must be considered include

- Types of fluids in the reservoir.
- Flow regimes.
- Reservoir geometry.
- Number of flowing fluids in the reservoir.

SECTION 3.1 TYPES OF FLUIDS

The isothermal compressibility coefficient is essentially the controlling factor in identifying the type of the reservoir fluid. In general, reservoir fluids are classified into three groups:

- Incompressible fluids.
- Slightly compressible fluids.
- Compressible fluids.

The isothermal compressibility coefficient c is described mathematically by the following two equivalent expressions:

• In terms of fluid volume,

$$c = \frac{-1}{V} \frac{\partial V}{\partial p}$$
 (3-1)

• In terms of fluid density,

$$c = \frac{1}{\rho} \frac{\partial \rho}{\partial p} \tag{3-2}$$

• where V and ρ are the volume and density of the fluid, respectively.

Incompressible Fluids

An incompressible fluid is defined as the fluid whose volume (or density) does not change with pressure; i.e.,

$$\frac{\partial \mathbf{V}}{\partial \mathbf{p}} = 0$$

$$\frac{\partial \rho}{\partial p} = 0$$

Incompressible fluids do not exist; this behavior, however, may be assumed in some cases to simplify the derivation and the final form of many flow equations.

Slightly Compressible Fluids

These "slightly" compressible fluids exhibit small changes in volume, or density, with changes in pressure. Knowing the volume V_{ref} of a slightly compressible liquid at a reference (initial) pressure p_{ref} , the changes in the volumetric behavior of this fluid as a function of pressure p can be mathematically described by integrating Equation 3-1 to give

$$-c\int_{p_{ref}}^{p} dp = \int_{V_{ref}}^{V} \frac{dV}{V}$$

$$e^{c(p_{ref} - p)} = \frac{V}{V_{ref}}$$
(3-3)

$$V = V_{ref} \, e^{c \left(p_{ref} - p \right)}$$

where p = pressure, psia

 $V = volume at pressure p, ft^3$

 $p_{ref} = initial$ (reference) pressure, psia

 V_{ref} = fluid volume at initial (reference) pressure, psia

The e^x may be represented by a series expansion as

$$e^{x} = 1 + x + \frac{x^{2}}{2!} + \frac{x^{2}}{3!} + \dots + \frac{x^{n}}{n!}$$
 (3-4)

Because the exponent x [which represents the term c ($p_{ref} - p$)] is very small, the e^x term can be approximated by truncating Equation 3-4 to

$$e^{x} = 1 + x \tag{3-5}$$

Combining Equation 3-5 with Equation 3-3 gives

$$V = V_{ref} [1 + c(p_{ref} - p)]$$
 (3-6)

A similar derivation is applied to Equation 3-2 to give

$$\rho = \rho_{ref}[1-c(p_{ref}-p)] \tag{3-7} \label{eq:3-7}$$

where V = volume at pressure p

 $\rho = density \ at \ pressure \ p$

 $V_{ref} = volume \ at \ initial \ (reference) \ pressure \ p_{ref}$

 $\rho_{ref} = density$ at initial (reference) pressure p_{ref}

It should be pointed out that crude oil and water systems fit into this category.

Compressible Fluids

These are fluids that experience large changes in volume as a function of pressure. All gases are considered compressible fluids. The truncation of the series expansion, as given by Equation 3-5, is not valid in this category and the complete expansion as given by Equation 3-4 is used. The isothermal compressibility of any compressible fluid is described by the following expression:

$$c_{g} = \frac{1}{p} - \frac{1}{z} \left(\frac{\partial z}{\partial p} \right)_{T} \tag{3-8}$$

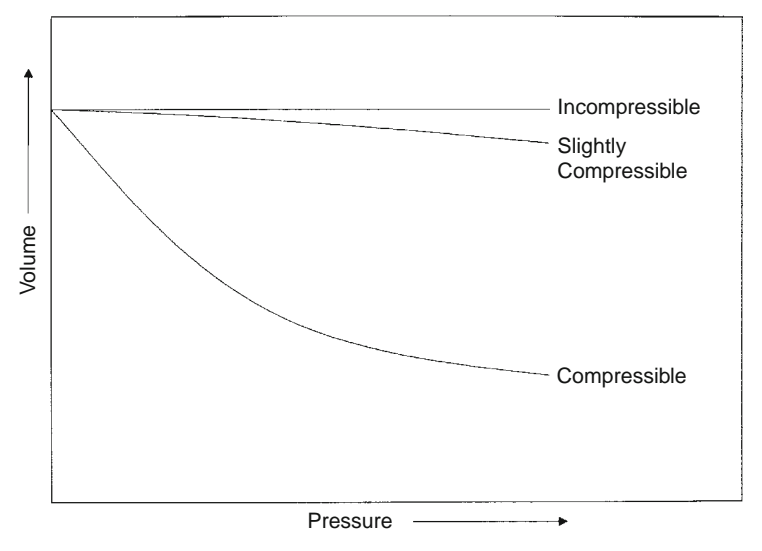


FIGURE 3-1 Pressure-volume relationship.

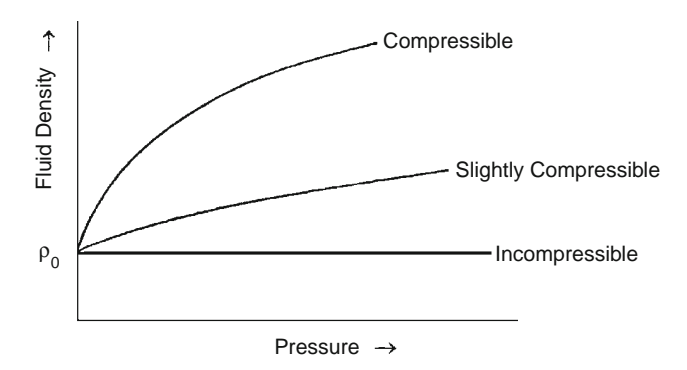


FIGURE 3-2 Fluid density versus pressure for different fluid types.

Figures 3-1 and 3-2 show schematic illustrations of the volume and density changes as a function of pressure for the three types of fluids.

SECTION 3.2 FLOW REGIMES

Basically, three types of flow regimes must be recognized in order to describe the fluid flow behavior and reservoir pressure distribution as a function of time:

- Steady-state flow.
- Unsteady-state flow.
- Pseudosteady-state flow.

Steady-State Flow

The flow regime is identified as a steady-state flow if the pressure at every location in the reservoir remains constant, i.e., does not change with time. Mathematically, this condition is expressed as

$$\left(\frac{\partial \mathbf{p}}{\partial \mathbf{t}}\right)_{\mathbf{i}} = 0 \tag{3-9}$$

This equation states that the rate of change of pressure p with respect to time t at any location i is 0. In reservoirs, the steady-state flow condition can occur only when the reservoir is completely recharged and supported by strong aquifer or pressure maintenance operations.

Unsteady-State Flow

The unsteady-state flow (frequently called *transient flow*) is defined as the fluid flowing condition at which the rate of change of pressure with respect to time at any position in the reservoir is not 0 or constant. This definition suggests that the pressure derivative with respect to time is essentially a function of both position i and time t; thus

$$\left(\frac{\partial \mathbf{p}}{\partial \mathbf{t}}\right) = \mathbf{f}(\mathbf{i}, \mathbf{t}) \tag{3-10}$$

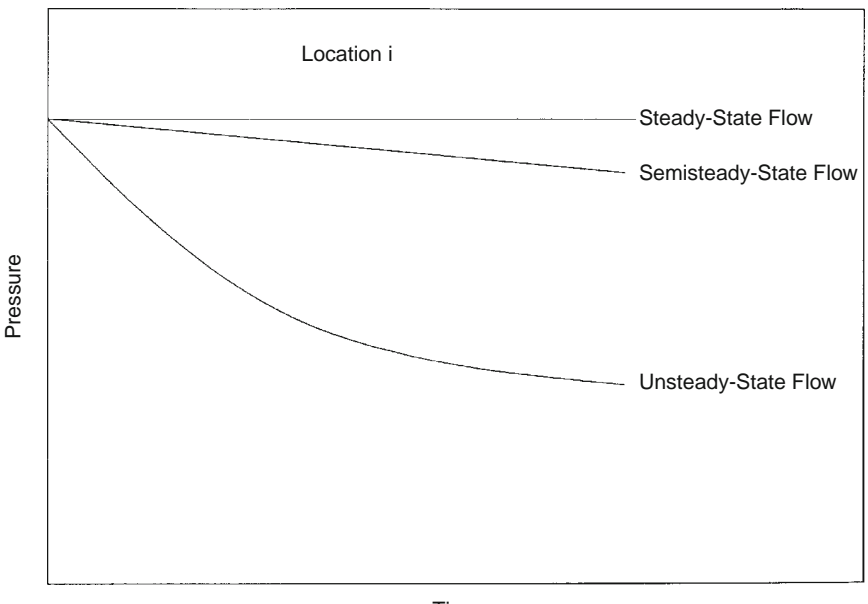
Pseudosteady-State Flow

When the pressure at different locations in the reservoir is declining linearly as a function of time, i.e., at a constant declining rate, the flowing condition is characterized as the pseudosteady-state flow. Mathematically, this definition states that the rate of change of pressure with respect to time at every position is constant, or

$$\left(\frac{\partial \mathbf{p}}{\partial \mathbf{t}}\right)_{\mathbf{i}} = \text{constant}$$
 (3-11)

It should be pointed out that the pseudosteady-state flow is commonly referred to as *semisteady-state flow* and *quasisteady-state flow*.

Figure 3-3 shows a schematic comparison of the pressure declines as a function of time of the three flow regimes.



Time

FIGURE 3-3 Flow regimes.

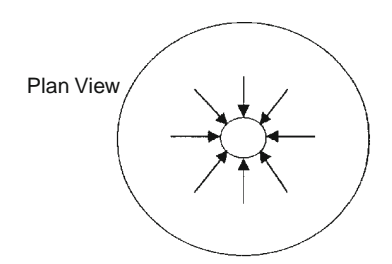
SECTION 3.3 RESERVOIR GEOMETRY

The shape of a reservoir has a significant effect on its flow behavior. Most reservoirs have irregular boundaries, and a rigorous mathematical description of geometry is often possible only with the use of numerical simulators. For many engineering purposes, however, the actual flow geometry may be represented by one of the following flow geometries:

- · Radial flow.
- · Linear flow.
- Spherical and hemispherical flow.

Radial Flow

In the absence of severe reservoir heterogeneities, flow into or away from a wellbore will follow radial flow lines from a substantial distance from the wellbore. Because fluids move toward the well from all directions and converge at the wellbore, the term *radial flow* is given to characterize the flow of fluid into the wellbore. Figure 3-4 shows idealized flow lines and iso-potential lines for a radial flow system.



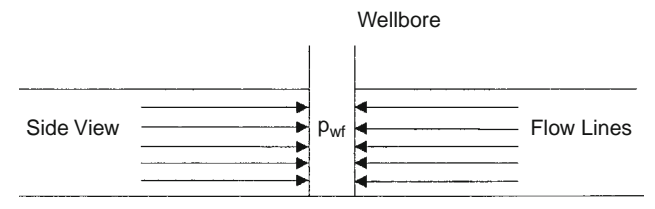


FIGURE 3-4 Ideal radial flow into a wellbore.

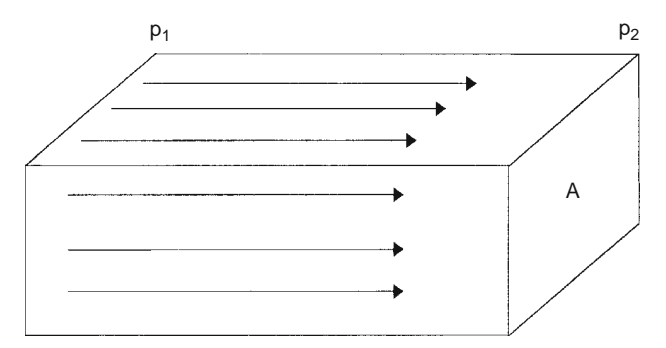


FIGURE 3-5 Linear flow.

Linear Flow

Linear flow occurs when flow paths are parallel and the fluid flows in a single direction. In addition, the cross-sectional area of flow must be constant. Figure 3-5 shows an idealized linear flow system. A common application of linear flow equations is the fluid flow into vertical hydraulic fractures, as illustrated in Figure 3-6.

Spherical and Hemispherical Flow

Depending upon the type of wellbore completion configuration, it is possible to have a spherical or hemispherical flow near the wellbore. A well

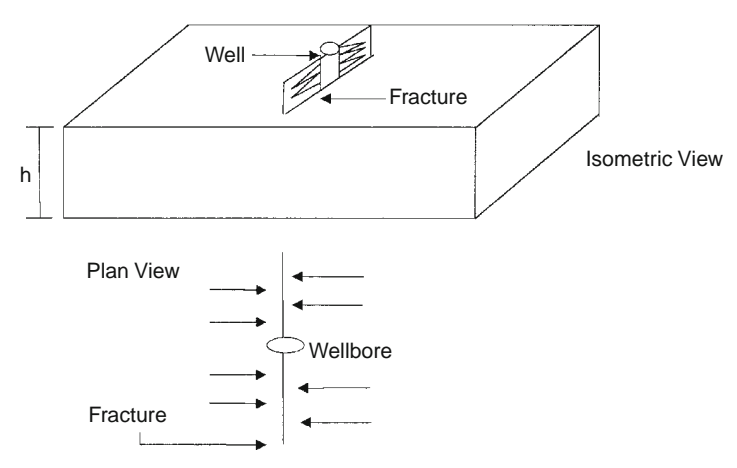


FIGURE 3-6 Ideal linear flow into vertical fracture.

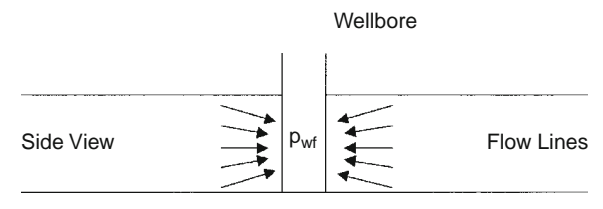


FIGURE 3-7 Spherical flow due to limited entry.

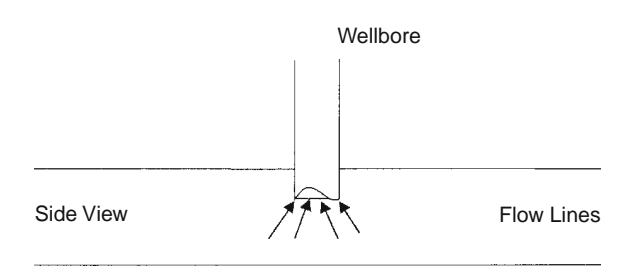


FIGURE 3-8 Hemispherical flow in a partially penetrating well.

with a limited perforated interval could result in spherical flow in the vicinity of the perforations, as illustrated in Figure 3-7. A well that only partially penetrates the pay zone, as shown in Figure 3-8, could result in hemispherical flow. The condition could arise where coning of bottom water is important.

SECTION 3.4 NUMBER OF FLOWING FLUIDS IN THE RESERVOIR

The mathematical expressions that are used to predict the volumetric performance and pressure behavior of the reservoir vary in form and complexity depending upon the number of mobile fluids in the reservoir. There are generally three cases of flowing systems:

- Single-phase flow (oil, water, or gas).
- Two-phase flow (oil-water, oil-gas, or gas-water).
- Three-phase flow (oil, water, and gas).

The description of fluid flow and subsequent analysis of pressure data become more difficult as the number of mobile fluids increases.

SECTION 3.5 FLUID FLOW EQUATIONS

The fluid flow equations that are used to describe the flow behavior in a reservoir can take many forms depending upon the combination of variables presented previously (i.e., types of flow, types of fluids, etc.). By combining the conservation of mass equation with the transport equation (Darcy's equation) and various equations of state, the necessary flow equations can be developed. Since all flow equations to be considered depend on Darcy's Law, it is important to consider this transport relationship first.

Darcy's Law

The fundamental law of fluid motion in porous media is Darcy's Law. The mathematical expression developed by Henry Darcy in 1856 states that the velocity of a homogeneous fluid in a porous medium is proportional to the pressure gradient and inversely proportional to the fluid viscosity. For a horizontal linear system, this relationship is

$$v = \frac{q}{A} = -\frac{k}{\mu} \frac{dp}{dx} \tag{3-12}$$

Here, v is the *apparent* velocity in centimeters per second and is equal to q/A, where q is the volumetric flow rate in cubic centimeters per second and A is the total cross-sectional area of the rock in square centimeters. In other words, A includes the area of the rock material as well as the area of the pore channels. The fluid viscosity, μ , is expressed in centipoise units, and the pressure gradient, dp/dx, is in atmospheres per centimeter, taken in the same direction as v and q. The proportionality constant, k, is the *permeability* of the rock expressed in darcy units.

The negative sign in Equation 3-12 is added because the pressure gradient is negative in the direction of flow, as shown in Figure 3-9.

For a horizontal-radial system, the pressure gradient is positive (see Figure 3-10) and Darcy's equation can be expressed in the following generalized radial form:

$$v = \frac{q_r}{A_r} = \frac{k}{\mu} \left(\frac{\partial p}{\partial r} \right)_r \tag{3-13}$$

where q_r = volumetric flow rate at radius r

 A_r = cross-sectional area to flow at radius r

 $(\partial p/\partial r)_r = pressure gradient at radius r$

 $\nu = apparent \ velocity \ at \ radius \ r$

The cross-sectional area at radius r is essentially the surface area of a cylinder. For a fully penetrated well with a net thickness of h, the cross-sectional area A_r is given by

$$A_r = 2\pi rh$$

Darcy's Law applies only when the following conditions exist:

- Laminar (viscous) flow.
- Steady-state flow.
- Incompressible fluids.
- Homogeneous formation.

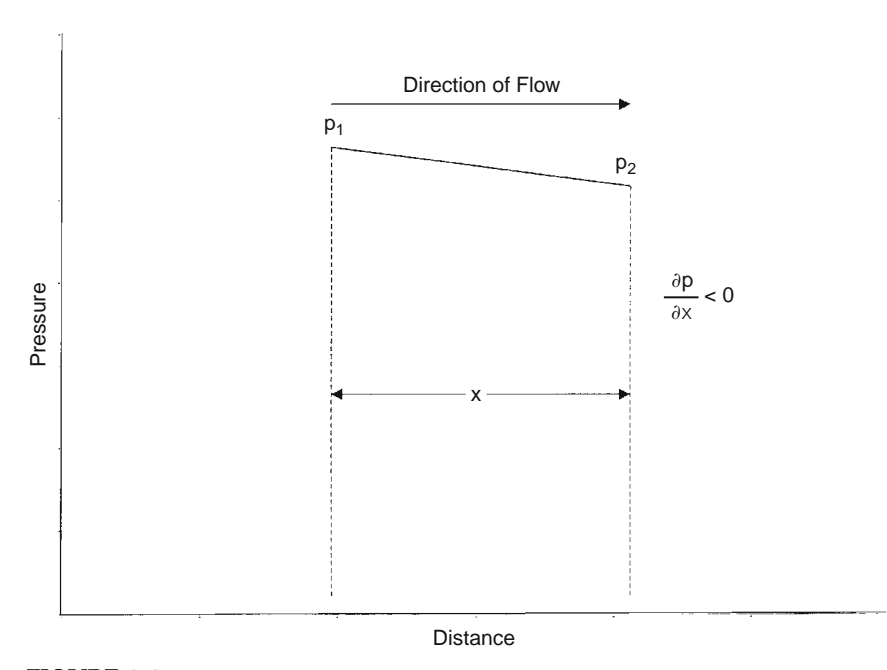


FIGURE 3-9 Pressure versus distance in a linear flow.

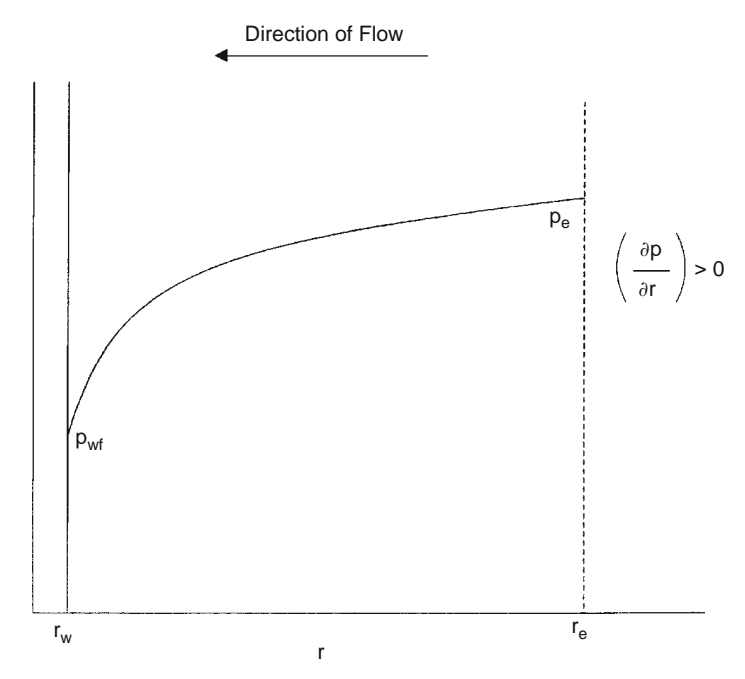


FIGURE 3-10 Pressure gradient in radial flow.

For turbulent flow, which occurs at higher velocities, the pressure gradient increases at a greater rate than does the flow rate, and a special modification of Darcy's equation is needed. When turbulent flow exists, the application of Darcy's equation can result in serious errors. Modifications for turbulent flow will be discussed later in this chapter.

SECTION 3.6 STEADY-STATE FLOW

As defined previously, steady-state flow represents the condition that exists when the pressure throughout the reservoir does not change with time. The applications of the steady-state flow to describe the flow behavior of several types of fluid in different reservoir geometries are presented next. These include

- Linear flow of incompressible fluids.
- Linear flow of slightly compressible fluids.
- Linear flow of compressible fluids.
- Radial flow of incompressible fluids.
- Radial flow of slightly compressible fluids.
- Radial flow of compressible fluids.
- Multiphase flow.

Linear Flow of Incompressible Fluids

In the linear system, it is assumed the flow occurs through a constant cross-sectional area A, where both ends are entirely open to flow. It is also assumed that no flow crosses the sides, top, or bottom, as shown in Figure 3-11.

If an incompressible fluid is flowing across the element dx, then the fluid velocity v and the flow rate q are constants at all points. The flow behavior in this system can be expressed by the differential form of Darcy's equation, i.e., Equation 3-12. Separating the variables of Equation 3-12 and integrating over the length of the linear system gives

$$\frac{q}{A}\int_{0}^{L}dx = -\frac{k}{\mu}\int_{p_{1}}^{p_{2}}dp$$

or

$$q = \frac{kA(p_1 - p_2)}{\mu L}$$

It is desirable to express this relationship in customary field units, or

$$q = \frac{0.001127 \text{ kA}(p_1 - p_2)}{\mu L} \tag{3-14}$$

where q = flow rate, bbl/day

k = absolute permeability, md

p = pressure, psia

 $\mu = viscosity$, cp

L = distance, ft

 $A = cross-sectional area, ft^2$

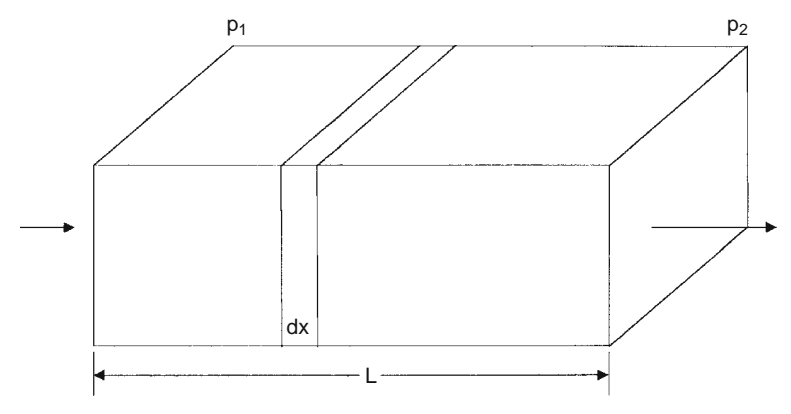


FIGURE 3-11 Linear flow model.

Example 3-1

An incompressible fluid flows in a linear porous media with the following properties:

$$\begin{array}{lll} L=2000 \text{ ft} & h=20 \text{ ft} & \text{width} = 300 \text{ ft} \\ k=100 \text{ md} & \varphi=15\% & \mu=2 \text{ cp} \\ p_1=2000 \text{ psi} & p_2=1990 \text{ psi} \end{array}$$

Calculate

- a. Flow rate in bbl/day.
- b. Apparent fluid velocity in ft/day.
- c. Actual fluid velocity in ft/day.

Solution

Calculate the cross-sectional area A:

$$A = (h)(width) = (20)(300) = 6000 \text{ ft}^2$$

a. Calculate the flow rate from Equation 3-14:

$$q = \frac{(0.001127)(100)(6000)(2000-1990)}{(2)(2000)} = 1.6905 \ bbl/day$$

b. Calculate the apparent velocity:

$$\nu = \frac{q}{A} = \frac{(1.6905)(5.615)}{6000} = 0.0016 \text{ ft/day}$$

c. Calculate the actual fluid velocity:

$$v = \frac{q}{\phi A} = \frac{(1.6905)(5.615)}{(0.15)(6000)} = 0.0105 \text{ ft/day}$$

The difference in the pressure $(p_1 - p_2)$ in Equation 3-14 is not the only driving force in a tilted reservoir. The gravitational force is the other important driving force that must be accounted for to determine the direction and rate of flow. The fluid gradient force (gravitational force) is always directed *vertically downward* while the force that results from an applied pressure drop may be in any direction. The force causing flow would then be the *vector sum* of these two. In practice, we obtain this result by introducing a new parameter, called *fluid potential*, which has the same dimensions as pressure, e.g., psi. Its symbol is Φ . The fluid potential at any point in the reservoir is defined as the pressure at that point less the pressure that would be exerted by a fluid head extending to an arbitrarily assigned datum level. Letting Δz_i be the vertical distance from a point i in the reservoir to this datum level,

$$\Phi_i = p_i - \Big(\frac{\rho}{144}\Big)\Delta z_i \eqno(3-15)$$

where ρ is the density in lb/ft³.

Expressing the fluid density in gm/cc in Equation 3-15 gives

$$\Phi_{i} = p_{i} - 0.433\gamma \Delta z_{i} \tag{3-16}$$

where Φ_i = fluid potential at point i, psi

 p_i = pressure at point i, psi

 Δz_i = vertical distance from point i to the selected datum level

 ρ = fluid density, lb/ft³ γ = fluid density, gm/cm³

The datum is usually selected at the gas-oil contact or oil-water contact; or at the highest point in formation. In using Equations 6-15 or 6-16 to calculate the fluid potential Φ_i at location i, the vertical distance Δz_i is assigned as a positive value when the point i is below the datum level and as a negative when it is above the datum level.

That is, if point i is above the datum level,

$$\Phi_i = p_i + \Big(\frac{\rho}{144}\Big) \Delta z_i$$

and

$$\Phi_i = p_i - 0.433 \gamma \Delta z_i$$

If point i is below the datum level,

$$\Phi_i = p_i - \Big(\!\frac{\rho}{144}\!\Big) \Delta z_i$$

and

$$\Phi_i = p_i - 0.433 \gamma \Delta z_i$$

Applying this generalized concept to Darcy's equation (Equation 3-14) gives

$$q = \frac{0.001127 \text{ kA}(\Phi_1 - \Phi_2)}{\mu L}$$
 (3-17)

It should be pointed out that the fluid potential drop $(\Phi_1 - \Phi_2)$ is equal to the pressure drop $(p_1 - p_2)$ only when the flow system is horizontal.

Example 3-2

Assume that the porous media with the properties as given in the previous example is tilted with a dip angle of 5° as shown in Figure 3-12. The incompressible fluid has a density of 42 lb/ft³. Resolve Example 3-1 using this additional information.

Solution

Step 1. For the purpose of illustrating the concept of fluid potential, select the datum level at half the vertical distance between the two points, i.e., at 87.15 ft, as shown in Figure 3-12.

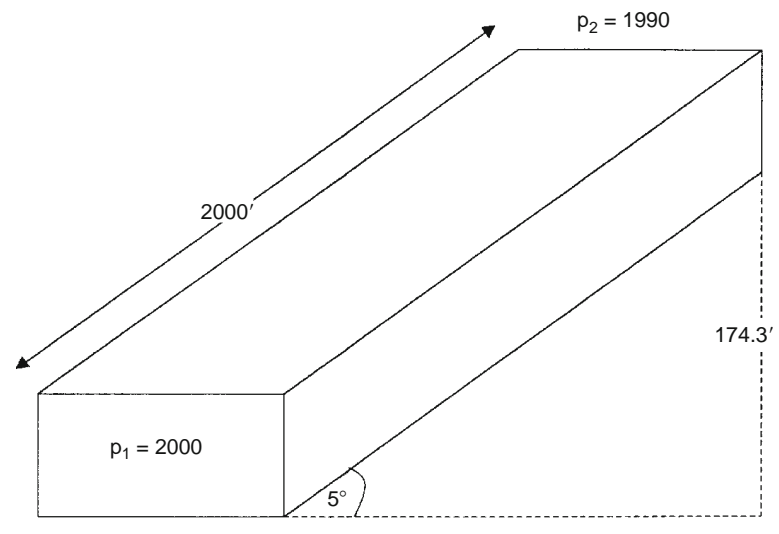


FIGURE 3-12 Example of a tilted layer.

Step 2. Calculate the fluid potential at points 1 and 2.

Since point 1 is below the datum level,

$$\Phi_1 = p_1 - \Big(\frac{\rho}{144}\Big)\Delta z_1 = 2000 - \bigg(\frac{42}{144}\bigg)(87.15) = 1974.58 \ psi$$

Since point 2 is above the datum level,

$$\Phi_2 = p_2 + \left(\frac{\rho}{144}\right) \Delta z_2 = 1990 + \left(\frac{42}{144}\right) (87.15) = 2015.42 \text{ psi}$$

Because $\Phi_2 > \Phi_1$, the fluid flows downward from point 2 to point 1. The difference in the fluid potential is

$$\Delta \Phi = 2015.42 - 1974.58 = 40.84 \text{ psi}$$

Notice, if we select point 2 for the datum level, then

$$\Phi_1 = 2000 - \left(\frac{42}{144}\right)(174.3) = 1949.16 \text{ psi}$$

$$\Phi_2 = 1990 + \left(\frac{42}{144}\right)(0) = 1990 \text{ psi}$$

These calculations indicate that, regardless of the position of the datum level, the flow is downward from 2 to 1 with

$$\Delta\Phi = 1990 - 1949.16 = 40.84~psi$$

Step 3. Calculate the flow rate:

$$q = \frac{(0.001127)(100)(6000)(40.84)}{(2)(2000)} = 6.9 \text{ bbl/day}$$

Step 4. Calculate the velocity:

Apparent velocity =
$$\frac{(6.9)(5.615)}{6000}$$
 = 0.0065 ft/day
Actual velocity = $\frac{(6.9)(5.615)}{(0.15)(6000)}$ = 0.043 ft/day

Linear Flow of Slightly Compressible Fluids

Equation 3-6 describes the relationship that exists between pressure and volume for slightly compressible fluids, or

$$V = V_{ref} \big[1 + c (p_{ref} - p) \big]$$

This equation can be modified and written in terms of flow rate as

$$q = q_{ref} [1 + c(p_{ref} - p)]$$
 (3-18)

where q_{ref} is the flow rate at some reference pressure p_{ref} . Substituting this relationship in Darcy's equation gives

$$\frac{q}{A} = \frac{q_{ref} \left[1 + c(p_{ref} - p)\right]}{A} = -0.001127 \frac{k}{\mu} \frac{dp}{dx}$$

Separating the variables and arranging gives

$$\frac{q_{ref}}{A} \int\limits_{0}^{L} dx = -0.001127 \frac{k}{\mu} \int\limits_{p_{1}}^{p_{2}} \left[\frac{dp}{1 + c(p_{ref} - p)} \right]$$

Integrating gives

$$q_{ref} = \left[\frac{0.001127 \text{ kA}}{\mu \text{ cL}} \right] \ln \left[\frac{1 + c(p_{ref} - p_2)}{1 + c(p_{ref} - p_1)} \right]$$
(3-19)

where $q_{\text{ref}} = \text{flow}$ rate at a reference pressure $p_{\text{ref}}\text{, bbl/day}$

 $p_1 = upstream \ pressure, \, psi$

 $p_2 = downstream pressure, psi$

k = permeability, md

 $\mu = \text{viscosity, cp}$

 $c = average liquid compressibility, psi^{-1}$

Selecting the upstream pressure p_1 as the reference pressure p_{ref} and substituting in Equation 3-19 gives the flow rate at point 1 as

$$q_1 = \left[\frac{0.001127 \text{ kA}}{\mu \text{ cL}} \right] \ln[1 + c(p_1 - p_2)] \tag{3-20}$$

Choosing the downstream pressure p_2 as the reference pressure and substituting in Equation 3-19 gives

$$q_2 = \left[\frac{0.001127 \text{ kA}}{\mu \text{ cL}}\right] \ln \left[\frac{1}{1 + c(p_2 - p_1)}\right]$$
(3-21)

where q_1 and q_2 are the flow rates at points 1 and 2, respectively.

Example 3-3

Consider the linear system given in Example 3-1 and, assuming a slightly compressible liquid, calculate the flow rate at both ends of the linear system. The liquid has an average compressibility of $21 \times 10^{-5} \, \mathrm{psi}^{-1}$.

Solution

Choosing the upstream pressure as the reference pressure gives

$$\begin{split} q_1 &= \left[\frac{(0.001127)(100)(6000)}{(2)(21\times 10^{-5})(2000)} \right] ln[1 + (21\times 10^{-5})(2000-1990)] \\ &= 1.689 \ bbl/day \end{split}$$

• Choosing the downstream pressure gives

$$\begin{split} q_2 &= \left[\frac{(0.001127)(100)(6000)}{(2)(21\times 10^{-5})(2000)} \right] ln \left[\frac{1}{1+(21\times 10^{-5})(1990-2000)} \right] \\ &= 1.692 \ bbl/day \end{split}$$

These calculations show that q_1 and q_2 are not largely different, which is due to the fact that the liquid is slightly incompressible and its volume is not a strong function of pressure.

Linear Flow of Compressible Fluids (Gases)

For a viscous (laminar) gas flow in a homogeneous-linear system, the real-gas equation of state can be applied to calculate the number of gas moles n at pressure p, temperature T, and volume V:

$$n = \frac{pV}{zRT}$$

At standard conditions, the volume occupied by the preceding n moles is given by

$$V_{sc} = \frac{n z_{sc} R T_{sc}}{p_{sc}}$$

Combining the two expressions and assuming $z_{\text{sc}}=1\ \text{gives}$

$$\frac{pV}{zT} = \frac{p_{sc} V_{sc}}{T_{sc}}$$

Equivalently, this relation can be expressed in terms of the flow rate as

$$\frac{5.615pq}{zT} = \frac{p_{sc}Q_{sc}}{T_{sc}}$$

Rearranging,

$$\left(\frac{p_{sc}}{T_{sc}}\right)\left(\frac{zT}{p}\right)\left(\frac{Q_{sc}}{5.615}\right) = q \tag{3-22}$$

where q = gas flow rate at pressure p in bbl/day

 $Q_{sc} = gas flow rate at standard conditions, scf/day$

z = gas compressibility factor

 T_{sc} , p_{sc} = standard temperature and pressure in ${}^{\circ}R$ and psia, respectively

Replacing the gas flow rate q with that of Darcy's Law, i.e., Equation 3-12, gives

$$\frac{q}{A} = \left(\frac{p_{sc}}{T_{sc}}\right) \left(\frac{zT}{p}\right) \left(\frac{Q_{sc}}{5.615}\right) \left(\frac{1}{A}\right) = -0.001127 \frac{k}{\mu} \frac{dp}{dx}$$

The constant 0.001127 is to convert from Darcy's units to field units. Separating variables and arranging yields

$$\left[\frac{q_{sc}p_{sc}T}{0.006328 k T_{sc}A}\right] \int_{0}^{L} dx = -\int_{p1}^{p2} \frac{p}{z\mu_{g}} dp$$

Assuming constant z and μ_g over the specified pressures, i.e., p_1 and $p_2\text{,}$ and integrating gives

$$Q_{sc} = \frac{0.003164 T_{sc} Ak \big(p_1^2 - p_2^2\big)}{p_{sc} TLz \mu_g}$$

 $\label{eq:qsc} \begin{aligned} \text{where } Q_{sc} = \text{gas flow rate at standard conditions, scf/day} \\ k = \text{permeability, md} \end{aligned}$

 $T = temperature, {}^{\circ}R$

 $\mu_g = gas \ viscosity, cp$

 $A = cross-sectional area, ft^2$

L = total length of the linear system, ft

Setting $p_{sc}=14.7$ psi and $T_{sc}=520^{\circ}R$ in the above expression gives

$$Q_{sc} = \frac{0.111924 \text{ A k}(p_1^2 - p_2^2)}{\text{TLz}\mu_g}$$
 (3-23)

It is essential to notice that those gas properties z and μ_g are a very strong function of pressure, but they have been removed from the integral to simplify the final form of the gas flow equation. The preceding equation is valid for applications when the pressure <2000 psi. The gas properties must be evaluated at the average pressure \overline{p} as defined next:

$$\overline{p} = \sqrt{\frac{p_1^2 + p_2^2}{2}} \tag{3-24}$$

Example 3-4

A linear porous media is flowing a 0.72 specific gravity gas at 120°F. The upstream and downstream pressures are 2100 psi and 1894.73 psi, respectively. The cross-sectional area is constant at 4500 ft². The total length is 2500 ft with an absolute permeability of 60 md. Calculate the gas flow rate in scf/day ($p_{sc} = 14.7$ psia, $T_{sc} = 520$ °R).

Solution

Step 1. Calculate average pressure by using Equation 3-24:

$$\overline{p} = \sqrt{\frac{2100^2 + 1894.73^2}{2}} = 2000 \ psi$$

Step 2. Using the specific gravity of the gas, calculate its pseudo-critical properties:

$$\begin{split} T_{pc} &= 168 + 325\gamma_g - 12.5\gamma_g^2 = 395.5^\circ R \\ p_{pc} &= 677 + 15.0\gamma_g - 37.5\gamma_g^2 = 668.4 \text{ psia} \end{split}$$

 $\begin{array}{l} \mbox{where} \ T_{pc} = \mbox{pseudo-critical temperature} \\ \mbox{$p_{pc} = $pseudo-critical pressure} \\ \mbox{$\gamma_g = $fluid density of gas} \end{array}$

Step 3. Calculate the pseudo-reduced pressure and temperature:

$$p_{pr} = \frac{2000}{668.4} = 2.99$$

$$T_{pr} = \frac{600}{395.5} = 1.52$$

Step 4. Determine the z-factor from the Standing-Katz chart (Figure 3-13) to give

$$z = 0.78$$

Step 5. Solve for the viscosity of the gas by applying the Lee-Gonzalez-Eakin method:

$$\begin{split} \mu_g &= 10^{-4} K \, exp \left[X \! \left(\frac{\rho_g}{62.4} \right) \right] \\ K &= \frac{(9.4 + 0.02 M_a) T^{1.5}}{209 + 19 M_a + T} \\ X &= 3.5 + \frac{986}{T} + 0.01 M_a \\ Y &= 2.4 - 0.2 X \end{split}$$

where $\mu_g = gas \ viscosity$

 $K = \text{Stewart-Burkhardt-Voo correlating parameter, } ^{\circ}R/\text{psia}$

 ρ_g = gas density at reservoir pressure and temperature, lb/ft³

 M_a = apparent molecular weight of the gas mixture

 $T = reservoir temperature, {}^{\circ}R$

Y = reduced density that can be obtained as the solution to the following equation:

$$F(Y) = X1 + \frac{Y + Y^2 + Y^3 + Y^4}{(1 - Y)^3} - (X2)Y^2 + (X3)Y^{X4} = 0$$

where $X1 = -0.06125p_{pr}t \ exp[-1.2(1-t)^2]$ $X2 = (14.76t - 9.76t^2 + 4.58t^3)$

 $X3 = (90.7t - 242.2t^2 + 42.4t^3)$

X4 = (2.18 + 2.82t)

t = reciprocal of the pseudo-reduced temperature, i.e., T_{pc}/T

This gives

$$\mu_g=0.0173\ cp$$

Step 6. Calculate the gas flow rate by applying Equation 3-23:

$$\begin{split} Q_{sc} &= \frac{(0.111924)(4500)(60)(2100^2 - 1894.73^2)}{(600)(0.78)(2500)(0.0173)} \\ &= 1,224,242 \, scf/day \end{split}$$

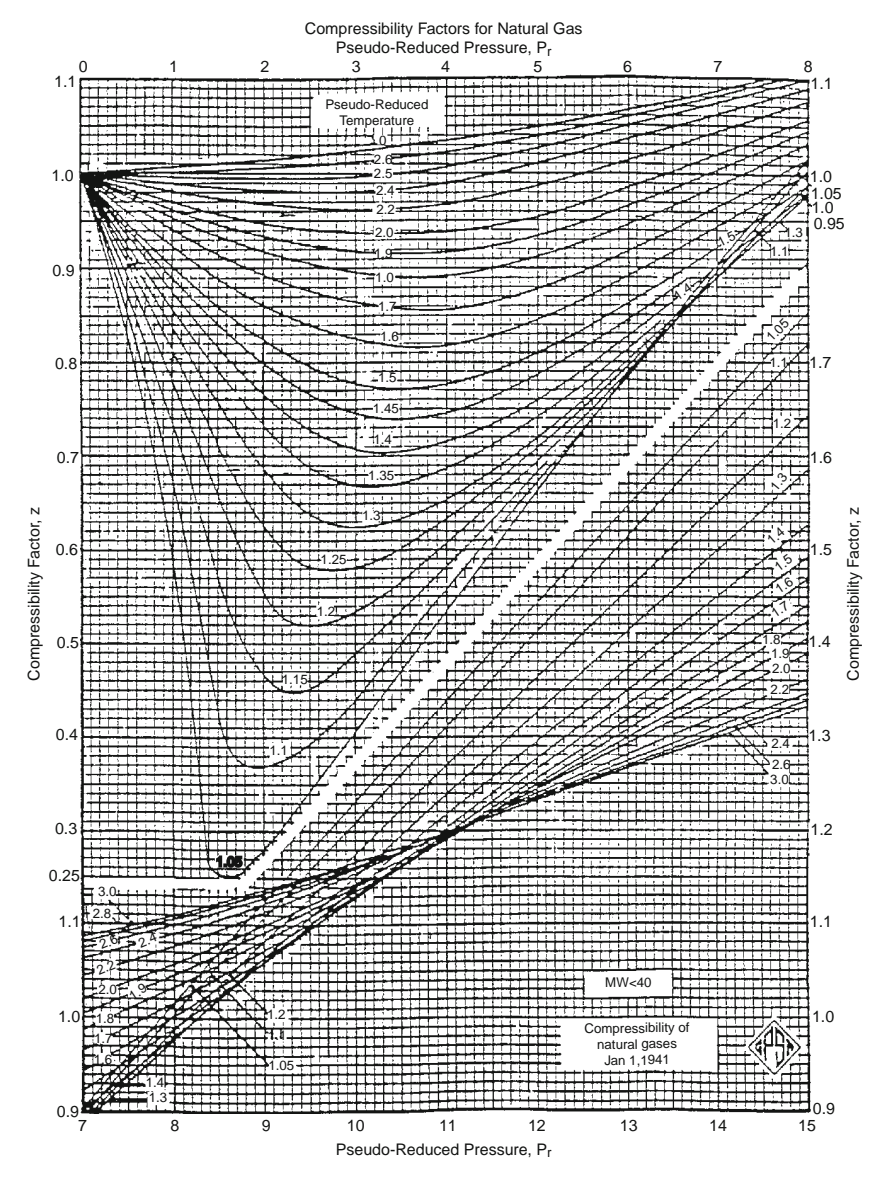


FIGURE 3-13 Standing and Katz compressibility factors chart. (Courtesy of GPSA and GPA Engineering Data Book, EO Edition, 1987.)

Radial Flow of Incompressible Fluids

In a radial flow system, fluids move toward the producing well from all directions. Before flow can take place, however, a pressure differential must exist. Thus, if a well is to produce oil, which implies a flow of fluids through the formation to the wellbore, the pressure in the formation at the wellbore must be less than the pressure in the formation at some distance from the well.

The pressure in the formation at the wellbore of a producing well is known as the *bottom-hole flowing pressure* (flowing BHP, p_{wf}).

Consider Figure 3-14, which schematically illustrates the radial flow of an incompressible fluid toward a vertical well. The formation is considered to have a uniform thickness h and a constant permeability k. Because the fluid is incompressible, the flow rate q must be constant at all radii. Due to the steady-state flowing condition, the pressure profile around the wellbore is maintained constant over time.

Let p_{wf} represent the maintained bottom-hole flowing pressure at the wellbore radius r_w and p_e denote the external pressure at the external or drainage radius. Darcy's equation as described by Equation 3-13 can be used to determine the flow rate at any radius r:

$$v = \frac{q}{A_r} = 0.001127 \frac{k}{\mu} \frac{dp}{dr}$$
 (3-25)

where $v = apparent fluid velocity, bbl/day-ft^2$

 $q = flow \ rate \ at \ radius \ r \text{, } bbl/day$

k = permeability, md

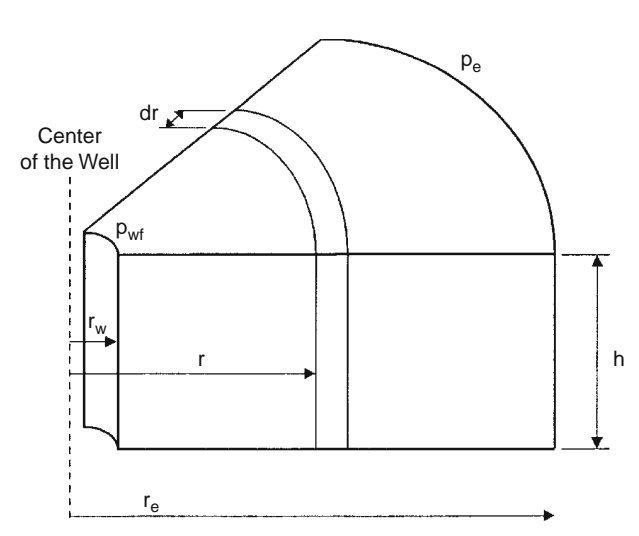


FIGURE 3-14 Radial flow model.

 $\mu = viscosity$, cp

0.001127 = conversion factor to express the equation in field units $A_r = cross\text{-sectional}$ area at radius r

The minus sign is no longer required for the radial system shown in Figure 3-14 as the radius increases in the same direction as the pressure. In other words, as the radius increases going away from the wellbore, the pressure also increases. At any point in the reservoir the cross-sectional area across which flow occurs will be the surface area of a cylinder, which is $2\pi rh$, or

$$v = \frac{q}{A_r} = \frac{q}{2\pi rh} = 0.001127 \frac{k}{\mu} \frac{dp}{dr}$$

The flow rate for a crude oil system is customarily expressed in surface units, i.e., stock-tank barrels (STB), rather than reservoir units. Using the symbol Q_0 to represent the oil flow as expressed in STB/day, then

$$q = B_0 Q_0$$

where B_o is the oil formation volume factor bbl/STB. The flow rate in Darcy's equation can be expressed in STB/day to give

$$\frac{Q_o B_o}{2\pi rh} = 0.001127 \frac{k}{\mu_o} \frac{dp}{dr}$$

Integrating this equation between two radii, r_1 and r_2 , when the pressures are p_1 and p_2 yields

$$\int_{r_1}^{r_2} \left(\frac{Q_o}{2\pi h} \right) \frac{dr}{r} = 0.001127 \int_{P_1}^{P_2} \left(\frac{k}{\mu_o B_o} \right) dp \tag{3-26}$$

For an incompressible system in a uniform formation, Equation 3-26 can be simplified to

$$\frac{Q_o}{2\pi h} \int_{r_1}^{r_2} \frac{dr}{r} = \frac{0.001127 \text{ k}}{\mu_o B_o} \int_{P_1}^{P_2} dp$$

Performing the integration gives

$$Q_o = \frac{0.00708 \; kh(p_2 - p_1)}{\mu_o B_o \; ln(r_2/r_1)} \label{eq:Qo}$$

Frequently the two radii of interest are the wellbore radius $r_{\rm w}$ and the external or drainage radius $r_{\rm e}$. Then,

$$Q_{o} = \frac{0.00708 \text{ kh}(p_{e} - p_{w})}{\mu_{o} B_{o} \ln(r_{e}/r_{w})}$$
(3-27)

where $Q_o = oil$, flow rate, STB/day

 $p_e = external pressure, psi$

 p_{wf} = bottom-hole flowing pressure, psi

k = permeability, md

 $\mu_o = oil \ viscosity, \ cp$

 $B_o = oil$ formation volume factor, bbl/STB

h = thickness, ft

 r_e = external or drainage radius, ft

 r_w = wellbore radius, ft

The external (drainage) radius r_e is usually determined from the well spacing by equating the area of the well spacing with that of a circle; i.e.,

$$\pi r_e^2 = 43{,}560~A$$

or

$$r_{e} = \sqrt{\frac{43,560 \text{ A}}{\pi}} \tag{3-28}$$

where A is the well spacing in acres.

In practice, neither the external radius nor the wellbore radius is generally known with precision. Fortunately, they enter the equation as a logarithm, so that the error in the equation will be less than the errors in the radii.

Equation 3-27 can be arranged to solve for the pressure p at any radius r to give

$$p = p_{wf} + \left[\frac{Q_o B_o \mu_o}{0.00708 \text{ kh}} \right] \ln \left(\frac{r}{r_w} \right)$$
 (3-29)

Example 3-5

An oil well in the Nameless Field is producing at a stabilized rate of 600 STB/day at a stabilized bottom-hole flowing pressure of 1800 psi. Analysis of the pressure buildup test data indicates that the pay zone is characterized by a permeability of 120 md and a uniform thickness of 25 ft. The well drains an area of approximately 40 acres. The following additional data are available:

$$\begin{array}{ll} r_w = 0.25 \text{ ft} & A = 40 \text{ acres} \\ B_o = 1.25 \text{ bbl/STB} & \mu_o = 2.5 \text{ cp} \end{array} \label{eq:rw}$$

Calculate the pressure profile (distribution) and list the pressure drop across 1-ft intervals from $r_{\rm w}$ to 1.25 ft, 4 to 5 ft, 19 to 20 ft, 99 to 100 ft, and 744 to 745 ft.

Solution

Step 1. Rearrange Equation 3-27 and solve for the pressure p at radius r:

$$\begin{split} p &= p_{wf} + \left[\frac{\mu_o B_o Q_o}{0.00708 \text{ kh}}\right] ln(r/r_w) \\ p &= 1800 + \left[\frac{(2.5)(1.25)(600)}{(0.00708)(120)(25)}\right] ln\left(\frac{r}{0.25}\right) \\ p &= 1800 + 88.28 ln\left(\frac{r}{0.25}\right) \end{split}$$

Step 2. Calculate the pressure at the designated radii:

r, ft	p, psi	Radius interval	Pressure drop
0.25	1800		
1.25	1942	0.25-1.25	1942 - 1800 = 142 psi
4	2045		1
5	2064	4–5	2064 - 2045 = 19 psi
19	2182		-
20	2186	19-20	2186 - 2182 = 4 psi
99	2328		_
100	2329	99-100	2329 - 2328 = 1 psi
744	2506.1		_
745	2506.2	744–745	2506.2 - 2506.1 = 0.1 psi

Figure 3-15 shows the pressure profile on a function of radius for the calculated data.

Results of this example reveal that the pressure drop just around the wellbore (i.e., 142 psi) is 7.5 times greater than at the 4–5 ft interval, 36 times greater than at 19–20 ft, and 142 times greater than at the 99–100 ft interval. The reason for this large pressure drop around the wellbore is that the fluid is flowing in from a large drainage of 40 acres.

The external pressure p_e used in Equation 3-27 cannot be measured readily, but p_e does not deviate substantially from initial reservoir pressure if a strong and active aquifer is present.

Several authors have suggested that the average reservoir pressure p_r , which often is reported in well test results, should be used in performing material balance calculations and flow rate prediction. Craft and Hawkins (1959) showed that the average pressure is located at about 61% of the drainage radius r_e for a steady-state flow condition. Substitute 0.61 r_e in Equation 3-29 to give

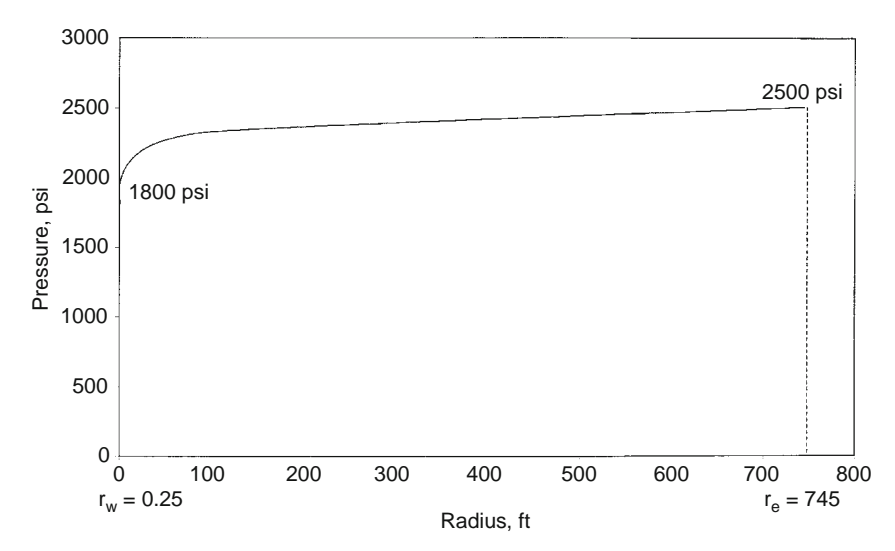


FIGURE 3-15 Pressure profile around the wellbore.

$$p(at~r=0.61~r_e) = p_r = p_{wf} + \left[\frac{Q_o B_o \mu_o}{7.08~kh}\right] ln \left(\frac{0.61~r_e}{r_w}\right) \label{eq:power_power}$$

or, in terms of flow rate,

$$Q_{o} = \frac{0.00708 \text{ kh}(p_{r} - p_{wf})}{\mu_{o} B_{o} \ln\left(\frac{0.61 \text{ r}_{e}}{r_{w}}\right)}$$
(3-30)

But, since $ln(0.61 \ r_e/r_w) = ln \bigg(\frac{r_e}{r_w}\bigg) - 0.5$,

$$Q_{o} = \frac{0.00708 \text{ kh}(p_{r} - p_{wf})}{\mu_{o} B_{o} \left[\ln \left(\frac{r_{e}}{r_{w}} \right) - 0.5 \right]}$$
(3-31)

Golan and Whitson (1986) suggested a method for approximating drainage area of wells producing from a common reservoir. The authors assumed that the volume drained by a single well is proportional to its rate of flow. Assuming constant reservoir properties and a uniform thickness, the approximate drainage area of a single well, A_w, is

$$A_{w} = A_{T} \left(\frac{q_{w}}{q_{T}} \right) \tag{3-32}$$

where $A_w = drainage$ area

 A_T = total area of the field

 $q_T = total flow rate of the field$

 $q_w = well flow rate$

Radial Flow of Slightly Compressible Fluids

Craft, Hawkins, and Terry (1990) used Equation 3-18 to express the dependency of the flow rate on pressure for slightly compressible fluids. If this equation is substituted into the radial form of Darcy's Law, the following is obtained:

$$\frac{q}{A_r} = \frac{q_{ref}[1 + c(p_{ref} - p)]}{2\pi rh} = 0.001127 \frac{k}{\mu} \frac{dp}{dr}$$

where q_{ref} is the flow rate at some reference pressure P_{ref}.

Separating the variables in this equation and integrating over the length of the porous medium gives

$$\frac{q_{ref}\mu}{2\pi kh} \int_{r_w}^{r_e} \frac{dr}{r} = 0.001127 \int_{p_{wf}}^{p_e} \frac{dp}{1 + c(p_{ref} - p)}$$

or

$$q_{ref} = \left[\frac{0.00708 \ kh}{\mu \ c \ln \left(\frac{r_e}{r_w} \right)} \right] \ln \left[\frac{1 + c(p_e - p_{ref})}{1 + c(p_{wf} - p_{ref})} \right] \label{eq:qref}$$

where q_{ref} is the oil flow rate at a reference pressure p_{ref} . Choosing the bottom-hole flow pressure p_{wf} as the reference pressure and expressing the flow rate in STB/day gives

$$Q_{o} = \left[\frac{0.00708 \text{ kh}}{\mu_{o} B_{o} c_{o} \ln \left(\frac{r_{e}}{r_{w}} \right)} \right] \ln [1 + c_{o} (p_{e} - p_{wf})]$$
(3-33)

where $c_o = isothermal$ compressibility coefficient, psi^{-1}

 $Q_{o} = oil \ flow \ rate, \ STB/day$

k = permeability, md

Example 3-6

The following data are available on a well in the Red River Field:

$$\begin{array}{lll} p_e = 2506 \; psi & p_{wf} = 1800 \\ r_e = 745 \; ft & r_w = 0.25 \\ B_o = 1.25 & \mu_o = 2.5 \\ k = 0.12 \; darcy & h = 25 \; ft \end{array} \quad c_o = 25 \times 10^{-6} \; psi^{-1}$$

Assuming a slightly compressible fluid, calculate the oil flow rate. Compare the result with that of incompressible fluid.

Solution

For a slightly compressible fluid, the oil flow rate can be calculated by applying Equation 3-33:

$$\begin{split} Q_o &= \left[\frac{(0.00708)(120)(25)}{(2.5)(1.25)(25\times 10^{-6})\ln(745/0.25)} \right] \\ &\times \ln[1+(25\times 10^{-6})(2506-1800)] = 595 \, STB/day \end{split}$$

Assuming an incompressible fluid, the flow rate can be estimated by applying Darcy's equation, i.e., Equation 3-27:

$$Q_o = \frac{(0.00708)(120)(25)(2506 - 1800)}{(2.5)(1.25)\ln(745/0.25)} = 600 \text{ STB/day}$$

Radial Flow of Compressible Gases

The basic differential form of Darcy's Law for a horizontal laminar flow is valid for describing the flow of both gas and liquid systems. For a radial gas flow, Darcy's equation takes the form

$$q_{gr} = \frac{0.001127 (2\pi rh)k}{\mu_g} \frac{dp}{dr}$$
 (3-34)

where $q_{gr} = gas$ flow rate at radius r, bbl/day

r = radial distance, ft

h = zone thickness, ft

 $\mu_g = gas \ viscosity$, cp

p = pressure, psi

0.001127 = conversion constant from darcy units to field units

The gas flow rate is usually expressed in scf/day. Referring to the gas flow rate at standard condition as Q_g , the gas flow rate q_{gr} under pressure and temperature can be converted to that of standard condition by applying the real-gas equation of state to both conditions, or

$$\frac{5.615 \text{ q}_{gr} \text{ p}}{zRT} = \frac{Q_g \text{ p}_{sc}}{z_{sc} \text{ R T}_{sc}}$$

or

$$\left(\frac{p_{sc}}{5.615T_{sc}}\right)\left(\frac{zT}{p}\right)Q_g = q_{gr} \tag{3-35}$$

where $p_{sc} = standard$ pressure, psia

 $T_{sc} = standard temperature, {}^{\circ}R$

 $Q_g = gas flow rate, scf/day$

 $q_{gr} = gas flow rate at radius r, bbl/day$

p = pressure at radius r, psia

T = reservoir temperature, °R

z = gas compressibility factor at p and T

 $z_{sc} = gas$ compressibility factor at standard condition $\cong 1.0$

Combining Equations 3-34 and 3-35 yields

$$\left(\frac{p_{sc}}{5.615\,T_{sc}}\right)\!\left(\!\frac{zT}{p}\!\right)\!Q_g = \frac{0.001127(2\pi rh)k}{\mu_g}\frac{dp}{dr}$$

Assuming that $T_{sc} = 520^{\circ}R$ and $p_{sc} = 14.7$ psia,

$$\left(\frac{T Q_g}{kh}\right) \frac{dr}{r} = 0.703 \left(\frac{2p}{\mu_g z}\right) dp \tag{3-36}$$

Integrate Equation 3-36 from the wellbore conditions (r_w and p_{wf}) to any point in the reservoir (r and p) to give

$$\int_{r_{w}}^{r} \left(\frac{T Q_{g}}{kh}\right) \frac{dr}{r} = 0.703 \int_{p_{wif}}^{p} \left(\frac{2p}{\mu_{g}z}\right) dp$$
 (3-37)

Impose Darcy's Law conditions on Equation 3-37; i.e.,

- Steady-state flow, which requires that Qg is constant at all radii,
- Homogeneous formation, which implies that k and h are constant, gives

$$\left(\frac{T Q_g}{kh}\right) \ln\left(\frac{r}{r_w}\right) = 0.703 \int_{p_{wf}}^{p} \left(\frac{2p}{\mu_g z}\right) dp$$

The term $\int_{wf}^{p} \left(\frac{2p}{\mu_g z}\right) dp$ can be expanded to give

$$\int\limits_{p_{wf}}^{p^{N}} \left(\frac{2p}{\mu_{g}z}\right) dp = \int\limits_{0}^{p} \left(\frac{2p}{\mu_{g}z}\right) dp - \int\limits_{0}^{p_{wf}} \left(\frac{2p}{\mu_{g}z}\right) dp$$

Combining these relationships yields

$$\left(\frac{T Q_{g}}{kh}\right) \ln\left(\frac{r}{r_{w}}\right) = 0.703 \left[\int_{0}^{p} \left(\frac{2p}{\mu_{g}z}\right) dp - \int_{0}^{p_{wf}} \left(\frac{2p}{\mu_{g}z}\right) dp\right]$$
(3-38)

The integral $\int_0^p 2p/(\mu_g z) dp$ is called the *real-gas potential* or *real-gas pseudopressure*, and it is usually represented by m(p) or ψ . Thus,

$$m(p) = \psi = \int_{0}^{p} \left(\frac{2p}{\mu_{g} z}\right) dp \tag{3-39}$$

Equation 3-38 can be written in terms of the real-gas potential to give

$$\left(\frac{T Q_g}{kh}\right) ln \frac{r}{r_w} = 0.703 (\psi - \psi_w)$$

or

$$\psi = \psi_{w} + \frac{Q_{g}T}{0.703 \text{ kh}} \ln \frac{r}{r_{w}}$$
 (3-40)

Equation 3-40 indicates that a graph of ψ versus ln r/r_w yields a straight line of slope (Q_g T/0.703 kh) and intercepts ψ_w (Figure 3-16).

The flow rate is given exactly by

$$Q_{g} = \frac{0.703 \text{ kh}(\psi - \psi_{w})}{T \ln \frac{r}{r_{w}}}$$
(3-41)

In the particular case when $r = r_e$,

$$Q_g = \frac{0.703 \text{ kh}(\psi_e - \psi_w)}{T \left(\ln \frac{r_e}{r_w} \right)}$$
 (3-42)

where ψ_e = real-gas potential as evaluated from 0 to p_e , psi^2/cp $\psi_{\rm w}$ = real-gas potential as evaluated from 0 to $P_{\rm wf}$, psi²/cp

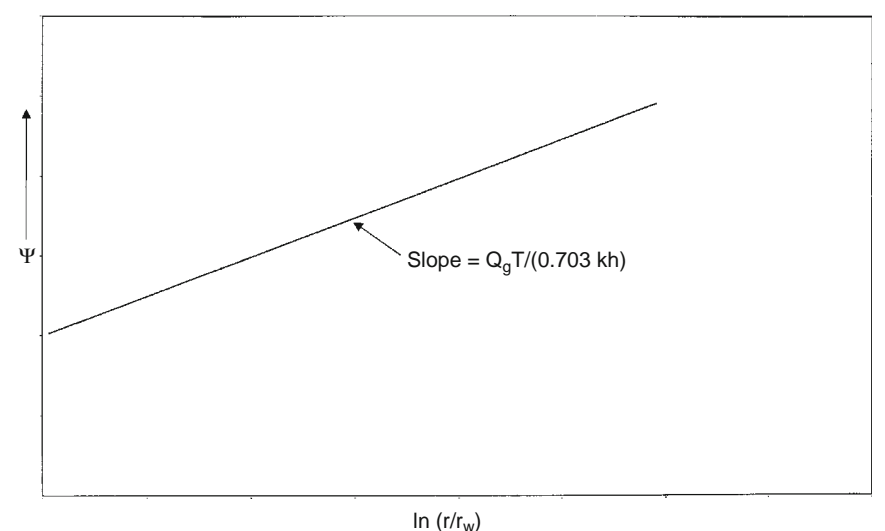


FIGURE 3-16 Graph of ψ versus ln (r/r_w).

k = permeability, md

h = thickness, ft

 r_e = drainage radius, ft

 $r_{\rm w}$ = wellbore radius, ft

 $Q_g = gas flow rate, scf/day$

The gas flow rate is commonly expressed in Mscf/day, or

$$Q_{g} = \frac{kh(\psi_{e} - \psi_{w})}{1422 T \left(ln \frac{r_{e}}{r_{w}} \right)}$$
(3-43)

where $Q_g = gas$ flow rate, Mscf/day.

Equation 3-43 can be expressed in terms of the average reservoir pressure p_r instead of the initial reservoir pressure p_e as

$$Q_{g} = \frac{kh(\psi_{r} - \psi_{w})}{1422 \text{ T} \left[ln \left(\frac{r_{e}}{r_{w}} \right) - 0.5 \right]}$$
(3-44)

To calculate the integral in Equation 3-43, the values of $2p/\mu_g z$ are calculated for several values of pressure p. Then $(2p/\mu_g z)$ versus p is plotted on a Cartesian scale and the area under the curve is calculated either numerically or graphically, where the area under the curve from p=0 to any pressure p represents the value of ψ corresponding to p. The following example will illustrate the procedure.

Example 3-7

The following PVT data from a gas well in the Anaconda Gas Field follows¹:

p(psi)	$\mu_{\rm g}({ m cp})$	z
0	0.0127	1.000
400	0.01286	0.937
800	0.01390	0.882
1200	0.01530	0.832
1600	0.01680	0.794
2000	0.01840	0.770
2400	0.02010	0.763
2800	0.02170	0.775
3200	0.02340	0.797
3600	0.02500	0.827
4000	0.02660	0.860
4400	0.02831	0.896

¹Data from D. Donohue and T. Ertekin, Gas Well Testing, Theory, Practice and Regulations, IHRDC Corporation (1982).

The well is producing at a stabilized bottom-hole flowing pressure of 3600 psi. The wellbore radius is 0.3 ft. The following additional data are available:

$$\begin{array}{ll} k=65 \text{ md} & \quad h=15 \text{ ft} \\ p_e=4400 \text{ psi} & \quad r_e=1000 \text{ ft} \end{array} \quad T=600^\circ R$$

Calculate the gas flow rate in Mscf/day.

Solution

Step 1. Calculate the term $\left(\frac{2p}{\mu_g z}\right)$ for each pressure as shown next:

p(psi)	μ _g (cp)	z	$\frac{2p}{\mu_g z} \left(\frac{psia}{cp} \right)$
0	0.0127	1.000	0
400	0.01286	0.937	66391
800	0.01390	0.882	130508
1200	0.01530	0.832	188537
1600	0.01680	0.794	239894
2000	0.01840	0.770	282326
2400	0.02010	0.763	312983
2800	0.02170	0.775	332986
3200	0.02340	0.797	343167
3600	0.02500	0.827	348247
4000	0.02660	0.860	349711
4400	0.02831	0.896	346924

- Step 2. Plot the term $\left(\frac{2p}{\mu_g z}\right)$ versus pressure as shown in Figure 3-17.
- Step 3. Calculate numerically the area under the curve for each value of p. These areas correspond to the real-gas potential ψ at each pressure. These ψ values are tabulated next; ψ versus p is also plotted in the figure).

p(psi)	$\psi\left(\frac{psi^2}{cp}\right)$
400	13.2×10^{6}
800	52.0×10^{6}
1200	113.1×10^{6}
1600	198.0×10^{6}
2000	304.0×10^{6}
2400	422.0×10^{6}
2800	542.4×10^{6}
3200	678.0×10^{6}
3600	816.0×10^{6}
4000	950.0×10^{6}
4400	1089.0×10^{6}

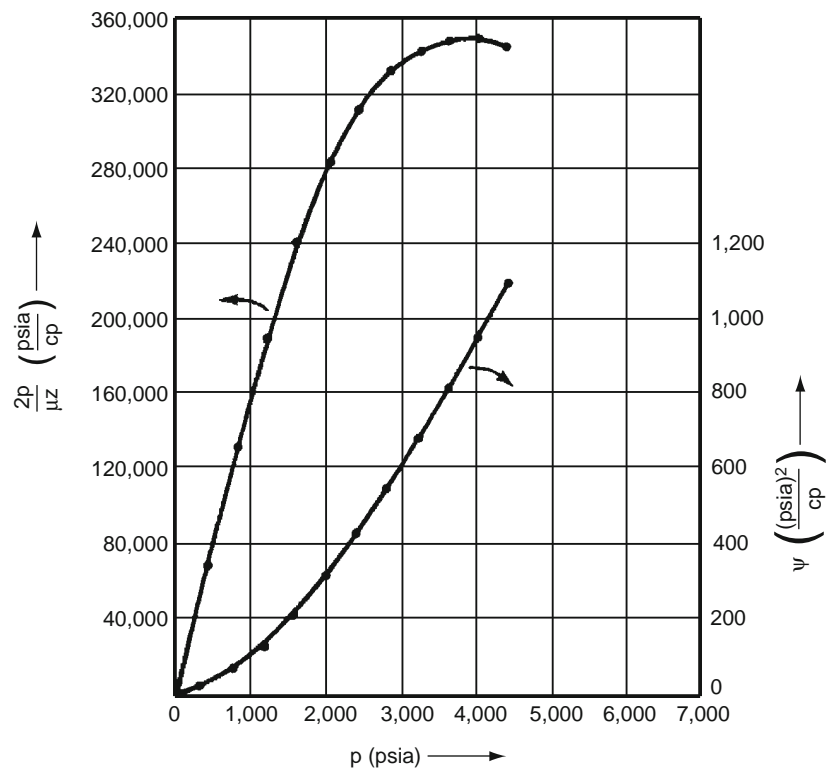


FIGURE 3-17 Real-gas pseudopressure data for Example 3-7. (After Donohue and Erkekin, 1982.)

Step 4. Calculate the flow rate by applying Equation 3-41.

$$\begin{split} p_w &= 816.0 \times 10^6 \quad p_e = 1089 \times 10^6 \\ Q_g &= \frac{(65)(15)(1089 - 816)10^6}{(1422)(600) \ln(1000/0.25)} = 37,614 \; Mscf/day \end{split}$$

Approximation of the Gas Flow Rate

The exact gas flow rate as expressed by the different forms of Darcy's Law, i.e., Equations 3-37 through 3-44, can be approximated by removing the term $2/\mu_g z$ outside the integral as a constant. It should be pointed out that the $\mu_g z$ is considered constant only under a pressure range of <2000 psi. Equation 3-43 can be rewritten as

$$Q_{g} = \left[\frac{kh}{1422 \, T \ln \left(\frac{r_{e}}{r_{w}}\right)}\right] \int_{p_{wf}}^{p_{e}} \left(\frac{2p}{\mu_{g} \, z}\right) dp$$

Removing the term and integrating gives

$$Q_{g} = \frac{kh(p_{e}^{2} - p_{wf}^{2})}{1422 T(\mu_{g}z)_{avg} ln(\frac{r_{e}}{r_{w}})}$$
(3-45)

 $\begin{array}{c} \text{where } Q_g = \text{gas flow rate, Mscf/day} \\ k = \text{permeability, md} \end{array}$

The term $(\mu_g z)_{avg}$ is evaluated at an average pressure \overline{p} that is defined by the following expression:

$$\overline{p} = \sqrt{\frac{p_{wf}^2 + p_e^2}{2}}$$

This approximation method is called the *pressure-squared* method and is limited to flow calculations when the reservoir pressure is less than 2000 psi.

Example 3-8

Using the data given in Example 3-7, re-solve for the gas flow rate by using the pressure-squared method. Compare with the exact method (i.e., real-gas potential solution).

Solution

Step 1. Calculate the arithmetic average pressure:

$$\overline{p} = \left\lceil \frac{4400^2 + 3600^2}{2} \right\rceil^5 = 4020 \; psi$$

Step 2. Determine the gas viscosity and gas compressibility factor at 4020 psi:

$$\begin{array}{c} \mu_g = 0.0267 \\ z = 0.862 \end{array}$$

Step 3. Apply Equation 3-45:

$$\begin{split} Q_g = & \frac{(65)(15)[4400^2 - 3600^2]}{(1422)(600)(0.0267)(0.862) \ln(1000/0.25)} \\ = & 38,314 \, \text{Mscf/day} \end{split}$$

Step 4. Results show that the pressure-squared method approximates the exact solution of 37,614 with an absolute error of 1.86%. This error is due to the limited applicability of the pressure-squared method to a pressure range of <2000 psi.

Horizontal Multiple-Phase Flow

When several fluid phases are flowing simultaneously in a horizontal porous system, the concept of the effective permeability to each phase and the associated physical properties must be used in Darcy's equation. For a radial system, the generalized form of Darcy's equation can be applied to each reservoir as follows:

$$\begin{split} q_o &= 0.001127 \left(\frac{2\pi rh}{\mu_o}\right) k_o \frac{dp}{dr} \\ q_w &= 0.001127 \left(\frac{2\pi rh}{\mu_w}\right) k_w \frac{dp}{dr} \\ q_g &= 0.001127 \left(\frac{2\pi rh}{\mu_g}\right) k_g \frac{dp}{dr} \end{split}$$

where k_o , k_w , k_g = effective permeability to oil, water, and gas, md μ_o , μ_w , μ_g = viscosity to oil, water, and gas, cp q_o , q_w , q_g = flow rates for oil, water, and gas, bbl/day k = absolute permeability, md

Many correlations of permeability use the effective phase saturation as a correlating parameter. The effective phase saturation is defined by the following set of relationships:

$$S_{o}^{*} = \frac{S_{o}}{1 - S_{wc}}$$

$$S_{w}^{*} = \frac{S_{w} - S_{wc}}{1 - S_{wc}}$$

$$S_{g}^{*} = \frac{S_{g}}{1 - S_{wc}}$$

where S_o^* , S_w^* , S_g^* = effective oil, water, and gas saturation, respectively S_o , S_w , S_g = oil, water, and gas saturation, respectively S_{wc} = connate (irreducible) water saturation

The effective permeability can be expressed in terms of the relative and absolute permeability, as just presented, to give

$$k_o = k_{ro}k$$

$$k_w = k_{rw}k$$

$$k_g = k_{rg}k$$

Using this concept in Darcy's equation and expressing the flow rate in standard conditions yields

$$Q_o = 0.00708(rhk) \left(\frac{k_{ro}}{\mu_o B_o}\right) \frac{dp}{dr}$$
 (3-46)

$$Q_w = 0.00708 (rhk) \left(\frac{k_{rw}}{\mu_w B_w}\right) \frac{dp}{dr} \tag{3-47} \label{eq:qw}$$

$$Q_g = 0.00708 (rhk) \left(\frac{k_{rg}}{\mu_g B_g}\right) \frac{dp}{dr} \tag{3-48}$$

where Q_{o} , $Q_{w}=$ oil and water flow rates, STB/day

 B_{o} , B_{w} = oil and water formation volume factor, bbl/STB

 $Q_g = gas flow rate, scf/day$

 $B_g = gas$ formation volume factor, bbl/scf

 \ddot{k} = absolute permeability, md

The gas formation volume factor B_g is expressed as

$$B_g = 0.005035 \frac{zT}{p}, bbl/scf$$

Performing the regular integration approach on Equations 3-46 through 6-48 yields the following.

Oil Phase.

$$Q_{o} = \frac{0.00708(kh)(k_{ro})(p_{e} - p_{wf})}{\mu_{o}B_{o}\ln(r_{e}/r_{w})}$$
(3-49)

Water Phase.

$$Q_{w} = \frac{0.00708(kh)(k_{rw})(p_{e} - p_{wf})}{\mu_{w}B_{w}\ln(r_{e}/r_{w})}$$
(3-50)

Gas Phase. In terms of the real-gas potential,

$$Q_{g} = \frac{(kh)k_{rg}(\psi_{e} - \psi_{w})}{1422 T \ln(r_{e}/r_{w})}$$
(3-51)

In terms of the pressure squared,

$$Q_{g} = \frac{(kh)k_{rg}(p_{e}^{2} - p_{wf}^{2})}{1422(\mu_{g}z)_{avg}T\ln(r_{e}/r_{w})}$$
(3-52)

where $Q_g = gas$ flow rate, Mscf/day

 $\ddot{k} = absolute permeability, md$

 $T = temperature, {}^{\circ}R$

In numerous petroleum engineering calculations, it is convenient to express the flow rate of any phase as a ratio of other flowing phases. Two important flow ratios are the "instantaneous" water-oil ratio (WOR) and "instantaneous" gas-oil ratio (GOR). The generalized form of Darcy's equation can be used to determine both flow ratios.

The water-oil ratio is defined as the ratio of the water flow rate to that of the oil. Both rates are expressed in stock-tank barrels per day, or

$$WOR = \frac{Q_w}{Q_o}$$

Dividing Equation 3-46 by Equation 3-48 gives

$$WOR = \left(\frac{k_{rw}}{k_{ro}}\right) \left(\frac{\mu_o B_o}{\mu_w B_w}\right) \tag{3-53}$$

where $WOR = water-oil\ ratio,\ STB/STB$.

The instantaneous GOR, as expressed in scf/STB, is defined as the *total* gas flow rate, i.e., free gas and solution gas, divided by the oil flow rate, or

$$GOR = \frac{Q_o R_s + Q_g}{Q_o}$$

or

$$GOR = R_s + \frac{Q_g}{Q_o} \tag{3-54}$$

where GOR = "instantaneous" gas-oil ratio, scf/STB

 $R_{\rm s} = gas \ solubility, \ scf/STB$

 $Q_g = \bar{\text{free}}$ gas flow rate, scf/day

 $Q_o = oil flow rate, STB/day$

Substituting Equations 3-46 and 3-48 into Equation 3-54 yields

$$GOR = R_s + \left(\frac{k_{rg}}{k_{ro}}\right) \left(\frac{\mu_o B_o}{\mu_g B_g}\right) \tag{3-55}$$

where \boldsymbol{B}_{g} is the gas formation volume factor as expressed in bbl/scf.

SECTION 3.7 UNSTEADY-STATE FLOW

Consider Figure 3-18A, which shows a shut-in well that is centered in a homogeneous circular reservoir of radius r_e with a uniform pressure p_i throughout the reservoir. This initial reservoir condition represents the zero producing time. If the well is allowed to flow at a constant flow rate

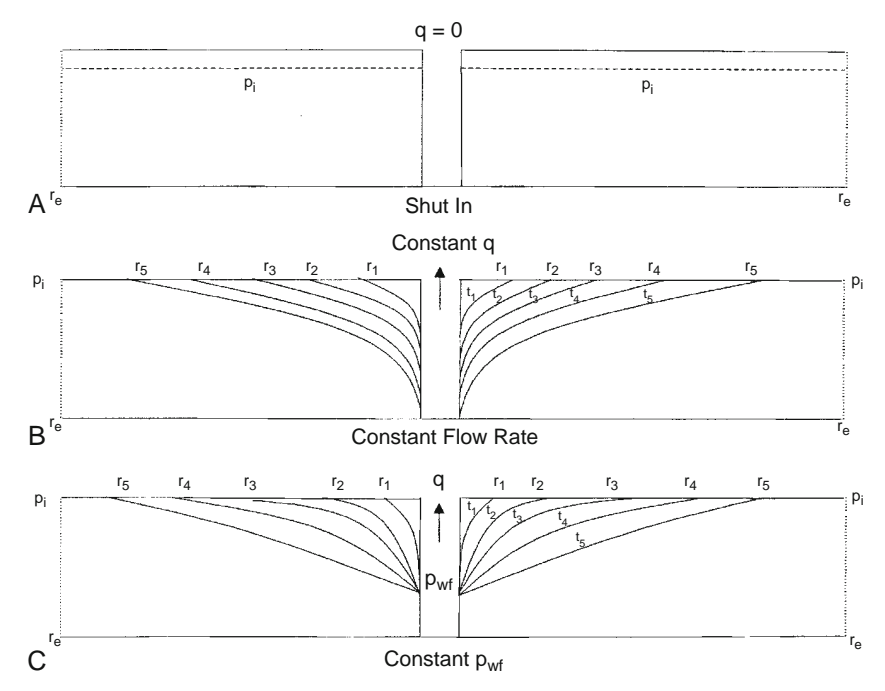


FIGURE 3-18 Pressure disturbance as a function of time.

of q, a pressure disturbance will be created at the sand face. The pressure at the wellbore, i.e., $p_{\rm wf}$, will drop instantaneously as the well is opened. The pressure disturbance will move away from the wellbore at a rate that is determined by

- · Permeability.
- Porosity.
- Fluid viscosity.
- Rock and fluid compressibilities.

Section B in Figure 3-18 shows that, at time t_1 , the pressure disturbance has moved a distance r_1 into the reservoir. Notice that the pressure disturbance radius is continuously increasing with time. This radius is commonly called *radius of investigation* and referred to as $r_{\rm inv}$. It is also important to point out that, as long as the radius of investigation has not reached the reservoir boundary, i.e., $r_{\rm e}$, the reservoir will be acting as if it is *infinite* in size. During this time we say that the reservoir is *infinite acting* because the outer drainage radius $r_{\rm e}$ can be mathematically *infinite*.

A similar discussion can be used to describe a well that is producing at a constant bottom-hole flowing pressure. Section C in Figure 3-18 schematically illustrates the propagation of the radius of investigation

with respect to time. At time t_4 , the pressure disturbance reaches the boundary, i.e., $r_{\rm inv}=r_{\rm e}$. This causes the pressure behavior to change.

Based on this discussion, the transient (unsteady-state) flow is defined as that time period during which the boundary has no effect on the pressure behavior in the reservoir and the reservoir will behave as if it is infinite in size. Section B in Figure 3-18 shows that the transient flow period occurs during the time interval $0 < t < t_t$ for the constant flow rate scenario and during the time period $0 < t < t_4$ for the constant p_{wf} scenario as depicted by Section C in Figure 3-18.

Basic Transient Flow Equation

Under the steady-state flowing condition, the same quantity of fluid enters the flow system as leaves it. In the unsteady-state flow condition, the flow rate into an element of volume of a porous media may not be the same as the flow rate out of that element. Accordingly, the fluid content of the porous medium changes with time. The variables in unsteady-state flow additional to those already used for steady-state flow therefore become

- Time, t.
- Porosity, φ.
- Total compressibility, c_t.

The mathematical formulation of the transient flow equation is based on combining three independent equations and a specifying set of boundary and initial conditions that constitute the unsteady-state equation. These equations and boundary conditions are briefly described:

- a. **Continuity Equation**. The continuity equation is essentially a material balance equation that accounts for every pound mass of fluid produced, injected, or remaining in the reservoir.
- b. **Transport Equation**. The continuity equation is combined with the equation for fluid motion (transport equation) to describe the fluid flow rate "in" and "out" of the reservoir. Basically, the transport equation is Darcy's equation in its generalized differential form.
- c. Compressibility Equation. The fluid compressibility equation (expressed in terms of density or volume) is used in formulating the unsteady-state equation with the objective of describing the changes in the fluid volume as a function of pressure.
- d. **Initial and Boundary Conditions**. Two boundary conditions and one initial condition are required to complete the formulation and the solution of the transient flow equation. The two boundary conditions are
 - The formation produces at a constant rate into the wellbore.
 - There is no flow across the outer boundary, and the reservoir behaves as if it were infinite in size, i.e., $r_e = \infty$.

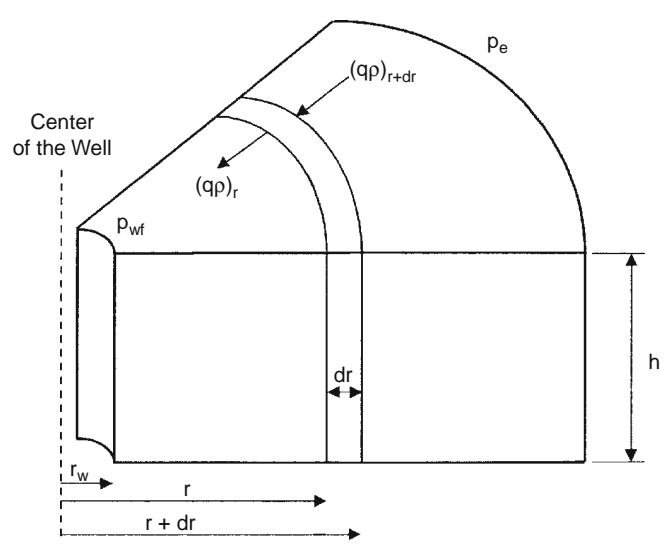


FIGURE 3-19 Illustration of radial flow.

The initial condition simply states that the reservoir is at a uniform pressure when production begins, i.e., time = 0.

Consider the flow element shown in Figure 3-19. The element has a width of dr and is located at a distance of r from the center of the well. The porous element has a differential volume of dV. According to the concept of the material-balance equation, the rate of mass flow into an element minus the rate of mass flow out of the element during a differential time Δt must be equal to the mass rate of accumulation during that time interval, or

$$\begin{bmatrix} \text{mass entering} \\ \text{volume element} \\ \text{during interval } \Delta t \end{bmatrix} - \begin{bmatrix} \text{mass leaving} \\ \text{volume element} \\ \text{during interval } \Delta t \end{bmatrix}$$

$$= \begin{bmatrix} \text{rate of mass} \\ \text{accumulation} \\ \text{during interval } \Delta t \end{bmatrix}$$
 (3-56)

The individual terms of Equation 3-56 are described next.

Mass Entering the Volume Element during Time Interval Δt

$$(Mass)_{in} = \Delta t [A\nu\rho]_{r+dr}$$
 (3-57)

where v = velocity of flowing fluid, ft/day $\rho =$ fluid density at (r + dr), lb/ft^3

A = Area at (r + dr)

 $\Delta t = \text{time interval, days}$

The area of element at the entering side is

$$A_{r+dr} = 2\pi(r+dr)h \tag{3-58}$$

Combining Equation 3-58 with 3-57 gives

$$[Mass]_{in} = 2\pi\Delta t(r + dr)h(\nu\rho)_{r+dr}$$
 (3-59)

Mass Leaving the Volume Element

Adopting the same approach as that of the leaving mass gives

$$[Mass]_{out} = 2\pi\Delta trh(\nu\rho)_{r}$$
 (3-60)

Total Accumulation of Mass

The volume of some element with a radius of r is given by

$$V = \pi r^2 h$$

Differentiating this equation with respect to r gives

$$\frac{dV}{dr} = 2\pi rh$$

or

$$\begin{split} dV &= (2\pi rh) dr \\ Total \ mass \ accumulation \ during \ \Delta t = dV[(\varphi\rho)_{t+\Delta t} - (\varphi\rho)_t] \end{split} \tag{3-61}$$

Substituting for dV yields

Total mass accumulation =
$$(2\pi rh)dr[(\phi\rho)_{t+\Delta t} - (\phi\rho)_t]$$
 (3-62)

Replacing the terms of Equation 3-56 with those of the calculated relationships gives

$$2\pi h(r+dr)\Delta t(\varphi\rho)_{r+dr}-2\pi hr\Delta t(\varphi\rho)_{r}=(2\pi rh)dr[(\varphi\rho)_{t+\Delta t}-(\varphi\rho)_{t}]$$

Dividing this equation by $(2\pi rh)dr$ and simplifying gives

$$\frac{1}{(r)dr}[(r+dr)(\nu\rho)_{r+dr}-r(\nu\rho)_{r}] = \frac{1}{\Delta t}[(\phi\rho)_{t+\Delta t}-(\phi\rho)_{t}]$$

or

$$\frac{1}{r}\frac{\partial}{\partial r}[r(\nu\rho)] = \frac{\partial}{\partial t}(\phi\rho) \tag{3-63}$$

where $\phi = \text{porosity}$ $\rho = \text{density, lb/ft}^3$ v = fluid velocity, ft/day Equation 3-63 is called the *continuity equation*, and it provides the principle of conservation of mass in radial coordinates.

The transport equation must be introduced into the continuity equation to relate the fluid velocity to the pressure gradient within the control volume dV. Darcy's Law is essentially the basic motion equation, which states that the velocity is proportional to the pressure gradient $(\partial p/\partial r)$.

From Equation 3-25,

$$\begin{split} \nu &= (5.615)(0.001127)\frac{k}{\mu}\frac{\partial p}{\partial r}\\ \nu &= (0.006328)\frac{k}{\mu}\frac{\partial p}{\partial r} \end{split} \tag{3-64}$$

where k = permeability, mdv = velocity, ft/day

Combining Equation 3-64 with Equation 3-63 results in

$$\frac{0.006328}{r} \frac{\partial}{\partial r} \left(\frac{k}{\mu} (\rho r) \frac{\partial p}{\partial r} \right) = \frac{\partial}{\partial t} (\phi \rho) \tag{3-65}$$

Expanding the right-hand side by taking the indicated derivatives eliminates the porosity from the partial derivative term on the right-hand side:

$$\frac{\partial}{\partial t}(\phi \rho) = \phi \frac{\partial \rho}{\partial t} + \rho \frac{\partial \phi}{\partial t}$$
 (3-66)

As shown in Part 2, porosity is related to the formation compressibility by the following:

$$c_{\rm f} = \frac{1}{\Phi} \frac{\partial \Phi}{\partial p} \tag{3-67}$$

Applying the chain rule of differentiation to $\partial \phi / \partial t$,

$$\frac{\partial \varphi}{\partial t} = \frac{\partial \varphi}{\partial p} \frac{\partial p}{\partial t}$$

Substituting Equation 3-67 into this equation,

$$\frac{\partial \varphi}{\partial t} = \varphi c_f \frac{\partial p}{\partial t}$$

Finally, substituting the preceding relation into Equation 3-66 and the result into Equation 3-65 gives

$$\frac{0.006328}{r} \frac{\partial}{\partial r} \left(\frac{k}{\mu} (\rho r) \frac{\partial p}{\partial r} \right) = \rho \varphi c_f \frac{\partial p}{\partial t} + \varphi \frac{\partial \rho}{\partial t} \tag{3-68}$$

Equation 3-68 is the general partial differential equation used to describe the flow of any fluid flowing in a radial direction in porous media. In addition to the initial assumptions, Darcy's equation has been added, which implies that the flow is laminar. Otherwise, the equation is not restricted to any type of fluid and is equally valid for gases or liquids. Compressible and slightly compressible fluids, however, must be treated separately in order to develop practical equations that can be used to describe the flow behavior of these two fluids. The treatments of the following systems are discussed:

- Radial flow of slightly compressible fluids.
- Radial flow of compressible fluids.

Radial Flow of Slightly Compressible Fluids

To simplify Equation 3-68, assume that the permeability and viscosity are constant over pressure, time, and distance ranges. This leads to

$$\left[\frac{0.006328 \text{ k}}{\mu r}\right] \frac{\partial}{\partial r} \left(r \rho \frac{\partial p}{\partial r}\right) = \rho \phi c_f \frac{\partial p}{\partial t} + \phi \frac{\partial \rho}{\partial t} \tag{3-69}$$

Expanding the equation gives

$$0.006328 \left(\frac{k}{\mu}\right) \left[\frac{\rho}{r} \frac{\partial p}{\partial r} + \rho \frac{\partial^2 p}{\partial r^2} + \frac{\partial p}{\partial r} \frac{\partial \rho}{\partial r}\right] = \rho \varphi c_f \left(\frac{\partial p}{\partial t}\right) + \varphi \left(\frac{\partial \rho}{\partial t}\right)$$

Using the chain rule in this relationship yields

$$0.006328 \left(\frac{k}{\mu}\right) \left[\frac{p}{r} \frac{\partial p}{\partial r} + p \frac{\partial^2 p}{\partial r^2} + \left(\frac{\partial \rho}{\partial \rho}\right)^2 \frac{\partial \rho}{\partial \rho}\right] = p \varphi c_f \left(\frac{\partial p}{\partial t}\right) + \varphi \left(\frac{\partial p}{\partial t}\right) \left(\frac{\partial p}{\partial \rho}\right)$$

Dividing the expression by the fluid density ρ gives

$$\begin{split} 0.006328 \bigg(\frac{k}{\mu}\bigg) & \left[\frac{1}{r} \frac{\partial p}{\partial r} + \frac{\partial^2 p}{\partial r^2} + \bigg(\frac{\partial p}{\partial r}\bigg)^2 \bigg(\frac{1}{\rho} \frac{\partial \rho}{\partial \rho}\bigg) \right] \\ & = \varphi c_f \bigg(\frac{\partial p}{\partial t}\bigg) + \varphi \frac{\partial p}{\partial t} \bigg(\frac{1}{\rho} \frac{\partial \rho}{\partial p}\bigg) \end{split}$$

Recall that the compressibility of any fluid is related to its density by

$$c = \frac{1}{\rho} \frac{\partial \rho}{\partial p}$$

Combining the preceding two equations gives

$$0.006328 \left(\frac{k}{\mu}\right) \left[\frac{\partial^2 p}{\partial r^2} + \frac{1}{r} \frac{\partial p}{\partial r} + c \left(\frac{\partial p}{\partial r}\right)^2\right] = \varphi c_f \left(\frac{\partial p}{\partial t}\right) + \varphi c \left(\frac{\partial p}{\partial t}\right)$$

The term $c \Big(\frac{\partial p}{\partial r} \Big)^2$ is considered very small and may be ignored:

$$0.006328 \left(\frac{k}{\mu}\right) \left[\frac{\partial^2 p}{\partial r^2} + \frac{1}{r} \frac{\partial p}{\partial r}\right] = \phi(c_f + c) \frac{\partial p}{\partial t} \tag{3-70}$$

Define total compressibility, c_t , as

$$c_t = c + c_f \tag{3-71}$$

Combining Equations 3-69 with 3-70 and rearranging gives

$$\frac{\partial^2 \mathbf{p}}{\partial \mathbf{r}^2} + \frac{1}{\mathbf{r}} \frac{\partial \mathbf{p}}{\partial \mathbf{r}} = \frac{\phi \mu c_t}{0.006328 \, \mathbf{k}} \frac{\partial \mathbf{p}}{\partial \mathbf{t}} \tag{3-72}$$

where the time t is expressed in days.

Equation 3-72 is called the *diffusivity equation*. It is one of the most important equations in petroleum engineering. The equation is used particularly in analysis of well testing data, where the time t is commonly recorded in hours. The equation can be rewritten as

$$\frac{\partial^2 \mathbf{p}}{\partial \mathbf{r}^2} + \frac{1}{\mathbf{r}} \frac{\partial \mathbf{p}}{\partial \mathbf{r}} = \frac{\phi \mu c_t}{0.000264 \, k} \frac{\partial \mathbf{p}}{\partial \mathbf{t}} \tag{3-73}$$

where k = permeability, md

r = radial position, ft

p = pressure, psia

 $c_t = total compressibility, psi^{-1}$

t = time, hrs

 ϕ = porosity, fraction

 $\mu = viscosity$, cp

When the reservoir contains more than one fluid, total compressibility should be computed as

$$c_t = c_o S_o + c_w S_w + c_g S_g + c_f$$
 (3-74)

where c_o , c_w , and c_g refer to the compressibility of oil, water, and gas, respectively, while S_o , S_w , and S_g refer to the fractional saturation of these fluids. Note that the introduction of c_t into Equation 3-72 does not make Equation 3-72 applicable to multiphase flow; the use of c_t , as defined by Equation 3-73, simply accounts for the compressibility of any *immobile* fluids that may be in the reservoir with the fluid that is flowing.

The term [0.000264 k/ $\phi\mu c_t$] (Equation 3-73) is called the *diffusivity* constant and is denoted by the symbol η , or

$$\eta = \frac{0.000264 \text{ k}}{\phi \mu c_t} \tag{3-75}$$

The diffusivity equation can then be written in a more convenient form as

$$\frac{\partial^2 \mathbf{p}}{\partial \mathbf{r}^2} + \frac{1}{\mathbf{r}} \frac{\partial \mathbf{p}}{\partial \mathbf{r}} = \frac{1}{\mathbf{n}} \frac{\partial \mathbf{p}}{\partial \mathbf{t}}$$
 (3-76)

The diffusivity equation as represented by Equation 3-76 is essentially designed to determine the pressure as a function of time t and position r.

Before discussing and presenting the different solutions to the diffusivity equation, it is necessary to summarize the assumptions and limitations used in developing Equation 3-76:

- 1. Homogeneous and isotropic porous medium.
- 2. Uniform thickness.
- 3. Single phase flow.
- 4. Laminar flow.
- 5. Rock and fluid properties independent of pressure.

Notice that for a steady-state flow condition, the pressure at any point in the reservoir is constant and does not change with time, i.e., $\partial p/\partial t = 0$, and therefore Equation 3-76 reduces to

$$\frac{\partial^2 \mathbf{p}}{\partial \mathbf{r}^2} + \frac{1}{\mathbf{r}} \frac{\partial \mathbf{p}}{\partial \mathbf{r}} = 0 \tag{3-77}$$

Equation 3-77 is called *Laplace's equation for steady-state flow*.

Example 3-9

Show that the radial form of Darcy's equation is the solution to Equation 3-77.

Solution

Step 1. Start with Darcy's Law as expressed by Equation 3-29:

$$p = p_{wf} + \left[\frac{Q_o B_o u_o}{0.00708 \ kh}\right] ln \bigg(\frac{r}{r_w}\bigg) \label{eq:pwf}$$

Step 2. For a steady-state incompressible flow, the term between the two brackets is constant and labeled as C, or

$$p = p_{wf} + [C] \ln \left(\frac{r}{r_w}\right)$$

Step 3. Evaluate this expression for the first and second derivative to give

$$\frac{\partial p}{\partial r} = [C] \left(\frac{1}{r}\right)$$

$$\frac{\partial^2 p}{\partial r^2} = [C] \left(\frac{-1}{r^2} \right)$$

Step 4. Substitute these two derivatives in Equation 3-77:

$$\frac{-1}{r^2}[C] + \left(\frac{1}{r}\right)[C]\left(\frac{-1}{r}\right) = 0$$

Step 5. Results of Step 4 indicate that Darcy's equation satisfies Equation3-77 and is indeed the solution to Laplace's equation.

To obtain a solution to the diffusivity equation (Equation 3-76), it is necessary to specify an initial condition and impose two boundary conditions. The initial condition simply states that the reservoir is at a uniform pressure p_i when production begins. The two boundary conditions require that the well is producing at a constant production rate and that the reservoir behaves as if it were infinite in size, i.e., $r_e = \infty$.

Based on the boundary conditions imposed on Equation 3-76, there are two generalized solutions to the diffusivity equation:

- Constant-terminal-pressure solution.
- Constant-terminal-rate solution.

The *constant-terminal-pressure solution* is designed to provide the cumulative flow at any particular time for a reservoir in which the pressure at one boundary of the reservoir is held constant. This technique is frequently used in water influx calculations in gas and oil reservoirs.

The *constant-terminal-rate solution* to the radial diffusivity equation solves for the pressure change throughout the radial system providing that the flow rate is held constant at one terminal end of the radial system, i.e., at the producing well. These are two commonly used forms of the constant-terminal-rate solution:

- The E_i-function solution.
- The dimensionless pressure p_D solution.

SECTION 3.8 CONSTANT-TERMINAL-PRESSURE SOLUTION

In the constant-rate solution to the radial diffusivity equation, the flow rate is considered to be constant at a certain radius (usually the wellbore radius) and the pressure profile around that radius is determined as a function of time and position. In the constant-terminal-pressure solution, the pressure is known to be constant at some particular radius and the solution is designed to provide the cumulative fluid movement across the specified radius (boundary).

The constant-pressure solution is widely used in water influx calculations.

SECTION 3.9 CONSTANT-TERMINAL-RATE SOLUTION

The constant-terminal-rate solution is an integral part of most transient test analysis techniques, such as with drawdown and pressure buildup analyses. Most of these tests involve producing the well at a *constant flow rate* and recording the flowing pressure as a function of time, i.e., $p(r_w, t)$. There are two commonly used forms of the constant-terminal-rate solution:

- The E_i-function solution.
- The dimensionless pressure p_D solution.

These are discussed here.

The E_i-Function Solution

Matthews and Russell (1967) proposed a solution to the diffusivity equation that is based on the following assumptions:

- Infinite-acting reservoir, i.e., the reservoir is infinite in size.
- The well is producing at a constant flow rate.
- The reservoir is at a uniform pressure, p_i, when production begins.
- The well, with a wellbore radius of r_w, is centered in a cylindrical reservoir of radius r_e.
- No flow across the outer boundary, i.e., at r_e.

Employing these conditions, the authors presented their solution in the following form:

$$p(r,t) = p_{i} + \left[\frac{70.6Q_{o}\mu_{o}b_{o}}{kh}\right]E_{i}\left[\frac{-948\phi\mu_{o}c_{t}r^{2}}{kt}\right] \tag{3-78}$$

where p(r, t) = pressure at radius r from the well after t hours

t = time, hrs

k = permeability, md

 $Q_o = flow rate, STB/day$

The mathematical function, E_{i} , is called the *exponential integral* and is defined by

$$E_{i}(-x) = -\int_{-\infty}^{\infty} \frac{e^{-u}du}{u} = \left[\ln x - \frac{x}{1!} + \frac{x^{2}}{2(2)} - \frac{x^{3}}{3(3!)} + \text{etc.} \right]$$
 (3-79)

Craft, Hawkins, and Terry (1990) presented the values of the E_i-function in tabulated and graphical forms as shown in Table 3-1 and Figure 3-20, respectively.

TABLE 3-1 Values of $-E_i$ (-x) as a Function of x (After Craft, Hawkins, and Terry, 1990)

х	-E _i (-x)	x	-E _i (-x)	х	-E _i (-x)
0.1	1.82292	4.3	0.00263	8.5	0.00002
0.2	1.22265	4.4	0.00234	8.6	0.00002
0.3	0.90568	4.5	0.00207	8.7	0.00002
0.4	0.70238	4.6	0.00184	8.8	0.00002
0.5	0.55977	4.7	0.00164	8.9	0.00001
0.6	0.45438	4.8	0.00145	9.0	0.00001
0.7	0.37377	4.9	0.00129	9.1	0.00001
0.8	0.31060	5.0	0.00115	9.2	0.00001
0.9	0.26018	5.1	0.00102	9.3	0.00001
1.0	0.21938	5.2	0.00091	9.4	0.00001
1.1	0.18599	5.3	0.00081	9.5	0.00001
1.2	0.15841	5.4	0.00072	9.6	0.00001
1.3	0.13545	5.5	0.00064	9.7	0.00001
1.4	0.11622	5.6	0.00057	9.8	0.00001
1.5	0.10002	5.7	0.00051	9.9	0.00000
1.6	0.08631	5.8	0.00045	10.0	0.00000
1.7	0.07465	5.9	0.00040		
1.8	0.06471	6.0	0.00036		
1.9	0.05620	6.1	0.00032		
2.0	0.04890	6.2	0.00029		
2.1	0.04261	6.3	0.00026		
2.2	0.03719	6.4	0.00023		
2.3	0.03250	6.5	0.00020		
2.4	0.02844	6.6	0.00018		
2.5	0.02491	6.7	0.00016		
2.6	0.02185	6.8	0.00014		
2.7	0.01918	6.9	0.00013		
2.8	0.01686	7.0	0.00012		
2.9	0.01482	7.1	0.00010		
3.0	0.01305	7.2	0.00009		
3.1	0.01149	7.3	0.00008		
3.2	0.01013	7.4	0.00007		

x	-E _i (-x)	x	$-E_i(-x)$	x	$-E_i(-x)$
3.3	0.00894	7.5	0.00007		
3.4	0.00789	7.6	0.00006		
3.5	0.00697	7.7	0.00005		
3.6	0.00616	7.8	0.00005		
3.7	0.00545	7.9	0.00004		
3.8	0.00482	8.0	0.00004		
3.9	0.00427	8.1	0.00003		
4.0	0.00378	8.2	0.00003		
4.1	0.00335	8.3	0.00003		
4.2	0.00297	8.4	0.00002		

TABLE 3-1 Values of $-E_i$ (-x) as a Function of x (After Craft, Hawkins, and Terry, 1990)—Cont'd

The E_i solution, as expressed by Equation 3-78, is commonly referred to as the *line-source solution*. The exponential integral E_i can be approximated by the following equation when its argument x is less than 0.01:

$$E_{i}(-x) = \ln(1.781x) \tag{3-80}$$

where the argument x in this case is given by

$$x=\frac{948\varphi\mu c_t r^2}{kt}$$

Equation 3-80 approximates the E_i -function with less than 0.25% error. Another expression that can be used to approximate the E_i -function for the range 0.01 < x < 3.0 is given by

$$E_{i}(-x) = a_{1} + a_{2} \ln(x) + a_{3} [\ln(x)]^{2} + a_{4} [\ln(x)]^{3} + a_{5}x + a_{6}x^{2} + a_{7}x^{3} + a_{8}/x$$
(3-81)

with the coefficients a_1 through a_8 having the following values:

$$\begin{array}{lll} a_1 = -0.33153973 & a_2 = -0.81512322 & a_3 = 5.22123384(10^{-2}) \\ a_4 = 5.9849819(10^{-3}) & a_5 = 0.662318450 & a_6 = -0.12333524 \\ a_7 = 1.0832566(10^{-2}) & a_8 = 8.6709776(10^{-4}) \end{array}$$

This relationship approximates the E_i -values with an average error of 0.5%.

It should be pointed out that, for x > 10.9, E_i (–x) can be considered 0 for all practical reservoir engineering calculations.

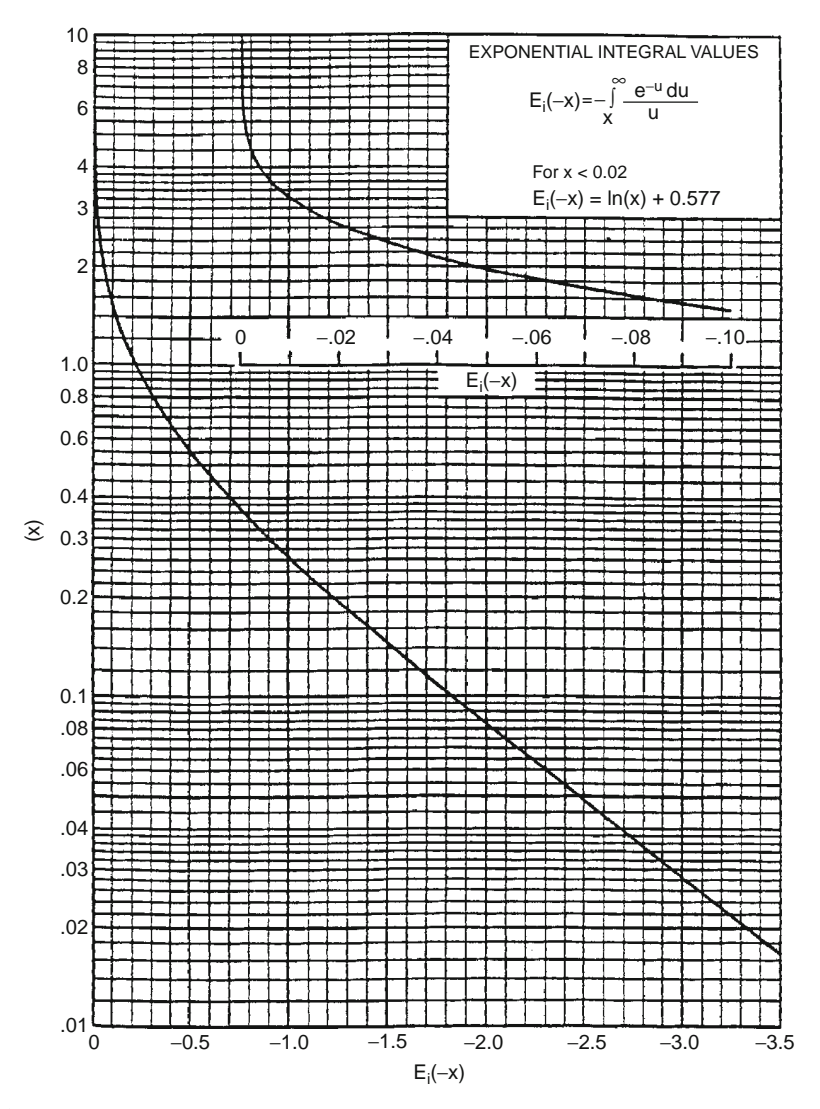


FIGURE 3-20 The E_i-function. (After Craft, Hawkins, and Terry, 1991.)

Example 3-10

An oil well is producing at a constant flow rate of 300 STB/day under unsteady-state flow conditions. The reservoir has the following rock and fluid properties:

$$\begin{array}{lll} B_o = 1.25 \ bbl/STB & \quad \mu_o = 1.5 \ cp & \quad c_t = 12 \times 10^{-6} \ psi^{-1} \\ k_o = 60 \ md & \quad h = 15 \ ft & \quad p_i = 4000 \ psi \\ \varphi = 15\% & \quad r_w = 0.25 \ ft\% & \end{array}$$

- 1. Calculate pressure at radii of 0.25, 5, 10, 50, 100, 500, 1000, 1500, 2000, and 2500 feet, for 1 hour. Plot the results as
 - a. Pressure versus logarithm of radius.
 - b. Pressure versus radius.
- 2. Repeat the above step for t=12 hours and 24 hours. Plot the results as pressure versus logarithm of radius.

Solution

Step 1. From Equation 3-78,

$$\begin{split} p(r,t) &= 4000 + \left[\frac{70.6(300)(1.5)(1.25)}{(60)(15)} \right] \\ &\times E_i \left[\frac{-948(0.15)(1.5)(12\times 10^{-6})r^2}{(60)(t)} \right] \\ p(r,t) &= 4000 + 44.125 \ E_i \left[-42.6(10^{-6})\frac{r^2}{t} \right] \end{split}$$

Step 2. Perform the required calculations after 1 hour in the following tabulated form:

Elapsed Time $t = 1 \text{ hr}$				
r, ft	$x = -42.6(10^{-6})\frac{r^2}{1}$	E _i (-x)	$p(r,1) = 4000 + 44.125 E_i(-x)$	
0.25	$-2.6625(10^{-6})$	-12.26*	3459	
5	-0.001065	-6.27 *	3723	
10	-0.00426	-4.88 *	3785	
50	-0.1065	-1.76^{\dagger}	3922	
100	-0.4260	-0.75^{\dagger}	3967	
500	-10.65	0	4000	
1000	-42.60	0	4000	
1500	-95.85	0	4000	
2000	-175.40	0	4000	
2500	-266.25	0	4000	

^{*}As calculated from Equation 3-29.

Step 3. Show results of the calculation graphically as illustrated in Figures 3-21 and 3-22.

[†]From Figure 3-20.

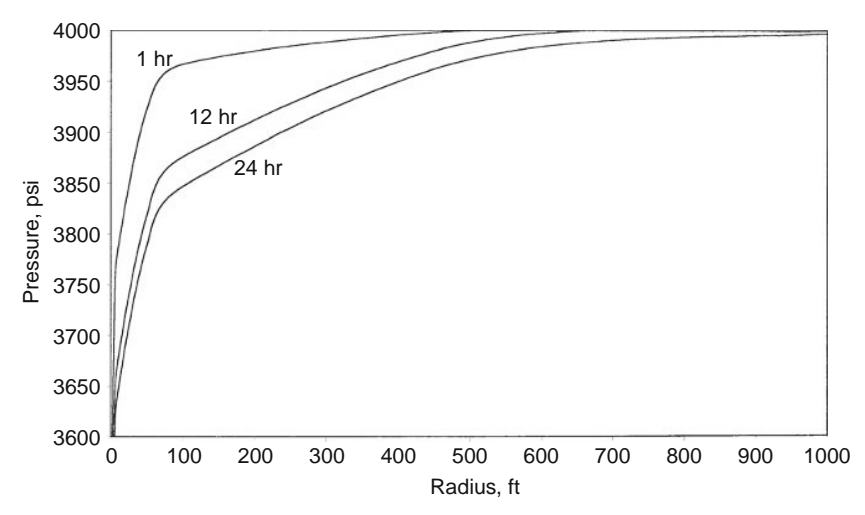


FIGURE 3-21 Pressure profiles as a function of time.

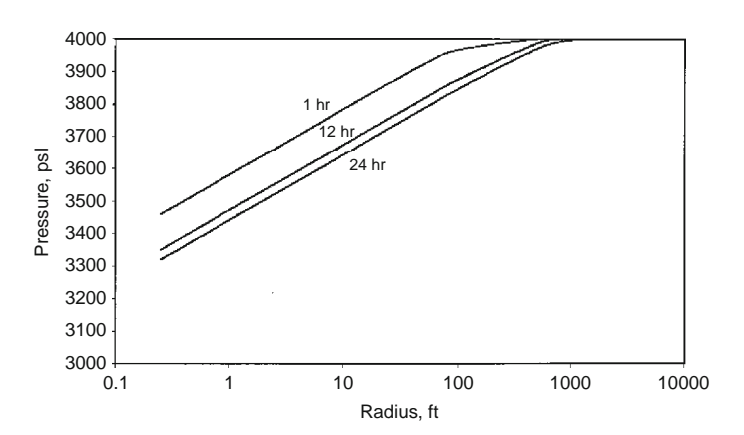


FIGURE 3-22 Pressure profiles as a function of time on a semilog scale.

Step 4. Repeat the calculation for t = 12 and 24 hrs.

Elapsed Time t = 12 hrs				
r, ft	$x = 42.6(10^{-6})\frac{r^2}{12}$	$E_i(-x)$	$p(r, 12) = 4000 + 44.125 E_i(-x)$	
0.25	$0.222(10^{-6})$	-14.74*	3350	
5	$88.75 (10^{-6})$	-8.75 *	3614	
10	$355.0 (10^{-6})$	−7.37 *	3675	
50	0.0089	-4.14 *	3817	
100	0.0355	-2.81^{\dagger}	3876	
500	0.888	-0.269	3988	

1000	3.55	-0.0069	4000
1500	7.99	$-3.77(10^{-5})$	4000
2000	14.62	0	4000
2500	208.3	0	4000

^{*}As calculated from equation 3-29.

[†]From Figure 3-20.

Elapsed Time $t = 24 \text{ hrs}$				
r, ft	$x = 42.6(10^{-6})\frac{r^2}{24}$	$E_i(-x)$	$p(r, 24) = 4000 + 44.125 E_i(-x)$	
0.25	-0.111 (10 ⁻⁶)	-15.44*	3319	
5	$-44.38 (10^{-6})$	-9.45 *	3583	
10	$-177.5 (10^{-6})$	-8.06*	3644	
50	-0.0045	-4.83*	3787	
100	-0.0178	-3.458 †	3847	
500	-0.444	-0.640	3972	
1000	-1.775	-0.067	3997	
1500	-3.995	-0.0427	3998	
2000	-7.310	$8.24 (10^{-6})$	4000	
2500	-104.15	0	4000	

^{*}As calculated from Equation 3-29.

Step 5. Results of Step 4 are shown graphically in Figure 3-22.

This example shows that most of the pressure loss occurs close to the wellbore; accordingly, near-wellbore conditions will exert the greatest influence on flow behavior. Figure 3-22 shows that the pressure profile and the drainage radius are continuously changing with time.

When the parameter x in the E_i -function is less than 0.01, the log approximation as expressed by Equation 3-80 can be used in Equation 3-78 to give

$$p(r,t) = p_i - \frac{162.6 Q_o B_o m_o}{kh} \left[log \left(\frac{kt}{\phi \mu_o c_t r^2} \right) - 3.23 \right]$$
 (3-82)

For most of the transient flow calculations, engineers are primarily concerned with the behavior of the bottom-hole flowing pressure at the wellbore, i.e., $r = r_w$. Equation 3-82 can be applied at $r = r_w$ to yield

$$p_{wf} = p_{i} - \frac{162.6 \, Q_{o} B_{o} m_{o}}{kh} \left[log \left(\frac{kt}{\phi \mu_{o} c_{t} r_{w}^{2}} \right) - 3.23 \right] \tag{3-83}$$

where k = permeability, md

t = time, hr

 $c_t = total compressibility, psi^{-1}$

[†]From Figure 3-20.

It should be noted that Equations 3-82 and 3-83 cannot be used until the flow time t exceeds the limit imposed by the following constraint:

$$t > 9.48 \times 10^4 \frac{\phi \mu_0 c_t r^2}{k} \tag{3-84}$$

where t = time, hr

k = permeability, md

Example 3-11

Using the data in Example 3-10, estimate the bottom-hole flowing pressure after 10 hours of production.

Solution

Step 1. Equation 3-83 can be used to calculate p_{wf} only if the time exceeds the time limit imposed by Equation 3-84, or

$$t = 9.48(10^4) \frac{(0.15)(1.5)(12 \times 10^{-6})(0.25)^2)}{60} = 0.000267 \text{ hr}$$
$$= 0.153 \text{ sec}$$

For all practical purposes, Equation 3-83 can be used anytime during the transient flow period to estimate the bottom-hole pressure.

Step 2. Since the specified time of 10 hrs is greater than 0.000267 hr, the p_{wf} can be estimated by applying Equation 3-83:

$$\begin{split} p_{wf} &= 4000 - \frac{162.6(300)(1.25)(1.5)}{(60)(15)} \\ &\times \left\{ log \left[\frac{(60)(10)}{(0.15)(1.5)(12\times 10^{-6})(0.25)^2} \right] - 3.23 \right\} = 3358 \; psi \end{split}$$

The second form of solution to the diffusivity equation is called the *dimensionless pressure drop* and is discussed next.

The Dimensionless Pressure Drop (pD) Solution

Well test analysis often makes use of the concept of dimensionless variables in solving the unsteady-state flow equation. The importance of dimensionless variables is that they simplify the diffusivity equation and its solution by combining the reservoir parameters (such as permeability and porosity) and thereby reduce the total number of unknowns.

To introduce the concept of the dimensionless pressure drop solution, consider for example Darcy's equation in a radial form, as given previously by Equation 3-27:

$$Q_{o} = 0.00708 \frac{kh(p_{e} - p_{wf})}{\mu_{o} B_{o} \, ln(r_{e}/r_{w})} \label{eq:Qo}$$

Rearrange the equation to give

$$\frac{p_{e} - p_{wf}}{\left(\frac{Q_{o} B_{o} \mu_{o}}{0.00708 \text{ kh}}\right)} = \ln\left(\frac{r_{e}}{r_{w}}\right)$$
(3-85)

It is obvious that the right-hand side of the equation has no units (i.e., dimensionless) and, accordingly, the left-hand side must be dimensionless. Since the left-hand side is dimensionless and $(p_e-p_{\rm wf})$ has the units of psi, it follows that the term $[Q_oB_o\mu_o/(0.00708~kh)]$ has units of pressure. In fact, any pressure difference divided by $[Q_oB_o\mu_o/(0.00708~kh)]$ is a dimensionless pressure. Therefore, Equation 3-85 can be written in a dimensionless form as

$$p_D = ln(r_{eD})$$

where

$$p_{D} = \frac{p_{e} - p_{wf}}{\left(\frac{Q_{o}B_{o}\mu_{o}}{0.00708 \text{ kh}}\right)}$$

This concept can be extended to consider unsteady-state equations where time is a variable. Define

$$r_{eD} = \frac{r_e}{r_w}$$

In transient flow analysis, the dimensionless pressure p_D is always a function of dimensionless time that is defined by the following expression:

$$p_{D} = \frac{p_{i} - p(r, t)}{\left(\frac{Q_{o}B_{o}\mu_{o}}{0.00708 \text{ kh}}\right)}$$
(3-86)

In transient flow analysis, the dimensionless pressure p_D is always a function of dimensionless time that is defined by the following expression:

$$t_{\rm D} = \frac{0.000264 \text{ kt}}{\phi \mu c_{\rm t} r_{\rm w}^2} \tag{3-87a}$$

This expression is only one form of dimensionless time. Another definition in common usage is $t_{\rm DA}$, the dimensionless time based on total drainage area:

$$t_{DA} = \frac{0.000264 \text{ kt}}{\phi \mu c_t A} = t_D \left(\frac{r_w^2}{A}\right) \tag{3-87b}$$

where A = total drainage area = πr_e^2

 $r_{e} = drainage radius$, ft

 $r_{\rm w}$ = wellbore radius, ft

The dimensionless pressure p_D also varies with location in the reservoir as represented by the dimensionless radial distances r_D and r_{eD} that are defined by

$$r_{\rm D} = \frac{r}{r_{\rm w}} \tag{3-88}$$

and

$$r_{eD} = \frac{r_e}{r_w} \tag{3-89}$$

where p_D = dimensionless pressure drop

 $r_{eD} = dimensionless$ external radius

 $t_D = dimensionless time$

 $r_D = dimensionless radius$

t = time, hr

p(r,t) = pressure at radius r and time t

k = permeability, md

 $\mu = viscosity$, cp

These dimensionless groups (i.e., p_D , t_D , and r_D) can be introduced into the diffusivity equation (Equation 3-76) to transform the equation into the following dimensionless form:

$$\frac{\partial^2 p_D}{\partial r_D^2} + \frac{1}{r_D} \frac{\partial p_D}{\partial r_D} = \frac{\partial p_D}{\partial t_D}$$
 (3-90)

Van Everdingen and Hurst (1949) proposed an analytical solution to the preceding equation by assuming

- The reservoir system is perfectly radial.
- The producing well is in the center and producing at a constant production rate of Q.
- Pressure p_i is uniform throughout the reservoir before production.
- ullet No flow occurs across the external radius r_e .

Van Everdingen and Hurst presented the solution to Equation 3-89 in a form of an infinite series of exponential terms and Bessel functions. The authors evaluated this series for several values of $r_{\rm eD}$ over a wide range of values for $t_{\rm D}$. Chatas (1953) and Lee (1982) conveniently tabulated these solutions for the following two cases:

- Infinite-acting reservoir
- Finite-radial reservoir

Infinite-Acting Reservoir

When a well is put in production at a constant flow rate after a shut-in period, the pressure in the wellbore begins to drop and causes a pressure disturbance to spread in the reservoir. The influence of the reservoir boundaries or the shape of the drainage area does not affect the rate at which the pressure disturbance spreads in the formation. That is why the transient state flow is also called the *infinite-acting state*. During the infinite-acting period, the declining rate of wellbore pressure and the manner by which the pressure disturbance spreads through the reservoir are determined by reservoir and fluid characteristics, such as

- Porosity, φ.
- Permeability, k.
- Total compressibility, ct.
- Viscosity, μ.

For an infinite-acting reservoir, i.e., $r_{eD} = \infty$, the dimensionless pressure drop function p_D is strictly a function of the dimensionless time t_D , or

$$p_D = f(t_D) \,$$

Chatas and Lee tabulated the p_D values for the infinite-acting reservoir as shown in Table 3-2. The following mathematical expressions can be used to approximate these tabulated values of p_D :

• For $t_D < 0.01$,

$$p_D = 2\sqrt{\frac{t_D}{\pi}} \tag{3-91}$$

• For $t_D > 100$,

$$p_D = 0.5[\ln(t_D) + 0.80907] \tag{3-92}$$

• For $0.02 < t_D < 1000$,

$$\begin{aligned} p_D &= a_1 + a_2 \ln(t_D) + a_3 [\ln(t_D)]^2 + a_4 [\ln(t_D)]^3 + a_5 t_D \\ &+ a_6 (t_D)^2 + a_7 (t_D)^3 + a_8 / t_D \end{aligned} \tag{3-93}$$

TABLE 3-2 p_D versus t_D —Infinite-Radial System, Constant-Rate at the Inner Boundary (After Lee, J., Well Testing, SPE Textbook Series.) (Permission to publish by the SPE, copyright SPE, 1982)

0 0 0.1 0.0005 0.0250 0.2 0.001 0.0352 0.3	0.4241 0.5024	60.0 70.0 80.0	2.4758 2.5501 2.6147
0.001 0.0352 0.3	0.5024	80.0	
			2 6147
	0.5645		4.014/
0.002 0.0495 0.4		90.0	2.6718
0.003 0.0603 0.5	0.6167	100.0	2.7233
0.004 0.0694 0.6	0.6622	150.0	2.9212
0.005 0.0774 0.7	0.7024	200.0	3.0636
0.006 0.0845 0.8	0.7387	250.0	3.1726
0.007 0.0911 0.9	0.7716	300.0	3.2630
0.008 0.0971 1.0	0.8019	350.0	3.3394
0.009 0.1028 1.2	0.8672	400.0	3.4057
0.01 0.1081 1.4	0.9160	450.0	3.4641
0.015 0.1312 2.0	1.0195	500.0	3.5164
0.02 0.1503 3.0	1.1665	550.0	3.5643
0.025 0.1669 4.0	1.2750	600.0	3.6076
0.03 0.1818 5.0	1.3625	650.0	3.6476
0.04 0.2077 6.0	1.4362	700.0	3.6842
0.05 0.2301 7.0	1.4997	750.0	3.7184
0.06 0.2500 8.0	1.5557	800.0	3.7505
0.07 0.2680 9.0	1.6057	850.0	3.7805
0.08 0.2845 10.0	1.6509	900.0	3.8088
0.09 0.2999 15.0	1.8294	950.0	3.8355
0.1 0.3144 20.0	1.9601	1,000.0	3.8584
30.0	2.1470		
40.0	2.2824		
50.0	2.3884		

$$\begin{split} &\text{Notes: For } t_D < 0.01, p_D \cong 2Z\sqrt{D}/x. \\ &\text{For } 100 < t_D < 0.25r_{eD}^2, \ p_D \cong 0.5(\ lnt_D + 0.80907). \end{split}$$

where

where
$$\begin{array}{lll} a_1=0.8085064 & a_2=0.29302022 & a_3=3.5264177(10^{-2}) \\ a_4=-1.4036304(10^{-3}) & a_5=-4.7722225(10^{-4}) & a_6=5.1240532(10^{-7}) \\ a_7=-2.3033017(10^{-10}) & a_8=-2.6723117(10^{-3}) \end{array}$$

Finite-Radial Reservoir

The arrival of the pressure disturbance at the well drainage boundary marks the end of the transient flow period and the beginning of the semi-steady (pseudo-) state. During this flow state, the reservoir boundaries and the shape of the drainage area influence the wellbore pressure response as well as the behavior of the pressure distribution throughout the reservoir. Intuitively, one should not expect the change from the transient to the semi-steady state in this bounded (finite) system to occur instantaneously. There is a short period of time that separates the transient state from the semi-steady state, which is called the *late-transient* state. Due to its complexity and short duration, the late-transient flow is not used in practical well test analysis.

For a finite radial system, the p_D-function is a function of both the dimensionless time and radius, or

$$p_D = f(t_D, r_{eD}) \,$$

where

$$r_{eD} = \frac{external\ radius}{wellbore\ radius} = \frac{r_e}{r_w} \tag{3-94}$$

Table 3-3 presents p_D as a function of t_D for $1.5 < r_{eD} < 10$. It should be pointed out that Van Everdingen and Hurst principally applied the p_D-function solution to model the performance of water influx into oil reservoirs. Thus, the authors' wellbore radius r_w was in this case the external radius of the reservoir and the r_e was essentially the external boundary radius of the aquifer. Therefore, the range of the red values in Table 3-3 is practical for this application.

Chatas (1953) proposed the following mathematical expression for calculating p_D .

For $25 < t_D$ and $0.25r_{eD}^2 < t_D$,

$$p_{D} = \frac{0.5 + 2t_{D}}{r_{eD}^{2} - 1} - \frac{r_{eD}^{4}[3 - 4\ln(r_{eD})] - 2r_{eD}^{2} - 1}{4(r_{eD}^{2} - 1)^{2}}$$
(3-95)

A special case of Equation 3-95 arises when $r_{eD}^2 \gg 1$; then

$$p_{\rm D} = \frac{2t_{\rm D}}{r_{\rm eD}^2} + \ln(r_{\rm eD}) - 0.75 \tag{3-96}$$

TABLE 3-3 p_D versus t_D —Finite-Radial System, Constant-Rate at the Inner Boundary (After Lee, J., Well Testing, SPE Textbook Series.) (Permission to publish by the SPE, copyright SPE, 1982)

r_{eD}	= 1.5	r _e	$_{\rm 2D} = 2.0$		r _{eD} =	= 2.5	r _{eD}	= 3.0)	r _{eD} =	3.5	r _{eD} =	= 4.0
t_D	p_{D}	t_{D}	p_{D}		t_D	p_{D}	t_{D}	p	D	t _D	p _D	t_D	p_{D}
0.06	0.251	0.22	2 0.44	3	0.40	0.565	0.52	0.6	27 1	.0	0.802	1.5	0.927
0.08	0.288	0.2	4 0.45	9	0.42	0.576	0.54	0.6	36 1	.1	0.830	1.6	0.948
0.10	0.322	0.20	6 0.47	6	0.44	0.587	0.56	0.6	45 1	.2	0.857	1.7	0.968
0.12	0.355	0.28	8 0.49	2	0.46	0.598	0.60	0.6	62 1	.3	0.882	1.8	0.988
0.14	0.387	0.30	0.50	7	0.48	0.608	0.65	0.6	83 1	.4	0.906	1.9	1.007
0.16	0.420	0.32	2 0.52	2	0.50	0.618	0.70	0.7	03 1	.5	0.929	2.0	1.025
0.18	0.452	0.3	4 0.53	6	0.52	0.628	0.75	0.7	21 1	.6	0.951	2.2	1.059
0.20	0.484	0.3	6 0.55	1	0.54	0.638	0.80	0.7	40 1	.7	0.973	2.4	1.092
0.22	0.516	0.38	8 0.56	5	0.56	0.647	0.85	0.7	58 1	.8	0.994	2.6	1.123
0.24	0.548	0.40	0.57	9	0.58	0.657	0.90	0.7	76 1	.9	1.014	2.8	1.154
0.26	0.580	0.42	2 0.59	3	0.60	0.666	0.95	0.7	91 2	0	1.034	3.0	1.184
0.28	0.612	0.4	4 0.60	7	0.65	0.688	1.0	0.8	06 2	25	1.083	3.5	1.255
0.30	0.644	0.40	6 0.62	1	0.70	0.710	1.2	0.8	65 2	50	1.130	4.0	1.324
0.35	0.724	0.48	8 0.63	4	0.75	0.731	1.4	0.9	20 2	75	1.176	4.5	1.392
0.40	0.804	0.50	0.64	8	0.80	0.752	1.6	0.9	73 3	.0	1.221	5.0	1.460
0.45	0.884	0.60	0.71	5	0.85	0.772	2.0	1.0	76 4	.0	1.401	5.5	1.527
0.50	0.964	0.70	0.78	2	0.90	0.792	3.0	1.3	28 5	0.0	1.579	6.0	1.594
0.55	1.044	0.80	0.849	9	0.95	0.812	4.0	1.5	78 6	.0	1.757	6.5	1.660
0.60	1.124	0.90	0.91	5	1.0	0.832	5.0	1.8	28			7.0	1.727
0.65	1.204	1.0	0.98	2	2.0	1.215						8.0	1.861
0.70	1.284	2.0	1.64	9	3.0	1.506						9.0	1.994
0.75	1.364	3.0	2.31	6	4.0	1.977						10.0	2.127
0.80	1.444	5.0	3.64	9	5.0	2.398							
r_{eD}	= 4.5	r _{eD} =	= 5.0	r _{eD}	= 6.0	r _{eD}	= 7.0	r _{eD}	= 8.0	r _{eD}	= 9.0	r _{eD} =	10.0
t_D	p_{D}	t _D	p _D	t _D	p_{D}	t_D	p_{D}	t_{D}	p_{D}	$\mathfrak{t}_{\mathrm{D}}$	p_{D}	t _D	p_{D}
2.0	1.023	3.0	1.167	4.0	1.275	6.0	1.436	8.0	1.556	10.0	1.651	12.0	1.732
2.1	1.040	3.1	1.180	4.5	1.322	6.5	1.470	8.5	1.582	10.5	1.673	12.5	1.750
2.2	1.056	3.2	1.192	5.0	1.364	7.0	1.501	9.0	1.607	11.0	1.693	13.0	1.768
2.3	1.702	3.3	1.204	5.5	1.404	7.5	1.531	9.5	1.631	11.5	1.713	13.5	1.784

TABLE 3-3 p_D versus t_D—Finite-Radial System, Constant-Rate at the Inner Boundary (After Lee, J., Well Testing, SPE Textbook Series.) (Permission to publish by the SPE, copyright SPE, 1982)—Cont'd

r_{eD}	= 4.5	r _{eD}	= 5.0	r _{eD}	= 6.0	r _{eD}	= 7.0	r _{eD}	= 8.0	r _{eD}	= 9.0	r _{eD} =	10.0
t_D	p_D	t_D	p_D	t_D	p_D	t_{D}	p_D	t_D	p_{D}	t_D	p_D	t_D	p_{D}
2.4	1.087	3.4	1.215	6.0	1.441	8.0	1.559	10.0	1.653	12.0	1.732	14.0	1.801
2.5	1.102	3.5	1.227	6.5	1.477	8.5	1.586	10.5	1.675	12.5	1.750	14.5	1.817
2.6	1.116	3.6	1.238	7.0	1.511	9.0	1.613	11.0	1.697	13.0	1.768	15.0	1.832
2.7	1.130	3.7	1.249	7.5	1.544	9.5	1.638	11.5	1.717	13.5	1.786	15.5	1.847
2.8	1.144	3.8	1.259	8.0	1.576	10.0	1.663	12.0	1.737	14.0	1.803	16.0	1.862
2.9	1.158	3.9	1.270	8.5	1.607	11.0	1.711	12.5	1.757	14.5	1.819	17.0	1.890
3.0	1.171	4.0	1.281	9.0	1.638	12.0	1.757	13.0	1.776	15.0	1.835	18.0	1.917
3.2	1.197	4.2	1.301	9.5	1.668	13.0	1.810	13.5	1.795	15.5	1.851	19.0	1.943
3.4	1.222	4.4	1.321	10.0	1.698	14.0	1.845	14.0	1.813	16.0	1.867	20.0	1.968
3.6	1.246	4.6	1.340	11.0	1.757	15.0	1.888	14.5	1.831	17.0	1.897	22.0	2.017
3.8	1.269	4.8	1.360	12.0	1.815	16.0	1.931	15.0	1.849	18.0	1.926	24.0	2.063
4.0	1.292	5.0	1.378	13.0	1.873	17.0	1.974	17.0	1.919	19.0	1.955	26.0	2.108
4.5	1.349	5.5	1.424	14.0	1.931	18.0	2.016	19.0	1.986	20.0	1.983	28.0	2.151
5.0	1.403	6.0	1.469	15.0	1.988	19.0	2.058	21.0	2.051	22.0	2.037	30.0	2.194
5.5	1.457	6.5	1.513	16.0	2.045	20.0	2.100	23.0	2.116	24.0	2.906	32.0	2.236
6.0	1.510	7.0	1.556	17.0	2.103	22.0	2.184	25.0	2.180	26.0	2.142	34.0	2.278
7.0	1.615	7.5	1.598	18.0	2.160	24.0	2.267	30.0	2.340	28.0	2.193	36.0	2.319
8.0	1.719	8.0	1.641	19.0	2.217	26.0	2.351	35.0	2.499	30.0	2.244	38.0	2.360
9.0	1.823	9.0	1.725	20.0	2.274	28.0	2.434	40.0	2.658	34.0	2.345	40.0	2.401
10.0	1.927	10.0	1.808	25.0	2.560	30.0	2.517	45.0	2.817	38.0	2.446	50.0	2.604
11.0	2.031	11.0	1.892	30.0	2.846					40.0	2.496	60.0	2.806
12.0	2.135	12.0	1.975							45.0	2.621	70.0	3.008
13.0	2.239	13.0	2.059							50.0	2.746	80.0	3.210
14.0	2.343	14.0	2.142							60.0	2.996	90.0	3.412
15.0	2.447	15.0	2.225							70.0	3.246	100.0	3.614

Notes: For t_D smaller than the values listed in this table for a given r_{eD} , reservoir is infinite acting.

Find p_D in Table 3-2.

For 25 <
$$t_D$$
 and t_D larger than values in table,
$$p_D \cong \frac{(1/2 + 2t_D)}{(r_{eD}^2 - 1)} - \frac{3r_{eD}^4 - 4r_{eD}^4 \ln r_{eD} - 2r_{eD}^2 - 1}{4(r_{eD}^2 - 1)^2}$$

For wells in rebounded reservoirs with $r_{eD}^2 \gg 1$,

$$p_{\mathrm{D}} \cong rac{2t_{\mathrm{D}}}{r_{\mathrm{eD}}^2} + \ln r_{\mathrm{eD}} - 3/4.$$

The computational procedure of using the p_D -function in determining the bottom-hole flowing pressure changing the transient flow period is summarized in the following steps:

- Step 1. Calculate the dimensionless time t_D by applying Equation 3-87.
- Step 2. Calculate the dimensionless radius r_{eD} from Equation 3-89.
- Step 3. Using the calculated values of $t_{\rm D}$ and $r_{\rm eD}$, determine the corresponding pressure function $p_{\rm D}$ from the appropriate table or equation.
- Step 4. Solve for the pressure at the desired radius, i.e., r_w, by applying Equation 3-86, or

$$p(r_w,t) = p_i - \left(\frac{Q_o B_o \mu_o}{0.00708 \ kh}\right) p_D \eqno(3-97)$$

Example 3-12

A well is producing at a constant flow rate of 300 STB/day under unsteady-state flow conditions. The reservoir has the following rock and fluid properties (see Example 3-10):

$$\begin{array}{lll} B_{o} = 1.25 \ bbl/STB & \mu_{o} = 1.5 \ cp & c_{t} = 12 \times 10^{-6} \ psi^{-1} \\ k = 60 \ md & h = 15 \ ft \\ \varphi = 15\% & r_{W} = 0.25^{'} & p_{i} = 4000 \ psi \end{array}$$

Assuming an infinite-acting reservoir, i.e., $r_{eD} = \infty$, calculate the bottom-hole flowing pressure after 1 hour of production by using the dimensionless pressure approach.

Solution

Step 1. Calculate the dimensionless time t_D from Equation 3-87:

$$t_D = \frac{0.000264(60)(1)}{(0.15)(1.5)(12\times 10^{-6}){(0.25)}^2} = 93,\!866.67$$

Step 2. Since $t_D > 100$, use Equation 3-92 to calculate the dimensionless pressure drop function:

$$p_D = 0.5[\,ln(93,\!866.67) + 0.80907] = 6.1294$$

Step 3. Calculate the bottom-hole pressure after 1 hour by applying Equation 3-97:

$$p(0.25,1) = 4000 - \left[\frac{(300)(1.25)(1.5)}{0.00708(60)(15)}\right](6.1294) = 3459 \ psi$$

This example shows that the solution as given by the p_D -function technique is identical to that of the E_i -function approach. The main difference between the two formulations is that the p_D -function can be used only to calculate the pressure at radius r when the flow rate Q is constant and known. In that case, the p_D -function application is essentially restricted to the wellbore radius because the rate is usually known. On the other hand, the E_i -function approach can be used to calculate the pressure at any radius in the reservoir by using the well flow rate Q.

It should be pointed out that, for an infinite-acting reservoir with $t_D > 100$, the p_D -function is related to the E_i -function by the following relation:

$$p_D = 0.5 \left[-E_i \left(\frac{-1}{4 t_D} \right) \right] \tag{3-98}$$

This example, i.e., Example 3-12, is not a practical problem, but it is essentially designed to show the physical significance of the $p_{\rm D}$ solution approach. In transient flow testing, we normally record the bottom-hole flowing pressure as a function of time. Therefore, the dimensionless pressure drop technique can be used to determine one or more of the reservoir properties, e.g., k or kh, as discussed later in this chapter.

Radial Flow of Compressible Fluids

Gas viscosity and density vary significantly with pressure and therefore the assumptions of Equation 3-76 are not satisfied for gas systems, i.e., compressible fluids. In order to develop the proper mathematical function for describing the flow of compressible fluids in the reservoir, the following two additional gas equations must be considered:

• Real density equation:

$$\rho = \frac{pM}{zRT}$$

• Gas compressibility equation:

$$c_{g} = \frac{1}{p} - \frac{1}{z} \frac{dz}{dp}$$

Combining these two basic gas equations with Equation 3-68 gives

$$\frac{1}{r}\frac{\partial}{\partial r}\left(r\frac{p}{\mu z}\frac{\partial p}{\partial r}\right) = \frac{\phi\mu c_t}{0.000264 \,k}\frac{p}{\mu z}\frac{\partial p}{\partial t} \tag{3-99}$$

where t = time, hr

k = permeability, md

 c_t = total isothermal compressibility, psi⁻¹

 $\phi = porosity$

Al-Hussainy, Ramey, and Crawford (1966) linearized this basic flow equation by introducing the real-gas potential m(p) to Equation 3-99. Recall the previously defined m(p) equation:

$$m(p) = \int_{0}^{p} \frac{2p}{\mu z} dp \tag{3-100}$$

Differentiating this relation with respect to p gives

$$\frac{\partial m(p)}{\partial p} = \frac{2p}{\mu z} \tag{3-101}$$

Obtain the following relationships by applying the chair rule:

$$\frac{\partial m(p)}{\partial r} = \frac{\partial m(p)}{\partial p} \frac{\partial p}{\partial r}$$
 (3-102)

$$\frac{\partial m(p)}{\partial t} = \frac{\partial m(p)}{\partial p} \frac{\partial p}{\partial t}$$
 (3-103)

Substituting Equation 3-101 into Equations 3-102 and 3-103 gives

$$\frac{\partial p}{\partial r} = \frac{\mu z}{2p} \frac{\partial m(p)}{\partial r}$$
 (3-104)

and

$$\frac{\partial p}{\partial t} = \frac{\mu z}{2p} \frac{\partial m(p)}{\partial t}$$
 (3-105)

Combining Equations 3-104 and 3-105 with 3-99 yields

$$\frac{\partial^2 m(p)}{\partial r^2} + \frac{1}{r} \frac{\partial m(p)}{\partial r} = \frac{\phi \mu c_t}{0.000264 \text{ k}} \frac{\partial m(p)}{\partial t}$$
(3-106)

Equation 3-106 is the radial diffusivity equation for compressible fluids. This differential equation relates the real-gas pseudopressure (real-gas potential) to the time t and the radius r. Al-Hussainy, Ramey, and Crawford (1966) pointed out that, in gas well testing analysis, the constant-rate solution has more practical applications than those provided by the constant-pressure solution. The authors provided the exact solution to Equation 3-106 that is commonly referred to as the m(p)-solution method. Two other solutions approximate the exact solution. These two

approximation methods are called the *pressure-squared method* and the *pressure-approximation method*. In general, there are three forms of the mathematical solution to the diffusivity equation:

- The m(p)-solution method (exact solution).
- The pressure-squared method (p²-approximation method).
- The pressure method (p-approximation method).

These three methods are presented as follows.

The m(p)-Solution Method (Exact Solution)

Imposing the constant-rate condition as one of the boundary conditions required to solve Equation 3-106, Al-Hussainy et al. (1966) proposed the following exact solution to the diffusivity equation:

$$m(p_{wf}) = m(p_i) - 57895.3 \left(\frac{p_{sc}}{T_{sc}}\right) \left(\frac{Q_g T}{kh}\right) \left[log\left(\frac{kt}{\phi \mu_i c_{ti} r_w^2}\right) - 3.23\right] \quad (3-107)$$

where p_{wf} = bottom-hole flowing pressure, psi

 p_e = initial reservoir pressure

 $Q_g = gas flow rate, Mscf/day$

t = time, hr

k = permeability, md

 $p_{sc} = standard \ pressure, \, psi$

 $T_{sc} = standard temperature, °R$

T = reservoir temperature

 $r_{\rm w}=$ wellbore radius, ft

h = thickness, ft

 $\mu_{i}=\mbox{gas}$ viscosity at the initial pressure, cp

 c_{ti} = total compressibility coefficient at p_i , psi^{-1}

 $\phi = porosity$

When $p_{sc}=14.7$ psia and $T_{sc}=520^{\circ}R$, Equation 3-107 reduces to

$$m(p_{wf}) = m(p_i) - \left(\frac{1637~Q_gT}{kh}\right) \left[log \left(\frac{kt}{\varphi \mu_i c_{ti} r_w^2}\right) - 3.23 \right] \tag{3-108} \label{eq:3-108}$$

Equation 3-108 can be written equivalently in terms of the dimensionless time t_D as

$$m(p_{wf}) = m(p_i) - \left(\frac{1637 \ Q_g T}{kh}\right) \left\lceil log\left(\frac{4 \ t_D}{\gamma}\right)\right\rceil \tag{3-109} \label{eq:3-109}$$

The dimensionless time was defined previously by Equation 3-86 as

$$t_D = \frac{0.000264 \ kt}{\varphi \mu_i c_{ti} r_w^2} \label{eq:tD}$$

The parameter γ is called *Euler's constant* and given by

$$\gamma = e^{0.5772} = 1.781 \tag{3-110}$$

The solution to the diffusivity equation as given by Equations 3-108 and 3-109 expresses the bottom-hole real-gas pseudopressure as a function of the transient flow time t. The solution as expressed in terms of m(p) is the recommended mathematical expression for performing gas-well pressure analysis due to its applicability in all pressure ranges.

The radial gas diffusivity equation can be expressed in a dimensionless form in terms of the dimensionless real-gas pseudopressure drop ψ_D . The solution to the dimensionless equation is given by

$$m(p_{wf}) = m(p_i) - \left(\frac{1422 \ Q_g T}{kh}\right) \psi_D \eqno(3-111)$$

 $\begin{aligned} \text{where } Q_g = \text{gas flow rate, Mscf/day} \\ k = \text{permeability, md} \end{aligned}$

The dimensionless pseudopressure drop ψ_D can be determined as a function of t_D by using the appropriate expression of Equations 3-91 through 3-96. When $t_D > 100$, ψ_D can be calculated by applying Equation 3-82, or

$$\psi_D = 0.5[\,ln(t_D) + 0.80907] \tag{3-112}$$

Example 3-13

A gas well with a wellbore radius of 0.3 ft is producing at a constant flow rate of 2000 Mscf/day under transient flow conditions. The initial reservoir pressure (shut-in pressure) is 4400 psi at 140°F. The formation permeability and thickness are 65 md and 15 ft, respectively. The porosity is recorded as 15%. Example 3-7 documents the properties of the gas as well as values of m(p) as a function of pressures. The table is reproduced here for convenience:

p	μ _g (cp)	z	m(p), psi²/cp
0	0.01270	1.000	0.000
400	0.01286	0.937	13.2×10^{6}
800	0.01390	0.882	52.0×10^{6}
1200	0.01530	0.832	113.1×10^{6}
1600	0.01680	0.794	198.0×10^{6}

2000 2400 2800 3200 3600 4000	0.01840 0.02010 0.02170 0.02340 0.02500 0.02660	0.770 0.763 0.775 0.797 0.827 0.860	304.0×10^{6} 422.0×10^{6} 542.4×10^{6} 678.0×10^{6} 816.0×10^{6} 950.0×10^{6}
4400	0.02831	0.896	1089.0×10^6

Assuming that the initial total isothermal compressibility is 3×10^{-4} psi⁻¹, calculate the bottom-hole flowing pressure after 1.5 hours.

Solution

Step 1. Calculate the dimensionless time t_D:

$$t_D = \frac{(0.000264)(65)(1.5)}{(0.15)(0.02831)(3\times 10^{-4})(0.3^2)} = 224,498.6$$

Step 2. Solve for $m(p_{wf})$ by using Equation 3-109:

$$\begin{split} m(p_{wf}) &= 1089 \times 10^6 - \frac{(1637)(2000)(600)}{(65)(15)} \left[log \left(\frac{(4)224,498.6}{e^{0.5772}} \right) \right] \\ &= 1077.5(10^6) \end{split}$$

Step 3. From the given PVT data, interpolate using the value of $m(p_{wf})$ to give a corresponding p_{wf} of 4367 psi.

An identical solution can be obtained by applying the ψ_D approach.

Step 1. Calculate ψ_D from Equation 3-112:

$$\psi_D = 0.5[\,ln(224,\!498.6) + 0.8090] = 6.565$$

Step 2. Calculate $m(p_{wf})$ by using Equation 3-111:

$$m(p_{wf}) = 1089 \times 10^6 - \bigg(\frac{1422(2000)(600)}{(65)(15)}\bigg)(6.565) = 1077.5 \times 10^6$$

The Pressure-Squared Approximation Method (p²-Method)

The first approximation to the exact solution is to remove the pressure-dependent term (μz) outside the integral that defines $m(p_{wf})$ and $m(p_i)$ to give

$$m(p_i) - m(p_{wf}) = \frac{2}{\overline{\mu}\overline{z}} \int_{p_{wf}}^{p_i} p dp$$
 (3-113)

or

$$m(p_i) - m(p_{wf}) = \frac{p_i^2 - p_{wf}^2}{\overline{\mu} \overline{z}}$$
 (3-114)

The bars over μ and z represent the values of the gas viscosity and deviation factor as evaluated at the average pressure \overline{p} . This average pressure is given by

$$\overline{p} = \sqrt{\frac{p_i^2 + p_{wf}^2}{2}} \tag{3-115}$$

Combining Equation 3-114 with Equation 3-108, 3-109, or 3-111 gives

$$p_{wf}^{2} = p_{i}^{2} - \left(\frac{1637Q_{g}T \overline{\mu} \overline{z}}{kh}\right) \left[\log\left(\frac{kt}{\phi \mu_{i} c_{ti} r_{w}^{2}}\right) - 3.23\right]$$
(3-116)

or

$$p_{wf}^{2} = p_{i}^{2} - \left(\frac{1637Q_{g}T \overline{\mu} \overline{z}}{kh}\right) \left[\log\left(\frac{4t_{D}}{\gamma}\right)\right]$$
(3-117)

or, equivalently,

$$p_{wf}^2 = p_i^2 - \left(\frac{1422Q_g T \overline{\mu} \overline{z}}{kh}\right) \psi_D$$
 (3-118)

The approximation solution forms indicate that the product (μz) is assumed constant at the average pressure \overline{p} . This effectively limits the applicability of the p^2 -method to reservoir pressures <2000. It should be pointed out that, when the p^2 -method is used to determine p_{wf} , it is perhaps sufficient to set $\overline{\mu} \overline{z} = \mu_i z$.

Example 3-14

A gas well is producing at a constant rate of 7454.2 Mscf/day under transient flow conditions. The following data are available:

$$\begin{array}{lll} k = 50 \; md & h = 10 \; ft & \varphi = 20\% & p_i = 1600 \; psi \\ T = 600^{\circ}R & r_w = 0.3 \; ft & c_{ti} = 6.25 \times 10^{-4} psi^{-1} \end{array}$$

The gas properties are tabulated as

p	μ _g , cp	z	m(p), psi ² /cp
0	0.01270	1.000	0.000
400	0.01286	0.937	13.2×10^{6}
800	0.01390	0.882	52.0×10^{6}
1200	0.01530	0.832	113.1×10^6
1600	0.01680	0.794	198.0×10^6

Calculate the bottom-hole flowing pressure after 4 hours by using

- a. The m(p)-method.
- b. The p^2 -method.

Solution

a. The m(p)-Method

Step 1. Calculate t_D:

$$t_D = \frac{0.000264(50)(4)}{(0.2)(0.0168)(6.25 \times 10^{-4})(0.3^2)} = 279,365.1$$

Step 2. Calculate ψ_D :

$$\psi_D = 0.5[ln(279,\!365.1) + 0.80907] = 6.6746$$

Step 3. Solve for $m(p_{wf})$ by applying Equation 3-111:

$$m(p_{wf}) = (198 \times 10^6) - \left[\frac{1422(7454.2)(600)}{(50)(10)}\right] 6.6746 = 113.1 \times 10^6$$

The corresponding value of $p_{\rm wf} = 1200$ psi.

b. The p^2 -Method

Step 1. Calculate ψ_D by applying Equation 3-112:

$$\psi_D = 0.5[\ln(279,365.1) + 0.80907] = 6.6477$$

Step 2. Calculate p_{wf}^2 by applying Equation 3-118:

$$\begin{split} p_{wf}^2 &= 1600^2 - \left[\frac{(1422)(7454.2)(600)(0.0168)(0.794)}{(50)(10)} \right] \\ &\times 6.6747 = 1,427,491 \\ p_{wf} &= 1195 \text{ psi} \end{split}$$

Step 3. The absolute average error is 0.4%.

The Pressure-Approximation Method

The second method of approximation to the exact solution of the radial flow of gases is to treat the gas as a *pseudoliquid*.

Recall that the gas formation volume factor $B_{\rm g}$ as expressed in bbl/scf is given by

$$B_{g} = \left(\frac{p_{sc}}{5.615T_{sc}}\right) \left(\frac{zT}{p}\right)$$

Solving this expression for p/z gives

$$\frac{p}{z} = \left(\frac{Tp_{sc}}{5.615T_{sc}}\right) \left(\frac{1}{B_g}\right)$$

The difference in the real gas pseudopressure is given by

$$m(p_i) - (p_{wf}) = \int_{p_{wf}}^{p_i} \frac{2p}{\mu z} dp$$

Combining these two expressions gives

$$m(p_i) - m(p_{wf}) = \frac{2Tp_{sc}}{5.615T_{sc}} \int_{p_{wf}}^{p_i} \left(\frac{1}{\mu B_g}\right) dp$$
 (3-119)

Fetkovich (1973) suggested that, at high pressures (p > 3000), $1/\mu B_g$ is nearly constant as shown schematically in Figure 3-23. Imposing Fetkovich's condition on Equation 3-119 and integrating gives

$$m(p_i) - m(p_{wf}) = \frac{2T p_{sc}}{5.615 T_{sc} \overline{\mu} \overline{B}_g} (p_i - p_{wf})$$
 (3-120)

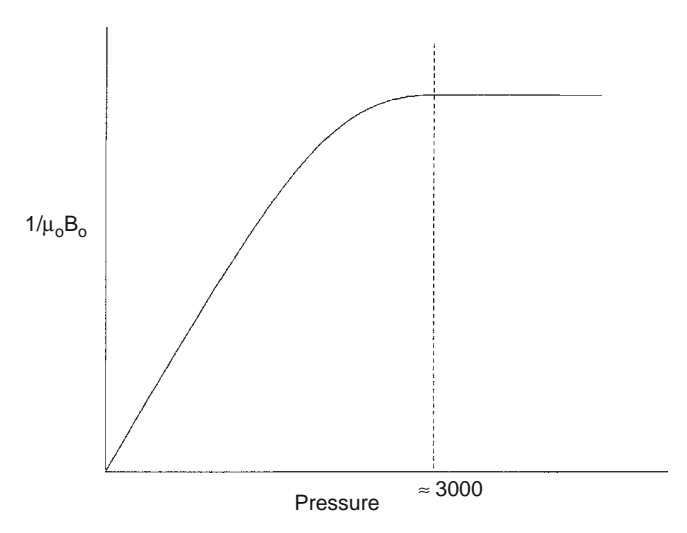


FIGURE 3-23 $1/\mu_o B_o$ versus pressure.

Combining Equation 3-120 with Equation 3-108, 3-109, or 3-111 gives

$$p_{wf} = p_i - \left(\frac{162.5 \times 10^3 Q_g \overline{\mu} \overline{B}_g}{kh}\right) \left[log \left(\frac{kt}{\varphi \overline{\mu} \ \overline{c}_t r_w^2}\right) - 3.23 \right] \eqno(3-121)$$

or

$$p_{wf} = p_i - \left[\frac{162.5(10^3)Q_g\overline{\mu}\overline{B}_g}{kh}\right] \left[log\left(\frac{4t_D}{\gamma}\right)\right] \tag{3-122}$$

or equivalently in terms of dimensionless pressure drop:

$$p_{wf} = p_{i} - \left[\frac{141.2(10^{3})Q_{g}\overline{\mu}\overline{B}_{g}}{kh} \right] p_{D}$$
 (3-123)

where $Q_g = gas$ flow rate, Mscf/day

 \ddot{k} = permeability, md

 \overline{B}_g = gas formation volume factor, bbl/scf

t = time, hr

 $p_D = dimensionless pressure drop$

 $t_D = dimensionless time$

It should be noted that the gas properties, i.e., μ , B_g , and c_t , are evaluated at pressure \overline{p} as defined next:

$$\overline{p} = \frac{p_i + p_{wf}}{2} \tag{3-124}$$

Again, this method is limited to applications above 3000 psi. When solving for p_{wf} , it might be sufficient to evaluate the gas properties at p_i .

Example 3-15

Resolve Example 3-13 by using the p-approximation method and compare with the exact solution.

Solution

Step 1. Calculate the dimensionless time t_D:

$$t_D = \frac{(0.000264)(65)(1.5)}{(0.15)(0.02831)(3\times 10^{-4})(0.3^2)} = 224,498.6$$

Step 2. Calculate Bg at pi:

$$B_g = 0.00504 \frac{(0.896)(600)}{4400} = 0.0006158 \; bbl/scf$$

Step 3. Calculate the dimensionless pressure p_D by applying Equation 3-92:

$$p_D = 0.5[\,ln(224,\!498.6) + 0.80907] = 6.565$$

Step 4. Approximate p_{wf} from Equation 3-123:

$$\begin{aligned} p_{wf} &= 4400 - \left[\frac{141.2 \times 10^3 (2000) (0.02831) (0.0006158)}{(65) (15)} \right] 6.565 \\ &= 4367 \ psi \end{aligned}$$

The solution is identical to the exact solution.

It should be pointed out that Examples 3-10 through 3-15 are designed to illustrate the use of different solution methods. These examples are not practical, however, because in transient flow analysis, the bottom-hole flowing pressure is usually available as a function of time. All the previous methodologies are essentially used to characterize the reservoir by determining the permeability k or the permeability-thickness product (kh).

SECTION 3.10 PSEUDOSTEADY-STATE FLOW

In the unsteady-state flow cases discussed previously, it was assumed that a well is located in a very large reservoir and producing at a constant flow rate. This rate creates a pressure disturbance in the reservoir that travels throughout this infinite-size reservoir. During this transient flow period, reservoir boundaries have no effect on the pressure behavior of the well. Obviously, the time period when this assumption can be imposed is often very short in length. As soon as the pressure disturbance reaches all drainage boundaries, it ends the transient (unsteady-state) flow regime. A different flow regime begins that is called *pseudosteady* (*semisteady*)-state flow. It is necessary at this point to impose different boundary conditions on the diffusivity equation and derive an appropriate solution to this flow regime.

Consider Figure 3-24, which shows a well in a radial system that is producing at a constant rate for a long enough period that eventually affects the entire drainage area. During this semisteady-state flow, the change in pressure with time becomes the same throughout the drainage area. Section B in Figure 3-24 shows that the pressure distributions become parallel at successive time periods. Mathematically, this important condition can be expressed as

$$\left(\frac{\partial p}{\partial t}\right)_r = constant$$

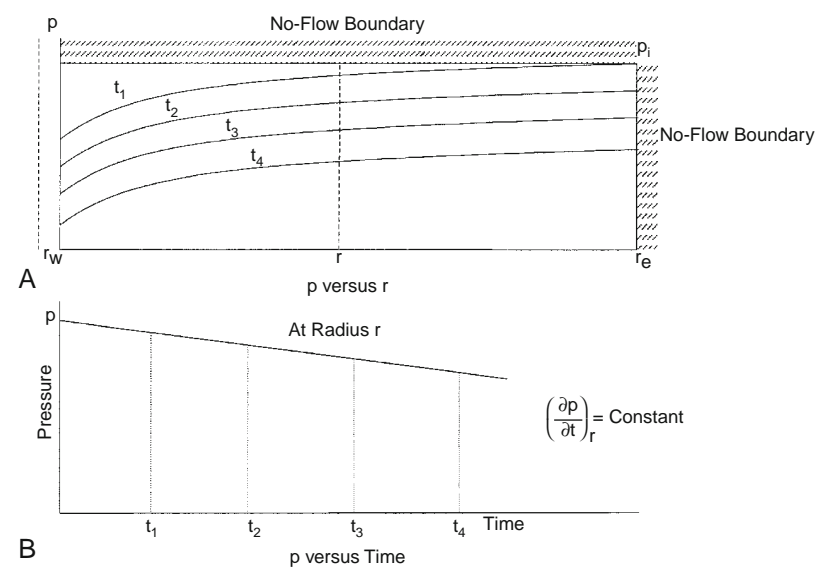


FIGURE 3-24 Semisteady-state flow regime.

The constant referred to in this equation can be obtained from a simple material balance using the definition of the compressibility:

$$c = \frac{-1}{V} \frac{dV}{dp}$$

Arranging,

$$cVdp = -dV$$

Differentiating with respect to time t,

$$cV\frac{dp}{dt} = -\frac{dV}{dt} = q$$

or

$$\frac{\mathrm{dp}}{\mathrm{dt}} = -\frac{\mathrm{q}}{\mathrm{cV}}$$

Expressing the pressure decline rate dp/dt in the preceding relation in psi/hr gives

$$\frac{dp}{dt} = -\frac{q}{24 \text{ cV}} = -\frac{Q_0 B_0}{24 \text{ cV}}$$
 (3-125)

where q = flow rate, bbl/day

 $Q_o = \text{flow rate, STB/day}$

dp/dt = pressure decline rate, psi/hr

V = pore volume, bbl

For a radial drainage system, the pore volume is given by

$$V = \frac{\pi r_e^2 h \phi}{5.615} = \frac{Ah\phi}{5.615}$$
 (3-126)

where $A = drainage area, ft^2$

Combining Equation 3-126 with Equation 3-125 gives

$$\frac{dp}{dt} = -\frac{0.23396 \text{ q}}{c_t \pi r_e^2 \text{ h}\phi} = \frac{-0.23396 \text{ q}}{c_t \text{ Ah}\phi}$$
(3-127)

Examination of the preceding expression reveals the following important characteristics of the behavior of the pressure decline rate dp/dt during the semisteady-state flow:

- The reservoir pressure declines at a higher rate with an increase in the fluids production rate.
- The reservoir pressure declines at a slower rate for reservoirs with higher total compressibility coefficients.
- The reservoir pressure declines at a lower rate for reservoirs with larger pore volumes.

Example 3-16

An oil well is producing at a constant oil flow rate of 1200 STB/day under a semisteady-state flow regime. Well testing data indicate that the pressure is declining at a constant rate of 4.655 psi/hr. The following additional data are available:

$$\begin{array}{ll} h=25~ft & \varphi=15\% & B_o=1.3~bbl/STB \\ c_t=12\times 10^{-6}~psi^{-1} & \end{array} \label{eq:balance}$$

Calculate the well drainage area.

Solution

- $q = Q_o B_o$
- q = (1200) (1.3) = 1560 bbl/day
- Apply Equation 3-127 to solve for A:

$$-4.655 = -\frac{0.23396(1560)}{12 \times 10^{-6}(A)(25)(0.15)}$$

$$A = 1,742,400 \text{ ft}^2$$

or

$$A = 1,742,400/43,560 = 40 \text{ acres}$$

Matthews, Brons, and Hazebroek (1954) pointed out that, once the reservoir is producing under the *semisteady-state condition*, each well will drain from within its own no-flow boundary independently of the other

wells. For this condition to prevail, the pressure decline rate dp/dt must be approximately constant throughout the entire reservoir; otherwise flow would occur across the boundaries causing a readjustment in their positions. Because the pressure at every point in the reservoir is changing at the same rate, it leads to the conclusion that the average reservoir pressure is changing at the same rate. This average reservoir pressure is essentially set equal to the volumetric average reservoir pressure \overline{p}_r . It is the pressure that is used to perform flow calculations during the semi-steady-state flowing condition. In the preceding discussion, \overline{p}_r indicates that, in principle, Equation 3-127 can be used to estimate it by replacing the pressure decline rate dp/dt with $(p_i - \overline{p}_r)/t$, or

$$p_i - \overline{p}_r = \frac{0.23396 \ qt}{c_t \ Ah\varphi}$$

or

$$\overline{p}_{r} = p_{i} - \frac{0.23396 \text{ qt}}{c_{t} \text{ Ah}\phi}$$
 (3-128)

where t is approximately the elapsed time since the end of the transient flow regime to the time of interest.

It should be noted that, when performing material balance calculations, the volumetric average pressure of the entire reservoir is used to calculate the fluid properties. This pressure can be determined from the individual well drainage properties as follows:

$$\overline{p}_{r} = \frac{\sum_{i} \overline{p}_{ri} V_{i}}{\sum_{i} V_{i}}$$
 (3-129)

where V_i = pore volume of the ith drainage volume,

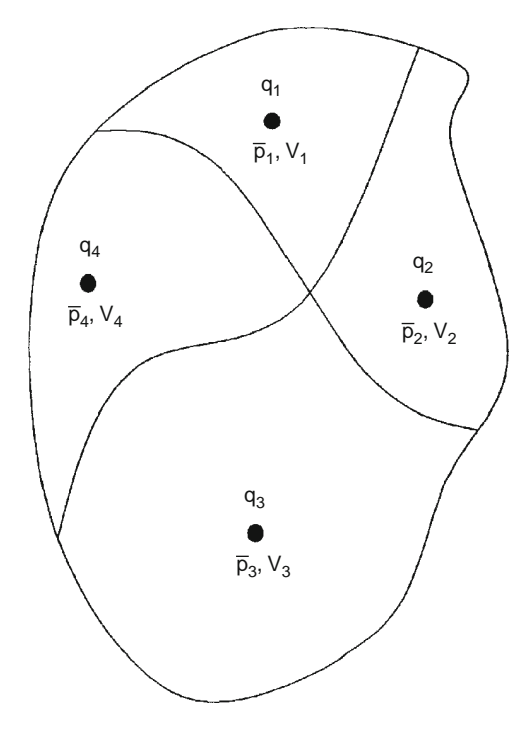
 \overline{p}_{ri} = volumetric average pressure within the ith drainage volume.

Figure 3-25 illustrates the concept of the volumetric average pressure. In practice, the V_i values are difficult to determine, and therefore, it is common to use the flow rate q_i in Equation 3-128:

$$\overline{p}_{r} = \frac{\sum_{i} (\overline{p}_{ri} q_{i})}{\sum_{i} q_{i}}$$
 (3-130)

The flow rates are measured on a routing basis throughout the lifetime of the field, thus facilitating the calculation of the volumetric average reservoir pressure, \overline{p}_r . Alternatively, the average reservoir pressure can be expressed in terms of the individual wells' average drainage pressure decline rates and fluid flow rates by

FIGURE 3-25 Volumetric average reservoir pressure.



$$\overline{p}_{\mathrm{r}} = \frac{\displaystyle\sum_{j} [(\overline{p}\,q)_{j}/(\partial \overline{p}/\partial t)_{j}]}{\displaystyle\sum_{j} [q_{j}/(\partial \overline{p}/\partial t)_{j}]}$$

However, since the material balance equation is usually applied at regular intervals of 3 to 6 months (i.e., $\Delta t = 3$ –6 months), throughout the life of the field, the average field pressure can be expressed in terms of the incremental net change in underground fluid withdrawal, $\Delta(F)$, as

$$\overline{p}_{r} = \frac{\displaystyle\sum_{j} \frac{\overline{p}_{j} \Delta(F)_{j}}{\Delta \overline{p}_{j}}}{\displaystyle\sum_{i} \frac{\Delta(F)_{j}}{\Delta \overline{p}_{j}}}$$

Where the total underground fluid withdrawals at time t and $t+\Delta t$ are given by

$$\begin{split} F_t &= \int\limits_0^t [Q_o B_o + Q_w B_w + (Q_g - Q_o R_s - Q_w R_{sw}) B_g] dt \\ F_{t+\Delta t} &= \int\limits_0^{t+\Delta t} [Q_o B_o + Q_w B_w + (Q_g - Q_o R_s - Q_w R_{sw}) B_g] dt \end{split}$$

with

$$\Delta(F) = F_{t+\Delta t} - F_t$$

where $R_s = gas$ solubility, scf/STB

 $R_{sw} = gas$ solubility in the water, scf/STB

 $B_g = gas$ formation volume factor, bbl/scf

 $Q_0 = \text{oil flow rate, STB/day}$

 $q_o = oil flow rate, bbl/day$

 $Q_w = \text{water flow rate, STB/day}$

 $q_w = water flow rate, bbl/day$

 $Q_g = gas flow rate, scf/day$

The practical applications of using the pseudosteady-state flow condition to describe the flow behavior of the following two types of fluids follow:

- Radial flow of slightly compressible fluids.
- Radial flow of compressible fluids.

Radial Flow of Slightly Compressible Fluids

The diffusivity equation as expressed by Equation 3-73 for the transient flow regime is

$$\frac{\partial^2 p}{\partial r^2} + \frac{1}{r} \frac{\partial p}{\partial r} = \left(\frac{\varphi \mu c_t}{0.000264k} \right) \frac{\partial p}{\partial t}$$

For the semisteady-state flow, the term $(\partial p/\partial t)$ is constant and is expressed by Equation 3-127. Substituting Equation 3-127 into the diffusivity equation gives

$$\frac{\partial^2 p}{\partial r^2} + \frac{1}{r} \frac{\partial p}{\partial r} = \left(\frac{\varphi \mu c_t}{0.000264k}\right) \left(\frac{-0.23396q}{c_t \ Ah\varphi}\right)$$

or

$$\frac{\partial^2 \mathbf{p}}{\partial r^2} + \frac{1}{r} \frac{\partial \mathbf{p}}{\partial r} = \frac{-887.22 \text{ q}\mu}{\text{Ahk}}$$
 (3-131)

Equation 3-131 can be expressed as

$$\frac{1}{r}\frac{\partial}{\partial r}\left(r\frac{\partial p}{\partial r}\right) = -\frac{887.22\ q\mu}{(\pi r_{a}^{2})hk}$$

Integrating this equation gives

$$r\frac{\partial p}{\partial r} = -\frac{887.22q\mu}{(\pi r_{o}^{2})hk} \left(\frac{r^{2}}{2}\right) + c_{1}$$

Where c_1 is the constant of the integration and can be evaluated by imposing the outer no-flow boundary condition [i.e., $(\partial p/\partial r)_{r_e}=0$] on that relation to give

$$c_1 = \frac{141.2 \; q\mu}{\pi \; hk}$$

Combining the two expressions gives

$$\frac{\partial p}{\partial r} = \frac{141.2 \text{ q}\mu}{hk} \left(\frac{1}{r} - \frac{r}{r_e^2} \right)$$

Integrating again,

$$\int_{p_e}^{p_i} dp = \frac{141.2 \text{ q}\mu}{hk} \int_{rw}^{re} \left(\frac{1}{r} - \frac{r}{r_e^2}\right) dr$$

Performing the integration and assuming (r_w^2/r_e^2) is negligible gives

$$(p_i - p_{wf}) = \frac{141.2 \text{ q}\mu}{kh} \left[ln \left(\frac{r_e}{r_w} \right) - \frac{1}{2} \right]$$
 (3-132)

A more appropriate form of the equation is to solve for the flow rate, to give

$$Q = \frac{0.00708 \text{ kh}(p_i - p_{wf})}{\mu B \left[\ln \left(\frac{r_e}{r_w} \right) - 0.5 \right]}$$
(3-133)

where Q = flow rate, STB/day

B = formation volume factor, bbl/STB

k = permeability, md

The volumetric average reservoir pressure \overline{p}_r is commonly used in calculating the liquid flow rate under the semisteady-state flowing condition. Introducing the \overline{p}_r into Equation 3-133 gives

$$Q = \frac{0.00708 \text{kh}(\overline{p}_{r} - p_{wf})}{\mu B \left[\ln \left(\frac{r_{e}}{r_{w}} \right) - 0.75 \right]}$$
(3-134)

Note that

$$ln\bigg(\frac{0.471r_e}{r_w}\bigg) = ln\bigg(\frac{r_e}{r_w}\bigg) - 0.75$$

This observation suggests that the volumetric average pressure $\overline{p}_{\rm r}$ occurs at about 47% of the drainage radius during the semisteady-state condition.

It is interesting to notice that the dimensionless pressure p_D solution to the diffusivity equation can be used to derive Equation 3-134. The p_D function for a bounded reservoir was given previously by Equation 3-96 for a bounded system as

$$p_D = \frac{2t_D}{r_{eD}^2} + \, ln(r_{eD}) - 0.75$$

where the three dimensionless parameters are given by Equations 3-86 through 3-88 as

$$\begin{split} p_D = & \frac{\frac{(p_i - p_{wf})}{QB\mu}}{0.00708 \text{ kh}} \\ t_D = & \frac{0.000264 \text{ kt}}{\phi\mu c_t r_w^2} \\ r_{eD} = & \frac{r_e}{r_w} \end{split}$$

Combining these four relationships gives

$$p_{wf} = p_i - \frac{Q B \mu}{0.00708 \ kh} \left[\frac{0.0005274 \ kt}{\varphi \mu c_t r_e^2} + \ ln \left(\frac{r_e}{r_w} \right) - 0.75 \right]$$

Solving Equation 3-129 for the time t gives

$$t = \frac{c_t \; A \; h \varphi \big(p_i - \overline{p}_r\big)}{0.23396 \; QB} = \frac{c_t \big(\pi r_e^2\big) h \varphi \big(p_i - \overline{p}_r\big)}{0.23396 \; QB}$$

Combining the two equations and solving for the flow rate Q yields

$$Q = \frac{0.00708 \text{ kh}(\overline{p}_r - p_{wf})}{\mu B \left[\ln \left(\frac{r_e}{r_w} \right) - 0.75 \right]}$$

It should be pointed out that the pseudosteady-state flow occurs regardless of the geometry of the reservoir. Irregular geometries also reach this state when they have been produced long enough for the entire drainage area to be affected.

Rather than developing a separate equation for each geometry, Ramey and Cobb (1971) introduced a correction factor that is called the *shape factor*, C_A , which is designed to account for the deviation of the drainage area from the ideal circular form. Shape factors, as listed in Table 3-4, account also for the location of the well within the drainage area. Introducing C_A into Equation 3-131 and performing the solution procedure gives the following two solutions:

TABLE 3-4 Shape Factors for Various Single-Well Drainage Areas (After Earlougher, R., Advances in Well Test Analysis, permission to publish by the SPE, copyright SPE, 1977)

In Bounded Reservoirs	$C_{\mathbf{A}}$	In C _A	$\frac{1}{2}ln\bigg(\frac{2.2458}{C_A}\bigg)$	Exact for t _{DA} >	Less than 1% Error for t _{DA} >	$ \begin{tabular}{ll} Use Infinite System \\ Solution with Less than \\ 1\% Error for t_{DA} < \\ \end{tabular} $
\overline{ullet}	31.62	3.4538	-1.3224	0.1	0.06	0.10
\odot	31.6	3.4532	-1.3220	0.1	0.06	0.10
\triangle	27.6	3.3178	-1.2544	0.2	0.07	0.09
60°	27.1	3.2995	-1.2452	0.2	0.07	0.09
1/3	21.9	3.0865	-1.1387	0.4	0.12	0.08
3 {	0.098	-2.3227	+1.5659	0.9	0.60	0.015
•	30.8828	3.4302	-1.3106	0.1	0.05	0.09
•	12.9851	2.5638	-0.8774	0.7	0.25	0.03
•	4.5132	1.5070	-0.3490	0.6	0.30	0.025
	3.3351	1.2045	-0.1977	0.7	0.25	0.01
• 1 2	21.8369	3.0836	-1.1373	0.3	0.15	0.025
1	10.8374	2.3830	-0.7870	0.4	0.15	0.025
1	4.5141	1.5072	-0.3491	1.5	0.50	0.06
1 2	2.0769	0.7309	-0.0391	1.7	0.50	0.02
1	3.1573	1.1497	-0.1703	0.4	0.15	0.005
2	0.5813	-0.5425	+0.6758	2.0	0.60	0.02

TABLE 3-4 Shape Factors for Various Single-Well Drainage Areas (After Earlougher, R., Advances in Well Test Analysis, permission to publish by the SPE, copyright SPE, 1977)—Cont'd

In Bounded Reservoirs	$C_{\mathbf{A}}$	ln C _A	$\frac{1}{2}ln\bigg(\frac{2.2458}{C_A}\bigg)$	Exact for t _{DA} >	Less than 1% Error for t _{DA} >	Use Infinite System Solution with Less than 1% Error for $t_{DA} <$
1	0.1109	-2.1991	+1.5041	3.0	0.60	0.005
• 1 4	5.3790	1.6825	-0.4367	0.8	0.30	0.01
1	2.6896	0.9894	-0.0902	0.8	0.30	0.01
1	0.2318	-1.4619	+1.1355	4.0	2.00	0.03
1	0.1155	-2.1585	+1.4838	4.0	2.00	0.01
• 1 5	2.3606	0.8589	-0.0249	1.0	0.40	0.025
In vertically fractured res	ervoirs	Use (x _e /	x _f)2 in place o	$f A/r_w^2$ for	fractured sy	stems
1	2.6541	0.9761	-0.0835	0.175	0.08	cannot use
1 0.2	2.0348	0.7104	+0.0493	0.175	0.09	cannot use
1 0.3	1.9986	0.6924	+0.0583	0.175	0.09	cannot use
1 0.5	1.6620	0.5080	+0.1505	0.175	0.09	cannot use
1	1.3127	0.2721	+0.2685	0.175	0.09	cannot use
1 1.0	0.7887	-0.2374	+0.5232	0.175	0.09	cannot use
In water-drive reservoirs						
•	19.1	2.95	-1.07	_	_	_
In reservoirs of unknown Production character						
\bullet	25.0	3.22	-1.20	_	_	

• In terms of the volumetric average pressure $\overline{p}_{r'}$

$$p_{wf} = \overline{p}_{r} - \frac{162.6 \,Q \,B\mu}{kh} \log \left[\frac{4A}{1.781 \,C_{A} r_{w}^{2}} \right]$$
 (3-135)

• In terms of the initial reservoir pressure p_i.

Recalling Equation 3-128, which shows the changes in the average reservoir pressure as a function of time and initial reservoir pressure p_i,

$$\overline{p}_{r} = p_{i} - \frac{0.23396 \text{ qt}}{c_{t}Ah\phi}$$

Combining this equation with Equation 3-135 gives

$$p_{wf} = \left[p_i - \frac{0.23396 \ Q \ Bt}{Ah\varphi c_t} \right] - \frac{162.6 \ Q \ B\mu}{kh} \ log \left[\frac{4A}{1.781 C_A r_w^2} \right] \eqno(3-136)$$

where k = permeability, md

 $A = drainage area, ft^2$

 C_A = shape factor

Q = flow rate, STB/day

t = time, hr

 $c_t = total compressibility coefficient, psi^{-1}$

Equation 3-135 can be arranged to solve for Q to give

$$Q = \frac{kh(\overline{p}_{r} - p_{wf})}{162.6B\mu \log \left[\frac{4A}{1.781C_{A}r_{w}^{2}}\right]}$$
(3-137)

It should be noted that, if Equation 3-137 is applied to a circular reservoir of a radius $r_{\rm e}$, then

$$A = \pi r_e^2$$

and the shape factor for a circular drainage area as given in Table 3-3 is

$$C_A = 31.62$$

Substituting in Equation 3-137, it reduces to

$$p_{wf} = \overline{p}_r - \left(\frac{QB\mu}{0.00708 \; kh} \right) \bigg[\, ln \bigg(\frac{r_e}{r_w} \bigg) - 0.75 \bigg] \label{eq:pwf}$$

This equation is identical to Equation 3-134.

Example 3-17

An oil well is developed at the center of a 40-acre square-drilling pattern. The well is producing at a constant flow rate of 800 STB/day

under a semisteady-state condition. The reservoir has the following properties:

$$\begin{array}{lll} \varphi = 15\% & h = 30 \text{ ft} & k = 200 \text{ md} \\ \mu = 1.5 \text{ cp} & B_o = 1.2 \text{ bbl/STB} & c_t = 25 \times 10^{-6} \text{ psi}^{-1} \\ p_i = 4500 \text{ psi} & r_w = 0.25 \text{ ft} & A = 40 \text{ acres} \end{array}$$

- Calculate and plot the bottom-hole flowing pressure as a function of time.
- b. Based on the plot, calculate the pressure decline rate. What is the decline in the average reservoir pressure from t=10 to $t=200\ hr?$

Solution

a. pwf Calculations

Step 1. From Table 3-3, determine C_A :

$$C_A = 30.8828$$

Step 2. Convert the area A from acres to ft²:

$$A = (40)(43,560) = 1,742,400 \text{ ft}^2$$

Step 3. Apply Equation 3-136:

$$P_{wf} = 4500 - 1.719 \; t - 58.536 \, log(2,027,\!436)$$

or

$$p_{wf} = 4493.69 - 1.719 t$$

Step 4. Calculate p_{wf} at different assumed times:

t, hr	$P_{\rm wf} = 44369 - 1.719 t$
10	4476.50
20	4459.31
50	4407.74
100	4321.79
200	4149.89

Step 5. Present the results of Step 4 in a graphical form as shown in Figure 3-26.

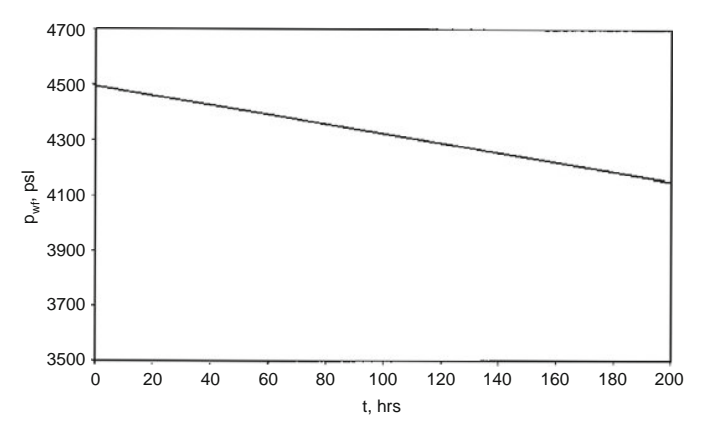


FIGURE 3-26 Bottom-hole flowing pressure as a function of time.

b. Pressure Decline Rate

It is obvious from Figure 3-26 and the preceding calculation that the bottom-hole flowing pressure is declining at a rate of 1.719 psi/hr, or

$$\frac{dp}{dt} = -1.719 \text{ psi/hr}$$

The significance of this example is that the rate of pressure decline during the pseudosteady state is the same throughout the drainage area. This means that the *average reservoir pressure*, p_r , is declining at the same rate of 1.719 psi; therefore the change in p_r from 10 to 200 hours is

$$\Delta \overline{p}_{\rm r} = (1.719)(200-10) = 326.6~psi$$

Example 3-18

An oil well is producing under a constant bottom-hole flowing pressure of 1500 psi. The current average reservoir pressure p_r is 3200 psi. The well is developed at the center of a 40-acre square-drilling pattern. Given the following additional information:

$$\begin{array}{lll} \varphi = 16\% & h = 15 \text{ ft} & k = 50 \text{ md} \\ \mu = 26 \text{ cp} & B_o = 1.15 \text{ bbl/STB} & c_t = 10 \times 10^{-6} \text{ psi}^{-1} \\ r_w = 0.25 \text{ ft} & \end{array}$$

calculate the flow rate.

Solution

Because the volumetric average pressure is given, solve for the flow rate by applying Equation 3-138.

$$Q = \frac{(50)(15)(3200 - 1500)}{(162.6)(1.15)(2.6)\log\left[\frac{(4)(40)(43,560)}{1.781(30.8828)(0.25^2)}\right]}$$
= 416 STB/day

Radial Flow of Compressible Fluids (Gases)

The radial diffusivity equation as expressed by Equation 3-106 was developed to study the performance of compressible fluid under unsteady-state conditions. The equation has the following form:

$$\frac{\partial^2 m(p)}{\partial r^2} + \frac{1}{r} \frac{\partial m(p)}{\partial r} = \frac{\phi \mu c_t}{0.000264 \text{ k}} \frac{\partial m(p)}{\partial t}$$

For the semisteady-state flow, the rate of change in the real-gas pseudopressure with respect to time is constant, i.e.,

$$\frac{\partial m(p)}{\partial t} = constant$$

Using the same technique as that described previously for liquids gives the following exact solution to the diffusivity equation:

$$Q_g = \frac{kh\left[m(\overline{p}_r) - m(p_{wf})\right]}{1422 T\left[ln\left(\frac{r_e}{r_w}\right) - 0.75\right]} \tag{3-138}$$

where $Q_g = gas$ flow rate, Mscf/day

 $T = \text{temperature, } ^{\circ}R$

k = permeability, md

Two approximations to this solution are widely used. These approximations are

- Pressure-squared approximation.
- Pressure-approximation.

Pressure-Squared Approximation Method

As outlined previously, this method provides us with compatible results to those of the exact solution approach when p < 2000. The solution has the following familiar form:

$$Q_g = \frac{kh(\overline{p}_r^2 - p_{wf}^2)}{1422 \text{ T } \overline{\mu} \, \overline{z} \left(\ln \frac{r_e}{r_w} - 0.75 \right)} \tag{3-139}$$

The gas properties \overline{z} and μ are evaluated at

$$\overline{p} = \sqrt{\frac{\left(\overline{p}_r\right)^2 + p_{wf}^2}{2}}$$

Pressure-Approximation Method

This approximation method is applicable at p > 3000 psi and has the following mathematical form:

$$Q_{g} = \frac{kh(\overline{p}_{r} - p_{wf})}{1422\overline{\mu}\overline{B}_{g}\left(\ln\frac{r_{e}}{r_{w}} - 0.75\right)}$$
(3-140)

with the gas properties evaluated at

$$\overline{p} = \frac{\overline{p}_r + p_{wf}}{2}$$

where $Q_g = gas$ flow rate, Mscf/day

k = permeability, md

 $\overline{B}_g = gas$ formation volume factor at average pressure, bbl/scf

The gas formation volume factor is given by the following expression:

$$\overline{B}_g = 0.00504 \frac{\overline{z}T}{\overline{p}}$$

In deriving the flow equations, the following two main assumptions were made:

- Uniform permeability throughout the drainage area.
- Laminar (viscous) flow.

Before using any of the previous mathematical solutions to the flow equations, each solution must be modified to account for the possible deviation from the preceding two assumptions. Introducing the following two correction factors into the solution of the flow equation can eliminate the above two assumptions:

- Skin factor.
- Turbulent flow factor.

Skin Factor

It is not unusual for materials such as mud filtrate, cement slurry, or clay particles to enter the formation during drilling, completion, or workover operations and reduce the permeability around the wellbore. This effect is commonly referred to as *wellbore damage* and the region of altered permeability is called the *skin zone*. This zone can extend from a few inches to several feet from the wellbore. Many other wells are stimulated by acidizing or fracturing, which in effect increases the permeability near the wellbore. Thus, the permeability near the wellbore is always different from the permeability away from the well, where the formation has not been affected by drilling or stimulation. A schematic illustration of the skin zone is shown in Figure 3-27.

Those factors that cause damage to the formation can produce additional localized pressure drop during flow. This additional pressure drop is commonly referred to as Δp_{skin} . On the other hand, well stimulation techniques will normally enhance the properties of the formation and increase the permeability around the wellbore, so that a decrease in pressure drop is observed. The resulting effect of altering the permeability around the wellbore is called the *skin effect*.

Figure 3-28 compares the differences in the skin zone pressure drop for three possible outcomes:

- First outcome. Δp_{skin} > 0 indicates an additional pressure drop due to wellbore damage, i.e., k_{skin} < k.
- Second outcome. Δp_{skin} < 0 indicates less pressure drop due to wellbore improvement, i.e., k_{skin} > k.
- Third outcome. $\Delta p_{skin} = 0$ indicates no changes in the wellbore condition, i.e., $k_{skin} = k$.

Hawkins (1956) suggested that the permeability in the skin zone, i.e., $k_{\rm skin}$, is uniform and the pressure drop across the zone can be

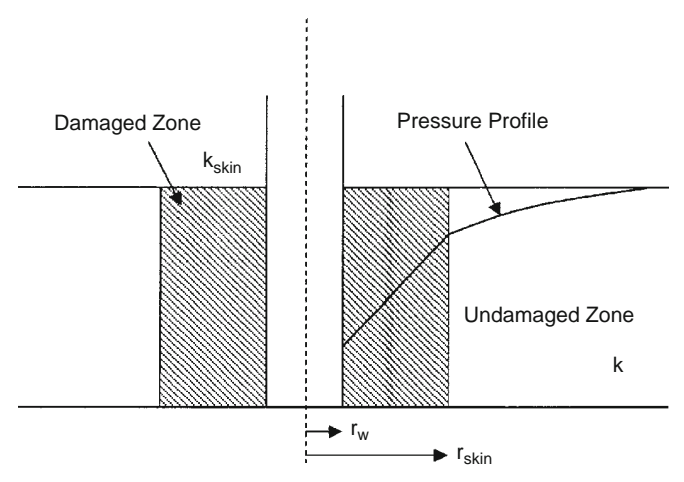


FIGURE 3-27 Near wellbore skin effect.

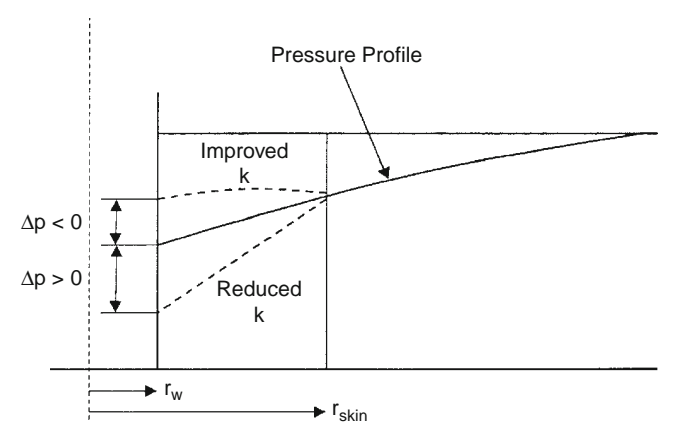


FIGURE 3-28 Representation of positive and negative skin effects.

approximated by Darcy's equation. Hawkins proposed the following approach:

$$\Delta p_{skin} = \begin{bmatrix} \Delta p \text{ in skin zone} \\ \text{due to } k_{skin} \end{bmatrix} - \begin{bmatrix} \Delta p \text{ in skin zone} \\ \text{due to } k \end{bmatrix}$$

Applying Darcy's equation gives

$$\Delta p_{skin} = \left[\frac{Q_o \; B_o \mu_o}{0.00708 \; h k_{skin}}\right] ln \left(\frac{r_{skin}}{r_w}\right) - \left[\frac{Q_o \; B_o \mu_o}{0.00708 \; h k}\right] ln \left(\frac{r_{skin}}{r_w}\right)$$

or

$$\Delta p_{skin} = \left(\!\frac{Q_o\,B_o\mu_o}{0.00708\,kh}\!\right)\!\left[\!\frac{k}{k_{skin}}\!-1\!\right]ln\!\left(\!\frac{r_{skin}}{r_w}\!\right)$$

where k = permeability of the formation, md $k_{skin} = permeability$ of the skin zone, md

The preceding expression for determining the additional pressure drop in the skin zone is commonly expressed in the following form:

$$\Delta p_{skin} = \left[\frac{Q_o B_o \mu_o}{0.00708 \text{ kh}} \right] s = 141.2 \left[\frac{Q_o B_o \mu_o}{\text{kh}} \right] s \tag{3-141}$$

where s is called the skin factor and defined as

$$s = \left[\frac{k}{k_{skin}} - 1\right] ln\left(\frac{r_{skin}}{r_{w}}\right)$$
 (3-142)

Equation 3-142 provides some insight into the physical significance of the sign of the skin factor. There are only three possible outcomes in evaluating the skin factor s:

- **Positive Skin Factor, s** > **0**. When a damaged zone near the wellbore exists, k_{skin} is less than k and hence s is a positive number. The magnitude of the skin factor increases as k_{skin} decreases and as the depth of the damage r_{skin} increases.
- Negative Skin Factor, s < 0. When the permeability around the well $k_{\rm skin}$ is higher than that of the formation k, a negative skin factor exists. This negative factor indicates an improved wellbore condition.
- **Zero Skin Factor**, $\mathbf{s} = \mathbf{0}$. Zero skin factor occurs when no alteration in the permeability around the wellbore is observed, i.e., $k_{skin} = k$.

Equation 3-142 indicates that a negative skin factor will result in a negative value of Δp_{skin} . This implies that a stimulated well will require less pressure drawdown to produce at rate q than an equivalent well with uniform permeability.

The proposed modification of the previous flow equation is based on the concept that the actual total pressure drawdown will increase or decrease by an amount of Δp_{skin} . Assuming that $(\Delta p)_{ideal}$ represents the pressure drawdown for a drainage area with a uniform permeability k, then

$$(\Delta p)_{actual} = (\Delta p)_{ideal} + (\Delta p)_{skin}$$

or

$$(p_i - p_{wf})_{actual} = (p_i - p_{wf})_{ideal} + \Delta p_{skin}$$
 (3-143)

The concept expressed by Equation 3-143 can be applied to all the previous flow regimes to account for the skin zone around the wellbore as follows.

Steady-State Radial Flow

Substituting Equations 3-27 and 3-141 into Equation 3-143 gives

$$(p_i-p_{wf})_{actual} = \left[\frac{Q_o~B_o\mu_o}{0.00708~kh}\right]ln \left(\frac{r_e}{r_w}\right) + \left[\frac{Q_o~B_o\mu_o}{0.00708~kh}\right]s$$

or

$$Q_{o} = \frac{0.00708 \text{ kh}(p_{i} - p_{wf})}{\mu_{o} B_{o} \left[\ln \frac{r_{e}}{r_{w}} + s \right]}$$
(3-144)

where $Q_o = oil$ flow rate, STB/day

k = permeability, md

h = thickness, ft

s = skin factor

 $B_o = oil formation volume factor, bbl/STB$

 $\mu_{o} = \text{oil viscosity, cp}$

 p_i = initial reservoir pressure, psi

 p_{wf} = bottom-hole flowing pressure, psi

Unsteady-State Radial Flow

 For Slightly Compressible Fluids. Combining Equations 3-83 and 3-141 with Equation 3-143 yields

$$\begin{split} p_i - p_{wf} &= 162.6 \Biggl(\frac{Q_o \; B_o \mu_o}{kh} \Biggr) \Biggl[log \frac{kt}{\varphi \mu c_t r_w^2} - 3.23 \Biggr] \\ &+ 141.2 \Biggl(\frac{Q_o \; B_o \mu_o}{kh} \Biggr) s \end{split}$$

or

$$p_{i} - p_{wf} = 162.6 \left(\frac{Q_{o} B_{o} \mu_{o}}{kh}\right) \left[log \frac{kt}{\phi \mu c_{t} r_{w}^{2}} - 3.23 + 0.87s \right] \tag{3-145}$$

• For Compressible Fluids. A similar approach to the preceding gives

$$m(p_{wf}) = m(p_i) - \frac{1637Q_gT}{kh} \left[log \frac{kt}{\varphi \mu c_t, r_w^2} - 3.23 + 0.87s \right] \eqno(3-146)$$

and, in terms of the pressure-squared approach, gives

$$p_{wf}^2 = p_i^2 - \frac{1637Q_gT\overline{z}\overline{\mu}}{kh} \left[log \frac{kt}{\phi \mu_i c_{ti} r_w^2} - 3.23 + 0.87s \right] \tag{3-147}$$

Pseudosteady-State Flow

• For Slightly Compressible Fluids. Introducing the skin factor into Equation 3-134 gives

$$Q_{o} = \frac{0.00708 \text{ kh}(\overline{p}_{r} - p_{wf})}{\mu_{o} B_{o} \left[\ln \left(\frac{r_{e}}{r_{w}} \right) - 0.75 + s \right]}$$
(3-148)

For Compressible Fluids.

$$Q_{g} = \frac{kh[m(\overline{p}_{r}) - m(P_{wf})]}{1422 T \left[ln\left(\frac{r_{e}}{r_{w}}\right) - 0.75 + s \right]}$$
(3-149)

Or, in terms of the pressure-squared approximation,

$$Q_{g} = \frac{kh(p_{r}^{2} - p_{wf}^{2})}{1422 \ T\overline{\mu} \ \overline{z} \left[\ln \left(\frac{r_{e}}{r_{w}} \right) - 0.75 + s \right]} \tag{3-150}$$

where $Q_g = gas$ flow rate, Mscf/day

 \ddot{k} = permeability, md

 $\begin{array}{l} T = \overset{1}{\text{temperature, }} °R \\ \left(\overline{\mu_g}\right) = \text{gas viscosity at average pressure } \overline{p}, \text{ cp} \\ \overline{z}_g = \text{gas compressibility factor at average pressure } \overline{p} \end{array}$

Example 3-19

Calculate the skin factor resulting from the invasion of the drilling fluid to a radius of 2 ft. The permeability of the skin zone is estimated at 20 md as compared with the unaffected formation permeability of 60 md. The wellbore radius is 0.25 ft.

Solution

Apply Equation 3-142 to calculate the skin factor:

$$s = \left[\frac{60}{20} - 1\right] \ln\left(\frac{2}{0.25}\right) = 4.16$$

Matthews and Russell (1967) proposed an alternative treatment for the skin effect by introducing the effective or apparent wellbore radius rwa that accounts for the pressure drop in the skin. They define rwa by the following equation:

$$r_{wa} = r_w e^{-s}$$
 (3-151)

All of the ideal radial flow equations can also be modified for the skin by simply replacing wellbore radius \mathbf{r}_{w} with the apparent wellbore radius rwa. For example, Equation 3-145 can be equivalently expressed as

$$p_{i} - p_{wf} = 162.6 \left(\frac{Q_{o} B_{o} \mu_{o}}{kh}\right) \left[\log \frac{kt}{\phi \mu_{o} c_{t} r_{wa}^{2}} - 3.23\right]$$
 (3-152)

Turbulent Flow Factor

All of the mathematical formulations presented so far are based on the assumption that laminar flow conditions are observed during flow. During radial flow, the flow velocity increases as the wellbore is approached. This increase in the velocity might cause the development of a turbulent flow around the wellbore. If turbulent flow does exist, it is most likely to occur with gases and causes an additional pressure drop similar to that caused by the skin effect. The term *non-Darcy flow* has been adopted by the industry to describe the additional pressure drop due to the turbulent (non-Darcy) flow.

Referring to the additional real-gas pseudopressure drop due to non-Darcy flow as $\Delta\psi$ non-Darcy, the total (actual) drop is given by

$$(\Delta \psi)_{actual} = (\Delta \psi)_{ideal} + (\Delta \psi)_{skin} + (\Delta \psi)_{non\text{-}Darcy}$$

Wattenburger and Ramey (1968) proposed the following expression for calculating $(\Delta \psi)_{\text{non-Darcy}}$:

$$(\Delta \Psi)_{\text{non-Darcy}} = 3.161 \times 10^{-12} \left[\frac{\beta T \gamma_g}{\mu_{\text{gw}} \text{ h}^2 \text{ r}_{\text{w}}} \right] Q_g^2$$
 (3-153)

This equation can be expressed in a more convenient form as

$$(\Delta \psi)_{\text{non-Darcy}} = FQ_g^2 \tag{3-154}$$

where F is called the non-Darcy flow coefficient and is given by

$$F = 3.161 \times 10^{-12} \left[\frac{\beta T \gamma_g}{\mu_{gw} h^2 r_w} \right]$$
 (3-155)

where $Q_g = gas$ flow rate, Mscf/day

 $\mu_{gw} = gas \ viscosity$ as evaluated at $p_{wf}\text{, }cp$

 $\gamma_g = gas \text{ specific gravity}$

h = thickness, ft

 $F = \text{non-Darcy flow coefficient, } psi^2/cp/(Mscf/day)^2$

 β = turbulence parameter

Jones (1987) proposed a mathematical expression for estimating the turbulence parameter β as

$$\beta = 1.88(10^{-10})(k)^{-1.47}(\phi)^{-0.53}$$
 (3-156)

where k = permeability, md

 ϕ = porosity, fraction

The term FQ_g^2 can be included in all the compressible gas flow equations in the same way as the skin factor. This non-Darcy term is interpreted as being a *rate-dependent skin*. The modification of the gas flow equations to account for the turbulent flow condition follows.

Unsteady-State Radial Flow

The gas flow equation for an unsteady-state flow is given by Equation 3-146 and can be modified to include the additional drop in the real-gas potential as

$$\begin{split} m(p_i) - m(p_{wf}) &= \left(\frac{1637Q_gT}{kh}\right) \left[log\frac{kt}{\varphi\mu_i c_{ti} r_w^2} - 3.23 + 0.87s \right] \\ &+ FQ_g^2 \end{split} \tag{3-157}$$

Equation 3-157 is commonly written in a more convenient form as

$$\begin{split} m(p_i) - m(p_{wf}) &= \left(\frac{16370Q_gT}{kh}\right) \\ &\times \left[\log\frac{kt}{\varphi\mu_i\;c_{ti}\;r_w^2} - 3.23 + 0.87s + 0.87\;DQ_g\right] \end{split} \tag{3-158}$$

where the term DQ_g is interpreted as the rate-dependent skin factor. The coefficient D is called the *inertial* or *turbulent flow factor* and is given by

$$D = \frac{Fkh}{1422 T} \tag{3-159}$$

The true skin factor s, which reflects the formation damage or stimulation, is usually combined with the non-Darcy rate-dependent skin and labeled as the *apparent* or *total skin factor*:

$$s' = s + DQ_{g} \tag{3-160}$$

or

$$\begin{split} m(p_i) - m(P_{wf}) &= \left(\frac{1637Q_g T}{kh}\right) \\ &\times \left[\log \frac{kt}{\varphi \mu_i \ c_{ti} \ r_w^2} - 3.23 + 0.87s'\right] \end{split} \tag{3-161}$$

Equation 3-161 can be expressed in the pressure-squared approximation form as

$$p_{i}^{2} - p_{wf}^{2} = \left[\frac{1637Q_{g} T\overline{z}\overline{\mu}}{kh}\right] \left[\log \frac{kt}{\phi \mu_{i} c_{ti} r_{w}^{2}} - 3.23 + 0.87 s'\right]$$
(3-162)

where $Q_g = gas$ flow rate, Mscf/day

t = time, hr

k = permeability, md

 $\mu_i = gas \text{ viscosity as evaluated at } p_i$, cp

Semisteady-State Flow

Equations 3-149 and 3-150 can be modified to account for the non-Darcy flow as follows:

$$Q_{g} = \frac{kh[m(\overline{p}_{r}) - m(p_{wf})]}{1422 T \left[ln\left(\frac{r_{e}}{r_{w}}\right) - 0.75 + s + DQ_{g} \right]}$$
(3-163)

or in terms of the pressure-squared approach:

$$Q_{g} = \frac{kh(\overline{p}_{r}^{2} - p_{wf}^{2})}{1422 \, T \, \overline{\mu} \, \overline{z} \left[\ln \left(\frac{r_{e}}{r_{w}} \right) - 0.75 + s + DQ_{g} \right]}$$
(3-164)

where the coefficient D is defined as

$$D = \frac{Fkh}{1422 T}$$
 (3-165)

Steady-State Flow

Similar to the modification procedure, Equations 3-44 and 3-45 can be expressed as

$$Q_{g} = \frac{kh[m(p_{i}) - m(p_{wf})]}{1422 T \left[ln \frac{r_{e}}{r_{w}} - 0.5 + s + DQ_{g} \right]}$$
(3-166)

$$Q_{g} = \frac{kh(\overline{p}_{e}^{2} - p_{wf}^{2})}{1422 \, T \, \overline{\mu} \, \overline{z} \left[\ln \frac{r_{e}}{r_{w}} - 0.5 + s + DQ_{g} \right]}$$
(3-167)

where D is defined by Equation 3-165.

Example 3-20

A gas well has an estimated wellbore damage radius of 2 feet and an estimated reduced permeability of 30 md. The formation has a permeability and porosity of 55 md and 12%. The well is producing at a rate

of 20 Mscf/day with a gas gravity of 0.6. The following additional data are available:

$$r_w = 0.25 \quad h = 20 \; ft \quad T = 140^\circ F \quad \mu_{\rm gw} = 0.013 \; cp \label{eq:rw}$$

Calculate the apparent skin factor.

Solution

Step 1. Calculate the skin factor from Equation 3-142:

$$s = \left\lceil \frac{55}{30} - 1 \right\rceil \ln \left(\frac{2}{0.25} \right) = 1.732$$

Step 2. Calculate the turbulence parameter β by applying Equation 3-154:

$$\beta = 1.88(10)^{-10}(55)^{-1.47}(0.12)^{-0.53} = 159.904 \times 10^6$$

Step 3. Calculate the non-Darcy flow coefficient from Equation 3-155:

$$F = 3.1612 \times 10^{-12} \left[\frac{159.904 \times 10^6 (600)(0.6)}{(0.013)(20)^2 (0.25)} \right] = 0.14$$

Step 4. Calculate the coefficient D from Equation 3-159:

$$D = \frac{(0.14)(55)(20)}{(1422)(600)} = 1.805 \times 10^{-4}$$

Step 5. Estimate the apparent skin factor by applying Equation 3-160:

$$s' = 1.732 + (1.805 \times 10^{-4})(20,\!000) = 5.342$$

SECTION 3.11 PRINCIPLE OF SUPERPOSITION

The solutions to the radial diffusivity equation as presented earlier in this chapter appear to be applicable for describing the pressure distribution only in an infinite reservoir that was caused by a constant production from a single well. Since real reservoir systems usually have several wells that are operating at varying rates, a more generalized approach is needed to study the fluid flow behavior during the unsteady-state flow period.

The principle of superposition is a powerful concept that can be applied to remove the restrictions that have been imposed on various forms of solution to the transient flow equation. Mathematically, the

superposition theorem states that any sum of individual solutions to the diffusivity equation is also a solution to that equation. This concept can be applied to account for the following effects on the transient flow solution:

- Effects of multiple wells.
- Effects of rate change.
- Effects of the boundary.
- Effects of pressure change.

Slider (1976) presented an excellent review and discussion of the practical applications of the principle of superposition in solving a wide variety of unsteady-state flow problems.

Effects of Multiple Wells

Frequently, it is desirable to account for the effects of more than one well on the pressure at some point in the reservoir. The superposition concept states that the total pressure drop at any point in the reservoir is the sum of the pressure changes at that point caused by flow in each of the wells in the reservoir. In other words, we simply superimpose one effect upon the other.

Consider Figure 3-29, which shows three wells that are producing at different flow rates from an infinite-acting reservoir, i.e., an unsteady-state flow reservoir. The principle of superposition shows that the total pressure drop observed at any well, e.g., Well 1, is

$$\begin{split} (\Delta p)_{\text{total drop at Well 1}} &= (\Delta p)_{\text{drop due to Well 1}} \\ &+ (\Delta p)_{\text{drop due to Well 2}} \\ &+ (\Delta p)_{\text{drop due to Well 3}} \end{split}$$

The pressure drop at Well 1 due to its own production is given by the log-approximation to the E_i-function solution presented by Equation 3-145, or

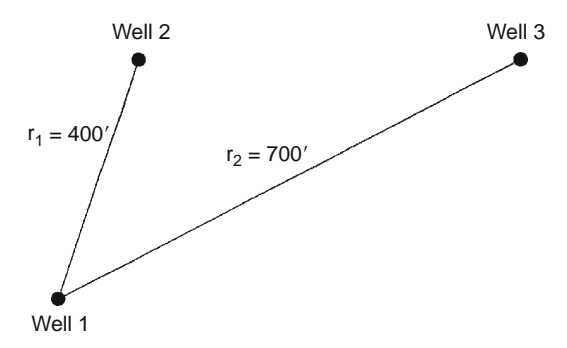


FIGURE 3-29 Well layout for Example 3-21.

$$\begin{split} (p_i - p_{wf}) &= (\Delta p)_{Well~1} = \frac{162.6Q_{o1}B_o\mu_o}{kh} \\ &\times \left[log\left(\frac{kt}{\varphi\mu c_t r_w^2}\right) - 3.23 + 0.87s \right] \end{split}$$

where t = time, hr

s = skin factor

k = permeability, md

 $Q_{o1} = oil flow rate from Well 1$

The pressure drop at Well 1 due to production at Wells 2 and 3 must be written in terms of the E_i -function solution as expressed by Equation 3-78. The log-approximation cannot be used because we are calculating the pressure at a long distance r from the well, i.e., the argument x > 0.01, or

$$\begin{split} \left(p_i - p_{wf}\right)_{total~at~Well~1} &= \left(\frac{162.6~Q_{o1}B_o\mu_o}{kh}\right) \\ &\times \left[\log\left(\frac{kt}{\varphi\mu c_t r_w^2}\right) - 3.23 + 0.87s\right] - \left(\frac{70.6Q_{o2}B_o\mu_o}{kh}\right) \\ &\times E_i \left[-\frac{948\varphi\mu c_t r_1^2}{kt}\right] - \left(\frac{70.6~Q_{o3}B_o\mu_o}{kh}\right) E_i \left[-\frac{948\varphi\mu c_t r_2^2}{kt}\right] \end{split}$$

where Q_{o1} , Q_{o2} , and Q_{o3} refer to the respective producing rates of Wells 1, 2, and 3.

This computational approach can be used to calculate the pressure at Wells 2 and 3. Further, it can be extended to include any number of wells flowing under the unsteady-state flow condition. It should also be noted that, if the point of interest is an operating well, the skin factor s must be included for that well only.

Example 3-21

Assume that the three wells as shown in Figure 3-29 are producing under a transient flow condition for 15 hours. The following additional data are available:

$Q_{o1} = 100 \text{ STB/day}$	h = 20 ft
$Q_{o2} = 160 \text{ STB/day}$	$\phi = 15\%$
$Q_{o3} = 200 \text{ STB/day}$	k = 40 md
$p_i = 4500 \text{ psi}$	$r_{\rm w}=0.25~{\rm ft}$
$B_o = 1.20 \text{ bbl/STB}$	$\mu_o = 2.0 \text{ cp}$
$c_t = 20 \times 10^{-6} \text{ psi}^{-1}$	$r_1 = 400 \text{ ft}$
$(S)_{Well\ 1} = -0.5$	$r_2=700\ ft$

If the three wells are producing at a constant flow rate, calculate the sand face flowing pressure at Well 1.

Solution

Step 1. Calculate the pressure drop at Well 1 caused by its own production by using Equation 3-145:

$$\begin{split} (\Delta p)_{Well~1} &= \frac{(162.6)(100)(1.2)(2.0)}{(40)(20)} \\ &\times \left[log \left(\frac{(40)(15)}{(0.15)(2)(20\times 10^{-6})(0.25)^2} \right) - 3.23 + 0.87(0) \right] \\ &= 270.2 \; psi \end{split}$$

Step 2. Calculate the pressure drop at Well 1 due to the production from Well 2:

$$\begin{split} \left(\Delta p\right)_{due\ to\ Well\ 2} &= -\frac{(70.6)(160)(1.2)(2)}{(40)(20)} \\ &\times E_i \left[-\frac{(948)(0.15)(2.0)(20\times 10^{-6})(400)^2}{(40)(15)} \right] \\ &= 33.888[-E_i(-1.5168)] \\ &= (33.888)(0.13) = 4.41\ psi \end{split}$$

Step 3. Calculate the pressure drop due to production from Well 3:

$$\begin{split} (\Delta p)_{due \ to \ Well \ 3} &= -\frac{(70.6)(200)(1.2)(2)}{(40)(20)} \\ & \times E_i \left[-\frac{(948)(0.15)(2.0)(20\times 10^{-6})(700)^2}{(40)(15)} \right] \\ &= (42.36)[-E_i(-4.645)] \\ &= (42.36)(1.84\times 10^{-3}) = 0.08 \ psi \end{split}$$

Step 4. Calculate the total pressure drop at Well 1:

$$(\Delta p)_{total \ at \ Well \ 1} = 270.2 + 4.41 + 0.08 = 274.69 \ psi$$

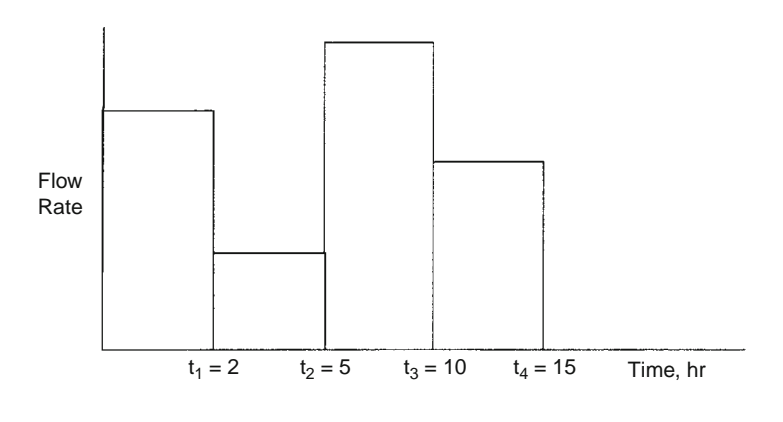
Step 5. Calculate p_{wf} at Well 1:

$$p_{wf} = 4500 - 274.69 = 4225.31 \text{ psi}$$

Effects of Variable Flow Rates

All of the mathematical expressions presented previously in this part require that the wells produce at a constant rate during the transient flow periods. Practically all wells produce at varying rates, and therefore, it is important that we be able to predict the pressure behavior when the rate changes. For this purpose, the concept of superposition states, "Every flow rate change in a well will result in a pressure response which is independent of the pressure responses caused by other previous rate changes." Accordingly, the total pressure drop that has occurred at any time is the summation of pressure changes caused separately by each net flow rate change.

Consider the case of a shut-in well, i.e., Q = 0, that was then allowed to produce at a series of constant rates for the different time periods shown in Figure 3-30. To calculate the total pressure drop at the sand



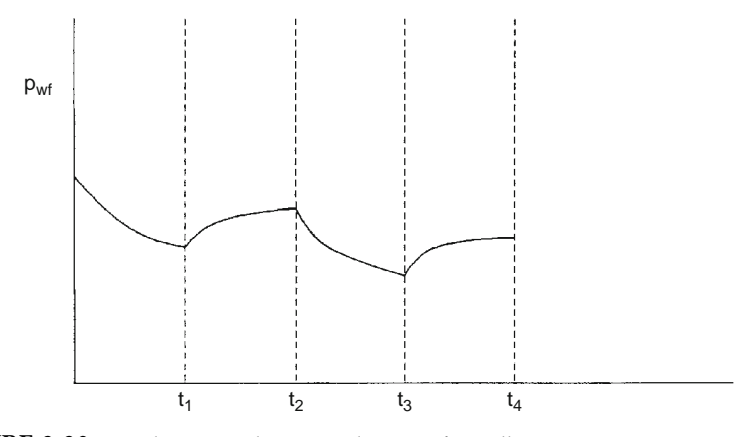


FIGURE 3-30 Production and pressure history of a well.

face at time t₄, the composite solution is obtained by adding the individual constant-rate solutions at the specified rate-time sequence, or

$$\begin{split} (\Delta p)_{total} &= (\Delta p)_{due~to(Q_{o1}-_0)} + (\Delta p)_{due~to(Q_{o2}-Q_{o1})} \\ &+ (\Delta p)_{due~to(Q_{o3}-Q_{o2})} + (\Delta p)_{due~to(Q_{o4}-Q_{o3})} \end{split}$$

This expression indicates that there are four contributions to the total pressure drop resulting from the four individual flow rates.

The first contribution results from increasing the rate from 0 to Q_1 and is in effect over the entire time period t_4 ; thus

$$\left(\Delta p\right)_{Q1-o} = \left[\frac{162.6(Q_1-0)B\mu}{kh}\right] \left[\ log \left(\frac{kt_4}{\varphi\mu c_t r_{w}^2}\right) - 3.23 + 0.87 \ s \right]$$

It is essential to notice the *change* in the rate, i.e., (new rate – old rate), that is used in the equation. It is the change in the rate that causes the pressure disturbance. Further, it should be noted that the "time" in the equation represents the *total elapsed time* since the change in the rate has been in effect.

The second contribution results from decreasing the rate from Q_1 to Q_2 at t_1 ; thus

$$\begin{split} \left(\Delta p\right)_{Q_2-Q_1} &= \left[\frac{162.6(Q_2-Q_1)B\mu}{kh}\right] \\ &\times \left[\log\left(\frac{k(t_4-t_1)}{\varphi\mu c_t r_w^2}\right) - 3.23 + 0.87~s\right] \end{split}$$

Using the same concept, the contributions from Q_2 to Q_3 and from Q_3 to Q_4 can be computed as

$$\begin{split} (\Delta p)_{Q_3-Q_2} &= \left[\frac{162.6(Q_3-Q_2)B\mu}{kh} \right] \\ &\times \left[\log \left(\frac{k(t_4-t_2)}{\varphi\mu c_t r_w^2} \right) - 3.23 + 0.87 \, s \right] \\ (\Delta p)_{Q_4-Q_3} &= \left[\frac{162.6(Q_4-Q_3)B\mu}{kh} \right] \\ &\times \left[\log \left(\frac{k(t_4-t_3)}{\varphi\mu c_t r_w^2} \right) - 3.23 + 0.87 \, s \right] \end{split}$$

This approach can be extended to model a well with several rate changes. Note, however, the approach is valid only if the well is flowing under the unsteady-state flow condition for the total time elapsed since the well began to flow at its initial rate.

Example 3-22

Figure 3-30 shows the rate history of a well that is producing under transient flow conditions for 15 hours. Given the following data:

$$\begin{array}{ll} p_i = 5000 \; psi & h = 20 \; ft \\ B_o = 1.1 \; bbl/STB & \varphi = 15\% \\ \mu_o = 2.5 \; cp & r_w = 0.3 \; ft \\ c_t = 20 \times 10^{-6} \; psi^{-1} & s = 0 \\ k = 40 \; md & s = 0 \end{array}$$

calculate the sand face pressure after 15 hours.

Solution

Step 1. Calculate the pressure drop due to the first flow rate for the entire flow period:

$$\begin{split} \left(\Delta p\right)_{Q_{1-0}} &= \frac{(162.6)(100-0)(1.1)(2.5)}{(40)(20)} \\ &\times \left\{ log \left[\frac{(40)(15)}{(0.15)(2.5)(20\times 10^{-6})(0.3)^2} \right] - 3.23 + 0 \right\} = 319.6 \; psi \end{split}$$

Step 2. Calculate the additional pressure change due to the change in flow rate from 100 to 70 STB/day:

$$\begin{split} \left(\Delta p\right)_{Q_2-Q_1} &= \frac{(162.6)(70-100)(1.1)(2.5)}{(40)(20)} \\ &\times \left\{ \log \left[\frac{(40)(15-2)}{(0.15)(2.5)(20\times 10^{-6})(0.3)^2} \right] - 3.23 \right\} = -94.85 \ psi \end{split}$$

Step 3. Calculate the additional pressure change due to the change in flow rate from 70 to 150 STB/day:

$$\begin{split} \left(\Delta p\right)_{Q_3-Q_2} &= \frac{(162.6)(150-70)(1.1)(2.5)}{(40)(20)} \\ &\times \left\{ \log \left[\frac{(40)(15-5)}{(0.15)(2.5)(20\times 10^{-6})(0.3)^2} \right] - 3.23 \right\} = 249.18 \text{ psi} \end{split}$$

Step 4. Calculate the additional pressure change due to the change in flow rate from 150 to 85 STB/day:

$$\begin{split} \left(\Delta p\right)_{Q_4-Q_3} &= \frac{(162.6)(85-150)(1.1)(2.5)}{(40)(20)} \\ &\times \left\{ log \left[\frac{(40)(15-10)}{(0.15)(2.5)(20\times 10^{-6})(0.3)^2} \right] - 3.23 \right\} = -190.44 \; psi \end{split}$$

Step 5. Calculate the total pressure drop:

$$(\Delta p)_{total} = 319.6 + (-94.85) + 249.18 + (-190.44) = 283.49 \text{ psi}$$

Step 6. Calculate the wellbore pressure after 15 hours of transient flow:

$$p_{wf} = 5000 - 283.49 = 4716.51 \text{ psi}$$

Effects of the Reservoir Boundary

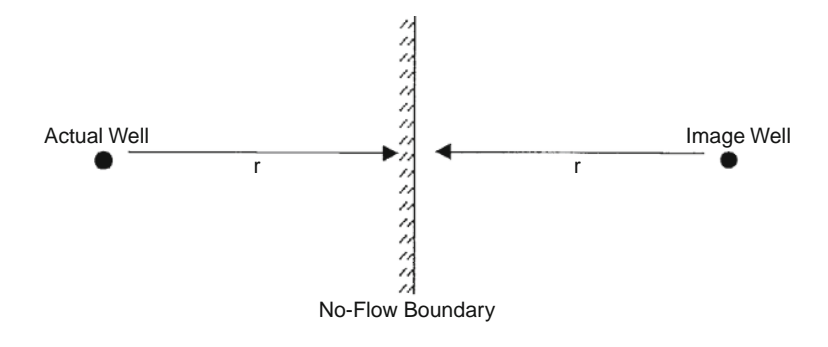
The superposition theorem can also be extended to predict the pressure of a well in a bounded reservoir. Consider Figure 3-31, which shows a well that is located a distance r from the no-flow boundary, e.g., sealing fault. The no-flow boundary can be represented by the following pressure gradient expression:

$$\left(\frac{\partial p}{\partial r}\right)_{boundary} = 0$$

Mathematically, the boundary condition can be met by placing an *image* well, identical to that of the actual well, on the other side of the fault at exactly distance r. Consequently, the effect of the boundary on the pressure behavior of a well would be the same as the effect of an image well located a distance 2r from the actual well

In accounting for the boundary effects, the superposition method is frequently called the *method of images*. Thus, for the system configuration given in Figure 3-31, the problem reduces to one of determining the effect of the image well on the actual well. The total pressure drop at the actual well will be the pressure drop due to its own production plus the additional pressure drop caused by an identical well at a distance of 2r, or

$$(\Delta p)_{total} = (\Delta p)_{actual\ well} + (\Delta p)_{due\ to\ image\ well}$$



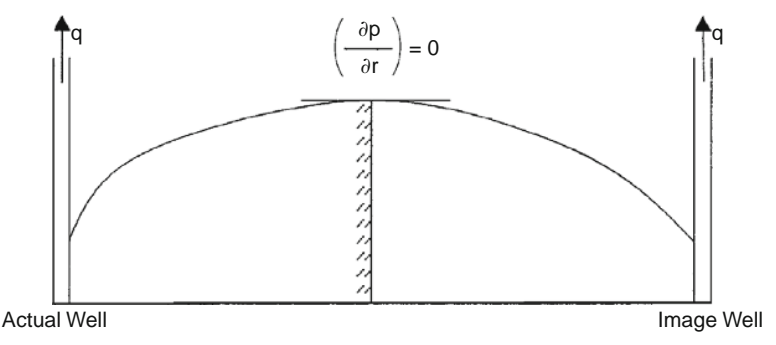


FIGURE 3-31 Method of images in solving boundary problems.

or

$$\begin{split} \left(\Delta p\right)_{total} &= \frac{162.6Q_oB_o\mu_o}{kh} \left[log\left(\frac{kt}{\varphi\mu_oc_tr_w^2}\right) - 3.23 + 0.87s \right] \\ &- \left(\frac{70.6Q_oB_o\mu_o}{kh}\right)E_i\left(-\frac{948\varphi\mu_oc_t(2r)^2}{kt}\right) \end{split} \tag{3-168} \label{eq:deltapprox}$$

Notice that this equation assumes the reservoir is infinite except for the indicated boundary. The effect of boundaries is always to cause a greater pressure drop than those drops calculated for infinite reservoirs.

The concept of image wells can be extended to generate the pressure behavior of a well located within a variety of boundary configurations.

Example 3-23

Figure 3-32 shows a well located between two sealing faults at 200 and 100 ft from the two faults. The well is producing under a transient flow condition at a constant flow rate of 200 STB/day.

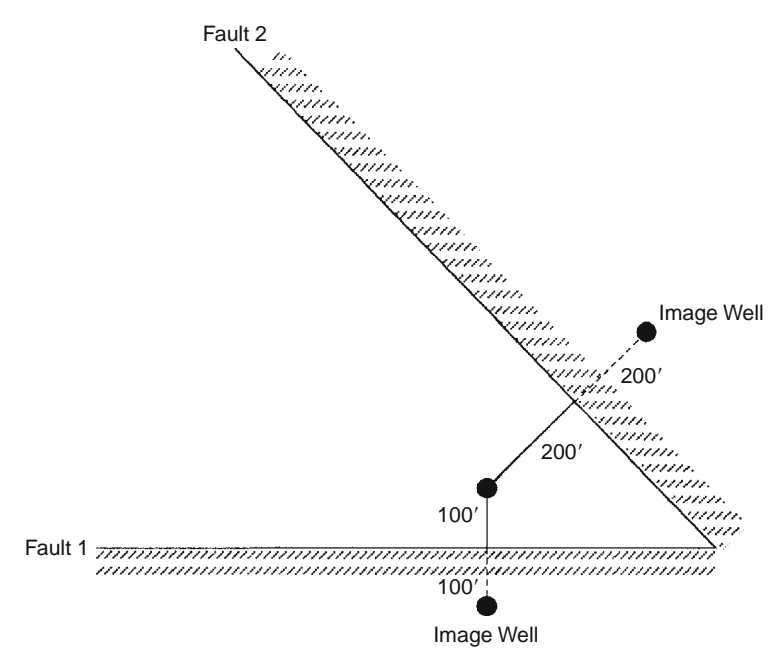


FIGURE 3-32 Well layout for Example 3-23.

Given

$$\begin{array}{ll} p_i = 500 \; psi & k = 600 \; md \\ B_o = 1.1 \; bbl/STB & \varphi = 17\% \\ \mu_o = 2.0 \; cp & h = 25 \; ft \\ r_w = 0.3 \; ft & s = 0 \\ c_t = 25 \times 10^{-6} \; psi^{-1} & \end{array}$$

calculate the sand face pressure after 10 hours.

Solution

Step 1. Calculate the pressure drop due to the actual well flow rate:

$$\begin{split} \left(\Delta p\right)_{actual} &= \frac{(162.6)(200)(1.1)(2.0)}{(60)(25)} \\ &\times \left\{ log \left[\frac{(60)(10)}{(0.17)(2)(0.17)(2)(25\times 10^{-6})(0.3)^2} \right] - 3.23 + 0 \right\} \\ &= 270.17 \end{split}$$

Step 2. Determine the additional pressure drop due to the first fault (i.e., Image Well 1):

$$\begin{split} \left(\Delta p\right)_{Image\ Well\ 1} &= -\frac{(70.6)(200)(1.1)(2.0)}{(60)(25)} \\ &\times E_i \left[-\frac{(948)(0.17)(2)(25\times 10^{-6})(2\times 100)^2}{(6)(10)} \right] \\ &= 20.71[-E_i(-0.537)] = 10.64\ psi \end{split}$$

Step 3. Calculate the effect of the second fault (i.e., Image Well 2):

$$\begin{split} \left(\Delta p\right)_{Image\ Well\ 2} &= 20.71 \left[-E_i \left(\frac{-948(0.17)(2)(25\times 10^{-6})(2\times 200)^2}{(60)(10)} \right) \right] \\ &= 20.71 [-E_i(-2.15)] = 1.0\ psi \end{split}$$

Step 4. total pressure drop is

$$(\Delta p)_{total} = 270.17 + 10.64 + 1.0 = 281.8 \ psi$$

Step 5.
$$p_{wf} = 5000 - 281:8 = 4718.2 \text{ psi.}$$

Accounting for Pressure-Change Effects

Superposition is also used in applying the constant-pressure case. Pressure changes are accounted for in this solution in much the same way that rate changes are accounted for in the constant-rate case.

SECTION 3.12 TRANSIENT WELL TESTING

Detailed reservoir information is essential to the petroleum engineer in order to analyze the current behavior and future performance of the reservoir. Pressure transient testing is designed to provide the engineer with a quantitative analysis of the reservoir properties. A transient test is essentially conducted by creating a pressure disturbance in the reservoir and recording the pressure response at the wellbore, i.e., bottomhole flowing pressure $p_{\rm wf}$, as a function of time. The pressure transient tests most commonly used in the petroleum industry include

- Pressure drawdown.
- Pressure buildup.
- Multirate.

- Interference.
- Pulse.
- Drill stem.
- Fall off.
- Injectivity.
- Step rate.

It has long been recognized that the pressure behavior of a reservoir following a rate change directly reflects the geometry and flow properties of the reservoir. Information available from a well test includes

- Effective permeability.
- Formation damage or stimulation.
- Flow barriers and fluid contacts.
- Volumetric average reservoir pressure.
- Drainage pore volume.
- Detection, length, and capacity of fractures.
- Communication between wells.

Only the drawdown and buildup tests are briefly described in the following two sections. Several excellent books comprehensively address the subject of well testing, notably:

- John Lee, Well Testing (1982).
- C. S. Matthews and D. G. Russell, *Pressure Buildup and Flow Tests in Wells* (1967).
- Robert Earlougher, Advances in Well Test Analysis (1977).
- R. Al-Hussainy and H. J. Ramsey, Jr., *Theory and Practice of the Testing of Gas Wells* (1975).
- Roland Horn, Modern Well Test Analysis (1995).

Drawdown Test

A pressure drawdown test is simply a series of bottom-hole pressure measurements made during a period of flow at constant producing rate. Usually the well is shut in prior to the flow test for a period of time sufficient to allow the pressure to equalize throughout the formation, i.e., to reach static pressure. A schematic of the ideal flow rate and pressure history is illustrated by Figure 3-33.

The fundamental objectives of drawdown testing are to obtain the average permeability, k, of the reservoir rock within the drainage area of the well and to assess the degree of damage or stimulation induced in the vicinity of the wellbore through drilling and completion practices. Other objectives are to determine the pore volume and to detect reservoir inhomogeneities within the drainage area of the well.

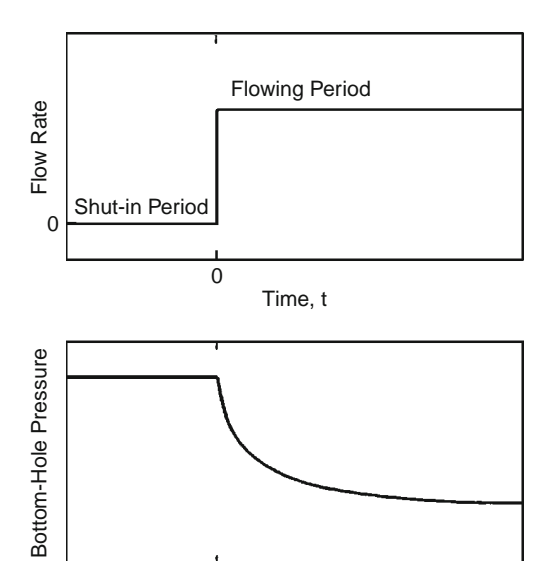


FIGURE 3-33 Idealized drawdown test.

During flow at a constant rate of Q_o , the pressure behavior of a well in an infinite-acting reservoir (i.e., during the unsteady-state flow period) is given by Equation 3-145 as

$$p_{wf} = p_i - \frac{162.6 \ Q_o B_o \mu}{kh} \left[log \left(\frac{kt}{\varphi \mu c_t r_w^2} \right) - 3.23 + 0.87 \ s \right]$$

where k = permeability, md

t = time, hr

 r_w = wellbore radius

0

Time, t

s = skin factor

The expression can be written as

$$\begin{split} p_{wf} &= p_i - \frac{162.6 \ Q_o B_o \mu}{kh} \\ &\times \left\lceil log(t) + log \left(\frac{k}{\varphi \mu c_t r_w^2}\right) - 3.23 + 0.87 \ s \right \end{split} \tag{3-169}$$

Equation 3-169 is essentially an equation of a straight line and can be expressed as

$$p_{wf} = a + m \log(t) \tag{3-170}$$

where

$$a = p_i - \frac{162.6Q_oB_o\mu}{kh} \left\lceil log \left(\frac{k}{\varphi\mu c_t r_w^2}\right) - 3.23 + 0.87 \ s \right\rceil$$

The slope m is given by

$$m = \frac{-162.6Q_{o}B_{o}\mu_{o}}{kh}$$
 (3-171)

Equation 3-170 suggests that a plot of p_{wf} versus time t on semilog graph paper would yield a straight line with a slope m in psi/cycle. This semilog straight-line relationship is illustrated by Figure 3-34.

Equation 3-171 can also be rearranged for the capacity kh of the drainage area of the well. If the thickness is known, then the average permeability is given by

$$k = \frac{-162.6Q_oB_o\mu_o}{mh}$$
 (3-172)

where k = average permeability, md

m = slope, psi/cycle (slope m is negative)

Clearly, kh/μ or k/μ also may be estimated.

The skin effect can be obtained by rearranging Equation 3-169 as

$$s = 1.151 \left(\frac{p_{wf} - p_i}{m} - \log t - \log \frac{k}{\varphi \mu c_t r_w^2} + 3.23 \right)$$

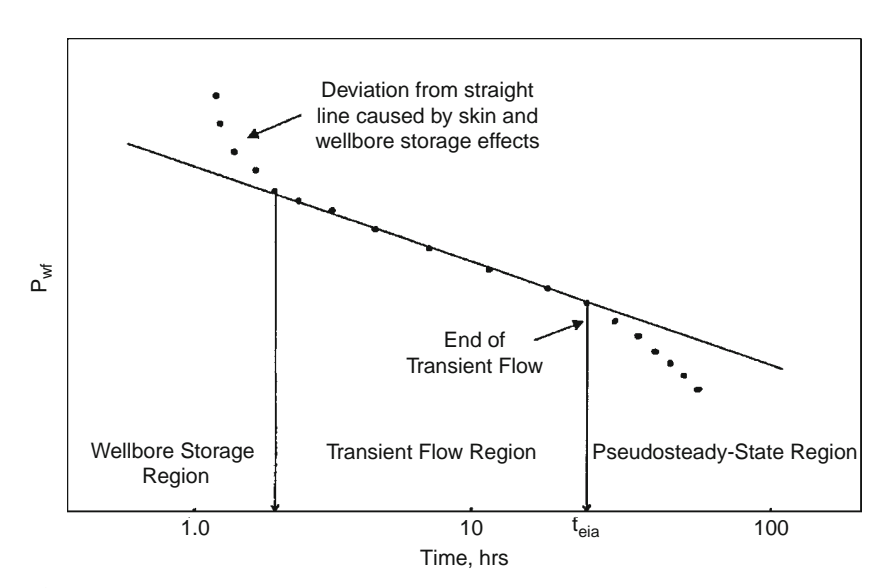


FIGURE 3-34 Semilog plot of pressure drawdown data.

or, more conveniently, if $p_{wf} = p_{1hr}$, which is found on the extension of the straight line at log t (1 hour), then

$$s = 1.151 \left(\frac{p_{1 \text{ hr}} - p_{i}}{m} - log \frac{k}{\phi \mu c_{t} r_{w}^{2}} + 3.23 \right) \tag{3-173}$$

In Equation 3-173, $p_{1 \text{ hr}}$ must be from the semilog straight line. If pressure data measured at 1 hour do not fall on that line, the line *must be extrapolated* to 1 hour and the extrapolated value of $p_{1\text{hr}}$ must be used in Equation 3-173. This procedure is necessary to avoid calculating an incorrect skin by using a wellbore-storage-influenced pressure. Figure 3-34 illustrates the extrapolation to $p_{1\text{hr}}$.

If the drawdown test is long enough, bottom-hole pressure will deviate from the semilog straight line and make the transition from infinite acting to pseudosteady state.

It should be pointed out that the pressure drop due to the skin, as expressed by Equation 3-141, can be written in terms of the transient flow slope, m, by combining the equations:

$$m = 162.6 \frac{Q_o B_o \mu_o}{kh}$$

$$\Delta Ps = 141.2 \left\lceil \frac{Q_o B_o \mu_o}{kh} \right\rceil s$$

Combining the two expressions gives

$$\Delta p_s = 0.87 \text{ m s}$$

Example 3-24²

Estimate oil permeability and skin factor from the drawdown data of Figure 3-35. The following reservoir data are available:

$$\begin{array}{ll} h = 130 \; ft & \varphi = 20\% \\ r_w = 0.25 \; ft & p_i = 1,154 \; psi \\ Q_o = 348 \; STB/D & m = -22 \; psi/cycle \\ B_o = 1.14 \; bbl/STB & \\ \mu_o = 3.93 \; cp & \\ c_t = 8.74 \times 10^{-6} \; psi^{-1} & \end{array}$$

Assuming that the wellbore storage effects are not significant, calculate

- Permeability.
- Skin factor.

²This example problem and the solution procedure are given by Earlougher, R., *Advances in Well Test Analysis*, Monograph Series, SPE, Dallas (1977).

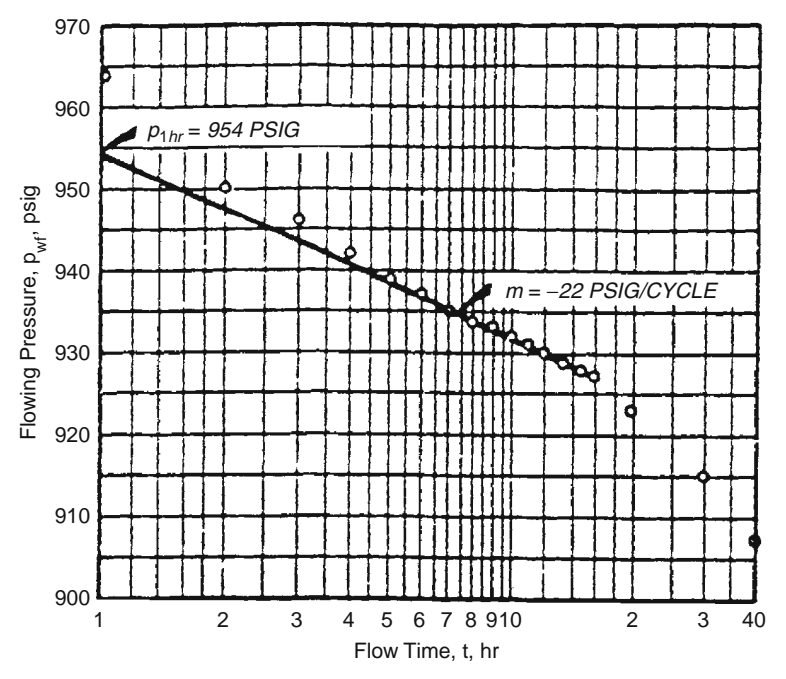


FIGURE 3-35 Earlougher's semilog data plot for the drawdown test. (Permission to publish by the SPE, copyright SPE, 1977.)

Solution

Step 1. From Figure 3-35, calculate p_{1hr} :

$$p_{1 \text{ hr}} = 954 \text{ psi}$$

Step 2. Determine the slope of the transient flow line:

$$m = -22 \: psi/cycle$$

Step 3. Calculate the permeability by applying Equation 3-172:

$$k = \frac{-(162.6)(348)(1.14)(3.93)}{(-22)(130)} = 89 \text{ md}$$

Step 4. Solve for the skin factor s using Equation 3-174:

$$s = 1.151 \left\{ \left(\frac{954 - 1,154}{-22} \right) - \log \left[\frac{89}{(0.2)(3.93)(8.74 \times 10^{-6})(0.25)^2} \right] + 3.2275 \right\} = 4.6$$

Basically, well test analysis deals with the interpretation of the well-bore pressure response to a given change in the flow rate (from 0 to a constant value for a drawdown test or from a constant rate to 0 for a buildup test). Unfortunately, the producing rate is controlled at the surface, not at the sand face. Because of the wellbore volume, a constant surface flow rate does not ensure that the entire rate is being produced from the formation. This effect is due to *wellbore storage*. Consider the case of a drawdown test. When the well is first open to flow after a shut-in period, the pressure in the wellbore drops. This drop in the wellbore pressure causes the following two types of wellbore storage:

- Wellbore storage effect caused by *fluid expansion*.
- Wellbore storage effect caused by changing fluid level in the casingtubing annulus.

As the bottom-hole pressure drops, the wellbore fluid expands and, thus, the initial surface flow rate is not from the formation but essentially from the fluid that had been stored in the wellbore. This is defined as the wellbore storage due to fluid expansion.

The second type of wellbore storage is due to a changing of the annulus fluid level (falling during a drawdown test and rising during a pressure buildup test). When the well is open to flow during a drawdown test, the reduction in pressure causes the fluid level in the annulus to fall. This annulus fluid production joins that from the formation and contributes to the total flow from the well. The falling fluid level is generally able to contribute more fluid than that by expansion.

The preceding discussion suggests that part of the flow will be contributed by the wellbore instead of the reservoir; i.e.,

$$q = q_f + q_{wb}$$

where q = surface flow rate, bbl/day

 $q_{\rm f} = formation \; flow \; rate, \; bbl/day \;$

 $q_{wb} = \text{flow rate contributed by the wellbore, bbl/day}$

As production time increases, the wellbore contribution decreases and the formation rate increases until it eventually equals the surface flow rate. During this period when the formation rate is changed, the measured drawdown pressures will not produce the ideal semilog straight-line behavior that is expected during transient flow. This indicates that the pressure data collected during the duration of the wellbore storage effect cannot be analyzed by using conventional methods.

Each of these two effects can be quantified in terms of the wellbore storage factor C, which is defined as

$$C = \frac{\Delta V_{wb}}{\Delta p}$$

where C = wellbore storage volume, bbl/psi

 ΔV_{wb} = change in the volume of fluid in the wellbore, bbl

This relationship can be applied to mathematically represent the individual effect of wellbore fluid expansion and falling (or rising) fluid level, to give the following:

• Wellbore Storage Effect Due to Fluid Expansion.

$$C = V_{wb}c_{wb}$$

where V_{wb} = total wellbore fluid volume, bbl

 $c_{wb} = average \ compressibility \ of \ fluid \ in \ the \ wellbore, \ psi^{-1}$

• Wellbore Storage Effect Due to Changing Fluid Level. If A_a is the cross-sectional area of the annulus, and ρ is the average fluid density in the wellbore, the wellbore storage coefficient is given by

$$C = \frac{144 \text{ A}_a}{5.615 \text{ p}}$$

with

$$A_{a} = \frac{\pi \Big[(ID_{C})^{2} - (OD_{T})^{2} \Big]}{4(144)}$$

where A_a = annulus cross-sectional area, ft²

 OD_T = outside diameter of the production tubing, in

 ID_C = inside diameter of the casing, in ρ = wellbore fluid density, lb/ft³

This effect is essentially small if a packer is placed near the producing zone. The total storage effect is the sum of both effects. It should be noted during oil well testing that the fluid expansion is generally insignificant due to the small compressibility of liquids. For gas wells, the primary storage effect is due to gas expansion.

To determine the duration of the wellbore storage effect, it is convenient to express the wellbore storage factor in a dimensionless form as

$$C_{\rm D} = \frac{5.615\,C}{2\pi h \varphi c_t r_w^2} = \frac{0.894\,C}{\varphi h c_t r_w^2}$$

where $C_D = \text{dimensionless}$ wellbore storage factor

C = wellbore storage factor, bbl/psi

 $c_t = total compressibility coefficient, psi^{-1}$

 $r_{\rm w} = \text{wellbore radius, ft}$

h = thickness, ft

Horne (1995) and Earlougher (1977), among other authors, have indicated that the wellbore pressure is directly proportional to the time during the wellbore storage-dominated period of the test and is expressed by

$$p_D = t_D/C_D$$

where $p_D = \mbox{dimensionless}$ pressure during wellbore storage domination time

 $t_D = dimensionless time$

Taking the logarithm of both sides of this relationship gives

$$log(p_D) = log(t_D) - log(C_D)$$

The expression has a characteristic that is diagnostic of wellbore storage effects. It indicates that a plot of p_D versus t_D on a log-log scale will yield a straight line of a unit slope during wellbore storage domination. Since p_D is proportional to Δp and t_D is proportional to time, it is convenient to log (p_i-p_{wf}) versus log (t) and observe where the plot has a slope of 1 cycle in pressure per cycle in time.

The log-log plot is a valuable aid for recognizing wellbore storage effects in transient tests (e.g., drawdown or buildup tests) when early-time pressure recorded data are available. It is recommended that this plot be made a part of transient test analysis. As wellbore storage effects become less severe, the formation begins to influence the bottom-hole pressure more and more, and the data points on the log-log plot fall below the unit-slope straight line and signific the end of the wellbore storage effect. At this point, wellbore storage is no longer important and standard semilog data-plotting analysis techniques apply. As a rule of thumb, that time usually occurs about 1 to 1½ cycles in time after the log-log data plot starts deviating significantly from the unit slope. This time may be estimated from

$$t_D > (60 + 3.5s) C_D \\$$

or approximately

$$t > \frac{(200,\!000+12,\!000\;s)C}{(kh/\mu)}$$

where t = total time that marks the end of the wellbore storage effect and the beginning of the semilog straight line, hr

k = permeability, md

s = skin factor

m = viscosity, cp

C = wellbore storage coefficient, bbl/psi

Example 3-25

The following data are given for an oil well that is scheduled for a drawdown test:

- Volume of fluid in the wellbore = 180 bbls.
- Tubing outside diameter = 2 in.
- Production casing inside diameter = 7.675 in.
- Average oil density in the wellbore = 45 lb/ft³.
- Additionally,

$$\begin{array}{lll} h = 20 \ ft & & \varphi = 15\% & r_w = 0.25 \ ft \\ \mu_o = 2 \ cp & k = 30 \ md & s = 0 \\ c_t = 20 \times 10^{-6} \ psi^{-1} & c_o = 10 \times 10^{-6} \ psi^{-1} \end{array}$$

If this well is placed under a constant production rate, how long will it take for wellbore storage effects to end?

Solution

Step 1. Calculate the cross-sectional area of the annulus A_a:

$$A_{a} = \frac{\pi \left[(7.675)^{2} - (2)^{2} \right]}{(4)(144)} = 0.2995 \text{ ft}^{2}$$

Step 2. Calculate the wellbore storage factor caused by fluid expansion:

$$\begin{split} C &= V_{wb} c_{wb} \\ C &= (180)(10 \times 10^{-6}) = 0.0018 \ bbl/psi \end{split}$$

Step 3. Determine the wellbore storage factor caused by the falling fluid level:

$$\begin{split} C &= \frac{144 \; A_a}{5.615 \; \rho} \\ C &= \frac{144 (0.2995)}{(5.615)(45)} = 0.1707 \; bbl/psi \end{split}$$

Step 4. Calculate the total wellbore storage coefficient:

$$C = 0.0018 + 0.1707 = 0.1725 \ bbl/psi$$

These calculations show that the effect of fluid expansion can generally be neglected in crude oil systems.

Step 5. Determine the time required for wellbore storage influence to end from

$$\begin{split} t &= \frac{(200,\!000+12,\!000\;s)C\;\mu}{kh} \\ t &= \frac{(200,\!000+0)(0.1725)(2)}{(30)(20)} = 115\;hrs \end{split}$$

The straight-line relationship as expressed by Equation 3-170 is valid only during the infinite-acting behavior of the well. Obviously, reservoirs are not infinite in extent; thus the infinite-acting radial flow period cannot last indefinitely. Eventually the effects of the reservoir boundaries will be felt at the well being tested. The time at which the boundary effect is felt is dependent on the following factors:

- Permeability k.
- Total compressibility c_t.
- Porosity φ.
- Viscosity μ.
- Distance to the boundary.
- Shape of the drainage area.

Earlougher (1977) suggests the following mathematical expression for estimating the duration of the infinite-acting period:

$$t_{eia} = \left[\frac{\varphi\mu c_t A}{0.000264~k}\right] (t_{DA})_{eia}$$

where t_{eia} = time to the end of the infinite-acting period, hr

 $A = well drainage area, ft^2$

 $c_t = total compressibility, psi^{-1}$

 $(t_{DA})_{eia}$ = dimensionless time to the end of the infinite-acting period

Earlougher's expression can be used to predict the end of transient flow in a drainage system of any geometry by obtaining the value of $(t_{DA})_{eia}$ from Table 3-4 as listed under "Use Infinite System Solution with Less than 1% Error for t_{DA} <." For example, for a well centered in a circular reservoir, $(t_{DA})_{eia} = 0.1$, and accordingly

$$t_{eia} = \frac{380 \varphi \mu c_t A}{k}$$

Hence, the specific steps involved in a drawdown test analysis are

- 1. Plot $(p_{\rm i}$ $p_{\rm wf})$ versus t on a log-log scale.
- 2. Determine the time at which the unit-slope line ends.

- 3. Determine the corresponding time at 1½ log cycle, ahead of the observed time in step 2. This is the time that marks the end of the wellbore storage effect and the start of the semilog straight line.
- 4. Estimate the wellbore storage coefficient from

$$C = \frac{qt}{24 \Delta p}$$

where t and Δp are values read from a point on the log-log unit-slope straight line and q is the flow rate in bbl/day.

- 5. Plot p_{wi} versus t on a semilog scale.
- 6. Determine the start of the straight-line portion as suggested in step 3 and draw the best line through the points.
- 7. Calculate the slope of the straight line and determine the permeability k and skin factor s by applying Equations 3-172 and 3-173, respectively.
- 8. Estimate the time to the end of the infinite-acting (transient flow) period, i.e., t_{eia}, which marks the beginning of the pseudosteady-state flow.
- 9. Plot all the recorded pressure data after $t_{\rm eia}$ as a function of time on a regular Cartesian scale. These data should form a straight-line relationship.
- 10. Determine the *slope* of the pseudosteady-state line, i.e., dp/dt (commonly referred to as m') and use Equation 3-127 to solve for the drainage area A:

$$A = \frac{-0.23396 \ QB}{c_t h \varphi(dp/dt)} = \frac{-0.23396 \ QB}{c_t h \varphi m^{'}}$$

where m' = slope of the semisteady-state Cartesian straight line

Q = fluid flow rate, STB/day

B = formation volume factor, bbl/STB

11. Calculate the shape factor C_A from an expression that has been developed by Earlougher (1977). Earlougher has shown that the reservoir shape factor can be estimated from the following relationship:

$$C_{A} = 5.456 \left(\frac{m}{m'}\right) \exp \left[\frac{2.303(p_{1 \text{ hr}} - p_{\text{int}})}{m}\right]$$

where m= slope of the transient semilog straight line, psi/log cycle m'= slope of the semisteady-state Cartesian straight line $p_{1hr}=$ pressure at t=1 hr from the semilog straight line, psi $p_{int}=$ pressure at t=0 from the semisteady-state Cartesian

straight line, psi

12. Use Table 3-4 to determine the drainage configuration of the tested well that has a value of the shape factor C_A closest to that of the calculated one, i.e., step 11.

Pressure Buildup Test

The use of pressure buildup data has provided the reservoir engineer with one more useful tool in the determination of reservoir behavior. Pressure buildup analysis describes the buildup in wellbore pressure with time after a well has been shut in. One of the principal objectives of this analysis is to determine the static reservoir pressure without waiting weeks or months for the pressure in the entire reservoir to stabilize. Because the buildup in wellbore pressure will generally follow some definite trend, it has been possible to extend the pressure buildup analysis to determine

- Effective reservoir permeability.
- Extent of permeability damage around the wellbore.
- Presence of faults and to some degree the distance to them.
- Any interference between producing wells.
- Limits of the reservoir where there is not a strong water drive or where the aquifer is no larger than the hydrocarbon reservoir.

Certainly all of this information will probably not be available from any given analysis, and the degree of usefulness of any of this information will depend on the experience in the area and the amount of other information available for correlation purposes.

The general formulas used in analyzing pressure buildup data come from a solution of the diffusivity equation. In pressure buildup and drawdown analyses, the following assumptions, with regard to the reservoir, fluid, and flow behavior, are usually made:

Reservoir

- Homogeneous.
- Isotropic.
- Horizontal, uniform thickness.

Fluid

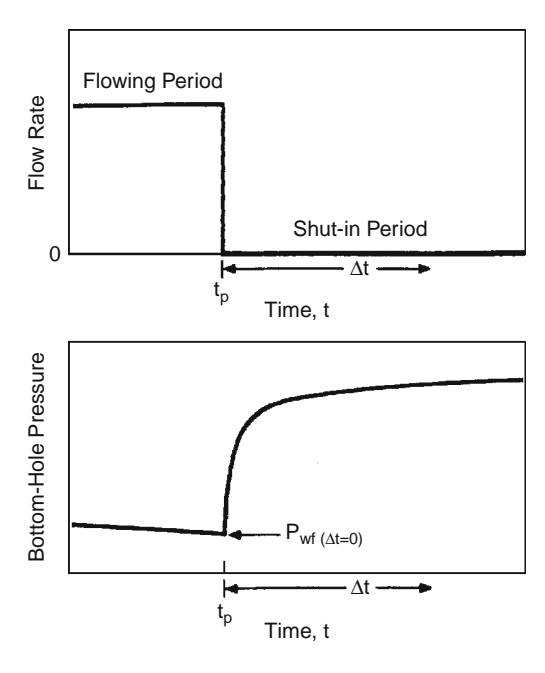
- Single phase.
- Slightly compressible.
- Constant μ_o and B_o .

Flow

- Laminar flow.
- No gravity effects.

Pressure buildup testing requires shutting in a producing well. The most common and the simplest analysis techniques require that the well produce at a constant rate, either from startup or long enough to establish a stabilized pressure distribution, before shut-in. Figure 3-36

FIGURE 3-36 Idealized pressure buildup test.



schematically shows rate and pressure behavior for an ideal pressure buildup test. In that figure, t_p is the production time and Δt is the running shut-in time. The pressure is measured immediately before shutin and is recorded as a function of time during the shut-in period. The resulting pressure buildup curve is analyzed for reservoir properties and wellbore condition.

Stabilizing the well at a constant rate before testing is an important part of a pressure buildup test. If stabilization is overlooked or is impossible, standard data analysis techniques may provide erroneous information about the formation.

A pressure buildup test is described mathematically by using the principle of superposition. Before the shut-in, the well is allowed to flow at a constant flow rate of Q_o STB/day for t_p days. At the time corresponding to the point of shut-in, i.e., t_p , a second well, superimposed over the location of the first well, is opened to flow at a constant rate equal to $-Q_o$ STB/day for Δt days. The first well is allowed to continue to flow at $+Q_o$ STB/day. When the effects of the two wells are added, the result is that a well has been allowed to flow at rate Q for time t_p and then shut in for time Δt . This simulates the actual test procedure. The time corresponding to the point of shut-in, t_p , can be estimated from the following equation:

$$t_{p} = \frac{24 N_{P}}{Q_{o}} \tag{3-174}$$

where N_p = well cumulative oil produced before shut-in, STB

Qo = stabilized well flow rate before shut-in, STB/day

 $t_p = total production time, hr$

Applying the superposition principle to a shut-in well, the total pressure change, i.e., $(p_i - p_{ws})$, which occurs at the wellbore during the shut-in time Δt , is essentially the sum of the pressure change caused by the constant flow rate Q and that of -Q, or

$$p_i - p_{ws} = (p_i - p_{wf})Q_o - 0 + (p_i - p_{wf})0 - Q_o$$

Substituting Equation 3-145 for each of the terms on the right-hand side of the above relationship gives

$$\begin{split} p_{ws} &= p_i - \frac{162.6(Q_o - 0)\mu B_o}{kh} \left[\log \frac{k(t_p + \Delta t)}{\phi \mu c_t r_w^2} - 3.23 + 0.875 \text{ s} \right] \\ &+ \frac{162.6(0 - Q_o)\mu B_o}{kh} \left[\log \frac{k(\Delta t)}{\phi \mu c_t r_w^2} - 3.23 + 0.875 \text{ s} \right] \end{split} \tag{3-175}$$

Expanding this equation and canceling terms,

$$p_{ws} = p_i - \frac{162.6Q_o\mu B}{kh} \left[log \frac{(t_p + \Delta t)}{\Delta t} \right]$$
 (3-176)

where p_i = initial reservoir pressure, psi

 p_{ws} = sand-face pressure during pressure buildup, psi

 $t_{\scriptscriptstyle D} =$ flowing time before shut-in, hr

 $\Delta t = \text{shut-in time, hr}$

The pressure buildup equation, i.e., Equation 3-175, was introduced by Horner (1951) and is commonly referred to as the *Horner equation*.

Equation 3-177 suggests that a plot of p_{ws} versus $(t_p + \Delta t)/\Delta t$ would produce a straight-line relationship with intercept p_i and slope –m, where

$$m = \frac{162.6 \ Q_o B_o \mu_o}{kh}$$

or

$$k = \frac{162.6 \ Q_o B_o \mu_o}{mh} \tag{3-177}$$

This plot, commonly referred to as the *Horner plot*, is illustrated in Figure 3-37. Note that, on the Horner plot, the scale of time ratio increases from left to right. Because of the form of the ratio, however, the shut-in time Δt increases from right to left. It is observed from Equation 3-176 that $p_{ws}=p_i$ when the time ratio is unity. Graphically, this means that the initial reservoir pressure, p_i , can be obtained by extrapolating the Horner plot straight line to $(t_p+\Delta t)/\Delta t=1$.

Earlougher (1977) pointed out that a result of using the superposition principle is that the skin factor, s, does not appear in the general pressure buildup equation, Equation 3-175. As a result, the skin factor does not appear in the simplified equation for the Horner plot, Equation 3-176. That means the Horner-plot slope is not affected by the skin factor; however, the skin factor still does affect the shape of the pressure buildup data. In fact, an early-time deviation from the straight line can be caused by the skin factor as well as by the wellbore storage, as

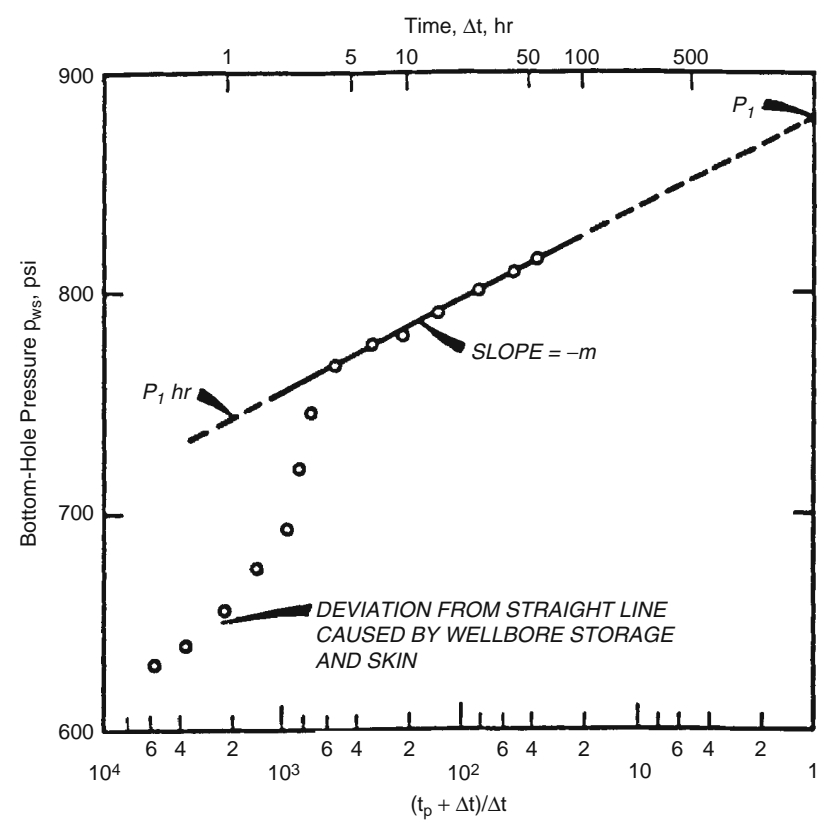


FIGURE 3-37 Horner plot. (After Earlougher, R. Advances in Well Test Analysis.) (Permission to publish by the SPE, copyright SPE, 1977.)

indicated in Figure 3-37. The deviation can be significant for the large negative skins that occur in hydraulically fractured wells. In any case, the skin factor does affect flowing pressure before shut-in, so skin may be estimated from the buildup test data plus the flowing pressure immediately before the buildup test:

$$s = 1.151 \left[\frac{p_{1 \text{ hr}} - p_{\text{wf}}(\Delta t = 0)}{m} - \log \frac{k}{\phi \mu c_t r_w^2} + 3.23 \right] \tag{3-178}$$

where p_{wf} ($\Delta t = 0$) = observed flowing bottom-hole pressure immediately before shut-in m = slope of the Horner plot k = permeability, md

$$\Delta p_{\rm skin} = 0.87 \text{ ms} \tag{3-179}$$

The value of p_{1hr} must be taken from the Horner straight line. Frequently, pressure data do not fall on the straight line at 1 hour because of wellbore storage effects or large negative skin factors. In that case, the semilog line must be extrapolated to 1 hour and the corresponding pressure is read.

It should be pointed out that, when a well is shut in for a pressure buildup test, the well is usually closed at the surface rather than the sand face. Even though the well is shut in, the reservoir fluid continues to flow and accumulates in the wellbore until the well fills sufficiently to transmit the effect of shut-in to the formation. This "after-flow" behavior is caused by the wellbore storage, and it has a significant influence on pressure buildup data. During the period of wellbore storage effects, the pressure data points fall below the semilog straight line. The duration of those effects may be estimated by making the log-log data plot described previously. For pressure buildup testing, plot log $[p_{ws} - p_{wf}]$ versus $\log (\Delta t)$. The bottom-hole flow pressure p_{wf} is observed immediately before shut-in. When wellbore storage dominates, that plot will have a unit-slope straight line; as the semilog straight line is approached, the log-log plot bends over to a gently curving line with a low slope.

In all pressure buildup test analyses, the log-log data plot should be made before the straight line is chosen on the semilog data plot. This log-log plot is essential to avoid drawing a semilog straight line through the wellbore storage-dominated data. The beginning of the semilog line can be estimated by observing when the data points on the log-log plot reach the slowly curving low-slope line and adding 1 to 1.5 cycles in time after the end of the unit-slope straight line. Alternatively, the time to the beginning of the semilog straight line can be estimated from

$$\Delta t > \frac{170,000C~e^{0.14s}}{(kh/\mu)}$$

where $\Delta t = \text{shut-in}$, time, hr

C = calculated wellbore storage coefficient, bbl/psi

k = permeability, md

s = skin factor

h = thickness, ft

Example 3-26³

Table 3–5 shows pressure buildup data from an oil well with an estimated drainage radius of 2,640 ft. Before shut-in, the well had produced at a stabilized rate of 4,900 STB/day for 310 hours. Known reservoir data are

$$\begin{array}{c} r_e = 2,640 \ \text{ft} \\ depth = 10,476 \ \text{ft} \\ r_w = 0.354 \ \text{ft} \\ c_t = 22.6 \times 10^{-6} psi^{-1} \\ Q_o = 4,900 \ STB/D \\ h = 482 \ \text{ft} \\ P_{wf}(\Delta t = 0) = 2,761 \ psig \\ \mu_o = 0.20 \ cp \\ \varphi = 0.09 \\ B_o = 1.55 \ bbl/STB \\ casing \ ID = 0.523 \ \text{ft} \\ t_p = 310 \ hr \end{array}$$

Calculate

- Average permeability k.
- Skin factor.
- Pressure drop due to skin.

Solution

Step 1. Plot p_{ws} versus $(t_p + \Delta t)/\Delta t$ on a semilog scale as shown in Figure 3-38.

Step 2. Identify the correct straight-line portion of the curve and determine the slope m to give

$$m = 40 \text{ psi/cycle}$$

³This example problem and solution procedure are given by Earlougher, R., *Advanced Well Test Analysis*, Monograph Series, SPE, Dallas (1977).

TABLE 3-5 Earlougher's Pressure Buildup Data (Permission to publish by the SPE, copyright SPE, 1977)

Δt (hours)	$t_p + \Delta t$ (hours)	$\frac{(t_p + \Delta t)}{\Delta t}$	p _{ws} (psig)
0.0	_	_	2,761
0.10	310.10	3,101	3,057
0.21	310.21	1,477	3,153
0.31	310.31	1,001	3,234
0.52	310.52	597	3,249
0.63	310.63	493	3,256
0.73	310.73	426	3,260
0.84	310.84	370	3,263
0.94	310.94	331	3,266
1.05	311.05	296	3,267
1.15	311.15	271	3,268
1.36	311.36	229	3,271
1.68	311.68	186	3,274
1.99	311.99	157	3,276
2.51	312.51	125	3,280
3.04	313.04	103	3,283
3.46	313.46	90.6	3,286
4.08	314.08	77.0	3,289
5.03	315.03	62.6	3,293
5.97	315.97	52.9	3,297
6.07	316.07	52.1	3,297
7.01	317.01	45.2	3,300
8.06	318.06	39.5	3,303
9.00	319.00	35.4	3,305
10.05	320.05	31.8	3,306
13.09	323.09	24.7	3,310
16.02	326.02	20.4	3,313
20.00	330.00	16.5	3,317
26.07	336.07	12.9	3,320
31.03	341.03	11.0	3,322
34.98	344.98	9.9	3,323
37.54	347.54	9.3	3,323

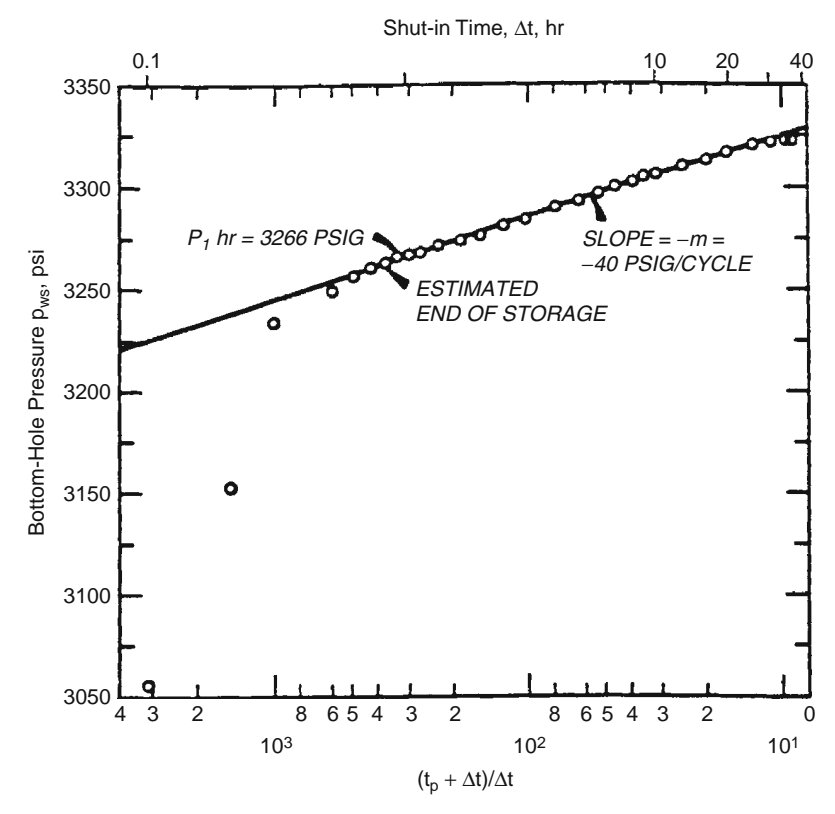


FIGURE 3-38 Earlougher's semilog data plot for the buildup test. (Permission to publish by the SPE, copyright SPE, 1977.)

Step 3. Calculate the average permeability by using Equation 3-177 to give

$$k = \frac{(162.6)(4,900)(1.55)(0.22)}{(40)(482)} = 12.8 \text{ md}$$

Step 4. Determine $p_{\rm wf}$ after 1 hour from the straight-line portion of the curve to give

$$p_{1 hr} = 3266 psi$$

Step 5. Calculate the skin factor by applying Equation 3-178.

$$s = 1.151 \left[\frac{3,266 - 2,761}{40} - \log \left(\frac{(12.8)(12)^2}{(0.09)(0.20)(22.6 \times 10^{-6})(4.25)^2} \right) + 3.23 \right] = 8.6$$

Step 6. Calculate the pressure drop due to skin from

$$\Delta p_{skin} = 0.87 \text{ ms} = 0.87(40)(8.6) = 299 \text{ psia}$$

SECTION 3.13 PROBLEMS

1. An incompressible fluid flows in a linear porous media with the following properties:

$$\begin{array}{ccc} L=2500 \ ft & h=30 \ ft & width=500 \ ft \\ k=50 \ md & \varphi=17\% & \mu=2 \ cp \\ inlet \ pressure=2100 \ psi & Q=4 \ bbl/day & \rho=45 \ lb/ft^3 \end{array}$$

Calculate and plot the pressure profile throughout the linear system.

- 2. Assume the reservoir linear system as described in problem 1 is tilted with a dip angle of 7°. Calculate the fluid potential through the linear system.
- 3. A 0.7 specific gravity gas is flowing in a linear reservoir system at 150°F. The upstream and downstream pressures are 2000 and 1800 psi, respectively. The system has the following properties:

$$\label{eq:local_local_local_local_local_local} \begin{split} L &= 2000 \text{ ft} \quad W = 300 \text{ ft} \quad h = 15 \text{ ft} \\ k &= 40 \text{ md} \quad \varphi = 15\% \end{split}$$

Calculate the gas flow rate.

4. An oil well is producing a crude oil system at 1000 STB/day and 2000 psi of bottom-hole flowing pressure. The pay zone and the producing well have the following characteristics:

$$\begin{array}{lll} h=35~ft & r_w=0.25~ft & drainage~area=40~acres\\ API=45^\circ & \gamma_g=0.72 & R_s=700~scf/STB\\ k=80~md & T=100^\circ F \end{array}$$

Assuming steady-state flowing conditions, calculate and plot the pressure profile around the wellbore.

5. Assuming steady-state flow and incompressible fluid, calculate the oil flow rate under the following conditions:

$$\begin{array}{llll} p_e = 2500 \; psi & p_{wf} = 2000 \; psi & r_e = 745 \; ft \\ r_w = 0.3 \; ft & \mu_o = 2 \; cp & B_o = 1.4 \; bbl/STB \\ h = 30 \; ft & k = 60 \; md & \end{array}$$

6. A gas well is flowing under a bottom-hole flowing pressure of 900 psi. The current reservoir pressure is 1300 psi. The following additional data are available:

$$\begin{array}{ll} T=140^{\circ}F & \quad \gamma_g=0.65 \quad \ \, r_w=0.3 \; ft \\ k=60 \; md \quad \ \, h=40 \; ft \quad \ \, r_e=1000 \; ft \end{array} \label{eq:gamma_spectrum}$$

Calculate the gas flow rate by using a

- Real-gas pseudopressure approach.
- Pressure-squared method.
- 7. An oil well is producing a stabilized flow rate of 500 STB/day under a transient flow condition. Given

$$\begin{array}{lll} B_o = 1.1 \ bbl/STB & \mu_o = 2 \ cp & c_t = 15 \times 10^{-6} \ psi^{-1} \\ k_o = 50 \ md & h = 20 \ ft & \varphi = 20\% \\ r_w = 0.3 \ ft & p_i = 3500 \ psi & \end{array}$$

calculate and plot the pressure profile after 1, 5, 10, 15, and 20 hours.

8. An oil well is producing at a constant flow rate of 800 STB/day under a transient flow condition. The following data are available:

$$\begin{array}{lll} B_o = 1.2 \ bbl/STB & \ \mu_o = 3 \ cp & \ c_t = 15 \times 10^{-6} \ psi^{-1} \\ k_o = 100 \ md & \ h = 25 \ ft & \ \phi = 15\% \\ r_w = 0.5 & \ p_i = 4000 \ psi & \ r_e = 1000 \ ft \end{array}$$

Using the E_i -function approach and the p_D -method, calculate the bottom-hole flowing pressure after 1, 2, 3, 5, and 10 hrs. Plot the results on a semilog scale and Cartesian scale.

9. A well is flowing under a drawdown pressure of 350 psi and produces at a constant flow rate of 300 STB/day. The net thickness is 25 ft. Given

$$r_e = 660 \; ft \quad r_w = 0.25 \; ft \quad \mu_o = 1.2 \; cp \quad B_o = 1.25 \; bbl/STB \label{eq:power_power}$$

- calculate
 - Average permeability.
 - Capacity of the formation.
- 10. An oil well is producing from the center of a 40-acre square-drilling pattern. Given

$$\begin{array}{lll} \varphi=20\% & h=15 \text{ ft} & k=60 \text{ md} \\ \mu_o=1.5 \text{ cp} & B_o=1.4 \text{ bbl/STB} & r_w=0.25 \text{ ft} \\ p_r=2000 \text{ psi} & p_{wf}=1500 \text{ psi} \end{array}$$

calculate the oil flow rate.

11. A shut-in well is located at a distance of 700 ft from one well and 1100 ft from a second well. The first well flows for 5 days at 180 STB/day, at which time the second well begins to flow at 280 STB/day. Calculate the pressure drop in the shut-in well when the second well has been flowing for 7 days. The following additional data are given:

$$\begin{array}{lll} p_i = 3000 \; psi & B_o = 1.3 \; bbl/STB & \mu_o = 1.2 \; cp & h = 60 \; ft \\ c_t = 15 \times 10^{-6} \; psi^{-1} & \varphi = 15\% & k = 45 \; md \end{array}$$

12. A well is opened to flow at 150 STB/day for 24 hours. The flow rate is then increased to 360 STB/day and lasts for another 24 hours. The well flow rate is then reduced to 310 STB/day for 16 hours. Calculate the pressure drop in a shut-in well 700 ft away from the well, given

$$\begin{array}{lll} \varphi = 15\% & h = 20 \text{ ft} & k = 100 \text{ md} \\ \mu_o = 2 \text{ cp} & B_o = 1.2 \text{ bbl/STB} & r_w = 0.25 \text{ ft} \\ p_i = 3000 \text{ psi} & c_t = 12 \times 10^{-6} \text{ psi}^{-1} \end{array}$$

13. A well is flowing under unsteady-state flowing conditions for 5 days at 300 STB/day. The well is located at 350 ft and 420 ft distance from two sealing faults. Given

calculate the pressure in the well after 5 days.

14. A drawdown test was conducted on a new well with results as follows:

t, hr	p _{wf} , psi
1.50	2978
3.75	2949
7.50	2927
15.00	2904
37.50	2876
56.25	2863
75.00	2848
112.50	2810
150.00	2790
225.00	2763

Given

$$\begin{array}{lll} p_i = 3400 \; psi & h = 25 \; ft & Q = 300 \; STB/day \\ c_t = 18 \times 10^{-6} \; psi^{-1} & \mu_o = 1.8 \; cp & B_o = 1.1 \; bbl/STB \\ r_w = 0.25 \; ft & \varphi = 12\% \end{array}$$

and assuming no wellbore storage, calculate

- Average permeability.
- Skin factor.
- 15. A drawdown test was conducted on a discovery well. The well was flowed at a constant flow rate of 175 STB/day. The fluid and reservoir data are

$$\begin{array}{lll} S_{wi} = 25\% & & \varphi = 15\% & & h = 30 \; ft & ct = 18 \times 10^{-6} \; psi^{-1} \\ r_w = 0.25 \; ft & & p_i = 4680 \; psi & & \mu_o = 1.5 \; cp & B_o = 1.25 \; bbl/STB \end{array}$$

771	1 1	1 1	1 - 1 -	
i ne	drawdown	test	aata	are

t, hr	p _{wf} , psi
0.6	4388
1.2	4367
1.8	4355
2.4	4344
3.6	4334
6.0	4318
8.4	4309
12.0	4300
24.0	4278
36.0	4261
48.0	4258
60.0	4253
72.0	4249
84.0	4244
96.0	4240
108.0	4235
120.0	4230
144.0	4222
180.0	4206

Calculate

- Drainage radius.
- Skin factor.
- Oil flow rate at a bottom-hole flowing pressure of 4300 psi, assuming a semisteady-state flowing condition.
- 16. A pressure buildup test was conducted on a well that had been producing at 146 STB/day for 53 hours. The reservoir and fluid data follow:

$$\begin{array}{lll} B_o = 1.29 \; bbl/STB & \;\; \mu_o = 0.85 \; cp & \;\; c_t = 12 \times 10^{-6} \; psi^{-1} \\ \varphi = 10\% & \;\; p_{wf} = 1426.9 \; psig & \;\; A = 20 \; acres \end{array}$$

The buildup data are as follows:

p _{ws} , psig
1451.5
1476.0
1498.6
1520.1
1541.5
1561.3
1581.9
1599.7
1617.9

1.667	1635.3
2.000	1665.7
2.333	1691.8
2.667	1715.3
3.000	1736.3
3.333	1754.7
3.667	1770.1
4.000	1783.5
4.500	1800.7
5.000	1812.8
5.500	1822.4
6.000	1830.7
6.500	1837.2
7.000	1841.1
7.500	1844.5
8.000	1846.7
8.500	1849.6
9.000	1850.4
10.000	1852.7
11.000	1853.5
12.000	1854.0
12.667	1854.0
14.620	1855.0

Calculate

- Average reservoir pressure.
- Skin factor.
- Formation capacity.

SECTION 3.14 REFERENCES

- R. Al-Hussainy, H.J. Ramey Jr., Application of Real Gas Flow Theory to Well Testing and Deliverability Forecasting, Jour. of Petroleum Technology, 1966, Theory and Practice of the Testing of Gas Wells, third ed., Energy Resources Conservation Board, Calgary, Canada, 1975.
- [2] R. Ál-Hussainy, H.J. Ramey Jr., P.B. Crawford, The Flow of Real Gases through Porous Media, Trans. AIME 624 (1966) 237.
- [3] A.T. Chatas, A Practical Treatment of Nonsteady-State Flow Problems in Reservoir Systems, Pet. Eng. (1953) B-44–B-56.
- [4] B. Craft, M. Hawkins, Applied Petroleum Reservoir Engineering, Prentice-Hall, 1959.
- [5] B. Craft, M. Hawkins, R. Terry, Applied Petroleum Reservoir Engineering, second ed., Prentice Hall, 1990.
- [6] L. Dake, Fundamentals of Reservoir Engineering, Elsevier, Amsterdam, 1978.
- [7] L.P. Dake, The Practice of Reservoir Engineering, Elsevier, Amsterdam, 1994.
- [8] D.H. Davis, Reduction in Permeability with Overburden Pressure, Trans. AIME 329 (1952) 195.
- [9] D. Donohue, T. Erkekin, Gas Well Testing, Theory and Practice, IHRDC, 1982.

- [10] R.C. Earlougher, Jr., Advances in Well Test Analysis, Monograph Vol. 5, Society of Petroleum Engineers of AIME. Millet the Printer, Dallas, TX, 1977.
- [11] M.J. Fetkovich, The Isochronal Testing of Oil Wells, in: SPE Paper 4529, presented at the SPE Annual meeting, Las Vegas, September 30–October 3, 1973.
- [12] M. Golan, C. Whitson, Well Performance, second ed., Prentice-Hall, Englewood Cliffs, NJ, 1986.
- [13] M. Hawkins, A Note on the Skin Effect, Trans. AIME (1956) 356.
- [14] R. Horne, Modern Well Test Analysis, Petroway, Inc., Palo Alto, CA, 1995.
- [15] D.R. Horner, Pressure Build-up in Wells, in: Proc., Third World Pet. Cong., Sec II, The Hague, 1951, pp. 503–523. Also Reprint Series, No. 9—Pressure Analysis Methods, Society of Petroleum Engineers of AIME, Dallas, 1967, pp. 25–43.
- [16] W. Hurst, Establishment of the Skin Effect and Its Impediment to Fluid Flow into a Wellbore, Petroleum Engineering 25 (1953) B–6.
- [17] S.C. Jones, Using the Inertial Coefficient, b, to Characterize Heterogeneity in Reservoir Rock, SPE Paper 16949, presented at the SPE Conference, Dallas, TX, Sept. 27–30, 1987.
- [18] S. Joshi, Horizontal Well Technology, Pennwell Publishing Company, 1991.
- [19] W. Lee, Well Testing, Society of Petroleum Engineers Textbook Series, Dallas, 1982.
- [20] J. Lee, R. Wattenbarger, Gas Reservoir Engineering, SPE Textbook Series, Vol. 5, SPE, 1996.
- [21] S. Matthews, F. Bronz, P. Hazebroek, A Method for the Determination of Average Pressure in a Bounded Reservoir, Trans. AIME 201 (1954) 82–191.
- [22] C.S. Matthews, D.G. Russell, Pressure Buildup and Flow Tests in Wells, Monograph Vol. 1, Society of Petroleum Engineers of AIME. Millet the Printer, Dallas, TX, 1967.
- [23] H. Ramey, W. Cobb, A General Pressure Buildup Theory for a Well in a Closed Drainage Area, JPT (1971) 1493–1505.
- [24] D.G. Russell, J.H. Goodrich, G.E. Perry, J.F. Bruskotter, Methods for Predicting Gas Well Performance, JPT (1966) 99–108; Trans. AIME, 237.
- [25] H.C. Slider, Practical Petroleum Reservoir Engineering Methods, Tulsa, OK, Petroleum Publishing Co., 1976.
- [26] A.F. Van Everdingen, The Skin Effect and Its Influence on the Productive Capacity of a Well, Trans. AIME 198 (1953) 171.
- [27] A.F. Van Everdingen, W. Hurst, The Application of the Laplace Transformation to Flow Problems in Reservoirs, Trans. AIME 186 (1949) 305–324.
- [28] R.A. Wattenbarger, H.J. Ramey Jr., Gas Well Testing with Turbulence. Damage and Wellbore Storage, JPT (1968) 877–887; Trans. AIME, 243.

Index

A	Darcy's law, 134
Absolute permeability correlations	gas flow rate, standard condition,
connate water, 84, 85	134–135
effective permeability, 86–87	number of gas moles, 133-134
Morris-Biggs equation, 85–86	unsteady-state radial flow, 206
relative permeability, 87	Connate water, 48
Timur equation, 85	Constant-terminal-pressure solution, 162
Absolute porosity, 32	Constant-terminal-rate solution
Areal heterogeneity, reservoir	dimensionless pressure drop (pD)
geostatistical estimation techniques, 105	solution
interpolation and extrapolation methods,	Bessel functions, 173
106	Darcy's equation, 171
pulse testing, 104–105	diffusivity equation, 172
Averaging absolute permeability	dimensionless variables, 170
geometric-average permeability, 83	finite-radial reservoir, 173, 175-178
harmonic-average permeability, 80-81	infinite-acting reservoir, 173-175
weighted-average permeability	radial distances, 172
layer 1, 77	transient flow analysis, 171
layer 2, 78	wellbore radius, 179
layer 3, 78–79	exponential integral (E _i)-function
layered beds, variable area, 78-79,	solution
79f	definition, 163
linear flow, layered beds, 77, 77f	diffusivity equation, 163
	line-source solution, 165
В	log approximation, 169
Bubble-point curve, 3	pressure profile and drainage
	radius, 168f, 169
C	values, 163, 164t, 166f
Capillary hysteresis	m(p)-solution method
drainage process, 49–50	constant-rate condition, 181
ink-bottle effect, 51	dimensionless time, 181-182
pressure curves, 50, 50f	Euler's constant, 182
Compressible fluids, 119	radial gas diffusivity equation,
constant-terminal-rate solution	182
gas compressibility equation, 179	pressure-approximation method
pressure-squared and pressure-	$1/\mu_o B_o$ vs. pressure, 186, 186f
approximation method, 180–181	gas formation volume factor,
radial diffusivity equation, 180-181	185–186
real density equation, 179	gas properties, 187
pseudosteady-state flow, 201, 207	pseudoliquid, 185
steady-state flow, linear flow	pressure-squared approximation
average pressure, 135	method, 183–185

Constant-terminal-rate solution (<i>Continued</i>) radial flow gas compressibility equation, 179 pressure-squared and pressure- approximation method, 180–181 radial diffusivity equation, 180–181 real density equation, 179 transient test analysis, 163 Cricondenbar (P _{cb}), 2 Cricondentherm (T _{ct}), 2	horizontal linear system, 125 horizontal-radial system, 125–127 pressure gradient, radial flow, 125–127,
Critical gas saturation (S _{gc}), 38	Gas reservoirs
Critical oil saturation (S _{oc}), 37	dry-gas reservoir
Critical point, 3	coefficients of equation, 25, 26t
Critical water saturation (S _{wc}), 38	generalized physical properties, 14–25, 25 <i>t</i>
_ D	hydrocarbon and nonhydrocarbon
Darcy's equation	components, 14, 15t
constant-terminal-rate solution, 171 horizontal multiple-phase flow, 151, 152 incompressible fluids, linear flow, 128,	phase diagram, 13, 13f ternary diagram, compositional boundaries, 13, 14f
130	near-critical gas-condensate reservoir
Klinkenberg effect, 75	isothermal reduction, 12
pseudosteady-state flow, 203-204	liquid-shrinkage curve, 11, 11f
Darcy's law	phase diagram, 11, 11f
cross-sectional area, 127	retrograde gas-condensate reservoir
horizontal linear system, 125	liquid dropout curve, 10, 10f
horizontal-radial system, 125–127	pressure-temperature phase
permeability, 65	diagram, 9–10, 9f
pressure gradient, radial flow, 125–127,	vaporization process, 10
126f pressure vs. distance, linear flow, 125, 126f	wet-gas reservoir, 12 Gas-oil contact (GOC), 51, 52
steady-state flow, 134	Gas-on contact (GOC), 31, 32
turbulent flow, 127	Н
Dew-point curve, 3	Harmonic-average permeability, 80–81
Displacement pressure, 47	Horizontal multiple-phase flow
Dry-gas reservoir	Darcy's equation, 151, 152
coefficients of equation, 25, 26t	effective phase saturation, 151
generalized physical properties, 14–25, 25t	gas formation volume factor, 152
hydrocarbon and nonhydrocarbon	gas-oil ratio (GOR), 153
components, 14, 15t	water-oil ratio (WOR), 153
phase diagram, 13, 13f	Horizontal permeability (k _h), 67
ternary diagram, compositional	Ī
boundaries, 13, 14f	I 50
Dykstra-Parsons permeability variation,	Imbibition process, 50
94–96	Incompressible fluids, 118 linear flow
E	average reservoir pressure, 141–142
Effective porosity, 33–36	constant cross-sectional area, 127
	Darcy's equation, 128, 130
F	drainage area, 142–143
Fluid flow equations	external pressure, 141
cross-sectional area, 127	external/drainage radius, 140

fluid density, 130 fluid potential, 129, 130 gravitational force, 129 radial flow apparent fluid velocity, 138–139 bottom-hole flowing pressure, 138 oil flow rate, 139–140 Initial saturation distribution combination-drive reservoir, 52, 53f free-water level (FWL), 54 pore-size distribution, 52–53, 53f	Oil reservoirs crude oils, 4 gas-cap reservoir, 4 liquid-shrinkage curve, 4, 5f, 7, 8f low-shrinkage oil, 5, 5f, 6f near-critical crude oil, 7, 8f ordinary black oil, 4, 4f saturated oil reservoir, 4 undersaturated oil reservoir, 3 volatile crude oil, 6, 6f, 7f
water saturation profile, 51, 52 <i>f</i> Interfacial tension, 40–41	Ordinary black oil, 4, 4f
Inverse distance method, 106	P
Inverse distance squared method, 106	Permeability, rock properties absolute permeability, 69
K	connate water, 84, 85
Klinkenberg effect	Darcy's law, 65
Darcy's equation, 75	effective permeability, 86–87
gas permeability measurements, 71, 72f	fluid flow equation, 65
gas pressure, 71–72, 73f	geometric-average permeability, 83
magnitude, 71–72, 72f	harmonic-average permeability, 80–81
Newton-Raphson iterative methods, 74, 75	Klinkenberg effect
radial flow model, 75, 75f	Darcy's equation, 75 gas permeability measurements, 71,
slip phenomenon, 73	72f
L	gas pressure, 71–72, 73f magnitude, 71–72, 72f
Laplace's equation, 161	Newton-Raphson iterative methods,
Leverett J-function, 61–64	74, 75
Linear flow	radial flow model, 75, 75f
layered beds, 77, 77f, 78–79, 79f	slip phenomenon, 73
reservoir geometry, 122–123, 123f, 124f	linear flow model, 66, 67f
series beds, 80, 80f, 81, 81f	Morris-Biggs equation, 85–86
steady-state flow	porous media samples, 67, 68, 68f
compressible fluids, 133–137 incompressible fluids, 127–132	relative permeability, 87 Timur equation, 85
slightly compressible fluids,	weighted-average permeability, 77
132–133	Phase envelope (two-phase region), 3
	Polygon method, 106
M	Porosity, 32–36
Mean pressure, 71	Pressure relations, capillary tubes, 41, 42f
Morris-Biggs equation, 85–86	Pressure-temperature diagram, 2–3
Movable oil saturation (S _{om}), 38	Pseudosteady-state flow
Multicomponent system, 2, 2f	compressibility, 189 compressible fluids, 201
N	flow regime, 188–189, 189f
Near-critical gas-condensate reservoir	pore volume, 190
isothermal reduction, 12	pressure decline rate, 190–191
liquid-shrinkage curve, 11, 11f	pressure-approximation method, 202
phase diagram, 11, 11f	pressure-squared approximation
Newton-Raphson iterative methods, 74, 75	method, 201–202

Pseudosteady-state flow (Continued)	constant-terminal-pressure solution,
skin factor, 206–207	162
Darcy's equation, 203-204	constant-terminal-rate solution, 162
definition, 204–205	diffusivity constant, 160
outcomes, 205	diffusivity equation, 160, 161, 162
positive and negative skin effects,	fluid density, 159
203, 204 <i>f</i>	Laplace's equation, steady-state
pressure drawdown, 205	flow, 161
skin zone, 202–203, 203f	Reservoir fluid behavior
steady-state radial flow, 205-206	classification, 1-29
unsteady-state radial flow, 206	gas reservoirs
wellbore damage, 202–203	dry-gas reservoir, 13, 14, 15t, 25t
slightly compressible fluids	near-critical gas-condensate
circular drainage area, 198	reservoir, 11, 12
diffusivity equation, 193	retrograde gas-condensate
flow rate, 194, 195	reservoir, 9, 10–11
integration constant, 194	wet-gas reservoir, 12
p _D function, 195	oil reservoirs
shape factor, 195–198, 196 <i>t</i>	crude oils, 4
turbulent flow factor, 210	gas-cap reservoir, 4
non-Darcy flow, 208	liquid-shrinkage curve, 4, 5f, 7, 8f
steady-state flow, 210	low-shrinkage oil, 5, 5f, 6f
turbulence parameter, 208–209	near-critical crude oil, 7, 8f
unsteady-state radial flow, 209–210	ordinary black oil, 4, 4f
underground fluid withdrawals,	saturated oil reservoir, 4
192–193	undersaturated oil reservoir, 3
volumetric average pressure, 191, 192f	volatile crude oil, 6, 6f, 7f
volumente average pressure, 171, 172,	pressure-temperature diagram, 2–3
Q	undefined petroleum fractions, 25–29
Quality lines, 3	Reservoir fluid flow
Quality Intest o	constant-terminal-pressure solution, 162
R	constant-terminal-rate solution
Radial flow	dimensionless pressure drop (p _D)
constant-terminal-rate solution	solution, 170–179
gas compressibility equation, 179	E _i -function solution, 163–170
pressure-squared and pressure-	m(p)-solution method, 181–183
approximation method, 180–181	pressure-approximation method,
radial diffusivity equation, 180–181	185–188
real density equation, 179	pressure-squared approximation
Klinkenberg effect, 75, 75f	method, 183–185
pseudosteady-state flow	radial flow, 179–181
compressible fluids, 201	Darcy's law
slightly compressible fluids,	cross-sectional area, 127
193–201	horizontal linear system, 125
reservoir geometry, 122, 123f	horizontal-radial system, 125–127
steady-state flow	pressure gradient, radial flow,
compressible gases, 144–150	125–127, 126 <i>f</i>
incompressible fluids, 138–142	pressure vs. distance, linear flow,
slightly compressible fluids,	125, 126 <i>f</i>
143–144	turbulent flow, 127
unsteady-state flow	flow regimes, 120–121
compressibility, 159, 160	fluid types

compressible fluids, 119	pressure disturbance, 153–155, 154f
density vs. pressure, 119, 120f	radial flow, 159-162
incompressible fluids, 118	radius of investigation, 154
isothermal compressibility	Reservoir heterogeneity
coefficient, 117–118	definition, 93–94
pressure-volume relationship, 119,	degree of homogeneity, 94
120 <i>f</i>	Dykstra-Parsons permeability variation,
slightly compressible fluids,	94–96
118–119	Lorenz coefficient
number of mobile fluids, 124-125	normalized flow capacity, 99-100,
pseudosteady-state flow	99f
compressibility, 189	permeability variation, 100, 100f
compressible fluids, 201	Residual oil saturation (S _{or}), 37–38
flow regime, 188–189, 189f	Retrograde gas-condensate reservoir
pore volume, 190	liquid dropout curve, 10, 10f
pressure decline rate, 190–191	pressure-temperature phase diagram,
pressure-approximation method,	9–10, 9f
202	vaporization process, 10
pressure-squared approximation	Rock compressibility
method, 201–202	pore compressibility
skin factor, 202–207	boundary conditions, 89–90
slightly compressible fluids,	formation compressibility, 89, 91, 92
193–201	reservoir pressure, 88
turbulent flow factor, 208-211	rock-bulk compressibility, 88
underground fluid withdrawals,	rock-matrix compressibility, 88
192–193	Rock properties
volumetric average pressure, 191,	absolute porosity, 32
192 <i>f</i>	areal heterogeneity
reservoir geometry	geostatistical estimation techniques,
linear flow, 122–123, 123f, 124f	105
radial flow, 122, 123f	interpolation and extrapolation
spherical and hemispherical flow,	methods, 106
123, 124 <i>f</i>	pulse testing, 104–105
steady-state flow	average saturation, 38–39
horizontal multiple-phase flow,	capillary pressure
151–153	capillary hysteresis, 49–51
linear flow, 127-137	data conversion, 64–65
radial flow, 138-142, 143-150	equipment, 46, 47f
superposition principle	gas-liquid system, 45
multiple wells, 212–214	initial saturation distribution, 51-61
pressure-change effects, 221	Leverett J-function, 61–64
reservoir boundary, 218–221	oil-water system, 45
superposition theorem, 211-212	pressure data, 47, 48f
variable flow rates, 215-218	two immiscible fluids, 43
transient well testing	types, 44
drawdown test, 222-232	variation, permeability, 48–49, 49f
petroleum industry, 221–222	wetting phase, 48
pressure buildup test, 233–241	critical gas saturation (S _{gc}), 38
unsteady-state flow	critical oil saturation (Soc), 37
basic transient flow equation,	critical water saturation (Swc), 38
155–159	effective porosity, 33–36
definition, 155	movable oil saturation (S _{om}), 38

Rock properties (Continued)	integration constant, 194
net pay thickness, 92–93	p _D function, 195
permeability	shape factor, 195–198, 196t
absolute permeability, 69	steady-state flow
connate water, 84, 85	linear flow, 132–133
Darcy's law, 65	radial flow, 143-144
effective permeability, 86–87	unsteady-state flow, 206
fluid flow equation, 65	compressibility, 159, 160
geometric-average permeability, 83	constant-terminal-pressure solution,
harmonic-average permeability,	162
80–81	constant-terminal-rate solution, 162
Klinkenberg effect, 71-76	diffusivity constant, 160
linear flow model, 66, 67f	diffusivity equation, 160, 161, 162
Morris-Biggs equation, 85–86	fluid density, 159
porous media samples, 67, 68, 68f	Laplace's equation, steady-state
relative permeability, 87	flow, 161
Timur equation, 85	Slip phenomenon, 73
weighted-average permeability, 77	Steady-state flow
pore compressibility	horizontal multiple-phase flow
boundary conditions, 89–90	Darcy's equation, 151, 152
formation compressibility, 89, 91, 92	effective phase saturation, 151
reservoir heterogeneity	gas formation volume factor, 152
definition, 93–94	gas-oil ratio (GOR), 153
degree of homogeneity, 94	water-oil ratio (WOR), 153
Dykstra-Parsons permeability	Laplace's equation, 161
variation, 94–96	linear flow
Lorenz coefficient, 99-101	compressible fluids, 133-137
reservoir pressure, 88	incompressible fluids, 127–132
residual oil saturation (S _{or}), 37–38	slightly compressible fluids,
rock-bulk compressibility, 88	132–133
rock-matrix compressibility, 88	radial flow
routine core analysis tests, 31	compressible gases, 144–150
special tests, 31–32	incompressible fluids, 138–142
surface and interfacial tension, 40-43	slightly compressible fluids,
wettability, 40	143–144
ę.	Surface tension, 40–41, 41f
S Softwartion mode management	Т
Saturation, rock properties	
average saturation, 38–39	Timur equation, 85
capillary forces, 37	Transient well testing
critical gas saturation (S _{gc}), 38	drawdown test
critical vistor saturation (S _{oc}), 37	average permeability, 224
critical water saturation (S_{wc}), 38 definition, 36	fundamental objectives, 222
	infinite-acting period, 231 log-log scale, 229
mathematical concept, 36–37	pressure behavior, 223
movable oil saturation (S _{om}), 38	
residual oil saturation (S _{or}), 37–38	semilog straight-line, 224, 224f, 225 skin effect, 224
Slightly compressible fluids, 118–119 pseudosteady-state flow, 206	specific steps, 231–233
circular drainage area, 198	transient flow slope, 225
diffusivity equation, 193 flow rate, 194, 195	wellbore pressure, 229 wellbore storage factor, 227–229

essure disturbance, 153–155, 154f lial flow compressibility, 159, 160 constant-terminal-pressure solution, 162 constant-terminal-rate solution, 162 diffusivity constant, 160 diffusivity equation, 160, 161, 162 fluid density, 159 Laplace's equation, steady-state flow, 161 lius of investigation, 154
V cal heterogeneity, reservoir gree of homogeneity, 94 kstra-Parsons permeability variation, 94–96 renz coefficient normalized flow capacity, 99–100, 99f permeability variation, 100, 100f cal permeability (k _v), 67 ille crude oil, 6, 6f, 7f W r-oil contact (WOC), 51, 52 hted-average permeability er 1, 77 er 2, 78 er 3, 78–79 ered beds, variable area, 78–79, 79f car flow, layered beds, 77, 77f gas reservoir, 12
i